Developmental Plasticity, Ecology, and Evolutionary Radiation of Nematodes of Diplogastridae

Dissertation

der Mathematisch-Naturwissenschaftlichen Fakultät

der Eberhard Karls Universität Tübingen

zur Erlangung des Grades eines

Doktors der Naturwissenschaften

(Dr. rer. nat.)

vorgelegt von

Vladislav Susoy

aus Berezniki, Russland

Tübingen

2015

Gedruckt mit Genehmigung der Mathematisch-Naturwissenschaftlichen Fakultät der Eberhard Karls Universität Tübingen.

Tag der mündlichen Qualifikation:	5 November 2015
Dekan:	Prof. Dr. Wolfgang Rosenstiel
1. Berichterstatter:	Prof. Dr. Ralf J. Sommer
2. Berichterstatter:	Prof. Dr. Heinz-R. Köhler
3. Berichterstatter:	Prof. Dr. Hinrich Schulenburg

Acknowledgements

I am deeply appreciative of the many people who have supported my work. First and foremost, I would like to thank my advisors, Professor Ralf J. Sommer and Dr. Matthias Herrmann for giving me the opportunity to pursue various research projects as well as for their insightful scientific advice, support, and encouragement. I am also very grateful to Matthias for introducing me to nematology and for doing an excellent job of organizing fieldwork in Germany, Arizona and on La Réunion.

I would like to thank the members of my examination committee: Professor Heinz-R. Köhler and Professor Hinrich Schulenburg for evaluating this dissertation and Dr. Felicity Jones, Professor Karl Forchhammer, and Professor Rolf Reuter for being my examiners.

I consider myself fortunate for having had Dr. Erik J. Ragsdale as a colleague for several years, and more than that to count him as a friend. We have had exciting collaborations and great discussions and I would like to thank you, Erik, for your attention, inspiration, and thoughtful feedback. I also want to thank Erik and Orlando de Lange for reading over drafts of this dissertation and spelling out some nuances of English writing. I am also grateful to Melanie Mayer for making a German translation of the summary of this dissertation.

I thank my collaborator Dr. Natsumi Kanzaki, whose attention to detail and unique skills have consistently been of great help. I also thank our wonderful technical assistants: Hanh, Metta, Gabi, Walli, Christian, Heike, Tobias, Aziza, and Christina, who helped me in various ways during my work. Special thanks to Jürgen Berger for electron microscopy and Christa Lanz for assistance with next generation sequencing.

I am grateful to present and past members of the Sommer lab. In particular, I want to thank Christian, Gabriel, Neel, and Praveen for bioinformatics support and Cameron, Vahan, Manuela, Jan, Martin, James, Arpita, Eduardo, Nermin, Akira, Isabella, Simone, and Dan for their expertise. I am also thankful to the many people who helped me with sample collection and assisted me during my field trips. Finally, I am appreciative of my friends and my family for supporting me throughout my graduate studies and the Max Planck Society for their generous support.

Contents

I Summary

Explaining organismal diversity and adaptation are the two central aims of evolutionary biology. In this thesis, I address these questions using a comparative evolutionary approach and nematodes of the family Diplogastridae as a study system. Systematic sampling of diplogastrid nematodes resulted in the discovery of numerous nematode species, their novel traits and ecological associations, providing reference points for consequent comparative evolutionary analyses. I first studied forces that drive evolutionary radiation and speciation in a host-symbiont system, specifically in a diverse group of predatory nematodes of the genus *Micoletzkya*, which are associated with bark beetles. I showed that nematode evolutionary radiation resulted from parallel divergence with their beetle hosts and was also shaped by preferential hosts shifts among closely related hosts, thus highlighting the roles of isolation and adaptation in the evolution of host-symbiont systems. I then built a new phylogenetic framework for the family Diplogastridae and used it to investigate the evolutionary implications of discrete phenotypic plasticity (polyphenism), specifically its impact on evolutionary tempo and the evolution of novelties. As a result, I identified that the origin of polyphenism coincided with a sharp increase in phenotypic complexity, which surprisingly decreased after secondary loss of plasticity; the rates of evolution, however, became even higher after phenotype fixation, which provided evidence for developmental character release. These results gave original support for a role of developmental plasticity in evolutionary diversification. Finally, I have discovered several new species of *Pristionchus*, which live in symbiosis with figs and fig wasps and show an extreme polyphenism with up to five discrete eco-morphotypes per species. This study revealed that adaptive radiation, or the rapid filling of contrasting ecological niches need not to be associated with diversifying selection on genotypes and can be based on discontinuous phenotypic plasticity.

II Zusammenfassung

Die zwei Hauptziele der Evolutionsbiologie sind die Erklärung der biologischen Vielfalt und der Adaptation. In dieser Arbeit befasse ich mich mit diesen Fragen unter Verwendung eines vergleichenden evolutionären Ansatzes und Nematoden der Familie Diplogastridae als Untersuchungssystem. Die systematische Probenentnahme diplogastrider Nematoden führte zur Entdeckung zahlreicher Nematodenarten, deren neuen Eigenschaften und ökologischen Assoziationen und lieferte Bezugspunkte für nachfolgende vergleichende evolutionäre Analysen. Zuerst untersuchte ich die Kräfte, die evolutionäre Radiation und Artenbildung in einem Wirt-Symbiont-System vorantreiben, nämlich in einer vielfältigen Gruppe räuberischer Nematoden der Gattung *Micoletzkya*, die mit Borkenkäfern assoziiert sind. Ich zeigte, dass die evolutionäre Radiation der Nematoden aus der parallelen Divergenz mit ihren Käferwirten resultierte und auch durch begünstigte Wirtswechsel zwischen nah verwandten Wirten geprägt wurde, was die Rolle der Isolation und der Adaptation in der Evolution von Wirt-Symbiont-Systemen hervorhebt. Als nächstes erstellte ich einen neuen phylogenetischen Rahmen für die Familie Diplogastridae und verwendete diesen um die evolutionären Folgen der diskontinuierlichen phänotypischen Plastizität (Polyphenismus) zu untersuchen, vor allem ihre Auswirkung auf evolutionäre Geschwindigkeit und die Evolution neuer Eigenschaften. Daraufhin erkannte ich, dass die Entstehung von Polyphenismus mit einer starken Zunahme an phänotypischer Komplexität übereinstimmte, die überraschenderweise nach einem sekundären Verlust der Plastizität wieder abnahm. Die Evolutionsraten wurden jedoch noch höher nach der phänotypischen Fixierung, was den Beweis für die Freigabe von Eigenschaften während der Entwicklung erbrachte. Diese Ergebnisse lieferten originelle Unterstützung für eine Rolle der Plastizität bei der evolutionären Diversifikation. Schließlich entdeckte ich einige neue *Pristionchus*-Arten, die in Symbiose mit Feigen und Feigenwespen leben und einen extremen Polyphenismus mit bis zu fünf diskreten Öko-Morphotypen pro Art aufweisen. Diese Arbeit zeigt, dass die adaptive Radiation oder das rasche Besetzen von gegensätzlichen ökologischen Nischen nicht mit diversifizierender Selektion von Genotypen assoziiert werden muss und auf diskontinuierlicher Plastizität basieren kann.

III List of publications

1. Susoy, V., Herrmann, M., Kanzaki, N., Kruger, M., Nguyen, C. N., Rödelsperger, C., Röseler, W., Weiler, C., Giblin-Davis, R. M., Ragsdale, E. J., Sommer, R. J. Large-scale diversification without genetic isolation in nematode symbionts of figs. *Science Advances* **2**, e1501031 (2016).
2. Susoy, V., Ragsdale, E. J., Kanzaki, N., Sommer, R. J. Rapid diversification associated with a macroevolutionary pulse of developmental plasticity. *eLife* **4**, e05463 (2015).
3. Wilecki, M., Lightfoot, J. W., Susoy, V., Sommer, R. J. Predatory feeding behaviour in *Pristionchus* nematodes is dependent on phenotypic plasticity and induced by serotonin. *The Journal of experimental biology* **218**, 1306-1313 (2015).
4. Susoy, V., Herrmann, M. Preferential host switching and codivergence shaped radiation of bark beetle symbionts, nematodes of *Micoletzkya* (Nematoda: Diplogastridae). *Journal of evolutionary biology* **27**, 889-898 (2014).
5. Kanzaki, N., Ragsdale, E. J., Susoy, V., Sommer, R. J. *Leptojacobus dorci* n. gen., n. sp. (Nematoda: Diplogastridae), an associate of *Dorcus* stag beetles (Coleoptera: Lucanidae). *Journal of nematology* **46**, 50-59 (2014).
6. Kanzaki, N., Ragsdale, E. J., Herrmann, M., Susoy, V., Sommer, R. J. Two androdioecious and one dioecious new species of *Pristionchus* (Nematoda: Diplogastridae): new reference points for the evolution of reproductive mode. *Journal of nematology* **45**, 172-194 (2013).
7. Susoy, V., Kanzaki, N., Herrmann, M. Description of the bark beetle associated nematodes *Micoletzkya masseyi* n. sp. and *M. japonica* n. sp. (Nematoda: Diplogastridae). *Nematology* **15**, 213-231 (2013).
8. Susoy, V., Herrmann, M. Validation of *Rhabditolaimus* Fuchs, 1914 (Nematoda: Diplogastridae) supported by integrative taxonomic evidence. *Nematology* **14**, 595-604 (2012).

1. Introduction

1.1 Diversity and divergence

Adaptive radiations play a central role in generating biological diversity and are a major characteristic of the evolution of life (Simpson, 1953; Schluter, 2000). The results of this process can be observed at all evolutionary depths and in most groups of living organisms. Well-known examples include the original radiations of eukaryotes, terrestrial plants, metazoans, insects, and vertebrates. Classic examples of recent diversifications are the radiation of Darwin's finches on Galapagos Islands and explosive speciation of Cichlid fishes in East African lakes (Brawand *et al*., 2014; Lamichhaney *et al*., 2015). In each of these instances, multiple phenotypically distinct lineages rapidly originated from a single ancestor following colonization of a new habitat. The process of adaptive radiation can be notionally divided into two components: lineage branching (speciation) and phenotypic divergence, and a basic principle of the process of adaptive radiation is that phenotypic divergence concurs with or follows genetic diversification. Indeed, the two processes are closely linked: phenotypic divergence within a species or population can result in habitat partitioning and assortative mating, leading to isolation and, consequently, decreased gene flow, and increased isolation can then promote even further genetic divergence. Lineage diversification and phenotypic divergence, however, do not need to be linked. There are examples of species radiations with little phenotypic or ecological divergence, and of substantial phenotypic divergence without speciation. Examples of the latter can be found in species with discrete phenotypic plasticity, or polyphenisms.

1.1.2 Divergence without speciation

1.1.2.1 Plasticity

Phenotypic plasticity is commonly defined as the ability of a single genotype to produce multiple phenotypes depending on environmental conditions (Bradshaw, 1965; Pigliucci, 2001, Whitman *et al*., 2009; Pfennig *et al*., 2010).

Plasticity is ubiquitous in nature and is arguably one of the basic features of life (Darwin, 1875; West-Eberhard, 2003; Nijhout, 2003). The notion of plasticity has a long history in the field of evolutionary biology, and yet its role in evolutionary processes remains controversial (Laland *et al*., 2014). Since the Modern Synthesis in the 1930-1940s, which combined the theory of evolution by natural selection with mendelian genetics through population genetics, much of evolutionary research has been focused on genes and selection as the sole force behind the evolution of adaptive traits (West-Eberhard, 2003; Sommer, 2009). In this framework genetic changes, which are random with respect to adaptation, work together with recombination to introduce selectable variation in natural populations, providing a substrate for natural selection. Adaptation is then the result of this accumulated genetic variation gradually modifying phenotype expression in a direction favored by selection. Under this set of assumptions, evolutionary processes, including the origin of novelties and phenotypically complex traits, can be explained through the change in allele frequencies of genes over time in populations under natural selection, and are subjected to Mendel's laws (Dobzhansky, 1937; Mayr, 1970).

Developmental biology was for the most part excluded from the Modern Synthesis, and so was phenotypic plasticity (Nicoglou, 2014). The environment had been seen just as a determinant of the direction of natural selection on genetically determined phenotypic variation, and development had been seen as the means by which genotypes were translated into phenotypes. Moreover, for a long time environmental sensitivity had been regarded as a source of instability and noise in genetics and was avoided whenever possible (Bradshaw, 2006). A result of this aversion to environmental stability was a tendency to work on model organisms showing little plasticity in expressed phenotypes of interest, and under controlled laboratory conditions. Likewise, systemic mutations that result in substantial body plan rearrangements (Goldschmidt, 1940) were largely ignored. Indeed, such practices of focusing on population genetics helped to formalize

evolutionary theory and achieve a quantitative understanding of the two major processes of evolution: adaptation and speciation (West-Eberhard, 2003). However, by prioritizing non-plastic traits and by leaving out the environment, the role of environmental sensitivity of development in evolutionary processes has been underrated for almost a century.

One of the early concepts that connected developmental biology and genetics was the concept of reaction norms. The term was first introduced by Woltereck (1909) to describe the plastic phenotypic reactions of *Daphnia* in continuously varying traits in response to an environmental change. Reaction norms gave support to the gradualist view of evolution, and also provided empirical evidence for an uncoupling of phenotype from genotype, as proposed by Johannsen (1911). Later, the concept of reaction norms was further developed and popularized by Dobzhansky (1955) and Schmalhausen (1949), who were interested in understanding the link between genotype and phenotype (see Schlichting and Pigliucci, 1998; Sarkar, 1999; and Nicoglou, 2014 for review). The norm of reaction is an expression curve of a single phenotype for a particular genotype, as a function of an environmental variable. In his experiments with *Drosophila*, Dobzhansky found that some mutant phenotypes were expressed only under certain culture conditions (Dobzhansky, 1937). Based on this finding, he suggested that genetic mutation does not change the trait, but instead modifies the reaction norm of that trait, and it is the particular reaction norm to the environmental stimulus that is inherited (Dobzhansky, 1937). Schmalhausen took the idea of the reaction norm and developed it further. He made a clear distinction between adaptive and non-adaptive norms of reaction. The former were related to the mechanism of evolution proposed by Baldwin in his paper “A new factor in evolution” (1896), later known as the Baldwin effect. According to Schmalhausen, an initial adaptive phenotypic response to a new environmental condition is followed by shifts in the reaction norm, specifically in the direction of the environmental change due to selection on genetic variation, if the shift in the environmental condition persists. Non-adaptive

modifications were inherent plastic reactions that had no historical context, i.e. when the organism experienced a totally new environment or were caused by a genetic disruption of a reaction norm (Schmalhausen, 1949). Unlike non-adaptive reactions, adaptive reaction norms are objects of natural selection, and can be canalized through a process of "stabilizing selection" (*sensu* Schmalhausen), which eventually restricts reaction norms within definite limits, appropriate for a particular stable environment (Schmalhausen, 1949; Pigliucci, 2010). A similar concept, known as genetic assimilation, was developed by Waddington (1942). According to Waddington, an initial plastic response to a shift in an environmental condition can be replaced by a genetic change that results in a similar phenotype, which should persist even in the absence of the environmental trigger. Genetic assimilation could occur through selection acting on previously hidden genetic variation or novel mutations. Using *Drosophila* as a model system, Waddington was able to experimentally demonstrate the phenomenon of genetic assimilation. In his experiments, a heat shock-induced Crossveinless phenotype became genetically fixed in a population after several rounds of selection for this heat shock-induced trait (Waddington, 1952). In an attempt to connect genetics, development, and evolution, Waddington developed the concept of epigenetic landscapes. Under this concept, both new genetic mutations and new environmental conditions can cause perturbations in development and are restricted (canalized) by the valleys of the epigenetic landscape. During genetic assimilation, a new trajectory is created that canalizes an initially anomalous response to a new environment or mutation (Waddington, 1974; West-Eberhard, 2003).

Although Waddington (1952) and others have presented clear evidence of genetic fixation of acquired characteristics using artificial selection experiments (Dworkin, 2005; Suzuki and Nijhout, 2006), the question of whether or not such processes also occur in populations under natural conditions remains controversial (Hall, 1992, Laland *et al*., 2014). Indeed, as some authors have pointed out, there is a fundamental difficulty in

distinguishing between character evolution by genetic assimilation and selection on genetic variants, because the outcome of both processes is essentially the same, and it might be possible to observe genetic assimilation only as it occurs, effectively under experimental conditions (Hall, 1992; Pigliucci and Murren, 2003; Pigliucci, 2010). Despite significant progress in the first part of the 20th century in bringing genetics, development, and evolution closer together, genes were still viewed as a blueprint for development. For example, in Waddington's epigenetic landscape metaphor, genes entirely specify the shape of the epigenetic landscape, which appears as a rigid construction, with the environment acting only as an external force that pushes development toward alternative genetically specified paths, but not changing the landscape itself (West-Eberhard, 2003). This notion was challenged by several in the next generation of biologists.

In the second half of the 20th century, multiple lines of evidence accumulated to suggest a larger role of phenotypic plasticity in evolution. Bradshaw (1965) emphasized the importance of environmental input in the determining of phenotypes. Using an optimality model to explain the evolution of plasticity, he argued that genetic control of trait plasticity is independent of the genetic control of the trait itself (Bradshaw, 1965; Nicoglou, 2014). This notion promoted further studies on genetic control of plasticity, which lead to the discovery of two major types of control: allelic sensitivity, which manifests as developmental modulation, and genes that act as regulators of plasticity in a switch-like manner. A debate started about whether phenotypic plasticity is a byproduct of selection acting on character states expressed in different environments (Via, 1993), or whether plasticity is a trait upon which natural selection can act directly (Scheiner, 1993a; Schlichting and Pigliucci, 1998; Nicoglou, 2014 and 2015). Later, the debate was partially regarded as semantic, as the two possibilities are not mutually exclusive (West-Eberhard, 2003), and with the discovery of several plasticity genes the controversy was resolved in favor of the latter opinion.

In her monograph *Developmental plasticity and evolution* Mary-Jane West-Eberhard (2003) developed a conceptual framework for a new extended evolutionary synthesis that would include development along with genes and environment. In this framework, the emphasis is put on phenotypes and not on genes: “genes are followers, not necessarily leaders, in phenotypic evolution” (West-Eberhard, 2003). Phenotypic and genetic accommodations play a central role in the process of adaptive evolution, according to West-Eberhard. She suggested that adaptive evolution occurs in four steps:

1. Trait origin. An environmental input or genetic mutation affects an aspect of a phenotype, causing it to change.

2. Phenotypic accommodation. Multiple aspects of the phenotype mutually adjust to the change, due to inherent plasticity. This immediate phenotypic response is likely to be adaptive.

3. Initial spread. Recurrence of the initiating factor (i.e. environmental change or mutation) produces a subpopulation of individuals that express the novel phenotype. In case of environmental induction, many individuals in the population are affected at the same time, providing more substrate for future selection.

4. Genetic accommodation. If the phenotype is advantageous, selection acting on a new or already existing genetic variation can fix it. Unlike genetic assimilation, genetic accommodation can result in either a decrease or an increase of environmental sensitivity.

Thus, both environment and mutations can contribute to a trait change, and this change is always followed by a multidimensional plastic response, which involves mutual adjustment of multiple phenotype aspects and is likely to be adaptive because it is based on ancestral adaptive plasticity (Pigliucci, 2010). Consequently, phenotypic variation, upon which natural selection can act, is not random in respect to adaptation, although the factors that underline this variation (i.e. environmental change and mutations) can be random. The most important role of mutation, according to West-Eberhard, is the long-term

storage of genetic variation rather than contribution to the origin of phenotypic novelties (West-Eberhard, 2003).

1.1.2.2 Alternative phenotypes

Continuous plasticity is universal in nature and can be observed at all levels of organismal organization, from single molecules to organisms and their behavior. Sometimes, however, plasticity is discrete, whereby the organisms express only alternative phenotypes with no intermediate forms. The most common form of discontinuous phenotypic plasticity is a dimorphism. The numerous examples of dimorphisms include commodore butterflies, which have seasonal color dimorphism (McLeod, 1968; Brakefield and Larsen, 1984), solitary and gregarious forms of the migratory locust (Nijhout, 1999), normal and protective morphs in *Daphnia* (Tollrian, 1995), and small- and large-horned male dung beetles (Moczek, *et al*., 2006). The degree of phenotypic difference between alternative phenotypes frequently exceeds that observed between genetically isolated populations of one species, different species of the same genus, and even species of different nominal genera. Often favored by a high degree of interspecific competition, polyphenisms help to partition ecological niches between individuals of the same population that otherwise would have been each other's strongest competitors (West-Eberhard, 2003). Among other factors that favor discrete plasticity are a highly variable but predictable environment, which changes slow proportionate to the lifespan of individuals, equal strength of selection across environments, availability of the phenotype-determining environmental cue that is correlated with the environment, and low cost of plasticity (Scheiner, 1993b).

Once induced by a mutation or environmental changes, alternative phenotypes have the potential to evolve semi-independently and in contrasting directions. Because expression of alternative phenotypes is conditional, they will always experience different sets of selective pressures, which fosters optimization of their phenotypes, sometimes resulting in forms

that have drastic differences in morphology and behavior. Moreover, unlike in the case of genetic variation, unfavorable conditions for one of the conditional alternatives does not need to result in its rapid elimination due to selection pressure; instead it can be protected from negative selection by conditional expression of the second phenotypic alternative for one or more generations. When the alternative is not expressed, it experiences relaxed selection, which allows genetic variation to accumulate, and when conditions are suitable for it, the alternative can be expressed again by many individuals in a population and be subjected to a strong positive selection. Such oscillating selection permits maintenance of both alternatives through facultative expression and environment matching, simultaneously favoring specialization of both phenotypes. Finally, it is argued that alternative phenotypes permit evolution of large-scale discontinuous adaptive novelties on a microevolutionary scale, by allowing rapid jumps between adaptive peaks without a need to cross the adaptive valley, as it would be necessary in case of standard gradual evolution (West-Eberhard, 1986, West-Eberhard, 2003). In contrary to a whidespread opinion that substantial phenotypic evolution is associated with periods of speciation (Eldredge and Gould, 1972; Gould and Eldredge, 1977; Orr and Smith, 1998), examples of polyphenic species show that extreme phenotypic divergence is possible with no genetic diversification at all.

1.1.2.3 Phenotype fixation and developmental character release

Although a high degree of dissimilarity between alternative phenotypes can be achieved, they are nonetheless expressed by the same genotype, and therefore their development cannot completely dissociate. Namely, non-specific modifiers of development shared by alternative phenotypes limit the degree of independent specialization that can be achieved, a phenomenon known as genetic correlation (West-Eberhard, 2003). Alternative phenotypes compete for their non-specific modifiers. Establishing a change in non-specific modifiers that favors only one form is expected only when that form is expressed at a very high frequency. If one alternative is expressed more

often, it will also experience more selective pressure, which might result in a greater degree of specialization. Eventually, one of the alternatives might be expressed all the time, or become fixed in a population, whereas the second alternative can be completely lost. The process of phenotype fixation is expected to be accompanied by developmental character release, whereby release from genetic correlations allows greater degree of specialization and at faster evolutionary rates. Character release simultaneously increases selection pressure on the phenotype due to its more frequent expression, and gives non-specific phenotype modifiers more freedom to specialize in the direction of the fixed phenotype (West-Eberhard, 2003).

1.1.2.4 Role of plasticity in evolution

In summary, there are several ways for developmental plasticity to affect evolution (discussed in West-Eberhard, 2003; Wund, 2012; Pfennig *et al*., 2010, Nijhout, 2015). First, plasticity increases the likelihood of a phenotypic change being adaptive, and, because of phenotypic accommodation, plasticity allows simultaneous coordinated change in many traits, which can lead to an adaptive or at least non-disruptive phenotype, and therefore may contribute to the evolution of complex novelties. Second, a plastic response to an environmental change helps to overcome suboptimal conditions, and therefore decreases the chance of lineage extinction; in addition, plasticity allows exploration of new environments. Third, plasticity facilitates the accumulation and release of genetic variation. Plastic responses both buffer the effect of new genetic variants and hinder the effect of negative selection on genetic variants in a non-inducing environment. Accumulated cryptic genetic variation can be released due to a new external (environmental) or internal (mutation) input and be used as material for genetic accommodation. Fourth, environmental induction affects the phenotypes of many individuals in a population at the same time, increasing the chance of the genetic accommodation of the novel phenotype. Finally, plasticity permits directional change under an oscillating selective pressure via evolution of alternative phenotypes. Moreover, developmental partitioning and semi-independent

evolution of alternative phenotypes allows specialization in contrasting directions and rapid jumps between adaptive peaks. It is argued that polyphenic stages contributed to major evolutionary transitions such as the evolution of photosynthesis, endosperm, early metazoan evolution, and terrestrial locomotion in tetrapods (West-Eberhard, 2003; Alegado *et al*., 2012; Standen *et al*., 2014).

Developmental plasticity still causes a lot of controversy among evolutionary biologists. Can the mainstream "gene-centric" theory accommodate processes associated with developmental plasticity? Or is a new extended evolutionary synthesis needed that would recognize developmental processes as a "creative element"? This remains a matter of debate (Laland *et al*., 2014; Pigliucci and Finkelman, 2014). It is clear, however, that empirical studies are needed to understand the role of plasticity in evolution as well as to test the outcomes and processes predicted by differing evolutionary theories. Two open questions specifically need to be addressed: whether and how ancestral plasticity affects the nature of phenotypic diversity, and whether genetic accommodation and developmental character release occur (Pfennig *et al*., 2010; Laland *et al*., 2014; West-Eberhard, 2003).

1.1.3 Evolutionary radiations and organismal interactions

Interactions between organisms modulate patterns of biodiversity. In host-symbiont systems, a long history of tight associations can give rise to codivergence, whereby the diversification of the associates tracks that of their hosts (Fig. 1). Sequences of successive codivergence events may lead to congruent phylogenetic histories of interacting taxa. Examples of systems where this phenomenon has been observed include gophers and lice, birds and lice, and figs and fig wasps (Hafner and Page, 1995; Hughes *et al*., 2007; Gruaud *et al*., 2012). In each of these examples, remarkable diversity of the symbionts is assumed to be a result of evolutionary radiation of their hosts. Factors that affect codivergence are: (i) transmission mode of symbionts within hosts' population, (ii) ability to disperse to a novel host, (iii) patterns of

host distribution, and (iv) adaptation of the symbiont to a particular host (Clayton *et al*., 2004). It is expected that vertical transmission of the symbionts, inability to disperse to a novel host, and coadaptation all facilitate parallel speciation. On the contrary, syntopy of the hosts and the absence of adaptation to a particular host make host switching more likely to happen.

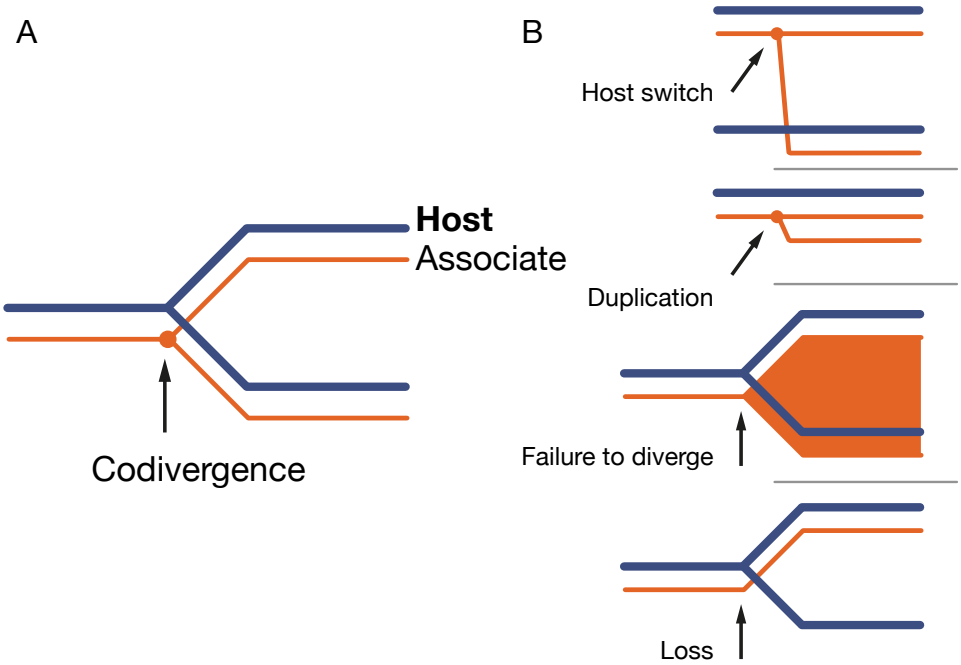

Figure 1.

Historical events that shape patterns of host-symbiont associations.

(**A**) When associates are transmitted vertically within populations of hosts, host speciation can lead to consequent speciation of the associates. Series of such events can result in phylogenetic histories of ecologically related organisms mirroring each other. (**B)** Host shifts, symbiont speciation without that of the host, failure to diverge, and symbiont loss can obscure patterns of codivergence. Modified from https://sites.google.com/site/cophylogeny/

Tight symbioses are of interest because they allow inferences about processes of diversification while also providing ecological and historical contexts for the studies of species adaptation to a well-defined environment. Nematodes are both species rich and broadly characterized by associations with plant and animal hosts. However, little is known about the forces that drive nematode speciation in such systems. Studies have shown that host switching is common among parasitic nematodes and a few cases of codivergence were observed in the nematode symbionts of insects (Giblin-

Davis *et al*., 2004). Mechanistic understanding of how isolation and specialization impact evolutionary radiation in systems with stable and highly specific relationships can be achieved when associations are amenable to direct observation and experimental manipulation.

1.1.4 Integrative approach in evolutionary biology

In an attempt to understand evolutionary processes, researchers in the field came to realize that the integration of multiple areas of biology is needed (Sommer, 2009). It is possible to bridge the gaps between population genetics, developmental biology, ecology, and behavioral studies with the novel model organisms now available and with revised research agendas. Recent technological advances, especially in sequencing technologies, genome-editing tools, and computational biology, have made it possible to carry out in-depth mechanistic studies on a wide range of organisms. At the same time, researchers working on classical genetic model organisms are expanding their studies by integrating approaches from adjacent disciplines, such as developmental biology and evolutionary ecology. The greatest advances can be achieved by focusing on systems that permit mechanistic studies (on genes and development) as well as microevolutionary, macroevolutionary and ecological observations.

Taxonomy is the basis for any macroevolutionary study. Only with deep taxon sampling and rigorous observations on phenotypes (including developmental mechanisms) is it possible to make evolutionary inferences. In the last two decades, taxonomic studies have been greatly facilitated by the introduction of molecular barcoding and molecular phylogenetic techniques, especially in the groups of organisms where the number of morphological characters useful for species delimitation is small. This has resulted not only in the discovery of a large number of cryptic species, which otherwise would have been hard or impossible to distinguish one from another, but also in a simplified and streamlined process for taxon sampling in various groups of organisms including bacteria, fungi, and nematodes (Herrmann *et al*., 2006a;

Félix *et al*., 2014). Moreover, a broad use of molecular phylogenetics has promoted the development of comparative phylogenetic techniques (Felsenstein, 1985; see Garamszegi, 2014 for review). The latter greatly expanded the repertoire of evolutionary methods, allowing the evolution of traits and genes to be traced (Huelsenbeck *et al*., 2003), investigating rates of character evolution in organism lineages (O'Meara *et al*., 2006; Eastman *et al*., 2011), as well as testing for correlation between characters in a phylogeny-informed manner (Felsenstein, 2012; Pagel and Meade, 2013).

1.2 Nematodes of Diplogastridae

The Diplogastridae are a nematode family characterized by the absence of valves (grinder) in the terminal bulb of the pharynx, an anisomorphic mouth (stegostom), dauer larvae that have oily, hydrophobic surfaces, three postembryonic stages, the absence of four cephalic sensillae in females and hermaphrodites, and the unique arrangement of male papillae. The monophyly of the group is supported by both morphological characters (Sudhaus and Fürst von Lieven, 2003) and molecular phylogenetic studies (Mayer, 2009). The family belongs to the paraphyletic group Rhabditina *sensu* Sudhaus (2011), and currently consists of 37 genera and more than 350 species (Giblin-Davis and Kanzaki, 2015).

The life cycle of diplogastrid nematodes includes four juvenile stages, separated by four molts (Fig. 2). Unlike in the majority of free-living nematodes, the first molt in Diplogastridae happens within the egg (Fürst von Lieven, 2005). Nematodes of Diplogastridae can either go through the direct cycle, or form dauer juveniles. The latter is a diapause larval stage, which helps the nematodes to survive harsh conditions and disperse. Although the direct life cycle of *P. pacificus* and many other diplogastrids can be completed within four days, the indirect cycle can take much longer, for dauer juveniles can survive for several months, and up to one year in *P. pacificus* (Mayer and Sommer, 2011).

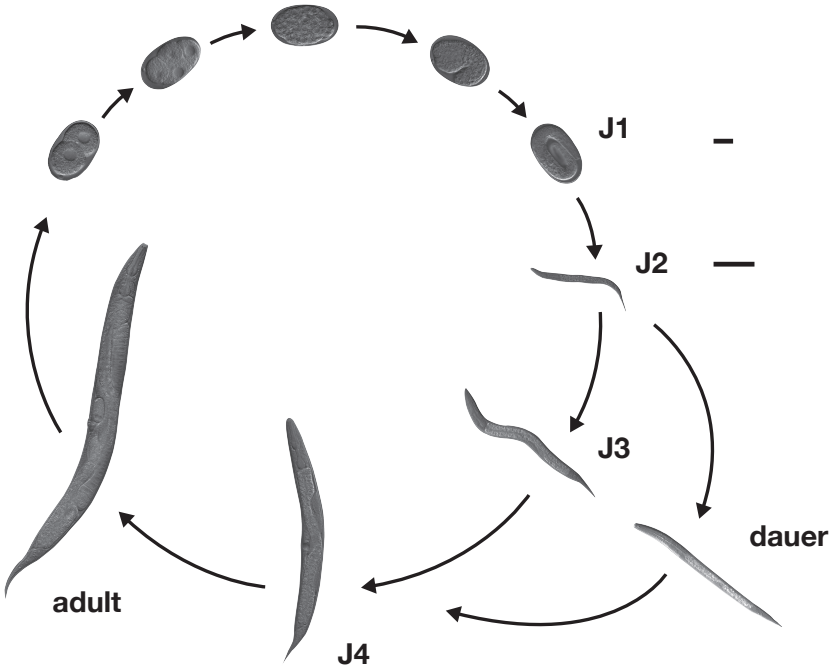

Figure 2.

Life cycle of *Pristionchus pacificus*.

P. pacificus and other nematodes of Diplogastridae have four juvenile stages, separated by molts. The first molt occurs inside the egg. Under harsh conditions, nematodes can form dauer juveniles, which can survive for several months and be transmitted by insect vectors. Scale bars: 20 µm for embryonic and 100 µm for post-embryonic stages. Pictures courtesy of Metta Riebesell.

Diplogastrid nematodes show a huge diversity of feeding structures (Fürst von Lieven and Sudhaus, 2000; Sudhaus and Fürst von Lieven, 2003). The most remarkable feature of diplogastrid nematodes is the presence of movable opposing teeth. The dental apparatus is typically represented by a large claw-like dorsal tooth, right subventral tooth, and a serrated plate on the left subventral side. Nematodes of Diplogastridae can use these structures to predate upon other nematodes, as well as for feeding on fungal spores and hyphae. Movable teeth are a novelty of Diplogastridae and have expanded the nematodes' food repertoire in comparison with strictly microbivorous nematodes of Rhabditidae, and as a consequence have allowed the colonization of new habitats.

1.2.1 Mouth dimorphism

Many species of Diplogastridae can express two alternative mouth phenotypes (Fürst von Lieven and Sudhaus, 2000). In the model organism *Pristionchus pacificus* and other diplogastrid species the alternatives are represented by “narrow-mouthed” stenostomatous (St) and “wide-mouthed” eurystomatous (Eu) forms (Fig. 3 A and B). The forms differ in size, shape and number of teeth, and in complexity and sclerotization of mouth structures. Specifically, the Eu form of all dimorphic species is characterized by a larger stoma, large claw-like dorsal and subventral teeth, and stronger sclerotization of mouthparts than that of the St form. Often, qualitative differences in morphology exist as well. For example, the St form of many *Pristionchus* spp. completely lacks a subventral tooth; the number of peaks on the left subventral plate is always greater in Eu than in St individuals (Ragsdale *et al*. 2015). In all species with mouth dimorphism, the mouth forms are discrete, with no intermediate forms observed.

Frequent occurrence of the dimorphism in species of Diplogastridae makes it possible to use comparative phylogenetic methods to study how gain and loss of plasticity affect macroevolution. Easy culturing of most species provides an opportunity to study the adaptive value of plasticity and behavioral aspects of it under controlled laboratory conditions. An array of functional and genetic tools, which are available for *P. pacificus* helps to achieve a comprehensive mechanistic understanding of developmental processes associated with plasticity (Sommer *et al*., 1996; Sommer and Sternberg, 1996; Srinivasan *et al*., 2002; Dieterich *et al*, 2008; Schlager *et al*., 2009; Witte *et al*., 2015; see Sommer, 2015 for review). Hundreds of wild *P. pacificus* isolates, which are available to laboratory study and show substantial phenotypic and genotypic variation, make micoevolutionary studies possible (Herrmann *et al*., 2010; McGaughran *et al*., 2014). Finally, the short generation time of *P. pacificus* and related nematodes permits artificial evolution studies. Hence, nematodes of Diplogastridae represent an ideal

system for studying discontinuous phenotypic plasticity, its evolution, and its role in the evolution of novelties.

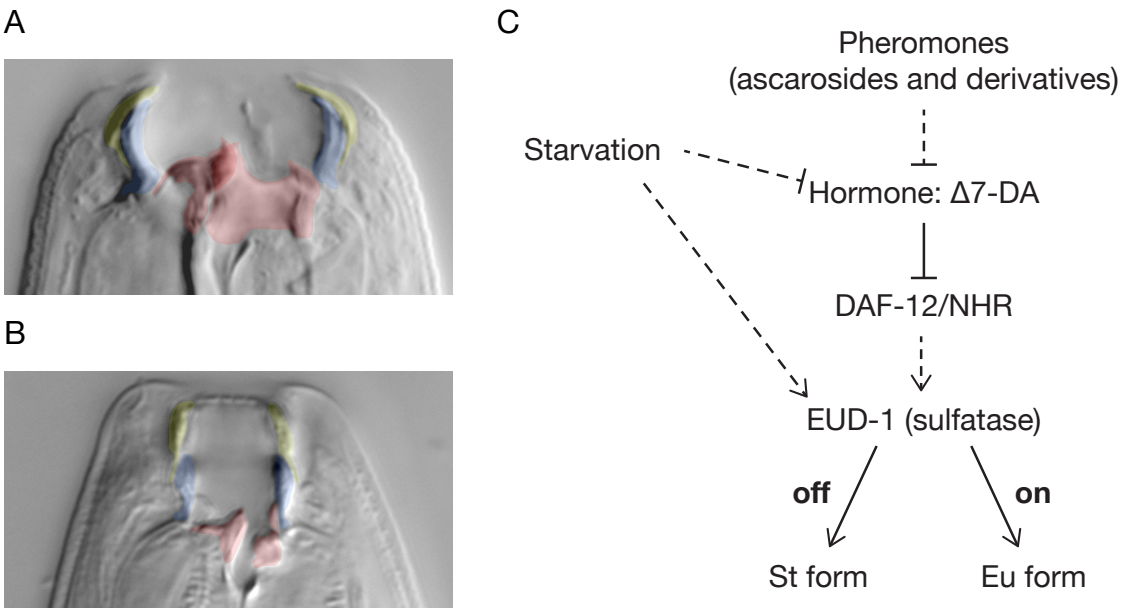

Figure 3.

Mouth dimorphism and its regulation.

(**A**) Eurystomatous (Eu) form of a diplogastrid nematode *Parapristionchus giblindavisi* is characterized by wide stoma and large opposing teeth. (**B**) *P. giblindavisi* Stenostomatous (St) form has narrow stoma and small teeth. False coloring marks individual compartments of the stoma (modified from Susoy *et al.*, 2015). (**C**) Model for the regulation of the mouth form development in *P. pacificus*. Starvation and nematode pheromones trigger expression of the Eu form through a sulfatase gene, which acts as a developmental switch (modified from Ragsdale, 2015).

1.2.2 Adaptive value of alternative mouth phenotypes

The mouth dimorphism of *Pristionchus* is a resource polyphenism, whereby phenotypic alternatives allow differential utilization of food and other resources. Experimental studies on behavior and development of Eu and St individuals of *P. pacificus* showed striking differences between the two forms in respect to resource use (Serobyan *et al*., 2013; Serobyan *et al*., 2014). Whereas Eu *P. pacificus* adults could predate on nematodes of other species, individuals that had the St mouth form showed almost no predatory behavior. However, when provided with abundant bacteria as food, St individuals completed their development faster than individuals that expressed the Eu phenotype. The latter could be explained by the St

phenotype demanding fewer resources for expression. Thus, both Eu and St phenotypes confer an adaptive advantage, but under different environmental conditions. When bacterial food is abundant, expression of the St mouth form allows faster development, and when microbial food is exhausted, expression of the Eu form enables alternative foods to be exploited, namely other nematodes.

1.2.3 Environmental induction of dimorphism

Induction of the two mouth phenotypes in species of Diplogastridae is influenced by environmental factors (Fig. 3C). Under standard laboratory conditions (i.e. nematodes cultured using *E. coli* strain OP50; no overcrowding or food deprivation are allowed), wild isolates of *P. pacificus* consist of 10 to 100 per cent St individuals (Ragsdale *et al*., 2013). It was shown that under starved conditions, nematodes of *P. pacificus* are more likely to become Eu than St (Bento *et al*., 2010). In addition, population density has an impact on mouth phenotype expression. Isolated individuals are more likely to express the St phenotype, whereas crowded conditions result in a high fraction of Eu individuals (Serobyan *et al*., 2013). Nematodes constantly secrete a large number of small molecules into their environment. Known as pheromones, some of these molecules play an important role in the regulation of the nematode life cycle and mating behavior (Butcher *et al*., 2007; Srinivasan *et al*., 2008; Pungaliya *et al*., 2009; Srinivasan *et al*., 2012). In *P. pacificus*, application of crude pheromone to nematode early larvae results in a high fraction of Eu form individuals in the population (Bento *et al*., 2010). A 2D NMR-spectroscopic screen of the *P. pacificus* exometabolome identified several small molecules that influence mouth phenotype development (Bose *et al*., 2012). Specifically, ascaroside derivatives dasc#1, pasc#9, and ascaroside ascr#1 strongly induce expression of the Eu form, while showing no effect on life cycle traits (i.e. dauer juvenile formation). In addition, nucleoside derivative npar#1 affects both plasticity and dauer formation, suggesting that dauer and dimorphism regulation partially overlap.

1.2.4 Genetic regulation of dimorphism

Developmental genetic studies in *P. pacificus* provided insight into the regulation of the mouth-form decision. Bento *et al*. (2010) showed that regulation of plasticity includes dafachronic acid (DA)-DAF-12 endocrine signaling module, which is conserved among nematodes and regulates dauer induction (Ogawa *et al*., 2009). Application of a steroidal hormone Δ7-dafachronic acid (DA), which is a ligand for the DAF-12 nuclear hormone receptor, resulted in a decrease in the Eu form in a concentration-dependent manner. Correspondingly, *Ppa-daf-12* mutant lines showed a lower fraction of Eu individuals, compared to wild type. Mutations in *Ppa-daf-12* and the application of Δ7-DA could suppress the effect of the *P. pacificus* crude pheromone on the mouth form frequency; however, they could not completely suppress the expression of the Eu phenotype, nor had they an effect on mouth-form frequency under starved conditions, suggesting that the DA-DAF-12 module does not act as a developmental switch.

Using a forward genetics approach, Ragsdale *et al*. (2013) identified a gene that acts as a developmental switch for the mouth dimorphism. The sulfatase-encoding gene *eud-1* is located on the X chromosome and is expressed in somatic and pharyngeal neurons, and is a specific regulator of plasticity (Fig. 3C). The effect of *eud-1* on the mouth phenotype is dosage dependent. Mutations in *eud-1* resulted in a complete loss of the Eu form. Individuals with only one functional copy of *eud-1* were more likely to express the Eu phenotype than individuals with no functional copy of *eud-1*, but less likely than the wild type. Overexpression of the wild type *eud-1* gene in a mutant background using multiple gene copies on an extrachromosomal array not only rescued the mutant phenotype but also resulted in 100% Eu individuals, a fraction higher than that of wild type. Similarly, overexpression of the gene in wild isolates with a high fraction of the St form, induced 100% Eu. Moreover, levels of expression of *eud-1* in the wild isolates of *P. pacificus* correlated with the St:Eu ratio. Treatment of *eud-1* mutants with pheromone dasc#1 showed no affect on the mouth form ratio, suggesting that

pheromone signaling acts through *eud-1*. Finally, application of Δ7-DA to the transgenic lines that overexpressed *eud-1* had no effect on the Eu frequency; thus, *eud-1* acts downstream or in parallel to the DA-DAF12 module. The function of *eud-1* is conserved between *P. pacificus* isolates and closely related species *P. exspectatus*. Phylogenetic analysis of *eud-1* homologs suggested that the *eud-1* gene originated from two duplications of an ancestral sulfatase gene. The first duplication happened in a lineage that included Diplogastridae, and the second in a lineage that included *Pristionchus*. Whether or not the X chromosome-linked sulfatase genes are always employed for regulation of dimorphism in different diplogastrid lineages still needs to be tested.

1.2.5 Ecology

Nematodes of Diplogastridae occupy a great number of habitats. First and foremost, diplogastrid species are often associated with insects. Many species of *Pristionchus* have a necromenic association with scarab and stag beetles (Herrmann *et al*., 2006 a,b); *Diplogasteriana* are exclusively found on *Nosodendron* (Paesler, 1939); genera *Parasitodiplogaster* and *Teratodiplogaster* live in obligate symbioses with fig wasps (Giblin-Davis *et al*., 2004; Giblin-Davis *et al*., 2006), and *Micoletzkya* and *Fuchsnema* with bark beetles (Rühm, 1956; Massey, 1974). *Koerneria* can be found in an association with stag beetles, and *Cephalobium* spp. and *Mehdinema* spp. are parasites of crickets. Although a dated phylogeny of Rhabditina would be necessary to test whether or not diversification of major diplogastrid lineages coincided with the evolutionary radiation of insects, it seems likely that at least at smaller evolutionary depths, radiation of diplogastrid genera was greatly influenced by that of their insect hosts, especially in those cases where the nematodes are transmitted vertically within hosts' populations (for example see Giblin-Davis *et al*., 2004). Another prominent habitat of many diplogastrids is dung, where multiple species of more than 7 different genera are found (Sudhaus and Fürst von Lieven, 2003), although in these instances insect associations are also possible or likely. Soil, fresh water, and rotten

plant material represent further sources of diplogastrid diversity. Finally, there are some rare cases of diplogastrid nematodes being associated with vertebrates. Examples include *Cutidiplogaster*, which was found on the skin of manatees (Fürst von Lieven *et al*., 2011), and species of *Longibucca*, which parasitize various tetrapods (Sudhaus and Fürst von Lieven, 2003). Taxon sampling in Diplogastridae, as well as in nematodes in general, is by no means complete. Recent systematic sampling attempts that targeted potential host insects resulted in discovery of many new species of Diplogastridae, particularly of the genus *Pristionchus* (Herrmann *et al*., 2006b; Kanzaki *et al*., 2012 a,b; Kanzaki *et al*., 2013 a,b) and several new genera (Kanzaki *et al*., 2012c; Herrmann *et al*., 2013; Ragsdale *et al*., 2014). It is therefore likely that rigorous examination of diverse habitats will result in the discovery of even greater number of diplogastrid taxa and their diverse ecological associations.

As discussed above, "the individual cannot be considered out of the context of its environment" (Bradshaw, 1965). One of the implications for the evolutionary studies of tight and specific associations observed in the family Diplogastridae is that they provide ecological context for the studies of adaptation. A small number of ecological interactions, compared to free-living nematodes, and a predictable environment in such systems as bark-beetle galleries and fig syconia, makes it possible to grasp most of the environmental complexity of such systems. Several studies have shown that not only do bark beetles and fig wasps have very consistent associations with animals (i.e. nematodes and mites), their associations with microbes and fungi are also very stable (Martinson *et al*., 2012; Hofstetter *et al*., 2015). Furthermore, codiversification (simultaneous diversification of two or more ecologically related lineages) and coevolution are expected when the associated organisms are vertically transmitted within populations of hosts. Therefore, examining such systems can open up an opportunity to look at the evolution of ecosystems.

1.3 Aims of this thesis

Explaining organismal diversity and adaptation are the two key goals of evolutionary biology. In this thesis, I address these questions using comparative phylogenetic approaches and nematodes of the family Diplogastridae as a study system. First, I conducted extensive sampling of diplogastrid nematodes, discovering many new or poorly known species, and introducing others to laboratory study. This served as the basis for consequent comparative evolutionary analyses. Second, I investigated forces that drive evolutionary radiation and speciation in a host-symbiont system, specifically in a diverse group of predatory nematodes associated with bark beetles. Finally, I studied developmental polyphenisms and their role in the macroevolution of complex phenotypic traits.

2. Results

2.1 Rapid diversification associated with a macroevolutionary pulse of developmental plasticity

V. Susoy, E.J. Ragsdale, N. Kanzaki, R.J. Sommer

eLife 4, e05463 (2015)

2.1.1 Synopsis

Developmental plasticity has been proposed to influence phenotypic evolution by facilitating adaptive change, but the macroevolutionary potential of plastic traits remained to be objectively tested. In this study, we focused on the evolution of feeding structures in a group of 90 nematodes, including *Pristionchus pacificus* and *Caenorhabditis elegans*, some species of which show a mouthpart dimorphism, moveable teeth, and predatory behavior. We first confirmed that the dimorphism where present was a polyphenism and not a genetic polymorphism. We then inferred history of the mouth dimorphism, which suggested that it evolved once and was lost multiple times. To test the effect of developmental plasticity on tempo of evolution, we measured the change in feeding structures using geometric morphometrics and structural complexity of the nematodes' stoma. Comparative analyses revealed a rapid process of diversification associated with evolution of plasticity. First, dimorphism was accompanied by a sharp increase in mouthpart complexity and elevated evolutionary rates, represented by a radiation of feeding-forms with structural novelties. Second, the subsequent fixation of a single phenotype coincided with a strong decrease in complexity but an even greater increase in rates of mouthpart evolution. Our results suggest that a macroevolutionary 'pulse' of plasticity promotes evolution of novelties, and even after the secondary fixation of phenotypes, historical presence of polyphenism permits sustained rapid evolutionary diversification.

2.1.2 Contributions

I designed the project, conducted all experimental work, and carried out data acquisition and analysis except tabulating complexity, which was done by Erik J. Ragsdale, who also contributed to project conception. Matthias Herrmann, Ralf J. Sommer, and Natsumi Kanzaki helped with nematode sampling. Natsumi Kanzaki created the original nematode drawings. The manuscript was prepared by Erik J. Ragsdale, Ralf J. Sommer, and me. I consider my contribution to this study to be approximately 80% of total work.

2.2 Large-scale diversification without genetic isolation in nematode symbionts of figs

V. Susoy, M. Herrmann, N. Kanzaki, M. Kruger, C.N. Nguyen, C. Rödelsperger, W. Röseler, C. Weiler, R.M. Giblin-Davis, E.J. Ragsdale, and R.J. Sommer

Science Advances ***2****, e1501031 (2016)*

2.2.1 Synopsis

Adaptive radiations produce biological diversity through ecological specialization associated with genetic diversification in multiplying lineages. Alternatively, specializations can arise from conditional expression of alternative phenotypes by a single genotype, but known examples are almost exclusively limited to dimorphism in nature. Here, we unveil an unprecedented case of adaptive radiation without genetic diversification. We show that upon colonizing the island-like micro-ecosystem of individual fig syconia, symbiotic nematodes of the genus *Pristionchus* have accumulated a polyphenism with up to five discrete eco-morphotypes per species. By integrating laboratory and field experiments with extensive genotyping of individuals, including the analysis of 49 genomes from a single species, we show that adaptive radiation, or the rapid filling of contrasting ecological niches can be based on discontinuous phenotypic plasticity, without diversifying selection on genotypes.

2.2.2 Contributions

I conducted all experimental work and carried out data acquisition and analysis except genomic data analysis, which was done by Christian Rödelsperger. Waltraud Röseler and Christian Weiler assisted with DNA sequencing. Matthias Herrmann, Meike Kruger, Chau N. Nguyen helped with nematode sampling. Natsumi Kanzaki did original nematode drawings. Ralf J. Sommer, Erik J. Ragsdale and I designed the project and wrote the manuscript. I consider my contribution to this study to be approximately 85% of total work.

2.3 Predatory feeding behaviour in *Pristionchus* nematodes is dependent on a phenotypic plasticity and induced by serotonin

M. Wilecki, J.W. Lightfoot, V. Susoy, R.J. Sommer

The Journal of experimental biology 218, 1306-1313 (2015)

2.3.1 Synopsis

Behavioral and morphological innovations are closely linked but their relationship is often scantily understood. Nematodes show a great diversity of feeding morphologies and behaviors to meet their ecological specializations. *Pristionchus* and their relatives display feeding activities that include consuming microbes and also predating other nematodes. Additionally, *Pristionchus* nematodes have an environmentally-induced mouth dimorphism triggered by a developmental switch. Through a mechanistic analysis of feeding behaviors, in particular in the model organism *P. pacificus*, we reveal two distinct feeding modes, which are different in pharyngeal rhythms and movement of the dorsal tooth. We found that the feeding mode switch is regulated by the neurotransmitter serotonin, which novel role appeared to be conserved across several predatory nematode species. We then investigated the effects of starvation, prey size and prey preference on *P. pacificus* predatory feeding, revealing predation to be an important component of the *Pristionchus* feeding repertoire thus providing an additional rich source of nutrition in addition to bacteria. Finally,

we found that mouth form has a strong impact on predation, with predatory behavior in the narrow mouthed (St) form being suppressed. Our results therefore provide insight into the regulation of predatory feeding and highlight *P. pacificus* as a model for understanding complex behavior evolution.

2.3.2 Contributions

I did mouth form phenotyping, phylogenetic analysis, and contributed to data analysis and study design. I consider my contribution to this study to be approximately 15% of total work.

2.4 Preferential host switching and codivergence shaped radiation of bark beetle symbionts, nematodes of *Micoletzkya* (Nematoda: Diplogastridae)

V. Susoy and M. Herrmann

Journal of evolutionary biology 27 (5), 889-898 (2014)

2.4.1. Synopsis

Host-symbiont systems are of interest to evolutionary biology because they permit inferences of speciation processes while also providing historical and ecological contexts for studies of adaptation. Species of the diplogastrid genus *Micoletzkya* have highly specific and stable symbiotic associations with bark beetles. In this study, we conducted a large-scale survey of bark beetles for the presence of *Micoletzkya* nematodes. Examination of more than 6,000 beetles of 85 species, mostly in Europe, North America, and Japan, resulted in the discovery of more than 450 *Micoletzkya* isolates. These isolates fell into 26 different putative species, majority of which showed remarkable host specificity. To test for parallel divergence between beetles and nematodes, we inferred multi-gene molecular phylogenies of *Micoletzkya* species and their corresponding hosts. Comparison of nematode and beetle phylogenies indicated that evolutionary history of bark beetles shaped that of the nematodes. However, the diversification of *Micoletzkya* could not be ascribed to parallel divergence alone. Our results indicate that preferential

host switching among closely related beetles also played a role. Whereas ecological and geographic isolation have modulated the diversification of *Micoletzkya* at shallow phylogenetic depths, adaptations towards related hosts have shaped cophylogenetic structure at a larger evolutionary scale.

2.4.2 Contributions

I designed the project, conducted sampling and experimental work, carried out data acquisition and analysis, and prepared the manuscript. Matthias Herrmann helped with sampling and contributed to project design. I consider my contribution to this study to be approximately 90% of the total work.

2.5 Validation of *Rhabditolaimus* Fuchs, 1914 (Nematoda: Diplogastridae) supported by integrative taxonomic evidence

V. Susoy and M. Herrmann

Nematology 14 (5), 595-604 (2012)

2.5.1 Synopsis

Taxonomic classification is useful where it mirrors the phylogenetic relationships of those taxa, as it can then serve to structure comparative analyses. Although current phylum-wide classifications of the nematodes are based on molecular phylogenetic evidence (De Ley and Blaxter, 2002; Hodda, 2007), finer-scale classification in groups is often still troubled by a reliance on typological characters, some of which are still indecisive due to plesiomorphy. Here, we apply morphology-independent tests to the systematic reorganization of diplogastrid nematodes. Among Diplogastridae, *Diplogasteroides sensu* Sudhaus and Fürst von Lieven (2003) is one of the few genera for which no synapomorphies have been identified, and morphology of some species of the genus casted doubt about its monophyly. Specifically, *Rhabditolaimus leuckarti*, the type species of the genus *Rhabditolaimus* Fuchs, 1914, which was later synonymized with *Diplogasteroides* (Sudhaus and Fürst von Lieven, 2003) showed morphology similar to species of another diplogastrid genus *Myctolaimus* (*sensu* Sudhaus

and Fürst von Lieven, 2003). We sampled individuals of *Hylobius abietis* (Coleoptera: Curculionidae), a type host of the type species of the genus *R. leuckarti* in central Europe. We then isolated *R. leuckarti*, and using phylogenetic inference showed that indeed it is closely related to species of *Myctolaimus*. Based on this and morphological evidence we propose to (i) reject all previous synonimisations of *Rhabditolaimus* and regard it as a valid nominal genus within Diplogastridae, (ii) transfer five species from *Diplogasteroides* to *Rhabditolaimus*, and (iii) consider *Myctolaimus sensu lato* as a junior synonym of *Rhabditolaimus*.

2.5.2 Contributions

I acquired, analyzed, and interpreted data and prepared the manuscript. Matthias Herrmann helped with sampling and contributed to project design and writing the manuscript. I consider my contribution to this study to be approximately 90% of total work.

2.6 Description of the bark beetle associated nematodes *Micoletzkya masseyi* n. sp. and *M. japonica* n. sp. (Nematoda: Diplogastridae)

V. Susoy, N. Kanzaki, and M. Herrmann

Nematology 15 (2), 213-231 (2013)

2.6.1 Synopsis

Diplogastrid nematodes of the genera *Micoletzkya* and *Fuchsnema* have specific associations with bark beetles (Coleoptera: Scolytidae). Over a course of a large-scale screening of bark beetles for the presence of symbiotic nematodes we obtained hundreds of nematode isolates, many of which could not be assigned to any previously known species. In this paper we describe two new nematode species as *Micoletzkya masseyi* and *M. japonica*, which were isolated from their beetle hosts, *Orthotomicus caelatus* and *Dryocoetes uniseriatus* in Canada and Japan respectively. The new species could be distinguished from all previously described species of *Micoletzkya* by morphology and specific ecological associations. We provide

detailed morphological and molecular characterization of the species, their life hystory, mouth dimorphism, and the first phylogeny of the genus.

2.6.2 Contributions

I acquired, analyzed, and interpreted data and prepared the manuscript. Natsumi Kanzaki helped with sampling and contributed to data acquisition. I assert my contribution to this study to be approximately 95% of total work.

2.7 *Leptojacobus dorci* n. gen., n. sp. (Nematoda: Diplogastridae), an associate of *Dorcus* stag beetles (Coleoptera: Lucanidae)

N. Kanzaki, E.J. Ragsdale, V. Susoy, and R.J. Sommer
Journal of nematology 46 (1), 50-59 (2014)

2.7.1 Synopsis

Many nematodes of Diplogastridae have phoretic, necromenic, and parasitic associations with insects. Therefore, insects represent a potential source of undocumented diplgogastrid diversity. Systematic examination of stag beetles (Coleoptera: Lucanidae) in particular revealed several new species of the genera *Pristionchus* and *Parapristionchus*. In this article we report a new species of diplogastrid nematodes from a stag beetle *Dorcus rectus* and assign it to a new nematode genus, based on morphological and phylogenetic evidence. Phylogenetic inferences suggested that a new genus might be an outgoup to all other known diplogastrid genera. Therefore, discovery of this taxon is valuable for understanding of the phylogenetic diversity and evolution of novelties in the diplogastrid family, particularly evolution of complex feeding structures and mouth polyphenisms.

2.7.2 Contributions

I contributed to sampling and study design, conducted sequencing and phylogenetic inference, and did microscopy and acquisition of morphological data. I consider my contribution to this study to be approximately 20% of the total work.

2.8 Two androdioecious and one dioecious new species of *Pristionchus* (Nematoda: Diplogastridae): new reference points for the evolution of reproductive mode

N. Kanzaki, E.J. Ragsdale, M. Herrmann, V. Susoy, and R.J. Sommer

Journal of nematology 45 (3), 172-194 (2013)

2.8.1 Synopsis

Androdioecious reproduction, which involves hermaphrodites and males, is found in few animal taxa, including rhabditid nematodes. There are several known cases of androdioecy in the genus *Pristionchus*, including the model nematode species *P. pacificus*. To understand the evolution of reproductive mode, dense taxon sampling, thorough morphological observation, and phylogenetic reconstruction are necessary. In this paper, we describe two new androdioecious species, *P. boliviae* n. sp. and *P. mayeri* n. sp., and one gonochoristic outgroup, *P. atlanticus* n. sp., based on morphological, molecular, and biological evidence. Phylogenetic relationships for the new and previously described species suggest that the new androdioecious species are sister taxa, indicating either speciation from an androdioecious ancestor or rapid convergent evolution of androdioecy in closely related species. Sexual characters of males distinguish the new species, and we present new morphological characters diagnosing six closely related *Pristionchus* species. Congruent with the predictions of "selfing syndrome", male papillae are remarkably variable in *P. boliviae* n. sp. and *P. mayeri* n. sp. In summary, description and phylogeny of new androdioecious species set up new reference points for mechanistic studies in the *Pristionchus* system by expanding its comparative evolutionary context.

2.8.2 Contributions

I did intraspecific and hybrid crosses, and genotyping of all males obtained as a result of these crosses. I consider my contribution to this study to be approximately 15% of the total work.

3. References

R. A. Alegado, L. W. Brown, S. Cao, R. K. Dermenjian, R. Zuzow, S. R. Fairclough, J. Clardy, N. King, A bacterial sulfonolipid triggers multicellular development in the closest living relatives of animals. *eLife* **1**, e00013 (2012).

J. M. Baldwin, A new factor in evolution. *The American Naturalist* **30**, 536-553 (1896).

G. Bento, A. Ogawa, R. J. Sommer, Co-option of the hormone-signalling module dafachronic acid-DAF-12 in nematode evolution. *Nature* **466**, 494-497 (2010).

N. Bose, A. Ogawa, S. H. von Reuss, J. J. Yim, E. J. Ragsdale, R. J. Sommer, F. C. Schroeder, Complex small-molecule architectures regulate phenotypic plasticity in a nematode. *Angewandte Chemie* **124**, 12606-12611 (2012).

A. D. Bradshaw, Evolutionary significance of phenotypic plasticity in plants. *Advances in Genetics* **13**, 115-155 (1965).

A. D. Bradshaw, Unraveling phenotypic plasticity–why should we bother? *New Phytologist* **170**, 644-648 (2006).

P. M. Brakefield, T. B. Larsen, The evolutionary significance of dry and wet season forms in some tropical butterflies. *Biological Journal of the Linnean Society* **22**, 1-12 (1984).

D. Brawand, C. E. Wagner, Y. I. Li, M. Malinsky, I. Keller, S. Fan, O. Simakov, A. Y. Ng, Z. W. Lim, E. Bezault, The genomic substrate for adaptive radiation in African cichlid fish. *Nature* **513**, 375-381 (2014).

R. A. Butcher, M. Fujita, F. C. Schroeder, J. Clardy, Small-molecule pheromones that control dauer development in *Caenorhabditis elegans*. *Nature Chemical Biology* **3**, 420-422 (2007).

D. H. Clayton, S. E. Bush, K. P. Johnson, Ecology of congruence: past meets present. *Systematic Biology* **53**, 165-173 (2004).

A. Cruaud, N. Rønsted, B. Chantarasuwan, L. S. Chou, W. L. Clement, A. Couloux, B. Cousins, G. Genson, R. D. Harrison, P. E. Hanson, An extreme case of plant–insect codiversification: figs and fig-pollinating wasps. *Systematic Biology* **61**, 1029-1047 (2012).

C. Darwin, *The variation of animals and plants under domestication*. (O. Judd & company, New York, 1868).

P. De Ley, M. L. Blaxter, in *The biology of nematodes,* D. L. Lee, Ed. (Taylor and Francis, London, 2002), pp. 1-30.

C. Dieterich, S. W. Clifton, L. N. Schuster, A. Chinwalla, K. Delehaunty, I. Dinkelacker, L. Fulton, R. Fulton, J. Godfrey, P. Minx, The *Pristionchus pacificus* genome provides a unique perspective on nematode lifestyle and parasitism. *Nature Genetics* **40**, 1193-1198 (2008).

T. Dobzhansky, *Genetics and the Origin of Species*. (Columbia University Press, New York, 1937).

T. Dobzhansky, *Evolution, genetics, and man*. (Wiley, New York, 1955).

I. Dworkin, A study of canalization and developmental stability in the sternopleural bristle system of *Drosophila melanogaster*. *Evolution* **59**, 1500-1509 (2005).

J. M. Eastman, M. E. Alfaro, P. Joyce, A. L. Hipp, L. J. Harmon, A novel comparative method for identifying shifts in the rate of character evolution on trees. *Evolution* **65**, 3578-3589 (2011).

M.-A. Felix, C. Braendle, A. D. Cutter, A streamlined system for species diagnosis in *Caenorhabditis* (Nematoda: Rhabditidae) with name designations for 15 distinct biological species. *PloS one* **9**, e94723 (2014).

J. Felsenstein, Phylogenies and the comparative method. *The American Naturalist* **125**, 1-15 (1985).

J. Felsenstein, A comparative method for both discrete and continuous characters using the threshold model. *The American Naturalist* **179**, 145-156 (2012).

G. Fuchs, Über Parasiten und andere biologisch an die Borkenkäfer gebundene Nematoden. 85. *Verhandlung der Gesellschaft Deutscher Naturforscher und Ärzte* **2**, 688-692 (1914).

L. Z. Garamszegi, *Modern phylogenetic comparative methods and their application in evolutionary biology*. (Springer, Berlin, 2014).

R. M. Giblin-Davis, K. A. Davies, G. S. Taylor, W. K. Thomas, in *Nematology, Advances and Perspectives,* Z. X. Chen, S. Y. Chen, D. W. Dickson, Eds. (Tsing-Hua University Press/CABI, New York, 2004), pp. 493-540.

R. M. Giblin-Davis, W. Ye, N. Kanzaki, D. Williams, K. Morris, W. K. Thomas, Stomatal ultrastructure, molecular phylogeny, and description of *Parasitodiplogaster laevigata* n. sp. (Nematoda: Diplogastridae), a parasite of fig wasps. *Journal of Nematology* **38**, 137 (2006).

R. Goldschmidt, *The material basis of evolution*. (Yale University Press, New Jersey, 1940).

N. E.-S. J. Gould, in *Models in Paleobiology,* T. J. M. Schopf, Ed. (Freeman, Cooper and Company, San Francisco, 1972), pp. 82-115.

S. J. Gould, N. Eldredge, Punctuated equilibria: the tempo and mode of evolution reconsidered. *Paleobiology* **3**, 115-151 (1977).

M. S. Hafner, R. D. Page, Molecular phylogenies and host-parasite cospeciation: gophers and lice as a model system. *Philosophical Transactions of the Royal Society B: Biological Sciences* **349**, 77-83 (1995).

B. K. Hall, Waddington's legacy in development and evolution. *American Zoologist* **32**, 113-122 (1992).

M. Herrmann, S. Kienle, J. Rochat, W. E. Mayer, R. J. Sommer, Haplotype diversity of the nematode *Pristionchus pacificus* on Réunion in the Indian Ocean suggests multiple independent invasions. *Biological Journal of the Linnean Society* **100**, 170-179 (2010).

M. Herrmann, W. E. Mayer, R. J. Sommer, Sex, bugs and Haldane's rule: the nematode genus *Pristionchus* in the United States. *Frontiers in Zoology* **3**, 1-15 (2006a).

M. Herrmann, W. E. Mayer, R. J. Sommer, Nematodes of the genus *Pristionchus* are closely associated with scarab beetles and the Colorado potato beetle in Western Europe. *Zoology* **109**, 96-108 (2006b).

M. Herrmann, E. J. Ragsdale, N. Kanzaki, R. J. Sommer, *Sudhausia aristotokia* n. gen., n. sp. and *S. crassa* n. gen., n. sp. (Nematoda: Diplogastridae): viviparous new species with precocious gonad development. *Nematology* **15**, 1001-1020 (2013).

M. Hodda, Phylum Nematoda. *Zootaxa* **1668**, 265-293 (2007).

R. W. Hofstetter, K. Klepzig, T. S. Davis, in *Bark Beetles: Biology and Ecology of Native and Invasive Species,* F. Vega, R. Hofstetter, Eds. (Elsevier, London, 2015), pp. 209-246.

J. P. Huelsenbeck, R. Nielsen, J. P. Bollback, Stochastic mapping of morphological characters. *Systematic Biology* **52**, 131-158 (2003).

J. Hughes, M. Kennedy, K. P. Johnson, R. L. Palma, R. D. Page, Multiple cophylogenetic analyses reveal frequent cospeciation between pelecaniform birds and *Pectinopygus* lice. *Systematic Biology* **56**, 232-251 (2007).

W. Johannsen, The genotype conception of heredity. *The American Naturalist* **45**, 129-159 (1911).

N. Kanzaki, R. M. Giblin-Davis, in Pristionchus pacificus*: A Nematode Model for Comparative and Evolutionary Biology,* R. J. Sommer, Ed. (Koninklijke Brill NV, Leiden, 2015), pp. 43-76.

N. Kanzaki, E. J. Ragsdale, M. Herrmann, W. E. Mayer, R. J. Sommer, Description of three *Pristionchus* species (Nematoda: Diplogastridae) from Japan that form a cryptic species complex with the model organism *P. pacificus*. *Zoological Science* **29**, 403-417 (2012a).

N. Kanzaki, E. J. Ragsdale, M. Herrmann, R. J. Sommer, Two new species of *Pristionchus* (Rhabditida: Diplogastridae): *P. fissidentatus* n. sp. from Nepal and La Réunion Island and *P. elegans* n. sp. from Japan. *Journal of Nematology* **44**, 80 (2012b).

N. Kanzaki, E. J. Ragsdale, M. Herrmann, W. E. Mayer, R. Tanaka, R. J. Sommer, *Parapristionchus giblindavisi* n. gen., n. sp. (Rhabditida: Diplogastridae) isolated from stag beetles (Coleoptera: Lucanidae) in Japan. *Nematology* **14**, 933-947 (2012c).

N. Kanzaki, E. J. Ragsdale, M. Herrmann, W. Röseler, R. J. Sommer, Two new species of *Pristionchus* (Nematoda: Diplogastridae) support the biogeographic importance of Japan for the evolution of the genus *Pristionchus* and the model system *P. pacificus*. *Zoological Science* **30**, 680-692 (2013a).

N. Kanzaki, E. J. Ragsdale, M. Herrmann, V. Susoy, R. J. Sommer, Two Androdioecious and One Dioecious New Species of *Pristionchus* (Nematoda: Diplogastridae): New Reference Points for the Evolution of Reproductive Mode. *Journal of Nematology* **45**, 172-194 (2013b).

N. Kanzaki, E. J. Ragsdale, V. Susoy, R. J. Sommer, *Leptojacobus dorci* n. gen., n. sp (Nematoda: Diplogastridae), an Associate of *Dorcus* Stag Beetles (Coleoptera: Lucanidae). *Journal of Nematology* **46**, 50-59 (2014).

K. Laland, T. Uller, M. Feldman, K. Sterelny, G. B. Müller, A. Moczek, E. Jablonka, J. Odling-Smee, G. A. Wray, H. E. Hoekstra, Does evolutionary theory need a rethink? *Nature* **514**, 161 (2014).

S. Lamichhaney, J. Berglund, M. S. Almén, K. Maqbool, M. Grabherr, A. Martinez-Barrio, M. Promerová, C.-J. Rubin, C. Wang, N. Zamani, Evolution of Darwin's finches and their beaks revealed by genome sequencing. *Nature* **518**, 371-375 (2015).

E. O. Martinson, E. A. Herre, C. A. Machado, A. E. Arnold, Culture-free survey reveals diverse and distinctive fungal communities associated with developing figs (*Ficus* spp.) in Panama. *Microbial Ecology* **64**, 1073-1084 (2012).

C. L. Massey, *Biology and taxonomy of nematode parasites and associates of bark beetles in the United States*. (Forest Service, US Dept. of Agriculture, Washington, DC, Washington, DC, 1974).

M. G. Mayer, R. J. Sommer, Natural variation in *Pristionchus pacificus* dauer formation reveals cross-preference rather than self-preference of nematode dauer pheromones. *Proceedings of the Royal Society of London B: Biological Sciences* **278**, 2784-2790 (2011).

W. E. Mayer, M. Herrmann, R. J. Sommer, Phylogeny of the nematode genus *Pristionchus* and implications for biodiversity, biogeography and the evolution of hermaphroditism. *BMC Evolutionary Biology* **7**, 104 (2007).

W. E. Mayer, M. Herrmann, R. J. Sommer, Molecular phylogeny of beetle associated diplogastrid nematodes suggests host switching rather than nematode-beetle coevolution. *BMC Evolutionary Biology* **9**, 212 (2009).

E. Mayr, *Populations, species, and evolution: an abridgment of animal species and evolution*. (Belknap Press of Harvard University Press, Cambridge, MA, 1970).

A. McGaughran, K. Morgan, R. J. Sommer, Environmental variables explain genetic structure in a beetle-associated nematode. *PLoS One* **9**, e87317 (2014).

L. McLeod, Controlled environment experiments with *Precis octavia* Cram (Nymphalidae). *J Res Lepidoptera* **7**, 1-18 (1968).

A. P. Moczek, T. E. Cruickshank, A. Shelby, When ontogeny reveals what phylogeny hides: gain and loss of horns during development and evolution of horned beetles. *Evolution* **60**, 2329-2341 (2006).

A. Nicoglou, in *Handbook of Evolutionary Thinking in the Sciences,* T. Heams, P. Huneman, G. Lecointre, M. Silberstein, Eds. (Springer Science, Dordrecht, 2014), pp. 285-318.

A. Nicoglou, The evolution of phenotypic plasticity: Genealogy of a debate in genetics. *Studies in History and Philosophy of Science Part C: Studies in History and Philosophy of Biological and Biomedical Sciences* **50**, 67-76 (2015).

H. F. Nijhout, Control Mechanisms of Polyphenic Development in Insects In polyphenic development, environmental factors alter some aspects of development in an orderly and predictable way. *Bioscience* **49**, 181-192 (1999).

H. F. Nijhout, Development and evolution of adaptive polyphenisms. *Evolution & development* **5**, 9-18 (2003).

H. F. Nijhout, To plasticity and back again. *eLife* **4**, e06995 (2015).

B. C. O'Meara, C. Ané, M. J. Sanderson, P. C. Wainwright, Testing for different rates of continuous trait evolution using likelihood. *Evolution* **60**, 922-933 (2006).

A. Ogawa, A. Streit, A. Antebi, R. J. Sommer, A conserved endocrine mechanism controls the formation of dauer and infective larvae in nematodes. *Current Biology* **19**, 67-71 (2009).

M. R. Orr, T. B. Smith, Ecology and speciation. *Trends in Ecology & Evolution* **13**, 502-506 (1998).

M. Pagel, A. Meade, BayesTraits v. 2.0. *Reading: University of Reading*, (2013).

D. W. Pfennig, M. A. Wund, E. C. Snell-Rood, T. Cruickshank, C. D. Schlichting, A. P. Moczek, Phenotypic plasticity's impacts on diversification and speciation. *Trends in Ecology & Evolution* **25**, 459-467 (2010).

M. Pigliucci, *Phenotypic plasticity: beyond nature and nurture*. (Johns Hopkins University Press, Baltimore, MD, 2001).

M. Pigliucci, in *Evolution-the extended synthesis,* M. Pigliucci, G. B. Müller, Eds. (MIT Press, Cambridge, MA, 2010), pp. 355-378.

M. Pigliucci, L. Finkelman, The Extended (Evolutionary) Synthesis Debate: Where Science Meets Philosophy. *BioScience* **64**, 511-516 (2014).

M. Pigliucci, C. J. Murren, C. D. Schlichting, Phenotypic plasticity and evolution by genetic assimilation. *Journal of Experimental Biology* **209**, 2362-2367 (2006).

C. Pungaliya, J. Srinivasan, B. W. Fox, R. U. Malik, A. H. Ludewig, P. W. Sternberg, F. C. Schroeder, A shortcut to identifying small molecule signals that regulate behavior and development in *Caenorhabditis elegans*. *Proceedings of the National Academy of Sciences* **106**, 7708-7713 (2009).

E. J. Ragsdale, in Pristionchus pacificus*: A Nematode Model for Comparative and Evolutionary Biology,* R. J. Sommer, Ed. (Koninklijke Brill NV, Leiden, 2015), pp. 301-329.

E. J. Ragsdale, N. Kanzaki, M. Herrmann, in Pristionchus pacificus*: A Nematode Model for Comparative and Evolutionary Biology,* R. J. Sommer, Ed. (Koninklijke Brill NV, Leiden, 2015), pp. 77-120.

E. J. Ragsdale, N. Kanzaki, R. J. Sommer, *Levipalatum texanum* n. gen., n. sp. (Nematoda: Diplogastridae), an androdioecious species from the south-eastern USA. *Nematology* **16**, 695-709 (2014).

E. J. Ragsdale, M. R. Müller, C. Rödelsperger, R. J. Sommer, A developmental switch coupled to the evolution of plasticity acts through a sulfatase. *Cell* **155**, 922-933 (2013).

W. Rühm, Die Nematoden der Ipiden. *Parasitologische Schriftenreihe* **6***,* 1-437 (1956).

S. Sarkar, From the Reaktionsnorm to the adaptive norm: the norm of reaction, 1909–1960. *Biology and Philosophy* **14**, 235-252 (1999).

S. M. Scheiner, Plasticity as a selectable trait: reply to Via. *The American Naturalist* **142**, 371-373 (1993a).

S. M. Scheiner, Genetics and evolution of phenotypic plasticity. *Annual Review of Ecology and Systematics* **24**, 35-68 (1993b).

B. Schlager, X. Wang, G. Braach, R. J. Sommer, Molecular cloning of a dominant roller mutant and establishment of DNA-mediated transformation in the nematode *Pristionchus pacificus*. *Genesis* **47**, 300-304 (2009).

C. D. Schlichting, M. Pigliucci, *Phenotypic evolution: a reaction norm perspective*. (Sinauer Associates Incorporated, Sunderland, MA, 1998).

D. Schluter, *The ecology of adaptive radiation*. Oxford series in ecology and evolution (Oxford University Press, Oxford, 2000).

I. I. Schmalhausen, *Factors of evolution: the theory of stabilizing selection*. (University of Chicago Press, Chicago, 1949).

V. Serobyan, E. J. Ragsdale, M. R. Müller, R. J. Sommer, Feeding plasticity in the nematode *Pristionchus pacificus* is influenced by sex and social context and is linked to developmental speed. *Evolution & Development* **15**, 161-170 (2013).

V. Serobyan, E. J. Ragsdale, R. J. Sommer, Adaptive value of a predatory mouth-form in a dimorphic nematode. *Proceedings of the Royal Society of London B: Biological Sciences* **281**, 20141334 (2014).

G. G. Simpson, *The major features of evolution*. (Columbia University Press, New York, 1953).

R. J. Sommer, L. K. Carta, S.-Y. Kim, P. W. Sternberg, Morphological, genetic and molecular description of *Pristionchus pacificus* sp. n. (Nematoda: Neodiplogasteridae). *Fundamental and Applied Nematology* **19**, 511-522 (1996).

R. J. Sommer, The future of evo–devo: model systems and evolutionary theory. *Nature Reviews Genetics* **10**, 416-422 (2009).

R. J. Sommer, in Pristionchus pacificus*: A Nematode Model for Comparative and Evolutionary Biology,* R. J. Sommer, Ed. (Koninklijke Brill NV, Leiden, 2015), pp. 19-41.

R. J. Sommer, P. W. Sternberg, Apoptosis and change of competence limit the size of the vulva equivalence group in *Pristionchus pacificus*: a genetic analysis. *Current Biology* **6**, 52-59 (1996).

J. Srinivasan, F. Kaplan, R. Ajredini, C. Zachariah, H. T. Alborn, P. E. Teal, R. U. Malik, A. S. Edison, P. W. Sternberg, F. C. Schroeder, A blend of small molecules regulates both mating and development in *Caenorhabditis elegans*. *Nature* **454**, 1115-1118 (2008).

J. Srinivasan, W. Sinz, C. Lanz, A. Brand, R. Nandakumar, G. Raddatz, H. Witte, H. Keller, I. Kipping, A. Pires-daSilva, A bacterial artificial chromosome-based genetic linkage map of the nematode *Pristionchus pacificus*. *Genetics* **162**, 129-134 (2002).

J. Srinivasan, S. H. Von Reuss, N. Bose, A. Zaslaver, P. Mahanti, M. C. Ho, O. G. O'Doherty, A. S. Edison, P. W. Sternberg, F. C. Schroeder, A modular library of small molecule signals regulates social behaviors in *Caenorhabditis elegans*. *PLoS-Biology* **10**, 147 (2012).

E. M. Standen, T. Y. Du, H. C. Larsson, Developmental plasticity and the origin of tetrapods. *Nature* **513**, 54-58 (2014).

W. Sudhaus, Phylogenetic systematisation and catalogue of paraphyletic "Rhabditidae" (Secernentea, Nematoda). *Journal of Nematode Morphology and Systematics* **14**, 113-178 (2011).

W. Sudhaus, A. F. von Lieven, A phylogenetic classification and catalogue of the Diplogastridae (Secernentea, Nematoda). *Journal of Nematode Morphology and Systematics* **6**, 43-89 (2003).

W. Sudhaus, D. Fitch, Comparative studies on the phylogeny and systematics of the Rhabditidae (Nematoda). *Journal of Nematology* **33**, 1 (2001).

V. Susoy, M. Herrmann, Validation of *Rhabditolaimus* Fuchs, 1914 (Nematoda: Diplogastridae) supported by integrative taxonomic evidence. *Nematology* **14**, 595-604 (2012)

V. Susoy, M. Herrmann, Preferential host switching and codivergence shaped radiation of bark beetle symbionts, nematodes of *Micoletzkya* (Nematoda: Diplogastridae). *Journal of Evolutionary Biology* **27**, 889-898 (2014).

V. Susoy, N. Kanzaki, M. Herrmann, Description of the bark beetle associated nematodes *Micoletzkya masseyi* n. sp and *M. japonica* n. sp (Nematoda: Diplogastridae). *Nematology* **15**, 213-231 (2013).

V. Susoy, E. J. Ragsdale, N. Kanzaki, R. J. Sommer, Rapid diversification associated with a macroevolutionary pulse of developmental plasticity. *eLife* **4**, e05463 (2015).

V. Susoy, M. Herrmann, N. Kanzaki, M. Kruger, C. N. Nguyen, C. Rödelsperger, W. Röseler, C. Weiler, R. M. Giblin-Davis, E. J. Ragsdale, R. J., Sommer. Large-scale diversification without genetic isolation in nematode symbionts of figs. *Science Advances* **2**, e1501031 (2016).

Y. Suzuki, H. F. Nijhout, Evolution of a polyphenism by genetic accommodation. *Science* **311**, 650-652 (2006).

R. Tollrian, Predator-induced morphological defenses: costs, life history shifts, and maternal effects in *Daphnia pulex*. *Ecology* **76**, 1691-1705 (1995).

J. D. Van Dyken, M. J. Wade, The genetic signature of conditional expression. *Genetics* **184**, 557-570 (2010).

S. Via, Adaptive phenotypic plasticity: target or by-product of selection in a variable environment? *The American Naturalist* **142**, 352-365 (1993).

A. F. von Lieven, The embryonic moult in diplogastrids (Nematoda)–homology of developmental stages and heterochrony as a prerequisite for morphological diversity. *Zoologischer Anzeiger - A Journal of Comparative Zoology* **244**, 79-91 (2005).

A. F. von Lieven, W. Sudhaus, Comparative and functional morphology of the buccal cavity of Diplogastrina (Nematoda) and a first outline of the phylogeny of this taxon. *Journal of Zoological Systematics and Evolutionary Research* **38**, 37-63 (2000).

A. F. von Lieven, S. Uni, K. Ueda, M. Barbuto, O. Bain, *Cutidiplogaster manati* n. gen., n. sp. (Nematoda: Diplogastridae) from skin lesions of a West Indian manatee (Sirenia) from the Okinawa Churaumi Aquarium. *Nematology* **13**, 51-59 (2011).

C. H. Waddington, Canalization of development and the inheritance of acquired characters. *Nature* **150**, 563-565 (1942).

C. H. Waddington, Selection of the genetic basis for an acquired character. *Nature* **169**, 625-626 (1952).

C. H. Waddington, A catastrophe theory of evolution. *Annals of the New York Academy of Sciences* **231**, 32-41 (1974).

M. J. West-Eberhard, Alternative adaptations, speciation, and phylogeny (a review). *Proceedings of the National Academy of Sciences* **83**, 1388-1392 (1986).

M. J. West-Eberhard, *Developmental plasticity and evolution*. (Oxford University Press, 2003).

D. W. Whitman, A. A. Agrawal, in *Phenotypic plasticity of insects: Mechanisms and Consequences,* D. W. Whitman, A. T. N., Eds. (Science Publishers, Inc, Enfield, N.H., 2009), pp. 1-63.

M. Wilecki, J. W. Lightfoot, V. Susoy, R. J. Sommer, Predatory feeding behaviour in *Pristionchus* nematodes is dependent on phenotypic plasticity and induced by serotonin. *Journal of Experimental Biology* **218**, 1306-1313 (2015).

H. Witte, E. Moreno, C. Rödelsperger, J. Kim, J.-S. Kim, A. Streit, R. J. Sommer, Gene inactivation using the CRISPR/Cas9 system in the nematode *Pristionchus pacificus*. *Development Genes and Evolution* **225**, 55-62 (2015).

R. Woltereck, Weitere experimentelle Untersuchungen über Artveränderung, speziell über das Wesen quantitativer Artunterschiede bei Daphnien. *Verhandlungen der Deutschen Zoologischen Gesellschaft* **19**, 110-173 (1909).

M. A. Wund, Assessing the impacts of phenotypic plasticity on evolution. *Integrative and Comparative Biology* **52**, 5-15 (2012).

F. Paesler, Massenvorkommen eines neuen Nematoden *Diplogaster schneideri* n. sp. im braunen Schleimfluß einer Roßkastanie. *Zoologische Zeitschrift* **126**, 138-140 (1939).

Vladislav Susoy

vladislav.susoy@tuebingen.mpg.de
DOB: 13.05.1986

Dep. of Integrative Evolutionary Biology
Max Planck Institute for Dev. Biology
Spemannstr. 37-39/IV
Tübingen, Germany 72076

EDUCATION

11/2009- Ph.D. candidate

Max Planck Institute for Developmental Biology,
Department of Integrative Evolutionary Biology,
Tübingen, Germany

Advisor: Prof. Ralf J. Sommer

Dissertation title: Developmental Plasticity, Ecology, and Adaptive Radiation of Nematodes of Diplogastridae

9/2007-7/2009 M.S. in Biological Sciences,
Ural State University, Faculty of Biology, Department of Zoology, Yekaterinburg, Russia

9/2003-6/2007 B.S. in Biological Sciences,
Ural State University, Faculty of Biology, Department of Zoology, Yekaterinburg, Russia

MAJOR RESEARCH INTERESTS

Phenotypic plasticity, behavior, neuroscience, molecular ecology, synthetic biology, evolution, nematodes.

LIST OF PUBLICATIONS

1. Susoy, V., Sommer, R. J. Stochastic and conditional regulation of nematode mouth-form dimorphisms. *Frontiers in Ecology and Evolution* (*in press*)

2. Susoy, V., Herrmann, M., Kanzaki, N., Kruger, M., Nguyen, C. N., Rödelsperger, C., Röseler, W., Weiler, C., Giblin-Davis, R. M., Ragsdale, E. J., Sommer, R. J. Large-scale diversification without genetic isolation in nematode symbionts of figs. *Science Advances* **2**, e1501031 (2016).

3. Susoy, V., Ragsdale, E. J., Kanzaki, N., Sommer, R. J. Rapid diversification associated with a macroevolutionary pulse of developmental plasticity. *eLife* **4**, e05463 (2015).

4. Wilecki, M., Lightfoot, J. W., Susoy, V., Sommer, R. J. Predatory feeding behaviour in *Pristionchus* nematodes is dependent on phenotypic plasticity and induced by serotonin. *Journal of Experimental Biology* **218**, 1306-1313 (2015).

5. Susoy, V., Herrmann, M. Preferential host switching and codivergence shaped radiation of bark beetle symbionts, nematodes of *Micoletzkya* (Nematoda: Diplogastridae). *Journal of Evolutionary Biology* **27**, 889-898 (2014).

6. Kanzaki, N., Ragsdale, E. J., Susoy, V., Sommer, R. J. *Leptojacobus dorci* n. gen., n. sp. (Nematoda: Diplogastridae), an associate of *Dorcus* stag beetles (Coleoptera: Lucanidae). *Journal of Nematology* **46**, 50-59 (2014).

7. Kanzaki, N., Ragsdale, E. J., Herrmann, M., Susoy, V., Sommer, R. J. Two androdioecious and one dioecious new species of *Pristionchus* (Nematoda: Diplogastridae): new reference points for the evolution of reproductive mode. *Journal of Nematology* **45**, 172-194 (2013).

8. Susoy, V., Kanzaki, N., Herrmann, M. Description of the bark beetle associated nematodes *Micoletzkya masseyi* n. sp. and *M. japonica* n. sp. (Nematoda: Diplogastridae). *Nematology* **15**, 213-231 (2013).

9. Susoy, V., Herrmann, M. Validation of *Rhabditolaimus* Fuchs, 1914 (Nematoda: Diplogastridae) supported by integrative taxonomic evidence. *Nematology* **14**, 595-604 (2012).

RESEARCH SKILLS

Laboratory skills: standard molecular lab techniques, genomic and RNA libraries preparation for the next generation sequencing, including development of low-input, single-nematode genomics and transcriptomics, DNA-mediated transformation via microinjection, reverse genetics using CRISPR/Cas9, brightfield, fluorescent, and scanning electron microscopy, fluorescent *in situ* hybridization (FISH), targeted and non-targeted metagenomics, nematode isolation and culturing, microbiology techniques. **Computational skills:** sequence analysis, phylogenetics, computational biology, and data analysis in R. **Soft skills:** project conception and design, supervision of Master's and first-year Ph.D. students.

MEETINGS AND CONFERENCES

Evolutionary Biology of *C. elegans* and Other Nematodes
Talk: "Evolutionary diversification through the gain and loss of plasticity", Hinxton, UK, 2014

Visions in Science
Max Planck Symposium, Berlin, Germany, 2014.

Max Planck Seminars
Talk: "A two-step process of evolutionary diversification associated with developmental plasticity", Tübingen, Germany, 2014.

Talk: "Radiation of beetles shaped diversification of symbiotic nematodes", Tübingen, Germany, 2013.

Meeting of the German Society of Nematology
Talk: “Evolutionary ecology of bark-beetle associated nematodes”, Berlin, Germany, 2012.

Max Planck Symposium Biodiversity, Berlin, Germany, 2012
German Society of General and Applied Entomology (DGaaE), Berlin, Germany, 2012 (talk).

International Symposium of the European Society of Nematologists, Vienna, Austria, 2010 (poster).

FIELD EXPERIENCE

2014, 2015, 2016 Field Station on Reunion Island. Collection of nematodes.
2013 Arizona. Collection of bark beetles and nematodes.
2010-2014 Multiple field trips in Germany. Collection of nematodes.

PROFESSIONAL REFERENCES

1. Dr. Ralf J. Sommer
   Director
   Department of Integrative Evolutionary Biology
   Max Planck Institute for Developmental Biology
   Tübingen, Germany
   Tel.: + 49 7071 601 371
   ralf.sommer@tuebingen.mpg.de

2. Dr. Erik J. Ragsdale
   Assistant Professor
   Department of Biology
   Indiana University
   IN 47405, USA
   Tel.: (812) 856-1946
   ragsdale@indiana.edu

3. Dr. Matthias Herrmann
   Group Leader
   Department of Integrative Evolutionary Biology
   Max Planck Institute for Developmental Biology
   Tübingen, Germany
   Tel.: + 49 7071 601 484
   matthias.herrmann@tuebingen.mpg.de

4. Dr. Robin Giblin-Davis
   Professor and Acting Center Co-Director
   Fort Lauderdale Research and Education Center
   University of Florida-IFAS
   Tel.: 954-577-6333
   giblin@ufl.edu

eLIFE elifesciences.org

SHORT REPORT

Rapid diversification associated with a macroevolutionary pulse of developmental plasticity

Vladislav Susoy[1], Erik J Ragsdale[1,2]*, Natsumi Kanzaki[3], Ralf J Sommer[1]*

[1]Department for Evolutionary Biology, Max Planck Institute for Developmental Biology, Tübingen, Germany; [2]Department of Biology, Indiana University, Bloomington, United States; [3]Forest Pathology Laboratory, Forestry and Forest Products Research Institute, Tsukuba, Japan

Abstract Developmental plasticity has been proposed to facilitate phenotypic diversification in plants and animals, but the macroevolutionary potential of plastic traits remains to be objectively tested. We studied the evolution of feeding structures in a group of 90 nematodes, including *Caenorhabditis elegans*, some species of which have evolved a mouthpart polyphenism, moveable teeth, and predatory feeding. Comparative analyses of shape and form, using geometric morphometrics, and of structural complexity revealed a rapid process of diversification associated with developmental plasticity. First, dimorphism was associated with a sharp increase in complexity and elevated evolutionary rates, represented by a radiation of feeding-forms with structural novelties. Second, the subsequent assimilation of a single phenotype coincided with a decrease in mouthpart complexity but an even stronger increase in evolutionary rates. Our results suggest that a macroevolutionary 'pulse' of plasticity promotes novelties and, even after the secondary fixation of phenotypes, permits sustained rapid exploration of morphospace.
DOI: 10.7554/eLife.05463.001

***For correspondence:** ragsdale@indiana.edu (EJR); ralf.sommer@tuebingen.mpg.de (RJS)

Competing interests: The authors declare that no competing interests exist.

Funding: See page 14

Received: 03 November 2014
Accepted: 03 February 2015
Published: 04 February 2015

Reviewing editor: Merijn R Kant, University of Amsterdam, Netherlands

Copyright Susoy et al. This article is distributed under the terms of the Creative Commons Attribution License, which permits unrestricted use and redistribution provided that the original author and source are credited.

Introduction

Developmental (phenotypic) plasticity has been proposed to affect evolution by facilitating adaptive change (***Pigliucci, 2001***; ***Schlichting, 2003***; ***West-Eberhard, 2003***; ***Moczek et al., 2011***) but the relevant processes resulting in evolutionary diversity remain elusive. Identification of a switch gene for a dimorphism recently confirmed the link between developmental switches and microevolutionary divergence (***Ragsdale et al., 2013***), although insights from genetic mechanisms have yet to be put into a macroevolutionary context. For example, whether plasticity accelerates evolution by allowing faster evolutionary responses (***Baldwin, 1896***; ***Waddington, 1953***; ***Suzuki and Nijhout, 2006***) or hinders it by allowing adaptation without the need for genetic assimilation (***Williams, 1966***) is still a matter of debate (e.g., ***de Jong, 2005***; ***Wund, 2012***). To know the macroevolutionary potential of developmental plasticity, objectively measured plastic traits must be compared by deep taxon sampling in a robust phylogenetic framework. Here, we test the role of developmental plasticity in evolutionary tempo and novelty by measuring change in feeding structures in a group of 90 nematodes, including *Caenorhabditis elegans*, of which some species show a mouthpart polyphenism, moveable teeth, and predatory feeding. As a result we identified both the gain and loss of a developmental dimorphism to be associated with rapid evolutionary diversification. We made the surprising finding that whereas the appearance of polyphenism coincided with increased complexity and evolutionary rates, these rates were even higher after the assimilation of a single phenotype.

The evolutionary and ecological success of nematodes is reflected by the extensive adaptation of their feeding structures, including hooks and stylets in animal- and plant-parasitic nematodes and

eLife digest Every animal and plant grows to a body plan that is defined by its genes. However, the body plan must be flexible enough to allow the organism to respond to whatever the world throws at it. This flexibility—known as developmental plasticity—allows an organism to change certain characteristics in order to survive in varying environmental conditions. For example, nerve cells in the brain need to be able to remodel to form memories.

It has been suggested that developmental plasticity can affect evolution because the ability to grow in different ways opens a diverse treasure trove of options from which to generate new forms and ways to exploit the environment. However, this potential had not previously been tested.

Susoy et al. looked at 90 species of roundworm that look different from one another, particularly in their mouths. Some of the worms have moveable teeth while others are simple and streamlined. Furthermore, of those examined, 23 species were found to be 'dimorphic' and have the ability to develop one of two types of mouth: either narrow or wide, depending on their prey.

Susoy et al. looked how similar the sequences of 14 genes were across all 90 species and used this information to build a family tree of how the roundworms are related to one another. Tracking which animals have dimorphic mouths on this tree produced an intriguing result: the strategy arose once in a single ancestor of the worms. Although this ability has been lost at least 10 times in the species that retained teeth, it has persisted in others through long periods of evolutionary time.

Next, Susoy et al. estimated the speed of evolution in these worms based on how quickly the characteristics of the worms' mouths had changed over evolutionary time. The gain of a dimorphic trait was associated with an increased rate of evolution and the appearance of many new species with diverse and more complex mouthparts. However, evolution was even faster where a dimorphism had been lost, even though the mouthparts generally became less complex.

Together, Susoy et al.'s findings demonstrate how developmental plasticity can introduce genetic diversity that can promote the evolution of new forms and species. The next challenges will be to find out how this genetic diversity is stored and released in the worms and to provide examples of the impact of environmental changes on developmental plasticity and shape.

DOI: 10.7554/eLife.05463.002

teeth in predatory species. The latter adaptation is found in the genetic model *Pristionchus pacificus* and other nematodes of the family Diplogastridae, in which cuticularized teeth and predation are sometimes associated with a dimorphism (***Fürst von Lieven and Sudhaus, 2000***). Dimorphic species execute either a 'narrow-mouthed' (stenostomatous, St) or 'wide-mouthed' (eurystomatous, Eu) morph, which differ in the size, shape, and complexity of their mouthparts (***Figure 1***). In *P. pacificus*, the St and Eu morphs are advantageous for feeding on bacteria and nematode prey, respectively (***Serobyan et al., 2013***, ***2014***). The dimorphism results from an irreversible decision during development, enabling a rapid optimization of morphology to the environment (***Bento et al., 2010***). This response is mediated by small-molecule pheromones (e.g., dasc#1, ascr#1) (***Bose et al., 2012***), endocrine signaling (dafachronic acid-DAF-12) (***Bento et al., 2010***), and a switch mechanism executed by the sulfatase EUD-1 (***Ragsdale et al., 2013***).

Results

To study the tempo and mode of evolution in nematode mouthparts, we analyzed 54 species of Diplogastridae, 23 of which we found to be dimorphic. The remaining 31 diplogastrid species were identified as monomorphic. We also analyzed 33 species of other Rhabditina (***De Ley and Blaxter, 2002***), which include *C. elegans* and the closest known outgroups of Diplogastridae (***Kiontke et al., 2007***; ***van Megen et al., 2009***). In contrast to Diplogastridae, all non-diplogastrid Rhabditina were monomorphic.

To test whether the dimorphism where present was a polyphenism, and not the result of genetic polymorphism (***Schwander and Leimar, 2011***), we exposed dimorphic species to cues potentially regulating their dimorphism. For assays we selected systematically inbred or genetically bottlenecked phylogenetic representatives. When exposed to signals of starvation, crowding, or the presence of nematode (*C. elegans*) prey, all species tested produced a higher number of Eu individuals in response ($p < 10^{-6}$, Fisher's exact test, for all induction experiments; ***Table 1***, ***Table 1—source data 1***). Thus, alternative conspecific morphs are the result of polyphenism across taxa of Diplogastridae.

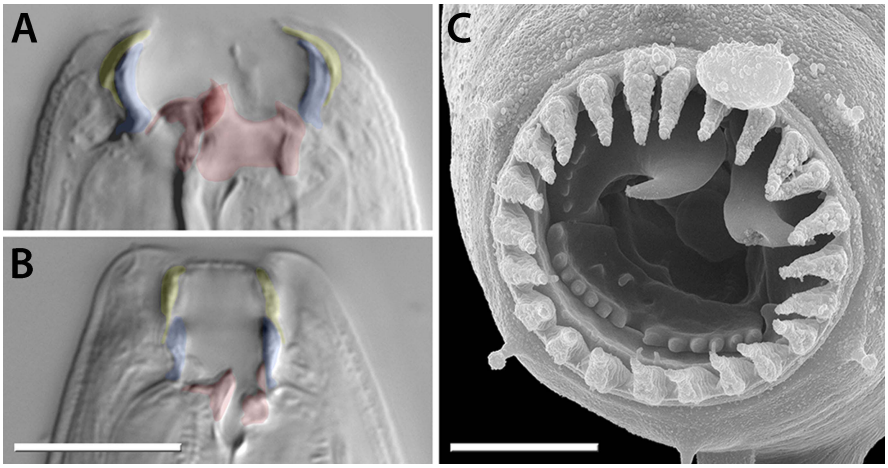

Figure 1. Mouth dimorphism and novelty in Diplogastridae. (**A**) The diplogastrid eurystomatous (Eu) morph, as shown here for *Parapristionchus giblindavisi*, is marked by a wider mouth, larger teeth, and often greater stomatal complexity than the stenostomatous (St) morph. (**B**) *P. giblindavisi*, St morph. False coloring in (**A** and **B**) indicates individual cuticular compartments of the mouth, providing a basis for tracking changes in homologous structures (yellow, cheilostom; blue, gymnostom; red, stegostom except telostegostom). View in (**A** and **B**) is right lateral and at same scale. Scale bar, 10 μm. (**C**) Opposing teeth, shown here for *Fictor* sp. 1, are a structural novelty of Diplogastridae and used for predatory feeding. Visible serrated plates are among other feeding innovations of Diplogastridae. Dorsal is right; scale bar, 5 μm.
DOI: 10.7554/eLife.05463.003

To determine the order and directionality of changes in mouthpart evolution, we inferred the phylogeny of Diplogastridae and outgroups using 14 genes in an alignment of 11,923 total and 6354 parsimony-informative sites (***Figure 2A***). Because our analysis included many taxa previously not analyzed by any molecular characters, newly inferred and highly supported relationships among taxa

Table 1. Environmental regulation of the mouth dimorphism across diplogastridae

Dimorphic nematode species	Treatment type	% Eu, treatment	% Eu, control	Odds ratio
Allodiplogaster sp. 1	Prey	100	0	
Allodiplogaster sudhausi	Prey	97	1	1080.976
Diplogasteriana n. sp.	Starved	24	0	
Fictor stercorarius	Prey	96	0	
Koerneria luziae	Starved	5	0	
Micoletzkya inedia	Prey	95	0	
Micoletzkya japonica	Prey	92	0	
Mononchoides sp. 1	Prey	98	10	120.272
Mononchoides sp. 3	Prey	100	6	
Neodiplogaster sp.	Prey	100	0	
Parapristionchus giblindavisi	Starved	34	6	8.428

The presence of prey nematode (*C. elegans*) larvae and the absence of bacterial food ('prey' treatment) induced development of the Eu morph in strains normally St-biased on an abundance of bacterial food (control). For species that could not reach adulthood on this regimen, conditions of overpopulation and starvation ('starved' treatment) similarly promoted the Eu morph. Effect size is given as the odds ratio (Fisher's exact test) where not infinite.
DOI: 10.7554/eLife.05463.004

Source data 1. Environmental induction of the Eu morph in dimorphic species. Results for individual replicates (plates) are shown.
DOI: 10.7554/eLife.05463.005

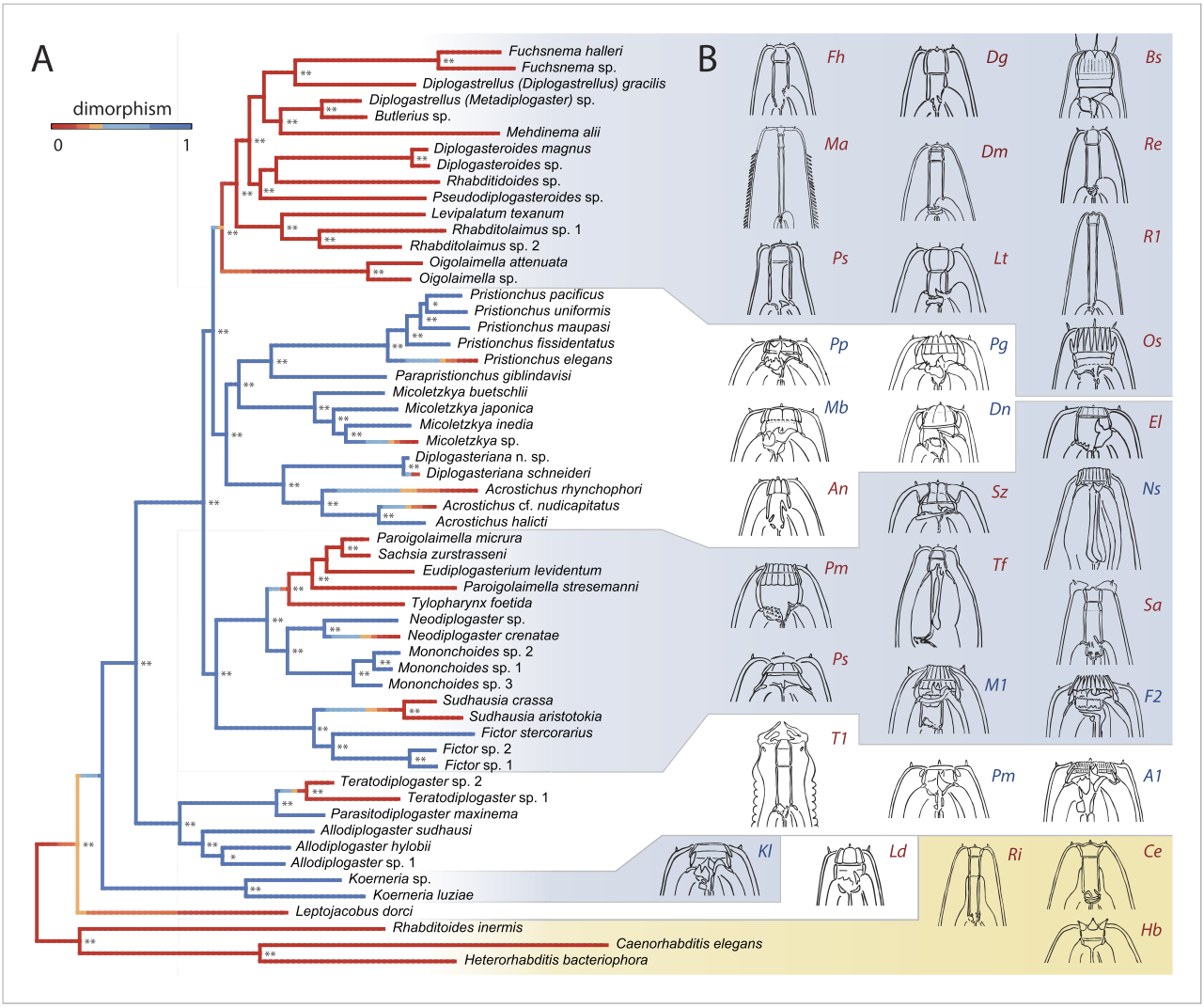

Figure 2. A radiation of feeding structures in diplogastrid nematodes. (**A**) Phylogenetic relationships inferred for nematodes of Rhabditina, including 54 species of Diplogastridae (***Figure 2—source data 1A,B***) from an alignment including SSU rRNA, LSU rRNA, and 11 ribosomal protein genes (for Diplogastridae, 468 kb excluding missing data), and RNA polymerase II. History of dimorphism inferred by stochastic character mapping on the set of sampled Bayesian posterior trees (consensus tree is shown). **100% posterior probability (PP); *99% PP. (**B**) Morphological diversity of mouthparts in Diplogastridae (light blue and white blocks), which are strikingly complex with respect to outgroups (yellow block). The origin of plasticity coincided with a radiation of complex feeding-forms, which variously include opposing teeth, bilateral asymmetry, and additional armature and articulations. In shape, form, and complexity, the mouths of outgroups (*Ri*, *Ce*, *Hb*) are more similar to the St than the Eu morph of dimorphic species. For dimorphic taxa, Eu morph is shown. Two-letter designations abbreviate Linnaean binomials of depicted species.

DOI: 10.7554/eLife.05463.006

The following source data is available for figure 2:

Source data 1. Nematode taxa used in this study, with isolation details given.

DOI: 10.7554/eLife.05463.007

allowed robust inferences of ancestral states. The inferred history of the mouth dimorphism revealed that it evolved once but was lost at least 10 times, and possibly 11 given the ambiguous position of *Leptojacobus dorci* (***Figure 2A***). Thus, the morphological diversity of diplogastrid mouthparts (***Figure 2B***) represents a radiation that accompanied the origin of polyphenism in those structures and involved many independent transitions to a monomorphic phenotype.

Next, we wanted to know whether the radiation of mouthparts in Diplogastridae that had dimorphism in their history represented a measurable increase in morphological variance with respect to outgroups. We quantified mouth morphology by recording 11 geometric landmarks

of the stoma that were considered homologous, as informed by fine-structural anatomy, across Diplogastridae and outgroups (**Baldwin et al., 1997**; **Ragsdale and Baldwin, 2010**) (**Figures 1A,B, 3A**). Analysis of landmark coordinates in Procrustes space for shape and form, the latter including shape + log-transformed centroid size (**Dryden and Mardia, 1998**; **Mitteroecker et al., 2004**), showed that non-diplogastrid Rhabditina occupy only a subset of the total morphospace colonized by Diplogastridae (**Figure 3A**, **Figure 3—figure supplement 1**, **Figure 3—source data 1A–D**). This represented greater disparity for Diplogastridae than for non-diplogastrid Rhabditina, whether disparity was measured as the sum of variances ($p < 10^{-5}$ when either St or both morphs represented dimorphic taxa) or by principal component analysis (PCA) volume (**Ciampaglio et al., 2001**) (**Figure 3B**, **Figure 3—source data 1E**). However, the disparity for either morph of dimorphic taxa was not different from that of non-diplogastrid Rhabditina. In contrast, diplogastrids that were secondarily monomorphic showed higher disparity than either morph in dimorphic taxa ($p < 0.02$ for both) (**Figure 3B**, **Figure 3—source data 1E**). Taken together, these findings show clear disparity differences between non-diplogastrid Rhabditina, dimorphic Diplogastridae, and secondarily monomorphic Diplogastridae.

We next tested if the observed morphospace occupation differences within Diplogastridae and across Rhabditina reflected shifts in evolutionary tempo, specifically with the gain or loss of the mouth polyphenism. Using the inferred phylogenies we measured the rate of change in shape and form (PC1) as a Brownian rate parameter under one-, two-, and three-rate parameter models (**O'Meara et al., 2006**). We found that the two-rate model that approximated different rate parameters for non-diplogastrid Rhabditina and Diplogastridae was favored over the single-rate model for both form ($\Delta AICc = 5.34$; $p = 0.01$, likelihood ratio test) and shape ($\Delta AICc = 11.71$; $p < 0.001$), with rates in Diplogastridae being higher (**Figure 3C,D**, **Figure 3—figure supplement 2**, **Figure 3—source data 1F,G**). Furthermore, a three-rate model that assumed a different rate parameter for each of the three nematode groups had the greatest fit compared with either a single-rate model ($\Delta AICc = 9.18$, $p = 0.038$ for form; $\Delta AICc = 14.79$, $p < 0.001$ for shape) or a model that assigned a different rate category to dimorphic diplogastrids ($\Delta AICc = 9.32$, $p < 0.01$ for form; $\Delta AICc = 15.27$, $p < 0.001$ for shape), and rates in monomorphic Diplogastridae were the highest (**Figure 3C**). For form evolution in particular, a two-rate model that assumed a different rate parameter for monomorphic Diplogastridae was a better fit than all other models, including that with a single category for Diplogastridae ($\Delta AICc = 5.23$). Congruent with these results, a comparison of posterior densities of rate estimates from the Bayesian sampling of a multirate Brownian-motion process (**Eastman et al., 2011**), which were extracted for individual nematode groups, indicated elevated rates of evolution in Diplogastridae relative to non-diplogastrid Rhabditina, with rates in secondarily monomorphic lineages being the fastest (**Figure 3—figure supplement 3**, **Figure 3—source data 1H**). Thus, our analyses of evolutionary rates show that diversification of shape and form in Diplogastridae increased with the appearance of the mouth plasticity but were highest after its subsequent loss.

We then wanted to know whether developmental plasticity also correlated with the complexity of mouthparts that distinguishes Diplogastridae from their closest relatives (**Figure 2B**). We tabulated complexity for all taxa by recording the number of stomatal structures or 'cusps', adapting a concept of complexity commonly applied to the dentition of vertebrates (**Harjunmaa et al., 2012**). Namely, we scored all structures or articulations that formed a $<135^{\circ}$ vertex with the wall of the stoma (**Figure 4—figure supplement 1**, **Figure 4—source data 1A**), summing the total to an index that was invariable for all specimens of a given species or, in dimorphic species, a particular morph (here, Eu). We then tested for phylogenetic correlations of this complexity index with the presence of plasticity. Plasticity was strongly correlated with greater complexity, as shown by their covariance tested either under the threshold model (**Felsenstein, 2012**) ($r = 0.78$, confidence interval 0.57–0.93) or a constant-variance random-walk model ($r = 0.45$; log Bayes factor = 20). Given the character histories of known taxa (**Figure 4**), this result reveals that the gain of the polyphenism was simultaneous with the onset of high complexity, including the origin of opposable teeth. In contrast, the loss of the polyphenism in monomorphic Diplogastridae was associated with a subsequent decrease in complexity.

Discussion

Our results provide original statistical and phylogenetic support for a role of developmental plasticity in evolutionary diversification. They are also congruent with a simple model for the role of plasticity in this process. First, the appearance of bimodal plasticity coincides with a burst of complexity and

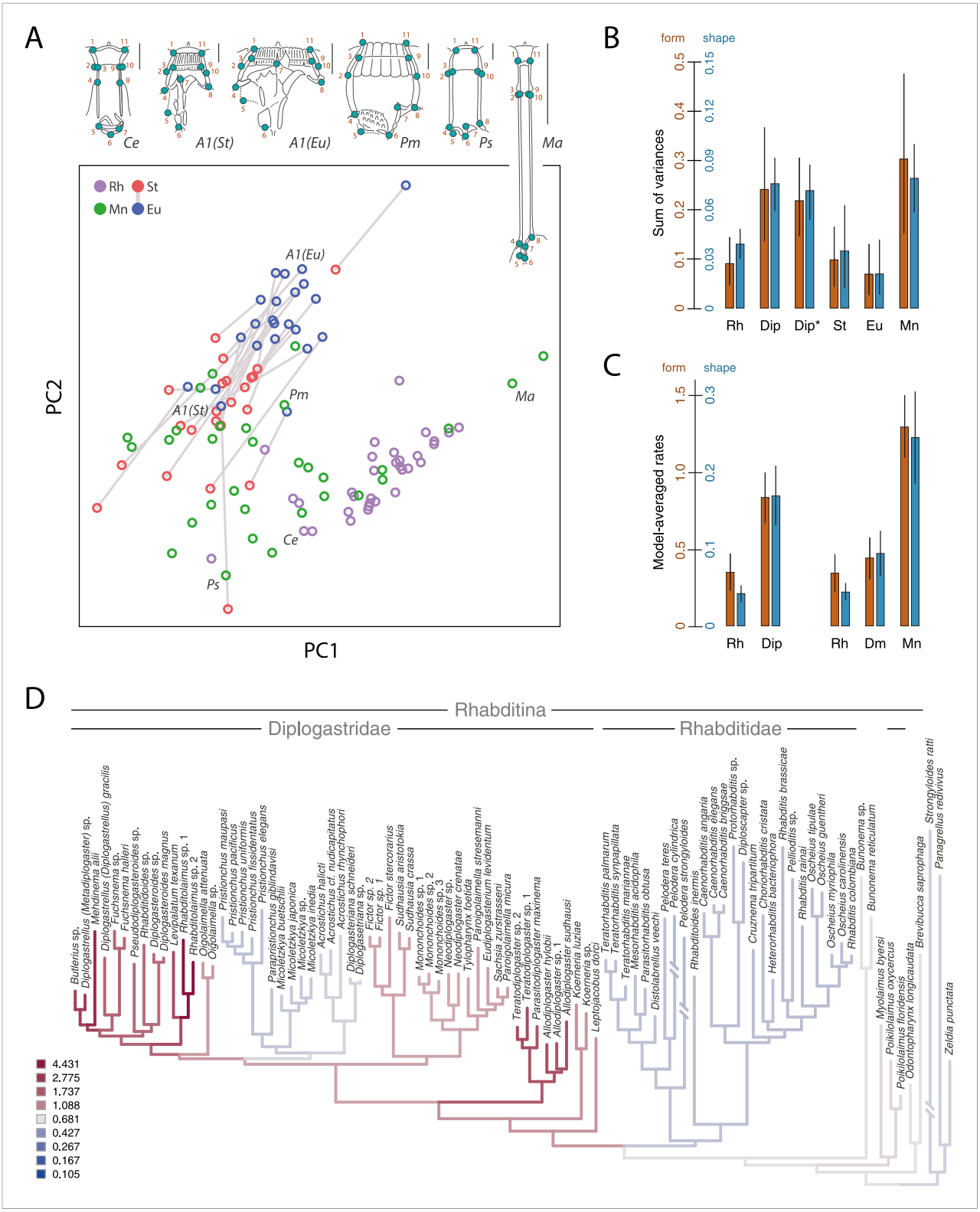

Figure 3. Developmental plasticity, morphological disparity, and evolutionary tempo in diplogastrid nematodes. (**A**) Stomatal morphology and positions of 11 two-dimensional landmarks (taxa coded in ***Figure 2***). Below is a projection of the first two principal components of stomatal shape-space. Purple circles represent non-diplogastrid Rhabditina (Rh), green circles mark monomorphic Diplogastridae (Mn); blue and red circles connected by lines mark St and Eu morphs, respectively, of dimorphic Diplogastridae. (**B**) Phenotypic disparity of non-diplogastrid Rhabditina (Rh), Diplogastridae (Dip, dimorphic taxa are represented by St morph; Dip*, by both morphs), and individually of St, Eu, and monomorphic (Mn) Diplogastridae, as estimated by the sum of

Figure 3. continued on next page

Figure 3. Continued

variances on shape- and form-space axes. Bars show mean values from 10,000 bootstrap replicates. Whiskers represent a 95% confidence interval. (**C**) Model-averaged relative estimates of evolutionary rates, as estimated under a Brownian motion model. Both a two-rate model (left) and a three-rate model (right) are shown (Dm, dimorphic Diplogastridae as represented by St morph). Bars are mean rates calculated across 5000 reconstructions of dimorphism history and 500 trees. Whiskers represent the standard deviation. (**D**) Rate estimates of stomatal form evolution in Rhabditina. In dimorphic taxa, rates are for St morph. Branch color indicates rates of evolutionary change; posterior rates are color-coded in legend.

DOI: 10.7554/eLife.05463.008

The following source data and figure supplements are available for figure 3:

Source data 1. Results from analyses of principle components, disparity, and evolutionary rates.

DOI: 10.7554/eLife.05463.009

Figure supplement 1. Projections of the first two principal components of Procrustes morphospace of stomatal landmarks.

DOI: 10.7554/eLife.05463.010

Figure supplement 2. Rate estimates of stomatal shape evolution in Rhabditina.

DOI: 10.7554/eLife.05463.011

Figure supplement 3. Posterior densities of rates of stomatal form and shape evolution in Rhabditina.

DOI: 10.7554/eLife.05463.012

increase in evolutionary tempo. By this model, developmental plasticity can facilitate novel structures and their associated developmental networks (***West-Eberhard, 2003***), as well as new complexity in behavioral or enzymatic function, thereby providing additional substrate for future selection. Following this macroevolutionary 'pulse' of plasticity, the secondary loss of plasticity is accompanied by a decrease in complexity but a strong acceleration of measured evolutionary rates, which in our study were most pronounced in form change. The surprising limitation of rates in dimorphic relative to secondarily monomorphic lineages might be explained in part by genetic correlation (***Cheverud, 1996***), or the inability of overlapping genetic programs controlling alternative phenotypes to completely dissociate. We speculate that, where correlated morphologies were initially governed by a dimorphism, assimilation of a single morph would then give the freedom for single phenotypes to specialize and diversify, a phenomenon proposed as developmental 'character release' (***West-Eberhard, 1986***).

A complementary means by which evolutionary rates increase after the loss of plasticity may be through the release of genetic variation built up as a by-product of relaxed selection (***Kawecki, 1994***; ***Snell-Rood et al., 2010***; ***Van Dyken and Wade, 2010***). This possibility might be realized through the following scenario. If populations experience fluctuating environments and alternative mouth morphologies confer fitness advantages in those environments, then environmental sensitivity (i.e., plasticity) will be maintained (***Moran, 1992***). The presence of plasticity necessarily leads to relaxed selection on genes underlying the production of either trait, particularly those downstream of a developmental switch, facilitating the accumulation of genetic variation (***Van Dyken and Wade, 2010***). If populations then encounter a stable, predictable environment, promoting the loss of plasticity (***Schwander and Leimar, 2011***), this variation can be selected and refined by constitutively exposing a single morph to that environment. This would allow more rapid evolution of novel phenotypes than would be possible through the generation and selection of new genetic variation (***Barrett and Schluter, 2008***; ***Lande, 2009***), thereby allowing rapid shifts to alternative niches such as novel diets (***Ledón-Rettig et al., 2010***). Combined with the ability of fixed morphs to more efficiently reach their fitness optima as permitted by character release, variation accumulated during periods of plasticity would thus enable rapid phenotypic specialization and diversification. Although accelerated rates of divergence due to built-up variation and character release should ultimately decline in monomorphic lineages (***West-Eberhard, 2003***; ***Lande, 2009***), the net result would be an extreme radiation of forms, as has occurred in diplogastrid nematodes.

In conclusion, the historical presence of polyphenism is strongly associated with evolutionary diversification. The degree to which the correlations observed are due to causation is presently unclear, although recent mechanistic advances in *P. pacificus* demonstrate the promise of functional genetic studies to test the causality of rapidly selected genes directly. Further work might also reveal that additional underlying causes, such as previously unseen ecological opportunities or selective pressures, may have jointly led to both complexity and plasticity. However, the simplicity of our results makes our proposed model sufficient to explain the observed correlations. We therefore hypothesize

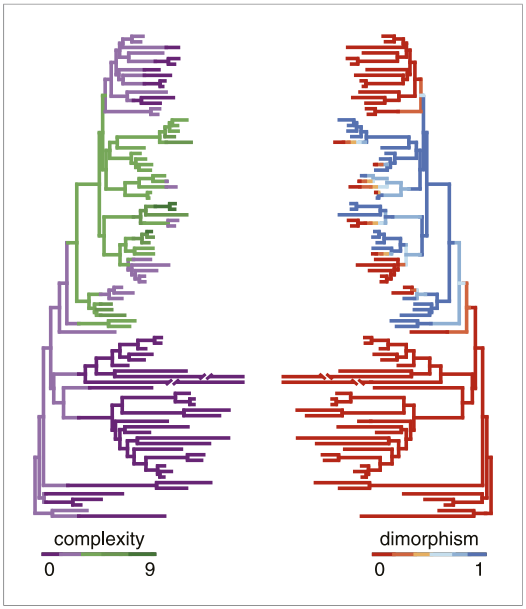

Figure 4. Correlation of polyphenism and complexity of nematode mouthparts. Painted branches show congruence of simulated character histories of dimorphism (right tree; 0 = absent, 1 = present) and stomatal complexity (left tree; complexity index ranges from 0 to 9). Covariance tests (see text) show that the apparent phylogenetic correlation between dimorphism and complexity is significant.

DOI: 10.7554/eLife.05463.013

The following source data and figure supplements are available for figure 4:

Source data 1. Matrix of structures tabulated to measure stomatal complexity.

DOI: 10.7554/eLife.05463.014

Figure supplement 1. Tabulating complexity of nematode mouthparts.

DOI: 10.7554/eLife.05463.015

that developmental plasticity is required to cross a threshold of complexity that affords the degrees of freedom necessary for further diversification of form, and even after the assimilation of monomorphy this diversification can continue to be realized. The difference in rates between ancestrally and secondarily monomorphic lineages suggest a deciding role for a history of plasticity in diversification. It is possible that the processes inferred to accompany the gain of plasticity apply also to other systems with taxonomically widespread polyphenism, which sometimes likewise show a general coincidence of plasticity and diversity (e.g., ***Emlen et al., 2005***; ***Pfennig and McGee, 2010***). In principle, the model we propose can be generalized to other systems through dense taxon sampling, a resolved phylogeny, and quantification of alternative morphologies.

Materials and methods

Nematodes

To investigate evolutionary rates, complexity, and character histories, we densely sampled nematodes of Rhabditina *sensu* ***De Ley and Blaxter (2002)*** (= Clade V *sensu* ***Blaxter et al., 1998***). Isolation details for all analyzed nematode taxa for which original sequence data were obtained are given in ***Figure 2—source data 1A***. Our taxonomic nomenclature follows previous systems (***Andrássy, 1984***, ***2005***; ***Sudhaus and Fürst von Lieven, 2003***) with additional genera described since those publications (***Ragsdale et al., 2014***). Our dataset included 54 species of Diplogastridae, in addition to 33 nematode species from all closest known outgroups to the family: 'Rhabditidae' sensu ***Sudhaus (2011)***, Brevibuccidae, Bunonematidae, Myolaimidae, and Odontopharyngidae. In the present study, 'non-diplogastrid Rhabditina' refers to the latter five families together. Rhabditidae were sampled such that they spanned all major clades of that group as identified in a previous study (***Kiontke et al., 2007***): the *Mesorhabditis* group and non-*Mesorhabditis* 'pleiorhabditids'; *Caenorhabditis*, the four deepest lineages of the *Rhabditis* group, and the remaining two deepest lineages of 'eurhabditids'; *Rhabditoides inermis*, a possible immediate outgroup to Diplogastridae; *Poikilolaimus*, the putative sister group to all other Rhabditidae and nested taxa. Three Clade IV (***Blaxter et al., 1998***) nematode species were included as outgroups in the dataset.

Phylogenetics

Dataset assembly

The phylogeny of Diplogastridae was inferred from concatenated alignments of 18S and 28S rRNA genes and 11 ribosomal protein-coding genes of 90 taxa. Genomic DNA was extracted from individual specimens and total RNA from 15–45 individuals per species (***Figure 2—source data 1B***). Genes of interest were amplified individually, and sequencing reactions were performed as previously described (***Mayer et al., 2009***). Sequences were assembled using Geneious 6.1.4. Sequences for 18S, 28S, ribosomal protein, and RNA polymerase II genes, which were either original in this study or retrieved from public databases, were included for non-diplogastrid Rhabditina and outgroups. 18S

and 28S rRNA sequences were aligned using the E-INS-I algorithm and default settings in MAFFT 7.1 (**Katoh and Standley, 2013**). Alignments were manually refined, and poorly aligned regions were eliminated manually. Alignments of 18S and 28S rRNA genes were 1598 and 3155 bp long, respectively, and included 859 and 1616 parsimony-informative sites. Sequences of each of the 11 ribosomal protein genes were aligned individually using default settings in Muscle 3.8 (**Edgar, 2004**) and were realigned by predicted translation; alignments were manually refined and stop-codon sites removed. The concatenated alignment of 11 ribosomal protein genes was 5475 bp long and included 2970 parsimony-informative positions. Aligned sequences for Diplogastridae contained 444 kb without missing data. The final dataset of diplogastrid sequences was more than four times larger than that used in the previously most inclusive phylogenetic study of the family (**Mayer et al., 2009**), and it included over three times as many species and twice as many diplogastrid genera. In the final concatenated alignment of rRNA and ribosomal protein genes for all diplogastrid species, the proportion of missing data was 20%, with a minimum of 70% of nematode species sampled per gene. The dataset of all taxa had 667 kb excluding missing data and was 11,923 bp long (**Supplementary file 1**), in which the fraction of missing data was 38%.

Inference methods

The phylogeny was inferred under Bayesian and maximum likelihood (ML) optimality criteria as implemented in MrBayes 3.2.2 (**Ronquist et al., 2012**) and RAxML 7.3 (**Stamatakis, 2006**), respectively. All inferences were performed on the CIPRES Science Gateway (**Miller et al., 2006**). For Bayesian inference, the dataset was partitioned into four subsets: two for 18S and 28S rRNA genes, which were analyzed using a 'mixed' + Γ model, and the third and fourth for the combined ribosomal protein genes and RNA polymerase II, respectively, which were analyzed under a codon + Γ model. Model parameters were unlinked across partitions. Four independent analyses, each containing four chains, were run for 55 million generations, with chains sampled every 1000 generations. After confirming convergence of runs and mixing of chains using Tracer 1.6 (**Drummond and Rambaut, 2007**), the first 50% generations were discarded as burn-in and the remaining topologies summarized to generate a 50% majority-rule consensus tree. For the ML analysis, our partitioning scheme divided the dataset into three subsets: two for the 18S and 28S rRNA genes, which were each analyzed using a GTR + Γ model, and the third subset for translated ribosomal protein and RNA polymerase II genes, analyzed under an inverse-gamma (IG) + Γ model. The latter model was selected based on an amino-acid substitution-model test as implemented ProtTest 3 (**Darriba et al., 2011**). 100 independent ML searches initiated with random starting trees were performed. Support values for the best-scoring tree were estimated from 1000 iterations of non-parametric bootstrapping.

Presence of polyphenism

We identified nematode species as dimorphic or monomorphic by screening at least 200 individuals in cultured populations under both well-fed and starved conditions, the latter of which is known to induce the Eu morph in *P. pacificus* (**Bento et al., 2010**). Dimorphism was diagnosed by the presence of morphs that differed (i) in the width and aspect ratio of the stoma and (ii) in the prominence and sclerotization of mouth structures (**Fürst von Lieven and Sudhaus, 2000**; **Serobyan et al., 2013**). In all examined species with mouth plasticity, the plasticity was discrete with no observed (and hence presumably rare) intermediate forms or reaction norms for morph-diagnostic morphology. Furthermore, each of the two morphs was stereotypic for a given species, such that morphology did not qualitatively vary with different induction cues. The mouth plasticity was therefore a discrete dimorphism of constant morphs in all species with the plasticity, consistent with previous observations of *P. pacificus*, for which multiple levels of starvation, pheromones, hormones, transgenes, enzyme-inhibiting salts, or environments previously experienced by wild-caught specimens all induced either of two morphs, albeit in differing ratios (**Bento et al., 2010**; **Bose et al., 2012**; **Ragsdale et al., 2013**; **Serobyan et al., 2013**). For species that could not be brought into culture (annotated as 'nc' in **Figure 2—source data 1A**), all of which were monomorphic, observations of collected isolates were corroborated by comprehensively reviewed previous taxonomic studies (**Sudhaus and Fürst von Lieven, 2003**) to confirm the absence of dimorphism. Taken together, previous reports and our own collections demonstrated that such species were monomorphic across multiple populations and environmental conditions. In each of the five cases of recent losses, namely those inferred to have occurred on a terminal branch within Diplogastridae, the assimilated morph was identified as the St morph. However, for inferred

ancient losses of the dimorphism, derived morphology made the homology of the assimilated morph impossible to determine reliably. Therefore, our analyses identify monomorphic and dimorphic taxa without distinguishing which of the two morphs was lost or assimilated.

Environmental induction of alternative morphs

To test whether the mouth dimorphism of diplogastrid nematodes was an environmental polyphenism and not genetic polymorphism, we exposed dimorphic species to environmental conditions potentially influencing expression of the two alternative mouth phenotypes. Specifically, we tested species (strains) with high frequency of St morph for environmental induction of the Eu morph. Although all strains tested had been kept in laboratory culture for at least one year prior to experiments, several strains (*Allodiplogaster sudhausi*, both *Micoletzkya* spp., *Parapristionchus giblindavisi*) were additionally inbred systematically for 10 generations.

In our first assay (***Table 1—source data 1***), 7 fertile St females or hermaphrodites (5 for *Allodiplogaster sudhausi*) were transferred from a stock culture well-fed with bacteria onto an NGM plate (no peptone, no cholesterol) supplied with approximately 70,000–100,000 arrested *C. elegans* larvae. In parallel, the same number of St females or hermaphrodites was transferred onto NGM plates with the same species of bacteria as that on stock culture plates: this was OP50 for most species, although some species (i.e., *Micoletzkya* spp.) required different bacterial strains to reproduce. Nematodes were allowed to feed on the provided food, lay eggs, and develop in the following generation. The mouth phenotype of all F1 females or hermaphrodites was scored when those individuals reached adulthood (5–10 days, depending on the species). Experiments were performed in triplicate for each species.

Because some species could not develop in the absence of microbial food, we employed a second strategy to test for environmental induction of the Eu morph in those strains. In this assay (***Table 1—source data 1***), 10–15 fertile females were transferred to plates seeded with a 500 µl bacterial lawn. After the time necessary for the populations of a species to complete one generation following the visible depletion of a bacterial lawn (*Diplogasteriana* n. sp., 6 weeks; *Koerneria luziae*, 2.5 weeks; *P. giblindavisi*, 2 weeks), adult females were screened for their mouth phenotype. In parallel, nematodes of the same species were maintained in well-fed culture, being transferred (10–15 females per replicate) to a new bacterial lawn, the next generation being screened for the mouth phenotype after 1 week. All adult females up to a sample size of 200 per plate were screened. Experiments were performed in triplicate for each species.

For both assays, significant differences in morph ratios between prey-fed and bacteria-fed nematodes were calculated using Fisher's exact test with the total number of assayed individuals pooled across replicates. Effect sizes of differences were estimated as the odds ratio by Fisher's exact test. The percentage of the Eu morph per treatment per species is reported in ***Table 1*** for pooled samples.

History of dimorphism

To infer the evolutionary history of the stomatal dimorphism, we used stochastic character mapping (***Nielsen, 2002***; ***Huelsenbeck et al., 2003***) as implemented in SIMMAP 1.5 (***Bollback, 2006***). This approach estimates probabilities of the states along phylogeny under continuous-time Markov models, incorporating uncertainty in tree topology, branch length, and ancestral character states. The best-fitting parameters of morphology priors, the overall substitution rate prior (gamma distribution prior), and the bias prior for two-state characters (beta distribution prior) were estimated using a Markov-chain Monte Carlo (MCMC) method as also implemented in SIMMAP. These calibration analyses were run for 500,000 generations, sampling the chain every 100 generations, using a 50% majority rule consensus tree summarized from the Markov chains of the Bayesian phylogenetic analysis; the first 50,000 generations were discarded as burn-in. For stochastic character mapping, 500 trees were randomly sampled, with the help of Mesquite 2.75 (***Maddison and Maddison, 2011***), from trees generated during the MCMC runs. The number of discrete categories, *k*, was set to 90 and 31 for the gamma and beta distributions, respectively. Trees were rescaled to a length of one before applying priors on the overall rate. For analyses of evolutionary rates and complexity correlation, 10 character histories were simulated on each of the 500 trees. The density maps of the dimorphism history (***Figures 2A, 3E***) were generated by summarizing posterior densities from 500 simulations of character histories on the ML tree in the R package phytools 0.3-72 (***Revell, 2012***).

Geometric morphometrics

To capture stomatal morphology, 11 fixed two-dimensional landmarks were placed at locally defined boundaries or points within the stoma (***Figure 3A***). Landmarks consisted of boundaries or points that were considered homologous across Rhabditina as predicted by fine-structural anatomy (***Baldwin et al., 1997***; ***Ragsdale and Baldwin, 2010***); stomatal terminology follows ***De Ley et al. (1995)***. Type-1 landmarks were recorded at the ventral and dorsal boundaries of the cheilostom with labial tissue (landmarks 1 and 11, respectively), the ventral and dorsal boundaries between the cheilostom and gymnostom (2 and 10, respectively), the ventral and dorsal boundaries between the gymnostom and stegostom (4 and 8, respectively), the posterior boundary of the dorsal telostegostom (6), and the dorsal gland orifice (7); type-2 landmarks included the anterior apex of the ventral and dorsal gymnostom (3 and 9, respectively) and the apex of medial curvature of the subventral telostegostom (5). To exclude contribution of the third dimension to morphometrics, all landmarks were recorded in exactly lateral view, as guaranteed by the body habitus of slide-mounted nematodes, that is, their sinusoidal spread along the sagittal plane.

For 68 nematode species, landmarks were recorded for multiple live specimens, which were mounted on 5% agar pads with 8 µl of 0.25 M sodium azide added as an anesthetic. Microscopy was performed using a Zeiss Axio Imager.Z1 equipped with a Spot RT-SE digital camera. Landmark positions were marked using live-view mode in Metamorph 7.1.3 (Molecular Devices, Sunnyvale, CA, USA), and after image acquisition they were digitalized using tpsDig2 (***Rohlf, 2008***). For 22 species, we used video vouchers and images from published sources for digitalization of landmarks. Our complete morphometric dataset consisted of 522 images and 90 nematode species (an average of 4.8 images per species or morph). Landmark positions and centroid sizes (square root of the sum of squared distances of landmarks to their centroid) were averaged for each species (or each morph for dimorphic species), whereafter landmarks were Procrustes-superimposed using MorphoJ (***Klingenberg, 2011***).

We used two approaches to analyze landmarks. First, we simultaneously accounted for variation in both stomatal shape and size by performing Procrustes form-space (size-shape space) analyses (***Dryden and Mardia, 1998***; ***Mitteroecker et al., 2004***). In this approach, Procrustes shape coordinates, which are the result of landmark centering, rotation, and scaling, are augmented by the natural-logarithm-transformed centroid size (i.e., as calculated prior to scaling) and subjected to principal component analysis (PCA). PCA on the Procrustes shape coordinates matrix was performed with an additional column appended containing log-transformed centroid size data using the 'prcomp' function in R 3.0.2 package Stats (***R Development Core Team, 2013***). In the second approach, we performed PCA analysis on Procrustes shape coordinates to reconstruct Procrustes shape-space (***Rohlf and Slice, 1990***). In contrast to form-space, shape-space in principle minimizes the effects of allometry, offering an alternative way to measure morphological change. When data for all species and morphs were combined (***Figure 3A***), the first and the second PC axes of form-space accounted for approximately 73% and 16% (68% and 12% for shape-space), respectively, of the variance. Thus, the cumulative proportion of the overall variance explained by PC1 and PC2 axes was 88% and 81% for form- and shape-space, respectively (***Figure 3—source data 1A,B***). In form-space analyses, loadings of the log centroid size onto PC1 and PC2 axes were 0.91 and 0.41 (***Figure 3—source data 1A,B***).

In addition to the PCA above, we performed phylogenetic PCA on both form and shape matrices for evolutionary rate analyses (***Revell, 2009***) to account for phylogenetic non-independence of morphometric data. The St morph represented dimorphic species in this PCA (***Figure 3—source data 1C,D***). Disparity analyses included several components of the standard PCA were retained (see below). All other analyses, which comprised phylogenetically corrected inference and tests of evolutionary rates requiring individual variables, used scores along the first PC axis of each phylogenetic PCA and which explained the vast majority of variance in either form or shape.

Disparity

Morphological variation (disparity) was examined in three groups, namely non-diplogastrid Rhabditina, dimorphic Diplogastridae, and monomorphic Diplogastridae. We used two approaches to investigate disparity: (i) the sum of univariate variances on form-space axes (multivariate variance) and (ii) PCA volume (***Figure 3—source data 1E***). These methods capture different aspects of morphological diversity and both are based on morphological distance measures, although neither controls for phylogenetic non-independence. The sum of variances, a variance-based metric, provides

an estimate of degree of difference among species in Procrustes morphospace. Alternatively, PCA volume gives an estimate of the amount of morphospace occupied by species; it is calculated as the product of the eigenvalues of the cross-distance matrix, divided by the square of the number of species. The sum of variances was previously shown by simulation-based studies to be relatively insensitive to variation in sample size, and both methods have relatively low sensitivity to missing data (***Ciampaglio et al., 2001***). The analyses were performed using the MATLAB package MDA (***Navarro, 2003***). PC axes that explained more than 5% of the overall variance (2 for form, 3 for shape) (***Figure 3—source data 1A,B***) were retained for calculations of the sum of variances and PCA volume. Rarefaction was performed to correct for sample-size dependence (***Ciampaglio et al., 2001***), such that the sample size was standardized to the number of species in the smallest group compared. To calculate means of disparity estimates, their standard deviations, and their 95% confidence intervals, 10,000 bootstrap replicates were performed. For pairwise comparisons of the sum of variances between groups, two-tailed p-values were estimated using 100,000 bootstrap replicates.

Evolutionary rates

We used two comparative methods that employ a Brownian motion (BM) model to estimate and compare rates of evolution of stomatal morphology among different nematode lineages: (i) a ML-based non-censored rate test (***O'Meara et al., 2006***) and (ii) a Bayesian reversible-jump approach (***Eastman et al., 2011***). In these approaches, the rate of evolution is measured as a rate parameter for the BM process by weighting the magnitude of change of the trait per unit of 'operational time' (***Pagel, 1997***). In our analyses, operational time was set to inferred genetic distance, that is, branch lengths inferred in our Bayesian phylogenetic analysis of four partitions of the 14 included genes. This metric is supported as an appropriate measure of time by mutation accumulation line experiments, which have indicated rates of molecular evolution to be nearly identical between distantly related nematodes of Rhabditina (***Weller et al., 2014***). Absolute time was not used because (i) relevant fossil data are not available to calibrate dates in the phylogeny and (ii) the number of generations per year is assumed to differ dramatically between nematode species due to differences in generation time and, given ecological differences (***Herrmann et al., 2006***; ***Kiontke et al., 2011***), presumed lengths of diapause (dauer) stages.

Non-censored rate test

To investigate how rates of morphological (form and shape) evolution change in the presence of plasticity, we estimated the relative fit of one-, two-, and three-rate parameter models using the 'Brownie.lite' function in the R package phytools 0.3-72 (***Revell, 2012***) (***Figure 3—source data 1F***). Five BM models were tested: (i) a single rate model that approximated the same rate parameter for non-diplogastrid Rhabditina, dimorphic Diplogastridae, and monomorphic Diplogastridae (1,1,1 model); (ii) a two-rate parameter model that assigned one rate category to non-diplogastrid Rhabditina and a different category to dimorphic and monomorphic Diplogastridae together (1,2,2 model); (iii) a two-rate model that approximated one rate parameter for non-diplogastrid Rhabditina and monomorphic diplogastrids but a different rate parameter for dimorphic Diplogastridae (1,2,1 model); (iv) a two-rate model that assumed the same rates for non-diplogastrid Rhabditina and dimorphic Diplogastridae but different rates for monomorphic Diplogastridae (1,1,2 model); (v) a three-rate model that assumed different rate parameters for each of the three nematode groups (1,2,3 model). We assessed the relative fit of models by comparing second-order Akaike Information Criterion (AICc) values (***Figure 3—source data 1F***). If the difference in values (ΔAICc) was greater than 4, the worse-fitting model was considered much less supported (***Burnham and Anderson, 2002***). Additionally, nested models were compared using a hypothesis-testing likelihood-ratio approach, that is, using a chi-square distribution (***Figure 3—source data 1F***; p-values are also given in main text). Tests were performed on 5000 trees with mapped character histories, which were randomly sampled from posterior distributions of post-burn-in trees generated by the MCMC runs of the phylogenetic analysis.

Bayesian sampling of shifts in trait evolution

We investigated variation in evolutionary rates across lineages of Rhabditina using a Bayesian reversible-jump approach (***Eastman et al., 2011***) as implemented in the R package Geiger 1.99-3 (***Harmon et al., 2008***) (***Figure 3—source data 1H***). This method estimates posterior rates of continuous trait evolution along individual branches of the phylogeny using reversible-jump MCMC sampling of a multirate BM process, without the need for specifying hypotheses a priori about the location of rate shifts. To achieve mixing of MCMC chains, we calibrated the proposal width using the

function 'calibrate.rjmcmc' and running the chain for 1 million generations, after which we used Tracer 1.6 to confirm mixing. Three MCMC analyses were then performed, with 30 million generations each, using the function 'rjmcmc.bm'. Analyses were run under a relaxed-BM model with the number of local clocks constrained to three and the proposal width set to 1.5. Chains were sampled every 5000 generations, the first 25% of generations was discarded as burn-in, and Tracer 1.6 was used to confirm chains mixing and convergence. Results from the three independent runs were combined, and weighted posterior rates of individual branches within each of the compared categories were extracted. The highest posterior density (HPD) intervals and means were estimated for the three nematode groups (***Figure 3—figure supplement 3***) and were compared using a two-tailed randomization test to determine whether posterior rates were different among groups (***Figure 3—source data 1H***).

Dimorphism and stomatal complexity

Tabulating complexity

To establish an index for the complexity of nematode mouthparts, we scored the total number of observed cuticular 'cusps' (***Harjunmaa et al., 2012***) and articulations, that is, structures projecting independently within the stoma. We define a 'structure' herein as any geometric deviation that is marked by a physical vertex of <135˚ from the cylindrical walls of the stoma or from the arched anterior margins of the pharyngeal radii (***Figure 4—figure supplement 1***). All recorded structures were discrete and stereotypic, that is, always present or absent, for each species or morph (for dimorphic taxa, the Eu morph was analyzed). Because such structures take a variety of shapes, all recorded structures are for clarity presented as a presence/absence character matrix (***Figure 4—source data 1***), which includes structures consistent with previous reports (***Fürst von Lieven, 2000***; ***Fürst von Lieven and Sudhaus, 2000***; ***Sudhaus and Fürst von Lieven, 2003***; ***Kanzaki et al., 2012***; ***Herrmann et al., 2013***; ***Ragsdale et al., 2014***). Iterative structures (i.e., serratae, rods, points, warts, serial denticles, and divisions of stomatal wall) were conservatively scored as a single structure, because such iterative structures were always co-dependent and were sometimes (i.e., for denticles, serratae, and warts) variable in number among individuals of a single species. Furthermore, such structures show that this additional within-character complexity correlates with size, analogous to what is observed in mammalian tooth development (***Harjunmaa et al., 2014***) or what might otherwise be expected in area-dependent patterning (***Turing, 1952***). Therefore, to minimize the effects of size on complexity in our analyses, all tabulated structures were those that were unique and constant within a species and which could be assigned homology where present in multiple species. Additionally, structures that bore multiple vertices or 'secondary complexity' distal to its deviation from the stoma (i.e., teeth, which could have multiple bends or peaks) were also coded as single structures. Finally, any character present as identical, symmetrical duplicates, which was due to the presence of two subventral sectors and hence also developmental co-dependence, was scored as a single structure. Examples of stomata with all of their structures recorded and labeled are shown in ***Figure 4—source data 1***.

All Diplogastridae and some non-diplogastrid Rhabditina were observed by differential interference contrast (DIC) microscopy. For other taxa, morphology was scored from published DIC video vouchers, DIC micrographs, and drawing interpretations; stomatal morphology for genera of Rhabditidae was additionally confirmed according to a recent key for the family (***Scholze and Sudhaus, 2011***). Observed structures comprised a total of 25 characters. For the set of analyzed taxa, the complexity index ranged from 0 to 9.

Character correlation

We tested for a correlation between presence of mouth dimorphism and stomatal complexity using the dataset that included all 87 species of Rhabditina and the threshold model (***Felsenstein, 2012***) as implemented in the R package phytools 0.3-72 (***Revell, 2012***). We ran 50 analyses of 500,000 generations each and using trees randomly sampled from the posterior distributions of trees generated by the phylogenetic analysis in MrBayes 3.2.2. After confirming chain convergence and discarding 25% of the posterior samples as burn-in, the outputs of the analyses were combined and used to calculate the maximum likelihood estimation of the correlation coefficient. The R package coda 0.16-1 (***Plummer et al., 2012***) was used to compute the highest posterior density intervals of those estimates.

Additionally, we tested for correlation between dimorphism and stomatal complexity by Bayesian MCMC sampling as implemented in BayesTraits V2 (beta) (***Pagel and Meade, 2013***). For this test, a constant-variance random-walk model was invoked. The regression coefficient was estimated as the ratio of covariance between dimorphism presence and complexity index to the variance of dimorphism presence. Significance of the trait correlation was tested by comparing the harmonic mean of the Bayes factor (BF) from runs under a dependent (correlation allowed) character model to that under an independent (correlation fixed to 0) model. A log(BF) >10 was considered to give very strong support for the best model. To incorporate phylogenetic uncertainty, the analysis was simulated on 50 trees sampled from the posterior distribution of trees from the phylogenetic analysis. MCMC chains were run for 10 million generations, sampling chains every 1000 generations.

Acknowledgements

We thank Waltraud Röseler, Aziza Aust, and Hanh Witte for helping with DNA preparation, Matthias Herrmann for help with nematode collecting, and Robin Giblin-Davis for providing several nematode strains.

Additional information

Funding

Funder	Author
Max-Planck-Gesellschaft (Max Planck Society)	Ralf J Sommer

The funder had no role in study design, data collection and interpretation, or the decision to submit the work for publication.

Author contributions

VS, EJR, Conception and design, Acquisition of data, Analysis and interpretation of data, Drafting or revising the article; NK, Sample collection, Acquisition of data; RJS, Sample collection, Drafting or revising the article

Additional files

Supplementary file

- Supplementary file 1. Two tree files and a multiple sequence alignment file.

DOI: 10.7554/eLife.05463.016

References

Andrássy I. 1984. *Klasse Nematoda*. Stuttgart: Fischer Verlag.

Andrássy I. 2005. *Free-living nematodes of Hungary, I (Nematoda errantia)*. Budapest: Hungarian National History Museum.

Baldwin JG, Giblin-Davis RM, Eddleman CD, Williams DS, Vida JT, Thomas WK. 1997. The buccal capsule of *Aduncospiculum halicti* (Nemata: Diplogasterina): an ultrastructural and molecular phylogenetic study. *Canadian Journal of Zoology* **75**:407–423. doi: 10.1139/z97-051.

Baldwin JM. 1896. A new factor in evolution. *The American Naturalist* **30**:441–451. doi: 10.1086/276408.

Barrett RD, Schluter D. 2008. Adaptation from standing genetic variation. *Trends in Ecology & Evolution* **23**:38–44. doi: 10.1016/j.tree.2007.09.008.

Bento G, Ogawa A, Sommer RJ. 2010. Co-option of the hormone signalling module dafachronic acid-DAF-12 in nematode evolution. *Nature* **466**:494–497. doi: 10.1038/nature09164.

Blaxter ML, De Ley P, Garey JR, Liu LX, Scheldeman P, Vierstraete A, Vanfleteren JR, Mackey LY, Dorris M, Frisse LM, Vida JT, Thomas WK. 1998. A molecular evolutionary framework for the phylum Nematoda. *Nature* **392**:71–75. doi: 10.1038/32160.

Bollback JP. 2006. SIMMAP: stochastic character mapping of discrete traits on phylogenies. *BMC Bioinformatics* **7**:88. doi: 10.1186/1471-2105-7-88.

Bose N, Ogawa A, von Reuss SH, Yim JJ, Ragsdale EJ, Sommer RJ, Schroeder FC. 2012. Complex small-molecule architectures regulate phenotypic plasticity in a nematode. *Angewandte Chemie* **51**:12438–12443. doi: 10.1002/anie.201206797.
Burnham KP, Anderson DR. 2002. *Model selection and multimodel interference: a practical information-theoretic approach*. New York: Springer.
Cheverud JM. 1996. Developmental integration and the evolution of pleiotropy. *American Zoologist* **36**:44–50.
Ciampaglio CN, Kemp M, McShea DW. 2001. Detecting changes in morphospace occupation patterns in the fossil record: characterization and analysis measures of disparity. *Palaeobiology* **27**:695–715. doi: 10.1666/0094-8373(2001)027<0695:DCIMOP>2.0.CO;2.
Darriba D, Taboada GL, Doallo R, Posada D. 2011. ProtTest 3: fast selection of best-fit models of protein evolution. *Bioinformatics* **27**:1164–1165. doi: 10.1093/bioinformatics/btr088.
de Jong G. 2005. Evolution of phenotypic plasticity: patterns of plasticity and the emergence of ecotypes. *The New Phytologist* **166**:101–117. doi: 10.1111/j.1469-8137.2005.01322.x.
De Ley P, Blaxter ML. 2002. Systematic position and phylogeny. In: Lee DL, editor. *The Biology of nematodes*. London: Taylor & Francis.
De Ley P, van de Velde MC, Mounport D, Baujard P, Coomans A. 1995. Ultrastructure of the stoma in *Cephalobidae*, *Panagrolaimidae*, and Rhabditidae, with a proposal for a revised stoma terminology in Rhabdtida (Nematoda). *Nematologica* **41**:153–182. doi: 10.1163/003925995X00143.
Drummond AJ, Rambaut A. 2007. BEAST: Bayesian evolutionary analysis by sampling trees. *BMC Evolutionary Biology* **7**:214. doi: 10.1186/1471-2148-7-214.
Dryden IL, Mardia KV. 1998. *Statistical shape analysis*. Chichester: Wiley.
Eastman JM, Alfaro ME, Joyce P, Hipp AL, Harmon LJ. 2011. A novel comparative method for identifying shifts in the rate of character evolution on trees. *Evolution* **65**:3578–3589. doi: 10.1111/j.1558-5646.2011.01401.x.
Edgar RC. 2004. MUSCLE: multiple sequence alignment with high accuracy and high throughput. *Nucleic Acids Research* **32**:1792–1797. doi: 10.1093/nar/gkh340.
Emlen DJ, Hunt J, Simmons LW. 2005. Evolution of sexual dimorphism and male dimorphism in the expression of beetle horns: phylogenetic evidence for modularity, evolutionary lability, and constraint. *The American Naturalist* **166**:Suppl 4S42–S68. doi: 10.1086/444599.
Felsenstein J. 2012. A comparative method for both discrete and continuous characters using the threshold model. *The American Naturalist* **179**:145–156. doi: 10.1086/663681.
Fürst von Lieven A. 2000. Vergleichende und funktionelle Morphologie der Mundhöhle der Diplogastrina (Nematoda) mit einem ersten Entwurf der Phylogenie dieses Taxons. Ph. D. dissertation, Freie Universität Berlin.
Fürst von Lieven A, Sudhaus W. 2000. Comparative and functional morphology on the buccal cavity of Diplogastrina (Nematoda) and a first outline of the phylogeny of this taxon. *Journal of Zoological Systematics and Evolutionary Research* **38**:37–63. doi: 10.1046/j.1439-0469.2000.381125.x.
Harjunmaa E, Kallonen A, Voutilainen M, Hämäläinen K, Mikkola ML, Jernvall J. 2012. On the difficulty of increasing dental complexity. *Nature* **483**:324–327. doi: 10.1038/nature10876.
Harjunmaa E, Seidel K, Häkkinen T, Renvoisé E, Corfe IJ, Kallonen A, Zhang ZQ, Evans R, Mikkola ML, Salazar-Ciudad I, Klein OD, Jernvall J. 2014. Replaying evolutionary transitions from the dental fossil record. *Nature* **512**:44–48. doi: 10.1038/nature13613.
Harmon LJ, Weir J, Brock C, Glor RE, Challenger W. 2008. GEIGER: investigating evolutionary radiations. *Bioinformatics* **24**:129–131. doi: 10.1093/bioinformatics/btm538.
Herrmann M, Mayer WE, Sommer RJ. 2006. Nematodes of the genus *Pristionchus* are closely associated with scarab beetles and the Colorado potato beetle in Western Europe. *Zoology* **109**:96–108. doi: 10.1016/j.zool.2006.03.001.
Herrmann M, Ragsdale EJ, Kanzaki N, Sommer RJ. 2013. *Sudhausia aristotokia* n. gen., n. sp. and *S. crassa* n. gen., n. sp. (Nematoda: Diplogastridae): viviparous new species with precocious gonad development. *Nematology* **15**:1001–1020. doi: 10.1163/15685411-00002738.
Huelsenbeck JP, Nielsen R, Bollback JP. 2003. Stochastic mapping of morphological characters. *Systematic Biology* **52**:131–138. doi: 10.1080/10635150390192780.
Kanzaki N, Ragsdale EJ, Herrmann M, Sommer RJ. 2012. Two new species of *Pristionchus* (Rhabditida: Diplogastridae): *P. fissidentatus* n. sp. from Nepal and La Réunion and *P. elegans* n. sp. from Japan. *Journal of Nematology* **44**:80–91.
Katoh K, Standley DM. 2013. MAFFT multiple alignment software version 7: improvements in performance and usability. *Molecular Biology and Evolution* **30**:772–780. doi: 10.1093/molbev/mst010.
Kawecki TJ. 1994. Accumulation of deleterious mutations and the evolutionary cost of being a generalist. *The American Naturalist* **144**:833–838. doi: 10.1086/285709.
Kiontke K, Barrière A, Kolotuev I, Podbilewicz B, Sommer R, Fitch DH, Félix MA. 2007. Trends, stasis, and drift in the evolution of nematode vulva development. *Current Biology* **17**:1925–1937. doi: 10.1016/j.cub.2007.10.061.
Kiontke KC, Félix MA, Ailion M, Rockman MV, Braendle C, Pénigault JB, Fitch DH. 2011. A phylogeny and molecular barcodes for *Caenorhabditis*, with numerous new species from rotting fruits. *BMC Evolutionary Biology* **11**:339. doi: 10.1186/1471-2148-11-339.
Klingenberg CP. 2011. MorphoJ: an integrated software package for geometric morphometrics. *Molecular Ecology Resources* **11**:353–357. doi: 10.1111/j.1755-0998.2010.02924.x.
Lande R. 2009. Adaptation to an extraordinary environment by evolution of phenotypic plasticity and genetic assimilation. *Journal of Evolutionary Biology* **22**:1435–1445. doi: 10.1111/j.1420-9101.2009.01754.x.

Ledón-Rettig CC, Pfennig DW, Crespi EJ. 2010. Diet and hormonal manipulation reveal cryptic genetic variation: implications for the evolution of novel feeding strategies. *Proceedings Biological sciences/The Royal Society* **277**: 3569–3578. doi: 10.1098/rspb.2010.0877.

Maddison WP, Maddison DR. 2011. *Mesquite: a modular system for evolutionary analysis. Version 2.75.* [http://mesquiteproject.org].

Mayer WE, Herrmann M, Sommer RJ. 2009. Molecular phylogeny of beetle associated diplogastrid nematodes suggests host switching rather than nematode-beetle coevolution. *BMC Evolutionary Biology* **9**:212. doi: 10.1186/1471-2148-9-212.

Miller MA, Pfeiffer W, Schwarz T. 2006. Creating the CIPRES science gateway for inference of large phylognetic trees. *Proceedings of the gateway computing environments workshop (GCE), 14 November.* New Orleans: p. 1–8.

Mitteroecker P, Gunz P, Bernhard M, Schaefer K, Bookstein FL. 2004. Comparison of cranial ontogenetic trajectories among great apes and humans. *Journal of Human Evolution* **46**:679–698. doi: 10.1016/j.jhevol.2004.03.006.

Moczek AP, Sultan SE, Foster SA, Ledón-Rettig CC, Dworkin I, Nijhout HF, Abouheif E, Pfennig DW. 2011. The role of developmental plasticity in evolutionary innovation. *Proceedings Biological sciences/The Royal Society* **278**: 2705–2713. doi: 10.1098/rspb.2011.0971.

Moran NA. 1992. The evolutionary maintenance of alternative phenotypes. *The American Naturalist* **139**:971–989. doi: 10.1086/285369.

Navarro N. 2003. MDA: a MATLAB-based program for morphospace-disparity analysis. *Computers & Geosciences* **29**:655–4. doi: 10.1016/S0098-3004(03)00043-8.

Nielsen R. 2002. Mapping mutations on phylogenies. *Systematic Biology* **51**:729–739. doi: 10.1080/10635150290102393.

O'Meara BC, Ané C, Sanderson MJ, Wainwright PC. 2006. Testing for different rates of continuous trait evolution using likelihood. *Evolution* **60**:922–933. doi: 10.1111/j.0014-3820.2006.tb01171.x.

Pagel M. 1997. Inferring evolutionary processes from phylogenies. *Zoologica Scripta* **26**:331–348. doi: 10.1111/j.1463-6409.1997.tb00423.x.

Pagel M, Meade A. 2013. *BayesTraits V2 (beta).* [http://www.evolution.rdg.ac.uk/BayesTraits.html].

Pfennig DW, McGee M. 2010. Resource polyphenism increases species richness: a test of the hypothesis. *Philosophical Transactions of the Royal Society of London Series B, Biological Sciences* **365**:577–591. doi: 10.1098/rstb.2009.0244.

Pigliucci M. 2001. *Phenotypic plasticity: beyond nature and nurture: syntheses in ecology and evolution.* Baltimore: Johns Hopkins University Press.

Plummer M, Best N, Cowles K, Vines K, Sarkar D, Almond R. 2012. coda: output analysis and diagnostics for MCMC. *R package version 0.16-1.* [http://CRAN.R-project.org/package=magic].

R Development Core Team. 2013. *R: a language and environment for statistical computing.* Vienna: R foundation for Statistical Computing. [http://www.R-project.org].

Ragsdale EJ, Baldwin JG. 2010. Resolving phylogenetic incongruence to articulate homology and phenotypic evolution: a case study from Nematoda. *Proceedings Biological Sciences/The Royal Society* **277**:1299–1307. doi: 10.1098/rspb.2009.2195.

Ragsdale EJ, Kanzaki N, Sommer RJ. 2014. *Levipalatum texanum* n. gen., n. sp. (Nematoda: Diplogastridae), an androdioecious species from the south-eastern USA. *Nematology* **16**:695–709. doi: 10.1163/15685411-00002798.

Ragsdale EJ, Müller MR, Rödelsperger C, Sommer RJ. 2013. A developmental switch coupled to the evolution of plasticity acts through a sulfatase. *Cell* **155**:922–933. doi: 10.1016/j.cell.2013.09.054.

Revell LJ. 2009. Size-correction and principal components for interspecific comparative studies. *Evolution* **63**: 3258–3268. doi: 10.1111/j.1558-5646.2009.00804.x.

Revell LJ. 2012. phytools: an R package for phylogenetic comparative biology (and other things). *Methods in Ecology and Evolution* **3**:217–223. doi: 10.1111/j.2041-210X.2011.00169.x.

Rohlf FJ. 2008. *TpsDig2: a program for landmark development and analysis.*Department of Ecology and Evolution, State University of New York at Stony Brook. [http://life.bio.sunysb.edu/morph/].

Rohlf FJ, Slice D. 1990. Extensions of the Procrustes method for optimal superimposition of landmarks. *Systematic Zoology* **39**:40–59. doi: 10.2307/2992207.

Ronquist F, Teslenko M, van der Mark P, Ayres DL, Darling A, Höhna S, Larget B, Liu L, Suchard MA, Huelsenbeck JP. 2012. MrBayes 3.2: efficient Bayesian phylogenetic inference and model choice across a large model space. *Systematic Biology* **61**:539–542. doi: 10.1093/sysbio/sys029.

Schlichting CD. 2003. Origins of differentiation via phenotypic plasticity. *Evolution & Development* **5**:98–105. doi: 10.1046/j.1525-142X.2003.03015.x.

Scholze VS, Sudhaus W. 2011. A pictorial key to the current genus groups of 'Rhabditidae'. *Journal of Nematode Morphology and Systematics* **14**:105–112.

Schwander T, Leimar O. 2011. Genes as leaders and followers in evolution. *Trends in Ecology & Evolution* **26**: 143–151. doi: 10.1016/j.tree.2010.12.010.

Serobyan V, Ragsdale EJ, Müller MR, Sommer RJ. 2013. Feeding plasticity in the nematode *Pristionchus pacificus* is influenced by sex and social context and is linked to developmental speed. *Evolution & Development* **15**: 161–170. doi: 10.1111/ede.12030.

Serobyan V, Ragsdale EJ, Sommer RJ. 2014. Adaptive value of a predatory mouth-form in a dimorphic nematode. *Proceedings Biological Sciences / The Royal Society* **281**:20141334. doi: 10.1098/rspb.2014.1334.

Snell-Rood EC, Van Dyken JD, Cruickshank T, Wade MJ, Moczek AP. 2010. Toward a population genetic framework of developmental evolution: the costs, limits, and consequences of phenotypic plasticity. *Bioessays* **32**:71–81. doi: 10.1002/bies.200900132.

Stamatakis A. 2006. RAxML-VI-HPC: maximum likelihood-based analyses with thousands of taxa and mixed models. *Bioinformatics* **22**:2688–2690. doi: 10.1093/bioinformatics/btl446.

Sudhaus W. 2011. Phylogenetic systemisation and catalogue of paraphyletic 'Rhabditidae' (Secernentea, Nematoda). *Journal of Nematode Morphology and Systematics* **14**:113–178.

Sudhaus W, Fürst von Lieven A. 2003. A phylogenetic classification and catalogue of the Diplogastridae (Secernentea, Nematoda). *Journal of Nematode Morphology and Systematics* **6**:43–90.

Suzuki Y, Nijhout HF. 2006. Evolution of a polyphenism by genetic accommodation. *Science* **311**:650–652. doi: 10.1126/science.1118888.

Turing AM. 1952. The chemical basis of morphogenesis. *Philosophical Transactions of the Royal Society of London Series B, Biological Sciences* **641**:37–72. doi: 10.1098/rstb.1952.0012.

Van Dyken JD, Wade MJ. 2010. The genetic signature of conditional expression. *Genetics* **184**:557–570. doi: 10.1534/genetics.109.110163.

van Megen H, van den Elsen S, Holterman M, Karssen G, Mooyman P, Bongers T, Holovachov O, Bakker J, Helder J. 2009. A phylogenetic tree of nematodes based on about 1200 full-length small subunit ribosomal DNA sequences. *Nematology* **11**:927–950. doi: 10.1163/156854109X456862.

Waddington CH. 1953. Genetic assimilation of an acquired character. *Evolution* **7**:118–126. doi: 10.2307/2405747.

Weller AM, Rödelsperger C, Eberhardt G, Molnar RI, Sommer RJ. 2014. Opposing forces of A/T-biased mutations and G/C-biased gene conversions shape the genome of the nematode *Pristionchus Pacificus*. *Genetics* **196**:1145–1152. doi: 10.1534/genetics.113.159863.

West-Eberhard MJ. 1986. Alternative adaptations, speciation, and phylogeny (a review). *Proceedings of the National Academy of Sciences of USA* **83**:1388–1392. doi: 10.1073/pnas.83.5.1388.

West-Eberhard MJ. 2003. *Developmental plasticity and evolution*. Oxford: Oxford University Press.

Williams GC. 1966. *Adaptation and natural selection*. Princeton: Princeton University Press.

Wund MA. 2012. Assessing the impacts of phenotypic plasticity on evolution. *Integrative and Comparative Biology* **52**:5–15. doi: 10.1093/icb/ics050.

Extended data for

Rapid diversification associated with a macroevolutionary pulse of developmental plasticity

Vladislav Susoy[1], Erik J. Ragsdale[1,2,*], Natsumi Kanzaki[3] & Ralf J. Sommer[1,*]

---

[1]Department of Evolutionary Biology, Max Planck Institute for Developmental Biology, Spemannstraße 37/4, 72076 Tübingen, Germany

[2]Department of Biology, Indiana University, 1001 E. 3rd Street, Bloomington, IN 47405, USA

[3]Forest Pathology Laboratory, Forestry and Forest Products Research Institute, 1 Matsunosato, Tsukuba, Ibaraki 305-8687, Japan

*For correspondence: ragsdale@indiana.edu, ralf.sommer@tuebingen.mpg.de

Additional data is available at http://elifesciences.org/content/4/e05463

Table 1-source data 1. Environmental induction of the Eu morph in dimorphic species. Results for individual replicates (plates) are shown.

Dimorphic nematode species	Treatment			Control		
	Eu, n	St, n	Eu, %	Eu, n	St, n	Eu, %
Deprivation of microbial food and presence of *C. elegans* larvae ("prey" treatment)						
Allodiplogaster sp. 1 (RS1982)	12	0	100	0	26	0
	23	0	100	0	21	0
	13	0	100	0	18	0
Allodiplogaster sudhausi (SB413B)	30	0	100	5	81	6
	30	2	94	0	67	0
	55	1	98	2	69	3
Fictor stercorarius (RS9003)	6	0	100	0	15	0
	8	1	89	0	12	0
	10	0	100	0	9	0
Micoletzkya inedia (RS5605)	17	4	81	0	40	0
	61	0	100	0	51	0
	23	1	96	0	52	0
Micoletzkya japonica (RS5524B)	34	0	100	0	72	0
	46	4	92	0	73	0
	39	6	87	0	55	0
Mononchoides sp. 1 (RS5441)	55	3	95	5	59	8
	43	0	100	1	36	3
	38	0	100	9	43	17
Mononchoides sp. 3 (RS9008)	49	0	100	2	37	5
	18	0	100	0	25	0
	26	0	100	4	26	13
Neodiplogaster sp. (RS9009)	41	1	98	0	47	0
	107	0	100	0	87	0
	62	0	100	0	45	0
Crowding and deprivation of food ("starved" treatment)						
Diplogasteriana n. sp. (RS9000)	12	18	40	0	200	0
	3	19	14	0	200	0
	3	21	13	0	200	0
Koerneria luziae (RS5613)	6	194	3	0	200	0
	16	184	8	0	200	0
	12	188	6	0	200	0
Parapristionchus giblindavisi (RS5555B)	31	48	39	5	95	5
	34	66	34	7	93	7
	29	71	29	5	95	5

Figure 2-source data 1. Nematode taxa used in this study, with isolation details given. Origins of strains are coded as follows: CGC, Caenorhabditis Genetics Center; JB, Baldwin lab (U. California, Riverside); MV, Viney lab (U. Bristol); NK, Kanzaki lab; RGD, Giblin-Davis lab (U. Florida-IFAS); RS, Sommer lab; SB, Sudhaus lab (Freie Universität Berlin). For other strains, references are given. nc, not culturable.

Nematode species	Strain	Isolation source	Location	Origin
		Diplogastridae		
Acrostichus cf. *nudicapitatus*	RS5083	Soil	Breitenholz, Germany	RS
Acrostichus halicti	JB120	*Halictus ligatus*	Davis, CA, USA	JB
Acrostichus rhynchophori	RGD193	*Rhynchophorus cruentatus*	Florida, USA	RGD
Allodiplogaster hylobii	RS5529	*Hylobius abietis*	Tübingen, Germany	RS
Allodiplogaster sp. 1	RS1982	*Melolontha melolontha*	Usedom, Germany	RS
Allodiplogaster sudhausi	SB413	Soil	Israel	SB
Butlerius sp.	nc	Frass from passalid beetle	New Caledonia	RS
Diplogasteriana n. sp.	RS9000	*Nosodendron unicolor*	Nebraska, USA	RS
Diplogasteriana schneideri	RS5440	*Nosodendron fasciculare*	Stuttgart, Germany	RS
Diplogasteroides magnus	RS1983	*Melolontha melolontha*	Tübingen, Germany	RS
Diplogasteroides sp.	RS5444	*Holotrichia* sp.	Kobe, Japan	RS
Diplogastrellus gracilis	SB306	-	Sweden	SB
Diplogastrellus sp.	RS5608	Frass from *Leptaulax* sp.	Christmas Island	RS
Eudiplogasterium levidentum	nc	Cow dung	Tübingen, Germany	RS
Fictor sp. 1	RS9001	*Trox* sp.	Cambodia	RS
Fictor sp. 2	RS9002	*Trox* sp.	Arizona, USA	RS
Fictor stercorarius	RS9003	Dung beetle	Tübingen, Germany	RS
Fuchsnema halleri	RS5531	*Ips typographus*	Tübingen, Germany	RS
Fuchsnema sp.	RS5537	*Gnathotrichus materiarius*	Tübingen, Germany	RS
Koerneria luziae	RS5613	Frass from *Dorcus ritsemae*	Indonesia	RS/NK
Koerneria sp.	RS9004	Frass from *Dorcus rectus*	Tsukuba, Japan	RS/NK
Leptojacobus dorci	RS9005	Frass from *Dorcus ritsemae*	Indonesia	RS/NK
Levipalatum texanum	RS5280	*Cyclocephala* sp.	Texas, USA	RS
Mehdinema alii	nc	*Gryllodes sigillatus*	Riverside, CA, USA	RS
Micoletzkya buetschlii	RS9006	*Ips typographus*	Tübingen, Germany	RS
Micoletzkya inedia	RS5605	*Dendroctonus ponderosae*	Arizona, USA	RS
Micoletzkya japonica	RS5524	*Dryocoetes uniseriatus*	Kasumigaura, Japan	RS
Micoletzkya sp.	RS5562	*Dryocoetes autographus*	Tübingen, Germany	RS
Mononchoides sp. 1	RS5441	*Geotrupes* sp.	Corsica, France	RS
Mononchoides sp. 2	RS9007	Scarabaeidae sp.	Mexico	RS
Mononchoides sp. 3	RS9008	-	New Caledonia	RS
Neodiplogaster crenatae	nc	*Scolytoplatypus daimio*	Shirakami, Japan	(1)
Neodiplogaster sp.	RS9009	Lucanidae sp.	Sulawesi	RS
Oigolaimella attenuata	SB353	*Reticulitermes lucifugus*	Corsica, France	SB
Oigolaimella sp.	RS9010	*Reticulitermes speratus*	Kagoshima, Japan	RS/NK
Parapristionchus giblindavisi	RS5555	*Dorcus rubrofemoratus*	Japan	RS

Parasitodiplogaster maxinema	nc	Syconium, *Ficus maxima*	Panama	(2)
Paroigolaimella micura	nc	Cow dung	Tübingen, Germany	RS
Paroigolaimella stresemanni	nc	Cow dung	Tübingen, Germany	RS
Pristionchus elegans	RS5229	*Phleotrupes auratus*	Japan	RS
Pristionchus fissidentatus	RS5133	Soil	Nepal	RS
Pristionchus maupasi	RS0143	*Melolontha melolontha*	Tübingen, Germany	RS
Pristionchus pacificus	PS312	Soil	Pasadena, CA, USA	RS
Pristionchus uniformis	RS0141	*Melolontha melolontha*	Menz, Germany	RS
Pseudodiplogasteroides sp.	SB257	Rotten cacti	Arizona, USA	SB
Rhabditidoides sp.	RS5443	*Geotrupes* sp.	Tübingen, Germany	RS
Rhabditolaimus sp. 1	RSA134	*Euplatypus parallelus*	La Réunion Island	RS
Rhabditolaimus sp. 2	RS5442	Prioninae sp.	Ghana	RS
Sachsia zurstrasseni	nc	Cow dung	Tübingen, Germany	RS
Sudhausia aristotokia	RS9011	*Onthophagus* sp.	Ghana	RS
Sudhausia crassa	RS9012	*Onthophagus* sp.	Pretoria, South Africa	RS
Teratodiplogaster sp. 1	nc	Syconium, *Ficus variegata*	Okinawa, Japan	RS/NK
Teratodiplogaster sp. 2	nc	Syconium, *Ficus* sp.	Vietnam	RS
Tylopharynx foetida	nc	*Geotrupes* sp.	Corsica	RS
Non-diplogastrid Rhabditina and outgroups				
Brevibucca saprophaga	SB261	-	-	(3)
Bunonema reticulatum	RS9013	Moss	Tübingen, Germany	RS
Bunonema sp.	RS9014	-	New Caledonia	RS
Caenorhabditis angaria	PS1010	*Metamasius hemipterus*	Florida, USA	(4)
Caenorhabditis briggsae	AF16	Soil	Ahmedabad, India	CGC
Caenorhabditis elegans	N2	Mushroom compost	Bristol, UK	CGC
Choriorhabditis cristata	RS5618	Basidiomycota mushroom	Tübingen, Germany	RS
Cruznema tripartitum	-	Soil	Campillo de Arenas, Spain	(5)
Diploscapter sp.	RS1965	Compost	Tübingen, Germany	RS
Distolabrellus veechi	-	Decaying organic substrate	India	(6)
Heterorhabditis bacteriophora	-	*Heliothis punctigera*	South Australia	CGC
Mesorhabditis acidophila	-	Snottites	Tabasco, Mexico	(7)
Myolaimus byersi	RGD233	*Hyophorbe verschaffeltii*	Florida, USA	(8)
Odontopharynx longicaudata	-	Soil	Netherlands	(9)
Oscheius carolinensis	-	Vermicompost	North Carolina, USA	(10)
Oscheius guentheri	-	Decaying rice plants	Hau Giang, Vietnam	(11)
Oscheius myriophila	RS1964	Soil	Oahu, HI, USA	RS
Oscheius tipulae	RS1990	-	Bogota, Colombia	RS
Panagrellus redivivus	PS1163	-	Harpenden, UK	CGC
Parasitorhabditis obtusa	RS5586	*Ips typographus*	Tübingen, Germany	RS
Pelodera cylindrica	RS5097	*Geotrupes* sp.	Tübingen, Germany	RS
Pelodera strongyloides	DF5022	Cow skin	Illinois, USA	CGC
Pelodera teres	-	Manure	Kashmir, India	(12)
Pellioditis sp.	RS5624	Basidiomycota mushroom	Tübingen, Germany	RS
Poikilolaimus floridensis	RGD617R	*Neotermes jouteli*	Florida, USA	(13)
Poikilolaimus oxycercus	SB200	Compost	Belgium	SB
Protorhabditis sp.	RS9015	Frass from *Dorcus rectus*	Tsukuba, Japan	RS

Rhabditis brassicae	RS5617	Basidiomycota mushroom	Tübingen, Germany	RS
Rhabditis colombiana	-	*Cyrtomenus bergi*	Cauca Valley, Colombia	(14)
Rhabditis rainai	-	*Coptotermes formosanus*	Louisiana, USA	(15)
Rhabditoides inermis	SB328	-	-	SB
Strongyloides ratti	ED321	*Rattus norvegicus*	Philadelphia, USA	MV
Teratorhabditis mariannae	RS0136	-	Tübingen, Germany	RS
Teratorhabditis palmarum	-	*Rhynchophorus palmarum*	Trinidad	(16)
Teratorhabditis synpapillata	-	*Rhynchophorus ferrugineus*	Kagoshima, Japan	(17)
Zeldia punctata	JB15	Soil	Riverside, CA, USA	JB

Supplementary references for Figure 2-source data 1:

1. Kanzaki N, Masuya H, Kubono T. 2008. Description of *Neodiplogaster crenatae* sp. n. and *N. acaloleptae* sp. n. (Nematoda: Diplogastridae) from Japan. *Nematology* **10**:545-560.
2. Kanzaki N, Giblin-Davis RM, Ye WM, Herre EA, Center BJ. 2013 Description of *Parasitodiplogaster pharmaconema* n. sp. and redescription of *P. maxinema* from *Ficus maxima* Mill. (Moraceae). *Nematology* **15**:957-974.
3. De Ley P, De Ley IT, Morris K, Abebe E, Mundo-Ocampo M, Yoder M, Heras J, Waumann D, Rocha-Olivares A, Burr AHJ, Baldwin JG, Thomas WK. 2005. An integrated approach to fast and informative morphological vouchering of nematodes for applications in molecular barcoding. *Phil Trans R Soc B* **360**:1945-1958.
4. Sudhaus W, Kiontke K, Giblin-Davis RM. 2010. Description of *Caenorhabditis angaria* n. sp. (Nematoda: Rhabditidae), an associate of sugarcane and palm weevils (Coleoptera: Curculionidae). *Nematology* **13**:61-78.
5. Abolafia J, Peña-Santiago R. 2009. Nematodes of the Order Rhabditida from Andalucía Oriental, Spain. The family Mesorhabditidae, with description of *Mesorhabditis carmenae* n. sp. *J Nematode Morphol Syst* **12**:41-64.
6. Tahseen Q, Shah AA, Khan R, Sultana R, Hussain A, Ahmad I. 2009. Biogeography and variations in allopatric populations of *Distolabrellus veechi* Anderson, 1983 (Nematoda: Rhabditidae). *Nematology* **11**:815-826.
7. Borgonie G, Dierick M, Houthoofd W, Willems M, Jacobs P, Bert W. 2010. Refuge from predation, the benefit of living in an extreme acidic environment? *Biol Bull* **219**:268-276.
8. Giblin-Davis RM, Kanzaki N, De Ley P, Williams DS, Schierenberg E, Ragsdale EJ, Zeng YS, Center BJ. 2010. Ultrastructure and life history of *Myolaimus byersi* n. sp. (Myolaimina: Myolaimidae), a phoretic associate of the crane fly, *Limonia schwarzi* (Alexander) (Limoniidae), in Florida. *Nematology* **12**:519-542.
9. Ye WM, Torres-Barragan A, Cardoza YJ. 2010. *Oscheius carolinensis* n. sp. (Nematoda: Rhabditidae), a potential entomopathogenic nematode from vermicompost. *Nematology* **12**:121-135.
10. van Megen H, van den Elsen S, Holterman M, Karssen G, Mooyman P, Bongers T, Holovachov O, Bakker J, Helder J. 2009. A phylogenetic tree of nematodes based on about 1200 full-length small subunit ribosomal DNA sequences. *Nematology* **11**:927-950.

11. Sudhaus W, Hooper DJ. 1990. *Rhabditis (Oscheius) guentheri* sp. n., an unusual species with reduced posterior ovary, with observations on the *Dolichura* and *Insectivora* groups (Nematoda: Rhabditidae). *Nematologica* **40**:508-533.
12. Hussain A, Tahseen Q, Khan R. 2006. Re-description of two species of *Pelodera* (Nematoda: Rhabditidae) from India. *Nematol Mediterr* **34**:55-62.
13. Kanzaki N, Giblin-Davis RM, Scheffrahn RH, Center BJ. 2009. *Poikilolaimus floridensis* n. sp. (Rhabditida: Rhabditidae) associated with termites (Kalotermitidae). *Nematology* **11**:203-216.
14. Stock SP, Caicedo AM, Calatayud PA. 2005. *Rhabditis (Oscheius) colombiana* n. sp. (Nematoda: Rhabditidae), a necromenic associate of the subterranean burrower bug *Cyrtomenus bergi* (Hemiptera: Cydnidae) from the Cauca Valley, Colombia. *Nematology* **7**:363-373.
15. Carta LK, Osbrink W. 2005. *Rhabditis rainai* n. sp. (Nematoda: Rhabditida) associated with the Formosan subterranean termite, *Coptotermes formosanus* (Isoptera: Rhinotermitidae). *Nematology* **7**:863-879.
16. Gerber K, Giblin-Davis RM. 1990. *Teratorhabditis palmarum* n. sp. (Nematoda: Rhabditidae): an associate of *Rhynchophorus palmarum* and *R. cruentatus*. *J Nematol* **22**:337-347.
17. Kanzaki N, Abe F, Giblin-Davis RM, Kiontke K, Fitch DHA, Hata K, Soné K. 2008. *Teratorhabditis synpapillata* Sudhaus, 1985 (Rhabditida: Rhabditidae) is an associate of the red palm weevil, *Rhynchophorus ferrugineus* (Coleoptera: Curculionidae). *Nematology* **10**:207-218.

Figure 3-source data 5. Estimates of morphological disparity of the stoma in Rhabditina. Groups compared were non-diplogastrid Rhabditina, monomorphic Diplogastridae, and dimorphic Diplogastridae. Disparity was measured as the principal component (PC) analysis volume and the sum of univariate variances. PC scores along the first two and three PC axes of Procrustes form and shape space, respectively, were used and are presented in the form mean±standard deviation (95% confidence interval). Eu, eurystomatous; St, stenostomatous.

Procrustes form-space				
Group	n	Rarefaction	Sum of variances	PCA volume
Non-diplogastrid Rhabditina	33	23	0.09±0.025 (0.046-0.144)	0.066±0.021 (0.032-0.112)
Monomorphic and St Diplogastridae	54	23	0.241±0.06 (0.135-0.367)	0.163±0.053 (0.078-0.279)
Monomorphic, Eu, and St Diplogastridae	77	23	0.218±0.041 (0.145-0.305)	0.13±0.032 (0.081-0.204)
St Diplogastridae	23	23	0.097±0.031 (0.043-0.166)	0.061±0.021 (0.027-0.109)
Eu Diplogastridae	23	23	0.068±0.027 (0.026-0.129)	0.044±0.02 (0.015-0.092)
Monomorphic Diplogastridae	31	23	**0.301±0.083 (0.151-0.475)**	**0.219±0.074 (0.099-0.383)**
Procrustes shape-space				
Group	n	Rarefaction	Sum of variances	PCA volume
Non-diplogastrid Rhabditina	33	23	0.0385±0.0045 (0.0297-0.0475)	0.0291±0.003 (0.023-0.0349)
Monomorphic and St Diplogastridae	54	23	0.0749±0.0082 (0.0584-0.0905)	0.0536±0.0076 (0.0386-0.0683)
Monomorphic, Eu, and St Diplogastridae	77	23	0.0705±0.0084 (0.0532-0.0865)	0.0513±0.0077 (0.0361-0.0661)
St Diplogastridae	23	23	0.0342±0.0132 (0.0117-0.0618)	0.0227±0.0107 (0.0063-0.0463)
Eu Diplogastridae	23	23	0.0205±0.0094 (0.0064-0.0411)	0.014±0.008 (0.0044-0.0329)
Monomorphic Diplogastridae	31	23	**0.0781±0.0105 (0.0575-0.0987)**	**0.0566±0.0093 (0.0386-0.0750)**

Figure 3-source data 6. Rates of stomatal evolution along the first principal component (PC) axis of Procrustes form- and shape-space. Rates were compared for non-diplogastrid Rhabditina (Rh), dimorphic Diplogastridae (Dm), and monomorphic Diplogastridae (Mn). Numbers indicate separate rate parameters for the designated groups. Model-averaged rates with standard deviation are shown.

Procrustes form-space						
Model (Rh-Dm-Mn)	Rate 1	Rate 2	Rate 3	-lnL	*k*	AICc
1-1-2	0.378±0.127	1.292±0.201	na	-38.682	3	**83.37**
1-2-3	0.340±0.124	0.438±0.136	1.273±0.202	-38.409	4	84.83
1-2-2	0.347±0.120	0.831±0.165	na	-41.330	3	88.67
1-1-1	0.644±0.145	na	na	-45.001	2	94.01
1-2-1	0.693±0.156	0.548±0.134	na	-44.073	3	94.15
Procrustes shape-space						
Model (Rh-Dm-Mn)	Rate 1	Rate 2	Rate 3	-lnL	*k*	AICc
1-2-3	0.044±0.012	0.094±0.029	0.244±0.06	38.107	4	**-68.20**
1-1-2	0.064±0.016	0.247±0.060	na	36.514	3	-67.02
1-2-2	0.042±0.011	0.169±0.039	na	35.585	3	-65.16
1-1-1	0.118±0.027	na	na	28.711	2	-53.41
1-2-1	0.125±0.031	0.104±0.026	na	29.468	3	-52.93

Figure 3-source data 7. Statistical comparison of non-nested models of stomatal evolution along the first principal component (PC) axis of Procrustes form- and shape-space using a chi-square distribution. Numbers indicate separate rate parameters for the designated groups. Rh, non-diplogastrid Rhabditina (Rh); Dm, dimorphic Diplogastridae; Mn, monomorphic Diplogastridae.

Procrustes form-space		
Null model (Rh-Dm-Mn)	Alternative model (Rh-Dm-Mn)	Chi-square p-values
1-1-1	1-2-1	0.2435
1-1-1	1-2-2	**0.0108**
1-1-1	1-1-2	**0.0011**
1-1-1	1-2-3	**0.0038**
1-2-1	1-2-3	**0.0058**
1-2-2	1-2-3	0.0923
1-1-2	1-2-3	0.7931
Procrustes shape-space		
Null model (Rh-Dm-Mn)	Alternative model (Rh-Dm-Mn)	Chi-square p-values
1-1-1	1-2-1	0.3236
1-1-1	1-2-2	**0.0007**
1-1-1	1-1-2	**0.0002**
1-1-1	1-2-3	**0.0002**
1-2-1	1-2-3	**0.0005**
1-2-2	1-2-3	0.1314
1-1-2	1-2-3	0.2968

Figure 3-source data 8. Highest posterior densities (HPD) of rates, and associated p-values obtained from two-tailed randomization tests, of stomatal form and shape evolution. Tests were performed for the branches assigned to non-diplogastrid Rhabditina, dimorphic Diplogastridae, and monomorphic Diplogastridae. CI, confidence interval.

Procrustes form-space				
Lineage	HPD mean (95% CI)	Non-diplogastrid Rhabditina	Dimorphic Diplogastridae	Monomorphic Diplogastridae
Non-diplogastrid Rhabditina	0.727 (0.117-1.482)	0.998		
Dimorphic Diplogastridae	1.402 (0.251-2.807)	0.391	0.987	
Monomorphic Diplogastridae	3.079 (0.606-7.335)	**0.041**	0.336	0.997
Procrustes shape-space				
Lineage	HPD mean (95% CI)	Non-diplogastrid Rhabditina	Dimorphic Diplogastridae	Monomorphic Diplogastridae
Non-diplogastrid Rhabditina	-1.074 (-1.523--0.560)	0.998		
Dimorphic Diplogastridae	-0.358 (-0.577--0.145)	**0.017**	0.998	
Monomorphic Diplogastridae	-0.282 (-0.525--0.053)	**0.012**	0.652	0.998

Figure 4-source data 1. Matrix of structures tabulated to measure stomatal complexity. Structures were recorded as described in text. Presence/absence of dimorphism is also given. 0 = absence, 1 = presence.

	Acrostichus cf. *nudicapitatus*	*Acrostichus halicti*	*Acrostichus rhynchophori*	*Allodiplogaster hylobii*	*Allodiplogaster* sp. 1	*Allodiplogaster sudhausi*	*Brevibucca saprophaga*	*Bunonema reticulatum*	*Bunonema* sp.	*Butlerius* sp.	*Caenorhabditis angaria*	*Caenorhabditis briggsae*
Complexity index	**3**	**4**	**3**	**5**	**6**	**5**	**0**	**0**	**0**	**3**	**1**	**1**
Glottoid apparatus[a]	0	0	0	0	0	0	0	0	0	0	1	1
Moveable dorsal tooth[a]	1	1	1	1	1	1	0	0	0	1	0	0
Fixed dorsal tooth[b]	0	0	0	0	0	0	0	0	0	0	0	0
Serratae on anterior gymnostom*	0	0	0	0	1	0	0	0	0	0	0	0
Pro-/mesostegomatal serratae*	0	0	0	0	0	0	0	0	0	0	0	0
Right subdorsal denticle[a]	0	0	0	0	0	0	0	0	0	0	0	0
Right subventral tooth[a]	0	0	0	1	1	1	0	0	0	0	0	0
Right subventral ridge of denticles[c]	0	0	0	0	0	0	0	0	0	0	0	0
Left subventral denticle or ridge*	1	1	1	1	1	1	0	0	0	0	0	0
Paired subventral denticles[a]	0	0	0	0	0	0	0	0	0	1	0	0
Duplicate left subventral ridge*	0	0	0	0	0	0	0	0	0	0	0	0
Right ventral denticle[c]	0	0	0	0	0	0	0	0	0	0	0	0
Lateral denticles[a]	0	1	0	0	0	0	0	0	0	0	0	0
Pairs of metastegostomatal rods[d]	0	0	0	0	0	0	0	0	0	0	0	0
Subventral stegostomatal warts[a]	0	0	0	0	0	0	0	0	0	0	0	0
Telostegostomatal ridge[e]	0	0	0	0	0	0	0	0	0	0	0	0
Triadial telostegostomatal points[d]	0	0	0	0	0	0	0	0	0	0	0	0
Dorsal, basal telostegostomatal fold*	0	0	0	0	0	0	0	0	0	0	0	0
Articulated apodemes[a]	0	0	0	1	1	1	0	0	0	0	0	0
Perradial telostegostomatal knobs[a]	0	0	0	0	0	0	0	0	0	0	0	0
Prostegostomatal row of denticles[b]	0	0	0	0	0	0	0	0	0	0	0	0
Gymnostomatal denticles[b]	0	0	0	0	0	0	0	0	0	0	0	0
Prostego-/gymnostomatal fold[e]	0	0	0	0	0	0	0	0	0	0	0	0
Radial gymnostomatal divisions*	0	0	0	0	0	0	0	0	0	0	0	0
Radial cheilostomatal divisions[a]	1	1	1	1	1	1	0	0	0	1	0	0
Stomatal dimorphism	0	1	0	1	1	1	0	0	0	0	0	0

[a]See Fürst von Lieven and Sudhaus (2000).
[b]See Fürst von Lieven (2000).
[c]See Kanzaki et al. (2012).
[d]See Herrmann et al. (2013).
[e]See Ragsdale et al. (2014).
*Original in this study.

Figure 4-source data 1, continued. Matrix of structures tabulated to measure stomatal complexity. Structures were recorded as described in text. Presence/absence of dimorphism is also given. 0 = absence, 1 = presence.

	Caenorhabditis elegans	*Choriorhabditis cristata*	*Cruznema tripartitum*	*Diplogasteriana* n. sp.	*Diplogasteriana schneideri*	*Diplogasteroides magnus*	*Diplogasteroides* sp.	*Diplogastrellus gracilis*	*Diplogastrellus (Metadiplogaster)* sp.	*Diploscapter* sp.	*Distolabrellus veechi*	*Eudiplogasterium levidentum*
Complexity index	**1**	**1**	**1**	**4**	**4**	**1**	**1**	**3**	**3**	**0**	**1**	**2**
Glottoid apparatus[a]	1	1	1	0	0	0	0	0	0	0	1	0
Moveable dorsal tooth[a]	0	0	0	1	1	1	1	1	1	0	0	1
Fixed dorsal tooth[b]	0	0	0	0	0	0	0	0	0	0	0	0
Serratae on anterior gymnostom*	0	0	0	0	0	0	0	0	0	0	0	0
Pro-/mesostegomatal serratae*	0	0	0	0	0	0	0	0	0	0	0	0
Right subdorsal denticle[a]	0	0	0	0	0	0	0	0	0	0	0	0
Right subventral tooth[a]	0	0	0	0	0	0	0	0	0	0	0	0
Right subventral ridge of denticles[c]	0	0	0	0	0	0	0	0	0	0	0	0
Left subventral denticle or ridge*	0	0	0	1	1	0	0	0	0	0	0	0
Paired subventral denticles[a]	0	0	0	0	0	0	0	1	1	0	0	0
Duplicate left subventral ridge*	0	0	0	0	0	0	0	0	0	0	0	0
Right ventral denticle[c]	0	0	0	0	0	0	0	0	0	0	0	0
Lateral denticles[a]	0	0	0	1	1	0	0	0	0	0	0	0
Pairs of metastegostomatal rods[d]	0	0	0	0	0	0	0	0	0	0	0	0
Subventral stegostomatal warts[a]	0	0	0	0	0	0	0	0	0	0	0	0
Telostegostomatal ridge[e]	0	0	0	0	0	0	0	0	0	0	0	0
Triadial telostegostomatal points[d]	0	0	0	0	0	0	0	0	0	0	0	0
Dorsal, basal telostegostomatal fold*	0	0	0	0	0	0	0	0	0	0	0	0
Articulated apodemes[a]	0	0	0	0	0	0	0	0	0	0	0	0
Perradial telostegostomatal knobs[a]	0	0	0	0	0	0	0	0	0	0	0	0
Prostegostomatal row of denticles[b]	0	0	0	0	0	0	0	0	0	0	0	0
Gymnostomatal denticles[b]	0	0	0	0	0	0	0	0	0	0	0	0
Prostego-/gymnostomatal fold[e]	0	0	0	0	0	0	0	0	0	0	0	0
Radial gymnostomatal divisions*	0	0	0	0	0	0	0	0	0	0	0	0
Radial cheilostomatal divisions[a]	0	0	0	1	1	0	0	1	1	0	0	1
Stomatal dimorphism	0	0	0	1	1	0	0	0	0	0	0	0

[a]See Fürst von Lieven and Sudhaus (2000).
[b]See Fürst von Lieven (2000).
[c]See Kanzaki et al. (2012).
[d]See Herrmann et al. (2013).
[e]See Ragsdale et al. (2014).
*Original in this study.

Figure 4-source data 1, continued. Matrix of structures tabulated to measure stomatal complexity. Structures were recorded as described in text. Presence/absence of dimorphism is also given. 0 = absence, 1 = presence.

	Fictor stercorarius	*Fictor* sp. 1	*Fictor* sp. 2	*Fuchsnema halleri*	*Fuchsnema* sp.	*Heterorhabditis bacteriophora*	*Koerneria luziae*	*Koerneria* sp.	*Leptojacobus dorci*	*Levipalatum texanum*	*Mehdinema alii*
Complexity index	**5**	**9**	**9**	**1**	**1**	**0**	**4**	**4**	**3**	**3**	**1**
Glottoid apparatus[a]	0	0	0	0	0	0	0	0	0	0	0
Moveable dorsal tooth[a]	1	1	1	1	1	0	1	1	1	1	1
Fixed dorsal tooth[b]	0	0	0	0	0	0	0	0	0	0	0
Serratae on anterior gymnostom*	0	1	1	0	0	0	0	0	0	0	0
Pro-/mesostegomatal serratae*	0	1	1	0	0	0	0	0	0	0	0
Right subdorsal denticle[a]	0	0	0	0	0	0	0	0	0	0	0
Right subventral tooth[a]	1	1	1	0	0	0	1	1	0	0	0
Right subventral ridge of denticles[c]	0	0	0	0	0	0	0	0	0	0	0
Left subventral denticle or ridge*	1	1	1	0	0	0	1	1	1	0	0
Paired subventral denticles[a]	0	0	0	0	0	0	0	0	0	0	0
Duplicate left subventral ridge*	0	1	1	0	0	0	0	0	0	0	0
Right ventral denticle[c]	0	0	0	0	0	0	0	0	0	0	0
Lateral denticles[a]	0	0	0	0	0	0	0	0	0	0	0
Pairs of metastegostomatal rods[d]	0	0	0	0	0	0	0	0	0	0	0
Subventral stegostomatal warts[a]	0	0	0	0	0	0	0	0	0	0	0
Telostegostomatal ridge[e]	0	0	0	0	0	0	0	0	0	1	0
Triadial telostegostomatal points[d]	1	1	1	0	0	0	0	0	0	0	0
Dorsal, basal telostegostomatal fold*	0	0	0	0	0	0	0	0	0	0	0
Articulated apodemes[a]	0	0	0	0	0	0	1	1	0	0	0
Perradial telostegostomatal knobs[a]	0	0	0	0	0	0	0	0	0	0	0
Prostegostomatal row of denticles[b]	0	0	0	0	0	0	0	0	0	0	0
Gymnostomatal denticles[b]	0	0	0	0	0	0	0	0	0	0	0
Prostego-/gymnostomatal fold[e]	0	0	0	0	0	0	0	0	0	1	0
Radial gymnostomatal divisions*	0	1	1	0	0	0	0	0	0	0	0
Radial cheilostomatal divisions[a]	1	1	1	0	0	0	0	0	1	0	0
Stomatal dimorphism	1	1	1	0	0	0	1	1	0	0	0

[a]See Fürst von Lieven and Sudhaus (2000).
[b]See Fürst von Lieven (2000).
[c]See Kanzaki et al. (2012).
[d]See Herrmann et al. (2013).
[e]See Ragsdale et al. (2014).
*Original in this study.

Figure 4-source data 1, continued. Matrix of structures tabulated to measure stomatal complexity. Structures were recorded as described in text. Presence/absence of dimorphism is also given. 0 = absence, 1 = presence.

	Mesorhabditis acidophila	*Micoletzkya buetschlii*	*Micoletzkya inedia*	*Micoletzkya japonica*	*Micoletzkya* sp.	*Mononchoides* sp. 1	*Mononchoides* sp. 2	*Mononchoides* sp. 3	*Myolaimus byersi*	*Neodiplogaster crenatae*	*Neodiplogaster* sp.
Complexity index	**1**	**4**	**4**	**4**	**4**	**8**	**6**	**6**	**0**	**4**	**4**
Glottoid apparatus[a]	1	0	0	0	0	0	0	0	0	0	0
Moveable dorsal tooth[a]	0	1	1	1	1	1	1	1	0	1	1
Fixed dorsal tooth[b]	0	0	0	0	0	0	0	0	0	0	0
Serratae on anterior gymnostom*	0	0	0	0	0	1	0	0	0	0	0
Pro-/mesostegomatal serratae*	0	0	0	0	0	1	0	0	0	0	0
Right subdorsal denticle[a]	0	0	0	0	0	1	1	1	0	0	0
Right subventral tooth[a]	0	1	1	1	1	1	1	1	0	1	1
Right subventral ridge of denticles[c]	0	0	0	0	0	0	0	0	0	0	0
Left subventral denticle or ridge*	0	1	1	1	1	1	1	1	0	0	0
Paired subventral denticles[a]	0	0	0	0	0	0	0	0	0	0	0
Duplicate left subventral ridge*	0	0	0	0	0	0	0	0	0	0	0
Right ventral denticle[c]	0	0	0	0	0	0	0	0	0	0	0
Lateral denticles[a]	0	0	0	0	0	0	0	0	0	0	0
Pairs of metastegostomatal rods[d]	0	0	0	0	0	0	0	0	0	0	0
Subventral stegostomatal warts[a]	0	0	0	0	0	0	0	0	0	0	0
Telostegostomatal ridge[e]	0	0	0	0	0	0	0	0	0	0	0
Triadial telostegostomatal points[d]	0	0	0	0	0	0	0	0	0	0	0
Dorsal, basal telostegostomatal fold*	0	0	0	0	0	1	1	1	0	0	0
Articulated apodemes[a]	0	0	0	0	0	0	0	0	0	0	0
Perradial telostegostomatal knobs[a]	0	0	0	0	0	0	0	0	0	1	1
Prostegostomatal row of denticles[b]	0	0	0	0	0	0	0	0	0	0	0
Gymnostomatal denticles[b]	0	0	0	0	0	0	0	0	0	0	0
Prostego-/gymnostomatal fold[e]	0	0	0	0	0	0	0	0	0	0	0
Radial gymnostomatal divisions*	0	0	0	0	0	0	0	0	0	0	0
Radial cheilostomatal divisions[a]	0	1	1	1	1	1	1	1	0	1	1
Stomatal dimorphism	0	1	1	1	0	1	1	1	0	0	1

[a]See Fürst von Lieven and Sudhaus (2000).
[b]See Fürst von Lieven (2000).
[c]See Kanzaki et al. (2012).
[d]See Herrmann et al. (2013).
[e]See Ragsdale et al. (2014).
*Original in this study.

Figure 4-source data 1, continued. Matrix of structures tabulated to measure stomatal complexity. Structures were recorded as described in text. Presence/absence of dimorphism is also given. 0 = absence, 1 = presence.

	Odontopharynx longicaudata	*Oigolaimella attenuata*	*Oigolaimella* sp.	*Oscheius carolinensis*	*Oscheius guentheri*	*Oscheius myriophila*	*Oscheius tipulae*	*Panagrellus redivivus*	*Parapristionchus giblindavisi*	*Parasitodiplogaster maxinema*	*Parasitorhabditis obtusa*
Complexity index	**3**	**3**	**3**	**1**	**1**	**1**	**1**	**0**	**4**	**3**	**0**
Glottoid apparatus[a]	0	0	0	1	1	1	1	0	0	0	0
Moveable dorsal tooth[a]	0	1	1	0	0	0	0	0	1	1	0
Fixed dorsal tooth[b]	1	0	0	0	0	0	0	0	0	0	0
Serratae on anterior gymnostom*	0	0	0	0	0	0	0	0	0	0	0
Pro-/mesostegomatal serratae*	0	0	0	0	0	0	0	0	0	0	0
Right subdorsal denticle[a]	0	0	0	0	0	0	0	0	0	0	0
Right subventral tooth[a]	0	1	1	0	0	0	0	0	1	1	0
Right subventral ridge of denticles[c]	0	0	0	0	0	0	0	0	0	0	0
Left subventral denticle or ridge*	0	0	0	0	0	0	0	0	1	0	0
Paired subventral denticles[a]	0	0	0	0	0	0	0	0	0	0	0
Duplicate left subventral ridge*	0	0	0	0	0	0	0	0	0	0	0
Right ventral denticle[c]	0	0	0	0	0	0	0	0	0	0	0
Lateral denticles[a]	0	0	0	0	0	0	0	0	0	0	0
Pairs of metastegostomatal rods[d]	0	0	0	0	0	0	0	0	0	0	0
Subventral stegostomatal warts[a]	0	0	0	0	0	0	0	0	0	0	0
Telostegostomatal ridge[e]	0	0	0	0	0	0	0	0	0	0	0
Triadial telostegostomatal points[d]	0	0	0	0	0	0	0	0	0	0	0
Dorsal, basal telostegostomatal fold*	0	0	0	0	0	0	0	0	0	0	0
Articulated apodemes[a]	0	0	0	0	0	0	0	0	0	1	0
Perradial telostegostomatal knobs[a]	0	0	0	0	0	0	0	0	0	0	0
Prostegostomatal row of denticles[b]	1	0	0	0	0	0	0	0	0	0	0
Gymnostomatal denticles[b]	1	0	0	0	0	0	0	0	0	0	0
Prostego-/gymnostomatal fold[e]	0	0	0	0	0	0	0	0	0	0	0
Radial gymnostomatal divisions*	0	0	0	0	0	0	0	0	0	0	0
Radial cheilostomatal divisions[a]	0	1	1	0	0	0	0	0	1	0	0
Stomatal dimorphism	0	0	0	0	0	0	0	0	1	1	0

[a]See Fürst von Lieven and Sudhaus (2000).
[b]See Fürst von Lieven (2000).
[c]See Kanzaki et al. (2012).
[d]See Herrmann et al. (2013).
[e]See Ragsdale et al. (2014).
*Original in this study.

Figure 4-source data 1, continued. Matrix of structures tabulated to measure stomatal complexity. Structures were recorded as described in text. Presence/absence of dimorphism is also given. 0 = absence, 1 = presence.

	Paroigolaimella micrura	*Paroigolaimella stresemanni*	*Pellioditis* sp.	*Pelodera cylindrica*	*Pelodera strongyloides*	*Pelodera teres*	*Poikilolaimus floridensis*	*Poikilolaimus oxycercus*	*Pristionchus elegans*	*Pristionchus fissidentatus*	*Pristionchus maupasi*
Complexity index	**3**	**3**	**1**	**1**	**1**	**1**	**1**	**1**	**5**	**6**	**4**
Glottoid apparatus[a]	0	0	1	1	1	1	1	1	0	0	0
Moveable dorsal tooth[a]	1	1	0	0	0	0	0	0	1	1	1
Fixed dorsal tooth[b]	0	0	0	0	0	0	0	0	0	0	0
Serratae on anterior gymnostom*	0	0	0	0	0	0	0	0	1	0	0
Pro-/mesostegomatal serratae*	0	0	0	0	0	0	0	0	0	0	0
Right subdorsal denticle[a]	0	0	0	0	0	0	0	0	0	0	0
Right subventral tooth[a]	0	0	0	0	0	0	0	0	1	1	1
Right subventral ridge of denticles[c]	0	0	0	0	0	0	0	0	0	1	0
Left subventral denticle or ridge*	0	0	0	0	0	0	0	0	1	1	1
Paired subventral denticles[a]	0	0	0	0	0	0	0	0	0	0	0
Duplicate left subventral ridge*	0	0	0	0	0	0	0	0	0	0	0
Right ventral denticle[c]	0	0	0	0	0	0	0	0	0	1	0
Lateral denticles[a]	0	0	0	0	0	0	0	0	0	0	0
Pairs of metastegostomatal rods[d]	0	0	0	0	0	0	0	0	0	0	0
Subventral stegostomatal warts[a]	1	1	0	0	0	0	0	0	0	0	0
Telostegostomatal ridge[e]	0	0	0	0	0	0	0	0	0	0	0
Triadial telostegostomatal points[d]	0	0	0	0	0	0	0	0	0	0	0
Dorsal, basal telostegostomatal fold*	0	0	0	0	0	0	0	0	0	0	0
Articulated apodemes[a]	0	0	0	0	0	0	0	0	0	0	0
Perradial telostegostomatal knobs[a]	0	0	0	0	0	0	0	0	0	0	0
Prostegostomatal row of denticles[b]	0	0	0	0	0	0	0	0	0	0	0
Gymnostomatal denticles[b]	0	0	0	0	0	0	0	0	0	0	0
Prostego-/gymnostomatal fold[e]	0	0	0	0	0	0	0	0	0	0	0
Radial gymnostomatal divisions*	0	0	0	0	0	0	0	0	0	0	0
Radial cheilostomatal divisions[a]	1	1	0	0	0	0	0	0	1	1	1
Stomatal dimorphism	0	0	0	0	0	0	0	0	0	1	1

[a]See Fürst von Lieven and Sudhaus (2000).
[b]See Fürst von Lieven (2000).
[c]See Kanzaki et al. (2012).
[d]See Herrmann et al. (2013).
[e]See Ragsdale et al. (2014).
*Original in this study.

Figure 4-source data 1, continued. Matrix of structures tabulated to measure stomatal complexity. Structures were recorded as described in text. Presence/absence of dimorphism is also given. 0 = absence, 1 = presence.

	Pristionchus pacificus	*Pristionchus uniformis*	*Protorhabditis* sp.	*Pseudodiplogasteroides* sp.	*Rhabditidoides* sp.	*Rhabditis brassicae*	*Rhabditis colombiana*	*Rhabditis rainai*	*Rhabditoides inermis*	*Rhabditolaimus* sp. 1	*Rhabditolaimus* sp. 2
Complexity index	**4**	**4**	**0**	**2**	**1**	**1**	**1**	**1**	**1**	**0**	**0**
Glottoid apparatus[a]	0	0	0	0	0	1	1	1	1	0	0
Moveable dorsal tooth[a]	1	1	0	1	1	0	0	0	0	0	0
Fixed dorsal tooth[b]	0	0	0	0	0	0	0	0	0	0	0
Serratae on anterior gymnostom*	0	0	0	0	0	0	0	0	0	0	0
Pro-/mesostegomatal serratae*	0	0	0	0	0	0	0	0	0	0	0
Right subdorsal denticle[a]	0	0	0	0	0	0	0	0	0	0	0
Right subventral tooth[a]	1	1	0	0	0	0	0	0	0	0	0
Right subventral ridge of denticles[c]	0	0	0	0	0	0	0	0	0	0	0
Left subventral denticle or ridge*	1	1	0	0	0	0	0	0	0	0	0
Paired subventral denticles[a]	0	0	0	0	0	0	0	0	0	0	0
Duplicate left subventral ridge*	0	0	0	0	0	0	0	0	0	0	0
Right ventral denticle[c]	0	0	0	0	0	0	0	0	0	0	0
Lateral denticles[a]	0	0	0	0	0	0	0	0	0	0	0
Pairs of metastegostomatal rods[d]	0	0	0	0	0	0	0	0	0	0	0
Subventral stegostomatal warts[a]	0	0	0	0	0	0	0	0	0	0	0
Telostegostomatal ridge[e]	0	0	0	0	0	0	0	0	0	0	0
Triadial telostegostomatal points[d]	0	0	0	0	0	0	0	0	0	0	0
Dorsal, basal telostegostomatal fold*	0	0	0	0	0	0	0	0	0	0	0
Articulated apodemes[a]	0	0	0	0	0	0	0	0	0	0	0
Perradial telostegostomatal knobs[a]	0	0	0	0	0	0	0	0	0	0	0
Prostegostomatal row of denticles[b]	0	0	0	0	0	0	0	0	0	0	0
Gymnostomatal denticles[b]	0	0	0	0	0	0	0	0	0	0	0
Prostego-/gymnostomatal fold[e]	0	0	0	1	0	0	0	0	0	0	0
Radial gymnostomatal divisions*	0	0	0	0	0	0	0	0	0	0	0
Radial cheilostomatal divisions[a]	1	1	0	0	0	0	0	0	0	0	0
Stomatal dimorphism	0	1	0	0	0	0	0	0	0	0	0

[a]See Fürst von Lieven and Sudhaus (2000).
[b]See Fürst von Lieven (2000).
[c]See Kanzaki et al. (2012).
[d]See Herrmann et al. (2013).
[e]See Ragsdale et al. (2014).
*Original in this study.

Figure 4-source data 1, continued. Matrix of structures tabulated to measure stomatal complexity. Structures were recorded as described in text. Presence/absence of dimorphism is also given. 0 = absence, 1 = presence.

	Sachsia zurstrasseni	*Strongyloides ratti*	*Sudhausia aristotokia*	*Sudhausia crassa*	*Teratodiplogaster* sp. 1	*Teratodiplogaster* sp. 2	*Teratorhabditis mariannae*	*Teratorhabditis palmarum*	*Teratorhabditis synpapillata*	*Tylopharynx foetida*	*Zeldia punctata*
Complexity index	**2**	**0**	**3**	**3**	**2**	**2**	**1**	**1**	**1**	**3**	**0**
Glottoid apparatus[a]	0	0	0	0	0	0	1	1	1	0	0
Moveable dorsal tooth[a]	1	0	1	1	1	1	0	0	0	1	0
Fixed dorsal tooth[b]	0	0	0	0	0	0	0	0	0	0	0
Serratae on anterior gymnostom*	0	0	0	0	0	0	0	0	0	0	0
Pro-/mesostegomatal serratae*	0	0	0	0	0	0	0	0	0	0	0
Right subdorsal denticle[a]	0	0	0	0	0	0	0	0	0	0	0
Right subventral tooth[a]	0	0	0	0	1	1	0	0	0	1	0
Right subventral ridge of denticles[c]	0	0	0	0	0	0	0	0	0	0	0
Left subventral denticle or ridge*	0	0	0	0	0	0	0	0	0	0	0
Paired subventral denticles[a]	0	0	0	0	0	0	0	0	0	0	0
Duplicate left subventral ridge*	0	0	0	0	0	0	0	0	0	0	0
Right ventral denticle[c]	0	0	0	0	0	0	0	0	0	0	0
Lateral denticles[a]	0	0	0	0	0	0	0	0	0	0	0
Pairs of metastegostomatal rods[d]	0	0	1	1	0	0	0	0	0	0	0
Subventral stegostomatal warts[a]	0	0	0	0	0	0	0	0	0	0	0
Telostegostomatal ridge[e]	0	0	0	0	0	0	0	0	0	0	0
Triadial telostegostomatal points[d]	0	0	1	1	0	0	0	0	0	0	0
Dorsal, basal telostegostomatal fold*	0	0	0	0	0	0	0	0	0	0	0
Articulated apodemes[a]	0	0	0	0	0	0	0	0	0	0	0
Perradial telostegostomatal knobs[a]	0	0	0	0	0	0	0	0	0	1	0
Prostegostomatal row of denticles[b]	0	0	0	0	0	0	0	0	0	0	0
Gymnostomatal denticles[b]	0	0	0	0	0	0	0	0	0	0	0
Prostego-/gymnostomatal fold[e]	0	0	0	0	0	0	0	0	0	0	0
Radial gymnostomatal divisions*	0	0	0	0	0	0	0	0	0	0	0
Radial cheilostomatal divisions[a]	1	0	0	0	0	0	0	0	0	0	0
Stomatal dimorphism	0	0	0	0	0	0	0	0	0	0	0

[a]See Fürst von Lieven and Sudhaus (2000).
[b]See Fürst von Lieven (2000).
[c]See Kanzaki et al. (2012).
[d]See Herrmann et al. (2013).
[e]See Ragsdale et al. (2014).
*Original in this study.

GENETICS

2016 © The Authors, some rights reserved; exclusive licensee American Association for the Advancement of Science. Distributed under a Creative Commons Attribution NonCommercial License 4.0 (CC BY-NC).
10.1126/sciadv.1501031

Large-scale diversification without genetic isolation in nematode symbionts of figs

Vladislav Susoy,[1] Matthias Herrmann,[1] Natsumi Kanzaki,[2] Meike Kruger,[3] Chau N. Nguyen,[4] Christian Rödelsperger,[1] Waltraud Röseler,[1] Christian Weiler,[1] Robin M. Giblin-Davis,[5] Erik J. Ragsdale,[6]* Ralf J. Sommer[1]*

Diversification is commonly understood to be the divergence of phenotypes accompanying that of lineages. In contrast, alternative phenotypes arising from a single genotype are almost exclusively limited to dimorphism in nature. We report a remarkable case of macroevolutionary-scale diversification without genetic divergence. Upon colonizing the island-like microecosystem of individual figs, symbiotic nematodes of the genus *Pristionchus* accumulated a polyphenism with up to five discrete adult morphotypes per species. By integrating laboratory and field experiments with extensive genotyping of individuals, including the analysis of 49 genomes from a single species, we show that rapid filling of potential ecological niches is possible without diversifying selection on genotypes. This uncoupling of morphological diversification and speciation in fig-associated nematodes has resulted from a remarkable expansion of discontinuous developmental plasticity.

INTRODUCTION

Radiations of species into underused habitats are a basic generator of biological diversity, and their results can be observed at all evolutionary depths and in most groups of living organisms (*1*, *2*). A fundamental principle of diversification is that phenotypic divergence coincides with or follows lineage branching, or speciation (*3*–*5*). However, the ability of "diverging selection" to occur within species, specifically those with discrete developmental plasticity, or polyphenism, suggests that morphological divergence need not be linked to lineage diversification (*6*). This phenomenon has been mostly observed as dimorphism, whereas examples of a greater number of divergent developmental phenotypes from a single genotype are exceedingly rare, usually limited to mating types, seasonal morphs, or clonal individuals with a common ecological function (*7*–*10*).

Here, we describe a remarkable case of extreme trophic diversification uncoupled from genetic isolation by the multiplication of a developmental polyphenism. We report exaggerated variation of feeding morphs within each of seven previously unknown nematode species (Fig. 1). All of these species were found in association with figs and their pollinator wasps, with the latter being known to transmit wasp-parasitic and floret-feeding nematodes (*11*–*16*). We analyze three new nematode species that have expanded an ancestral dimorphism to establish several new morphs and trophic guilds within figs. We describe the new species as *Pristionchus borbonicus* sp. nov., *Pristionchus sycomori* sp. nov., and *Pristionchus racemosae* sp. nov. (Phylum Nematoda, Family Diplogastridae), which were isolated from the figs *Ficus mauritiana* (La Réunion Island), *Ficus sycomorus* (South Africa), and *Ficus racemosa* (Vietnam) and their agaonid pollinators *Ceratosolen coecus*, *Ceratosolen arabicus*, and *Ceratosolen fusciceps*, respectively.

[1]Max Planck Institute for Developmental Biology, Department of Evolutionary Biology, Spemannstraße 37, Tübingen 72076, Germany. [2]Forest Pathology Laboratory, Forestry and Forest Products Research Institute, 1 Matsunosato, Tsukuba, Ibaraki 305-8687, Japan. [3]Department of Genetics, University of Pretoria, Pretoria 0002, South Africa. [4]Institute of Ecology and Biological Resources, Vietnam Academy of Science and Technology, 18 Hoang Quoc Viet Road, Hanoi, Vietnam. [5]Fort Lauderdale Research and Education Center, University of Florida–IFAS, 3205 College Avenue, Fort Lauderdale, FL 33314, USA. [6]Department of Biology, Indiana University, 915 East 3rd Street, Bloomington, IN 47405, USA.
*Corresponding author. E-mail: ragsdale@indiana.edu (E.J.R.); ralf.sommer@tuebingen.mpg.de (R.J.S.)

RESULTS

Extreme disparity of forms in an island-like microecosystem

Initial observations indicated that *Pristionchus* nematodes associated with figs show a high degree of morphological variation among adult forms, especially in their feeding structures. To determine the extent of this variation, we examined hundreds of nematode individuals and uncovered five distinct morphotypes associated with each of the three fig species mentioned above. Morphs associated with a single fig species differed qualitatively in their mouthpart complexity, or the total number of spatially independent structures or "cusps" arising from the nematode stoma (*17*), including the presence and number of movable teeth, serrated plates, and labial appendages (Figs. 1 and 2A). Furthermore, the shape and size of mouthparts for different morphs were strikingly disparate. Specifically, principal components analysis (PCA) of the geometric morphometrics of mouth shape and form (the latter including landmark-derived shape data + log centroid size) (*18*, *19*) showed the five morphs in each fig species to occupy different parts of Procrustes morphospace with no or little overlap in shape, form, or both (Fig. 2B). Overall, the degree of discontinuous morphological variation that we observed between individuals from figs exceeded that observed between nominal genera of the same family (*17*) and among all other examined species of *Pristionchus* combined (Fig. 3), with some morphs exhibiting fantastic structures that, to our knowledge, have no analogs in other known nematodes (Figs. 1, C and E, and 2A).

Morphological diversity from single genotypes

Despite the disparity of adult nematode morphotypes discovered in individual figs, we surprisingly found that all *Pristionchus* nematodes isolated from a given fig species always had identical 18S ribosomal RNA (rRNA) sequences. This suggested that the diverse participants identified in each microecosystem belonged to a single species. To confirm species identity, we sampled the putative genetic diversity of multiple individuals of all morphotypes for each *Pristionchus* species in question. To do this, we sequenced the individual genomes of 49 specimens of *P. borbonicus*, and we sequenced rapidly evolving mitochondrial genes (*20*) for *P. sycomori* and *P. racemosae*. The genetic distance within each species was smaller than that between isolates of its selfing

Downloaded from http://advances.sciencemag.org/ on February 10, 2016

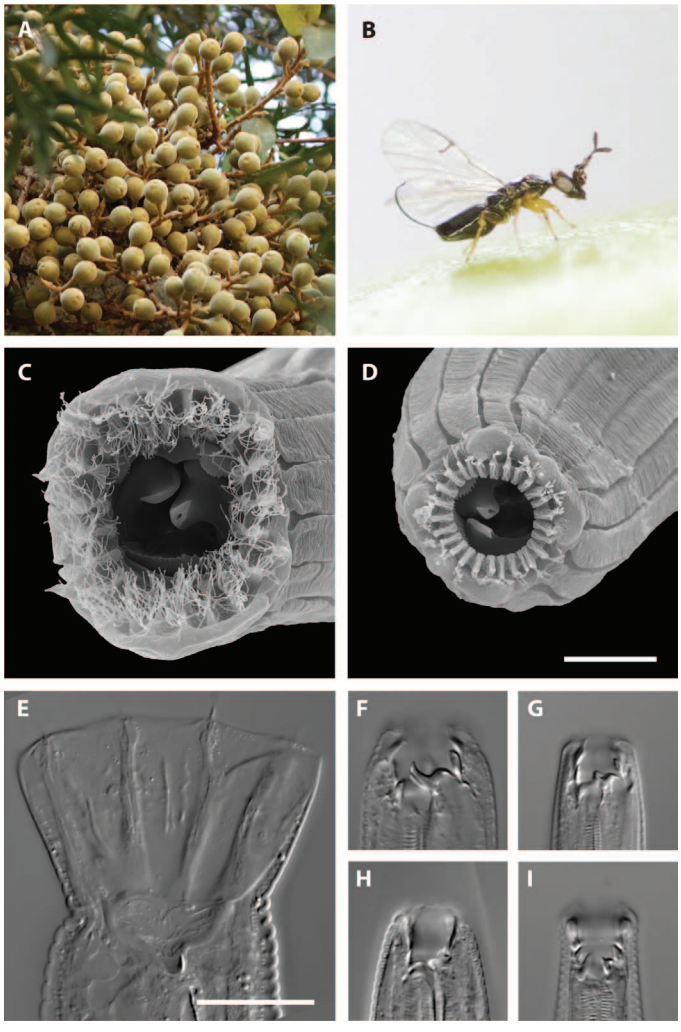

Fig. 1. Novelties and morphological diversity of nematode symbionts of figs. (**A**) Symbionts in the nematode genus *Pristionchus* are obligate associates of figs, such as *F. sycomorus* (shown here), in the African and Oriental tropics. (**B**) Fig-associated nematodes require transmission by pollinating wasps (*Ceratosolen* spp.), only a few of which are usually received by a given fig. (**C** and **D**) Two morphotypes (morphs I and II) of *P. borbonicus*, a symbiont of *F. mauritiana*. The beard-like labial morphology is a novelty known only for this species and *P. sycomori*. Scale bar, 10 μm. (**E** to **I**) Five alternative morphotypes of *P. racemosae*, a symbiont of the Australasian fig *F. racemosa*. Divergence of these morphs within species and with respect to the most closely related known fig associates is so great as to obscure homologies of traits or the morphs themselves. Scale bar, 20 μm.

congener *Pristionchus pacificus*: nucleotide diversity for *P. borbonicus* ($\pi = 0.0002$), in particular, was an order of magnitude lesser than for individual lineages of *P. pacificus* ($\pi = 0.002$) (*21*), and mitochondrial DNA (mtDNA) maximal sequence divergence between isolates of *P. sycomori* ($\hat{p} = 0.01$) and *P. racemosae* ($\hat{p} = 0.027$) was lesser than that for corresponding regions in *P. pacificus* ($\hat{p} = 0.054$ and $\hat{p} = 0.064$). To test whether genetic differences corresponded to any population structure among different morphotypes, we inferred a genotype network of more than 10,500 single-nucleotide polymorphic sites for individuals of *P. borbonicus* and mitochondrial haplotype networks for both *P. sycomori* and *P. racemosae*. No grouping of individuals by morphotype was observed, and different morphs instead had similar or identical haplotypes (Fig. 2, C to E). These results indicate the absence of reproductive isolation between different morphotypes within each species and that these morphotypes represent extreme intraspecific variation, possibly a polyphenism.

Condition dependence of diverse morphotypes

We next investigated the possibility that alternative morphotypes were the result of a polyphenism, specifically of condition-dependent induction. Examination of nematode populations in figs of *F. mauritiana* and *F. sycomorus* yielded four observations supporting polyphenism. First, surveys of nematodes by fig phase revealed differences in ratios of *Pristionchus* morphs between early and late interfloral figs. In figs that had recently received their pollinators, only a single minute, microbivorous morph of the associated *Pristionchus* species (morph V) emerged (Fig. 4A). Sequencing of individual nematodes present on the bodies of wasps that were captured exiting figs had confirmed that nematode species observed in figs, including *Pristionchus* spp., were transmitted as developmentally arrested (dauer) juveniles by the wasps (table S1). Therefore, morph V of *P. borbonicus* and *P. sycomori* represents postdispersal adults that are brought to young, receptive figs. Second, in generations of nematodes following this colonization event, morph V was never present, and instead, individuals of the four other morphs, including three types of putative carnivores (morphs I to III), were found (Fig. 4A and table S2). Third, observations of very late interfloral-phase figs revealed the occurrence of dauer larvae as progeny of morphs I to IV. After passage through the fig-wasp vector, these dauer larvae form phenotypes of morph V in early interfloral figs. Finally, we observed differences in ratios between sexes, suggesting that these morphs are induced from a single genotype in a sexually dimorphic manner (Fig. 4A), as described for the mouth polyphenism of other *Pristionchus* species (*22*).

To test whether different morphs were possible from the same nematode line, we developed a protocol to successfully rear one generation of fig-associated nematodes in laboratory culture. Indeed, we found that postdispersal adults (morph V) gave rise to an alternative nonpredatory morph of unknown function (morph IV) under laboratory conditions. Because nematodes could not be cultured further outside of the fig, environmental cues inducing the other morphs could not be identified. Taken together, surveys of nematode populations by fig phase and laboratory experiments indicate that the multiple morphs of fig-associated *Pristionchus* are the result of polyphenism and not genetic polymorphism.

Evidence for resource polyphenism

To test putative feeding specializations of individual morphs, we first inspected the behavior of nematode morphs in the laboratory. We found morphs I to III to be able to attack, kill, and feed on specimens of *Acrostichus* sp. and *Teratodiplogaster* sp., which frequently co-occur in the same figs (table S3). In addition, we screened the 49 genomes of individual specimens of *P. borbonicus* for the presence of non-*Pristionchus* nematode sequences. The presence of such sequences, presumably from the guts of sequenced individuals, would be an additional indicator of predatory behavior in the wild. Indeed, several individual genomes of morphs I and II showed an abundance of sequence reads for *Acrostichus* sp. and *Teratodiplogaster* sp., whereas such reads were not detected at high levels in morphs III to V (Fig. 4B). Thus, our metagenomic analysis distinguished morphs I and II as predators of other nematodes. A more detailed analysis of the feeding specializations of fig-associated *Pristionchus* awaits future studies of these minute animals in their tropical settings.

Downloaded from http://advances.sciencemag.org/ on February 10, 2016

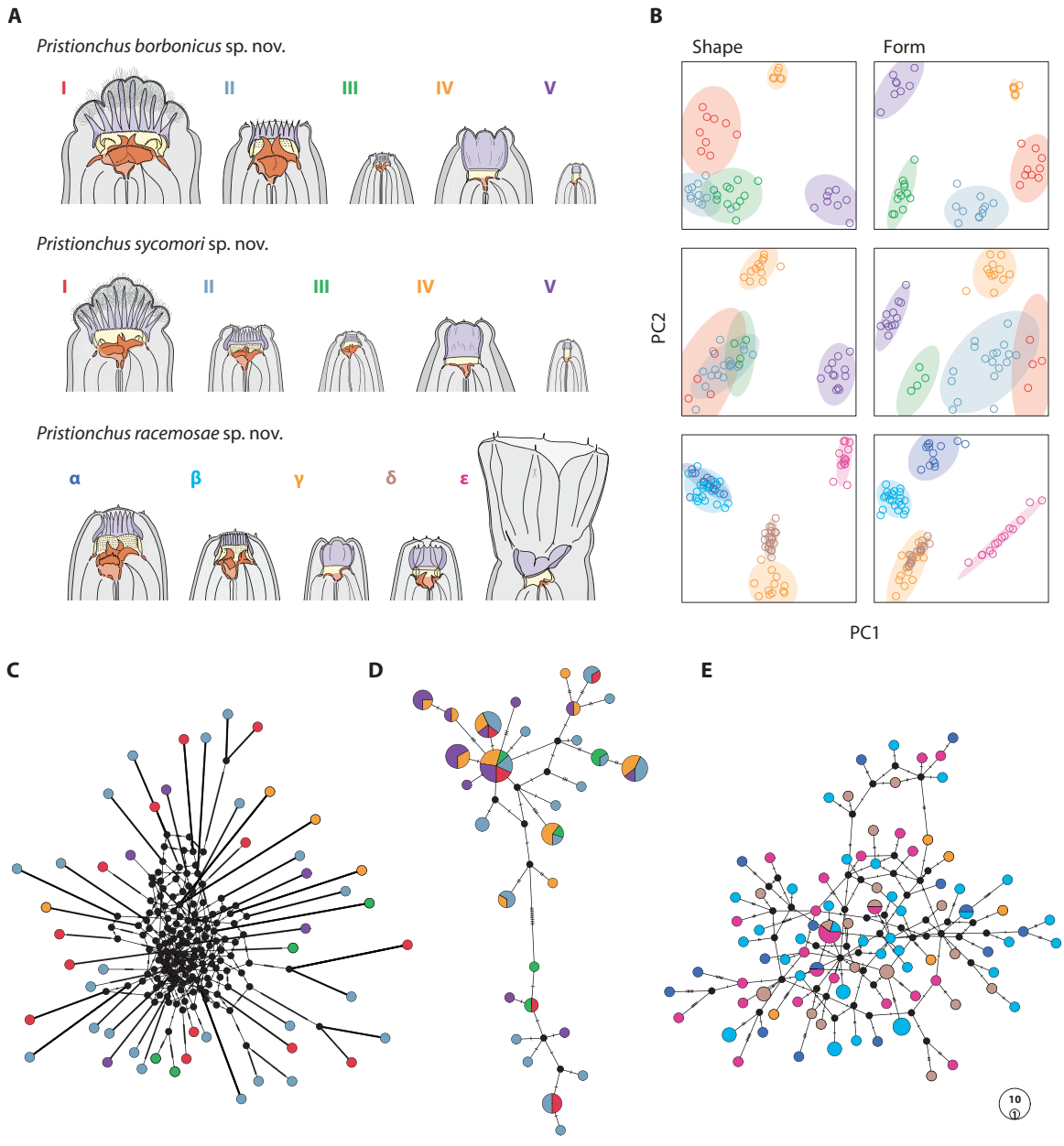

Fig. 2. Genetic and phenotypic diversity in fig-associated *Pristionchus* nematodes. (**A**) Discrete adult morphs of *P. borbonicus*, *P. sycomori*, and *P. racemosae*. Homologous mouthpart regions are color-coded across morphs and species. (**B**) Projections of the first two principal components of mouth shape and form (PC1, principal component 1; PC2, principal component 2). Colors indicate morphs, as coded by labels in (A). Ovals represent a 95% confidence interval of the mean. (**C**) Genotype network for 49 individuals of *P. borbonicus* based on 10,500 single-nucleotide polymorphic sites. (**D**) Haplotype network for 77 individuals of *P. sycomori* based on sequences of *ND1*, *Cytb*, and *COI* genes. (**E**) Haplotype network for 104 individuals of *P. racemosae* based on sequences of the *COI* gene. (C to E) Each circle represents a unique genotype or haplotype and is colored according to morphs, as coded by labels in (A); if greater than 1, pairwise differences between joined haplotypes are denoted by hatch marks and vertices, with the latter also showing theoretical intermediate nodes introduced by the algorithm; the size of circles is proportional to the number of individuals sharing the same haplotype.

Macroevolution via alternative phenotypes

Having uncovered a novel polyphenism of unprecedented complexity, we then explored the implications of such plasticity for macroevolution, or change following speciation events. Geometric morphometrics and PCA revealed that the addition of multiple morphs in fig-associated nematodes was accompanied by rapid divergence among morphs. Not only did some added morphs fall completely outside the range of phenotypes in other *Pristionchus* species, some morphs were irreconcilable with any of those of other species (for example, morphs I and V of *P. borbonicus* and *P. sycomori* and morph ε of *P. racemosae*) (Fig. 3A). Thus, diverging selection has occurred so rapidly that homologies of most morphs between African and Vietnamese lineages, which

Downloaded from http://advances.sciencemag.org/ on February 10, 2016

are both associated with a relatively narrow clade of host trees/wasps (*23*), can no longer be determined in terms of either morphometrics or presence of qualitative structures (Figs. 1, 2A, 3A, and 5). Given the degree of disparity between morphs of dubious homology, it is possible that diverging selection among morphs has been supplemented by the loss and gain of new or recurring alternative morphotypes, resulting in intraspecific divergence within lineage diversification (Fig. 3B).

DISCUSSION

Multiplication of morphs and morphological diversification without speciation

Here, we have revealed an extreme case of morphological diversification without genetic divergence or isolation. This intraspecific disparity was observed particularly in adult mouthparts, which in a phylum of animals relatively limited in external morphology are widely regarded as the primary trait for determining their position in the food web (*24*). Even before a complete account of the natural history of this unusual system has been achieved, based on morphological, behavioral, and metagenomic evidence, we speculate that the diversity of feeding forms reflects large-scale ecological diversification. For example, the small microbivorous morph (V) of *P. borbonicus* and *P. sycomori* may develop fast to compete for an ephemeral bacterial food source, a common strategy in nematodes with simple, tube-like mouths (*25*). In contrast, predatory morphs emerge in the following generations, coincident with the proliferation of cohabiting wasp-transmitted nematodes in the fluid-filled cavities retained within the figs. In the examined African figs, other nematode species include plant parasites (*Schistonchus* spp. and *Bursaphelenchus* spp.), wasp parasites (*Parasitodiplogaster*

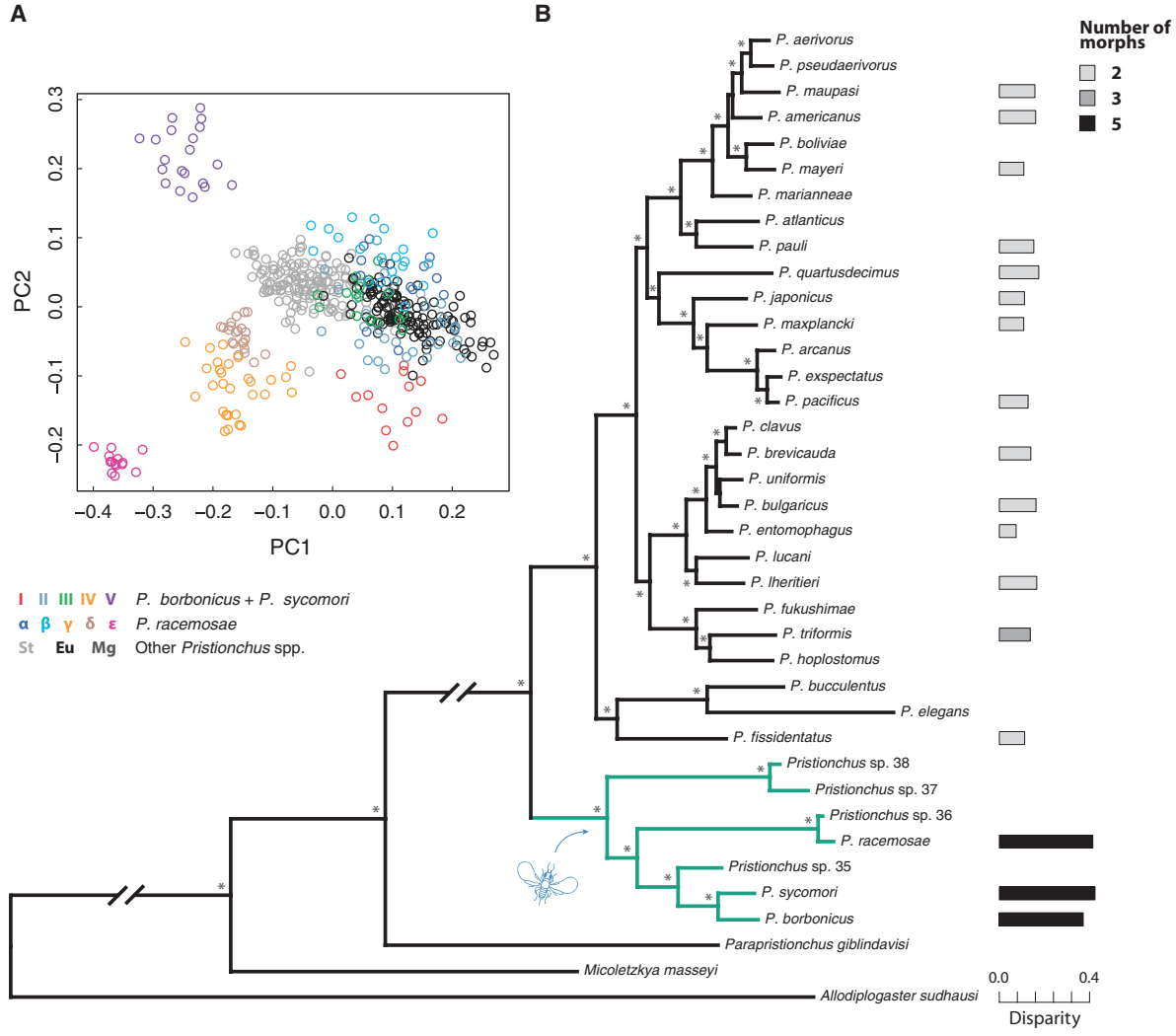

Fig. 3. Macroevolutionary disparity in fig symbionts relative to other *Pristionchus* species. (**A**) PCA of the mouth shape of 18 species of *Pristionchus* (PC1, principal component 1; PC2, principal component 2). Colors indicate morphs. (**B**) Phylogeny of *Pristionchus* spp. inferred from 18*S* and 28*S* rRNA genes and 27 ribosomal protein genes. Lineages that have radiated following a presumptively single fig colonization event are shown in green. Bars show disparity between morphs of selected polyphenic species, which was measured as maximal Euclidean pairwise distance in the morphospace between morph means. The color of bars is proportional to the number of morphs observed for a given fig-associated species. St, Eu, and Mg represent the two to three possible morphs in other *Pristionchus* species. Asterisk represents node support of 100% posterior probability.

Downloaded from http://advances.sciencemag.org/ on February 10, 2016

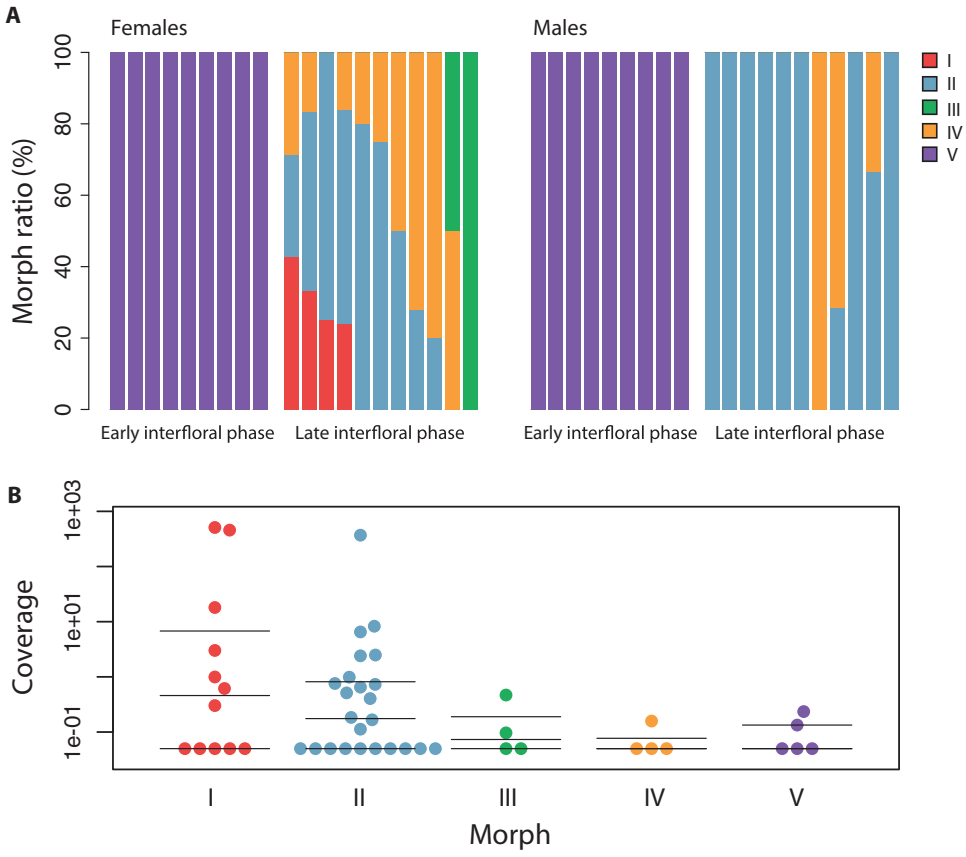

Fig. 4. Conditional dependence and sexual dimorphism of morph production in individual figs. (**A**) Individuals of *P. sycomori* in figs shortly after pollination are exclusively of the microbivorous morph in both males and females. In later stages of fig development, concomitant with the increase in complexity especially attributable to the presence and action of other wasp-transmitted nematode species, subsequent generations of *Pristionchus* nematodes give rise to alternative morphs, including both of predatory and of novel unknown function. Each bar represents the morph ratio in a single fig, with males and females for that fig represented in corresponding columns. Columns for late interfloral phase figs, which were not separated further by age, are ordered by composition only. (**B**) Predation in different morphs of *P. borbonicus*. Normalized coverage of 18*S* rRNA genes of non-*Pristionchus* nematodes detected in genomes of 49 individuals of *P. borbonicus* is shown. Thin lines mark 0.25, 0.5, and 0.75 quantiles.

spp.), omnivores (*Acrostichus* spp.), microbivores (*Caenorhabditis* spp.), and putative fungivores (*Teratodiplogaster* spp.) (table S3). Moreover, this intraspecific character displacement that has allowed niche partitioning within each nematode species is enabling *Pristionchus* nematodes to exploit the fig microecosystem in apparently novel, unknown ways, as indicated by at least one unprecedented form (morph ε) in the Vietnamese fig-associated *P. racemosae*. What makes this diversification remarkable is that the various morphotypes of all species were expressed at the same life stage, suggesting a hierarchy of developmental switches, in contrast to the ecological divergence that is typically limited to different developmental stages, as is common in zooplankton, holometabolous insects, and other nematodes.

Conditions for diversification without genetic isolation

The ability to produce any of five morphotypes at a single developmental stage, as evidenced by divergent feeding morphologies, is surprising in the absence of genetic isolation. The apparent uniqueness of this system therefore demands some explanation. First, a significant (albeit not exclusive) feature of *Pristionchus* fig symbionts is the ancestral presence of a feeding dimorphism (*17*) and its associated developmental switch (*22*), which may have disposed alternative morphs to relaxed selection on conditionally expressed phenotypes (*26*, *27*). Indeed, the macroevolutionary maintenance of this dimorphism apparently led to increased rates of morphological evolution in this nematode family (*17*) and thus may also have facilitated the genetic variation needed to add successive switches to the mouth polyphenism. Alternatively, an ancestral polyphenism may have facilitated the recurrence of forms, allowing the rapid re-establishment of morphotypes (*6*) to result in a multiplied polyphenism. For example, morphs α and β of *P. racemosae* show characters (that is, stomatal rugae) that are absent from all other *Pristionchus* and its closest outgroups but are present in distant lineages of Diplogastridae (*17*), indicating the possibility of recurrence, if not uncanny convergent evolution. A second distinguishing feature is the bottlenecked vertical transmission of nematodes by their insect vectors. This mode of transmission presumably precludes the reliable transmission of multiple genetically distinct morphs to new figs, which may have promoted the maintenance of polyphenism over genetic assimilation of alternative phenotypes. Third, the small physical dimensions and spatially overlapping niches within figs may simply preclude genetic isolation in sympatry. In principle, character displacement between "allopatric" species (that is, species coevolved with fig and wasp

Downloaded from http://advances.sciencemag.org/ on February 10, 2016

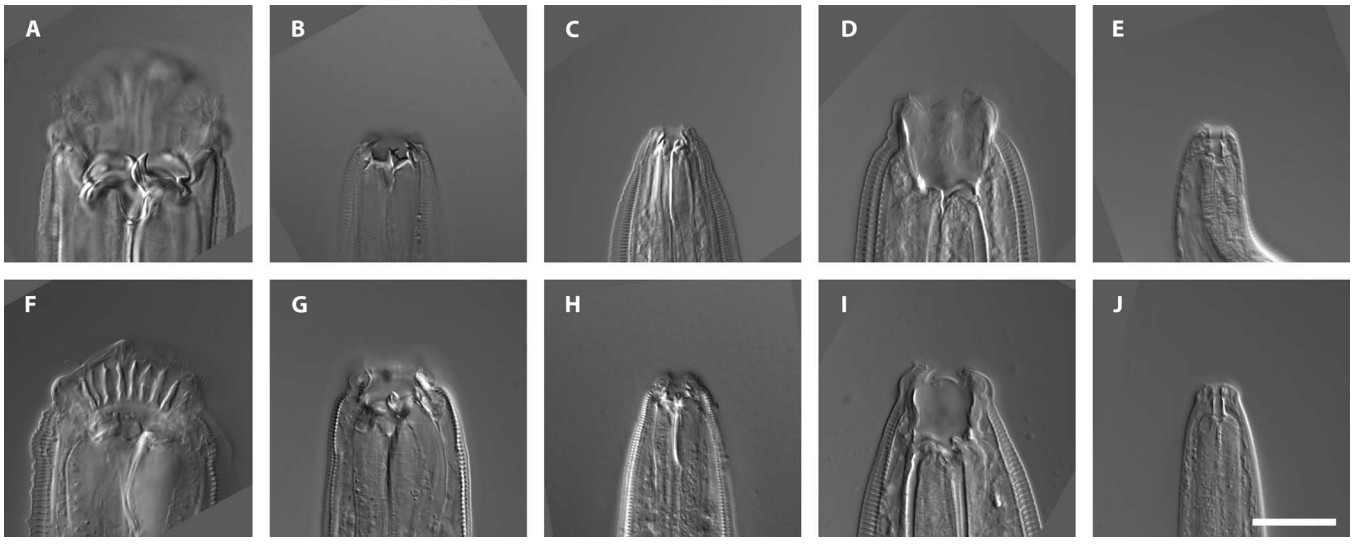

Fig. 5. Discrete morphs present in *P. borbonicus* (A to E) and *P. sycomori* (F to J). For both species, morphs are (from left to right) as follows: I, II, III, IV, and V. Scale bar, 20 μm.

hosts) with multiple phenotypes, which in this case would result from host switching by the wasp vector, could ultimately lead to the genetic assimilation of alternative forms in competing species (*28*). However, the repeated occurrence of five morphs suggests that any possible competition between otherwise allopatric species is not prevalent enough in this system to have led to the assimilation of alternative morphotypes in different species.

Conclusions

In summary, given the "empty niche" conditions predisposing an ecosystem to the trophic diversification of its colonists (in particular, low ecological complexity, previously limited immigration of species, and underutilized resources) (*2*), a pre-existing polyphenism, and vertically transmitted founder populations could have together facilitated macroevolutionary-scale diversification in fig-associated nematodes without lineage splitting. Despite the idiosyncrasies of the fig microecosystem, our findings support the prediction that "stem plasticity" in a lineage allows diversifying selection into multiple ecological roles (*6*, *29*). Thus, our findings reveal an alternative possibility to the principle that substantial phenotypic evolution only follows periods of speciation (*1*, *30*) and that developmental plasticity can lead to the multiplication of discontinuous novelties from a single genotype.

Taxonomy

P. borbonicus Susoy, Kanzaki, Herrmann, Ragsdale, and Sommer sp. nov. (Phylum Nematoda Potts, 1932; Order Rhabditida Chitwood, 1933; Family Diplogastridae Kreis, 1932).

Etymology. The species epithet is the Latin adjectival demonym for Île Bourbon, the former name for the island of the type locality of this species.

Holotype. Adult female of morph I is deposited in the University of California Riverside Nematode Collection (UCRNC).

Paratypes. Ten paratypes are deposited in the UCRNC, whereas 10 paratypes are deposited in the Swedish Museum of Natural History (Stockholm, Sweden).

Locality. Type specimens were collected at Grand Étang, La Réunion Island.

Type host and vector. Type specimens were isolated from within sycones of *F. mauritiana* Lamarck, 1788 (Moraceae), in association with *C. coecus* Coquerel, 1855 (Hymenoptera: Agaonidae).

Description. Body habitus, pharynx, female reproductive tract, male testis, and positions of ventral body openings are typical of *Pristionchus* nematodes (Fig. 1, C and D, Fig. 2A, and Fig. 5, A to E). Cuticle with fine annulation and thick, offset longitudinal alae are found on the entire body diameter, extending from the labial region to the tail, except for morph V, in which ridges are indistinct. Adults consist of five morphs. Because these morphs are of uncertain homology with respect to the eurystomatous and stenostomatous morphs of other *Pristionchus* species, we adopt a neutral nomenclature (that is, morphs I to V) for the new species:

Morph I: Body larger than those of other morphs, head widening just anterior to the labial region; lips large, lateral lips higher and wider than subventral and subdorsal lips; labial region with conspicuous "beard" (a circumstomatal ring of thin cuticular filaments originating from anterior cheilostom); pre-gymnostomatal cheilostom twice as high as gymnostom, with anteriorly tapering rugae separated from each other for most of their length; gymnostom thick, barrel-shaped, overlapping cheilostom for most of height, finely serrated at anterior margin; pro-mesostegostom projecting into one dorsal and two subventral anteriorly serrated lobes; metastegostom with claw-like dorsal tooth, claw-like right subventral tooth, and large, coarsely serrated left subventral ridge extending dorsally past most of the dorsal tooth; postdental region (telostegostom) deeper ventrally than dorsally, sclerotized.

Morph II: Head narrowing just anterior to the labial region; with six offset lips, lateral lips smaller than subventral and subdorsal lips; pre-gymnostomatal cheilostom same height as gymnostom, with closely spaced, tapering rugae, each tipped with several filaments and extending past the stomatal opening; gymnostom with thick walls, overlapping cheilostom for most of height, with heavy punctation and fine anterior serration; pro-mesostegostom with small projecting, serrated lobes; meta- and telostegostom as in morph I.

Morph III: Head tapered, with small but distinct lips; stoma small; cheilostom with sharp anterior taper, with minute, tightly packed rugae not extending past the stomatal opening; gymnostom thin, barrel-shaped,

Downloaded from http://advances.sciencemag.org/ on February 10, 2016

overlapping cheilostom for most of height, with fine punctation; small projecting lobes in mesostegostom indistinct or absent; metastegostom with small dorsal and right subventral claw-like teeth and left subventral plate with two or three denticles, telostegostom as in morph I.

Morph IV: With six offset, separate, and thin-walled bulging lips, subdorsal and subventral lips larger than lateral lips, with pointed labial papillae; cheilostom large, vacuous, undivided; gymnostom thin, smooth, narrower than and barely overlapping cheilostom; stegostom simple, smooth, except for a small dorsal bulge with thickened cuticle; telostegostom narrow, sclerotized.

Morph V: Body thin, smaller than other morphs, sometimes less than a third of the size of other morphs (that is, I and IV); stoma tube-like; cheilostom undivided, toroid-shaped; gymnostom slightly taller than cheilostom, barely overlapping the latter, anteriorly tapered; stegostom simple, smooth, except for a small dorsal bulge with thickened cuticle.

Eight pairs of genital papillae are arranged as <v1, v2, (C, v4), ad, (pd, Ph, v5 to v7)>, such that v3d is absent, v1 and v4 are each separated from v2 by ca. one anal body width, ad is equidistant between v4 and v5 to v7, and pd is clearly anterior to v5. Spicules have large manubrium, twisted lamina, and calomus anteriorly, with raised ventral ridge. Tail is filiform and long in males and females (ca. seven to nine cloacal/anal body widths) of morphs I to IV; tails of both sexes are short and conical in morph V.

Diagnosis. The new species is distinguished from all other Diplogastridae, except for *P. sycomori* sp. nov. and *P. racemosae* sp. nov., by the presence of five morphs and by having morphs of laterally symmetrical and laterally asymmetrical stomatal structures in the same species. It is distinguished from all species, except for *P. sycomori* sp. nov., by the presence of a form (morph I) with a "bearded" inner stomatal opening, the lateral sides of which are axially longer than the dorsal and ventral margins. The new species is distinguished from *P. sycomori* sp. nov. by morph V having a thin versus posteriorly widened cheilostomatal toroid and by its unique 18*S* rRNA barcode (ca. 850-bp fragment defined by primers SSU18A and SSU26R; GenBank accession number KT188856), which differs from that of *P. sycomori* sp. nov. by 15 unique sites.

P. sycomori Susoy, Kanzaki, Kruger, Ragsdale, and Sommer sp. nov.

Etymology. The species epithet is the Latin genitive for that of its fig host, *F. sycomorus*.

Holotype. Adult female of morph I is deposited in the UCRNC.

Paratypes. Ten paratypes are deposited in the UCRNC, whereas 10 paratypes are deposited in the Swedish Museum of Natural History (Stockholm, Sweden).

Locality. Type specimens were collected from the Manie van der Schijff Botanical Garden at the University of Pretoria (Pretoria, South Africa).

Type host and vector. Type specimens were isolated from within sycones of the sycamore fig *F. sycomorus* Linneaus, 1753 (Moraceae), in association with *C. arabicus* Mayr, 1906 (Hymenoptera: Agaonidae).

Description. Body habitus, pharynx, female reproductive tract, male testis, and positions of ventral body openings are typical of *Pristionchus* nematodes (Fig. 2A and Fig. 5, F to J). Cuticle with fine annulation and thick, offset longitudinal alae are found on the entire body diameter, extending from the labial region to the tail, except for morph V, in which ridges are indistinct. Adults consist of five morphs. The nomenclature of morphs follows that used for *P. borbonicus* sp. nov. (that is, I to V), with which homologies of morphs could be assigned:

Morph I: Body larger than those of other morphs, head not tapering anterior to the labial region; lips large, lateral lips higher and wider than subventral and subdorsal lips; labial region with conspicuous beard (a circumstomatal ring of thin cuticular filaments originating from anterior cheilostom); pre-gymnostomatal cheilostom twice as high as gymnostom, with anteriorly tapering rugae separated from each other for most of their length; gymnostom thick, barrel-shaped, overlapping cheilostom for most of height, finely serrated at anterior margin; pro-mesostegostom projecting into one dorsal and two subventral anteriorly serrated lobes; metastegostom with claw-like dorsal tooth, claw-like right subventral tooth, and coarsely serrated left subventral ridge slightly overlapping the dorsal tooth; telostegostom deeper ventrally than dorsally, sclerotized.

Morph II: Head narrowing just anterior to the labial region; with six offset lips, lateral lips smaller than subventral lips; pre-gymnostomatal cheilostom with same height as gymnostom, with closely spaced, tapering rugae, each tipped with several filaments and extending past the stomatal opening; gymnostom thick, overlapping cheilostom for most of height, with fine anterior serration and with heavy punctation on medial surface; pro-mesostegostom with small projecting lobes; meta- and telostegostom as in morph I.

Morph III: Head tapered, with clearly offset, squared lips; stoma small; cheilostom with sharp anterior taper, with minute, tightly packed rugae not extending past the stomatal opening; gymnostom thin, barrel-shaped, overlapping cheilostom for most of height, with fine punctation; small projecting lobes in pro-mesostegostom indistinct or absent; metastegostom with small dorsal and right subventral claw-like teeth and left subventral plate with two to three denticles; telostegostom as in morph I.

Morph IV: With six offset, separate, thick-walled bulging lips, subdorsal and subventral lips larger than lateral lips, with pointed labial papillae; cheilostom large, vacuous, undivided; gymnostom thin, smooth, narrower than and barely overlapping cheilostom; stegostom simple, smooth, except for a small dorsal bulge with thickened cuticle; telostegostom narrow, sclerotized.

Morph V: Body thin, smaller than other morphs, sometimes less than a third of the size of other morphs (that is, I and IV); stoma tube-like; cheilostom undivided, and distinctly wider posteriorly, such that wall is triangular in section; gymnostom clearly taller than cheilostom, barely overlapping the latter, anteriorly tapered; stegostom simple, smooth, except for a small dorsal bulge with thickened cuticle.

Tail is filiform and long in males and females (ca. seven to nine cloacal/anal body widths) of morphs I to IV; tails of both sexes are short and conical in morph V.

Diagnosis. The new species is distinguished from all other Diplogastridae, except for *P. borbonicus* sp. nov. and *P. racemosae* sp. nov. (see below), by the presence of five morphs and by having morphs of laterally symmetrical and laterally asymmetrical stomatal structures in the same species. It is distinguished from all species, except *P. borbonicus* sp. nov., by the presence of a form (morph I) with a bearded inner stomatal opening, the lateral sides of which are axially longer than the dorsal and ventral margins. The new species is distinguished from *P. borbonicus* sp. nov. as described above, including its unique 18*S* rRNA barcode (ca. 850-bp fragment defined by primers SSU18A and SSU26R; GenBank accession number KT188857).

Downloaded from http://advances.sciencemag.org/ on February 10, 2016

***P. racemosae* Susoy, Kanzaki, Nguyen, Ragsdale, and Sommer sp. nov.**

Etymology. The species epithet is the Latin genitive for that of its fig host, *F. racemosa*.

Holotype. Adult female of morph ε is deposited in the UCRNC.

Paratypes. Ten paratypes are deposited in the UCRNC, whereas 10 paratypes are deposited in the Swedish Museum of Natural History (Stockholm, Sweden).

Locality. Type specimens were collected from the campus of the Institute of Ecological and Biological Sciences, Vietnamese Academy of Science and Technology (Cau Giay, Hanoi, Vietnam).

Type host and vector. Type specimens were isolated from within sycones of the cluster fig *F. racemosa* Linneaus, 1753 (Moraceae), in association with *C. fusciceps* Mayr, 1885 (Hymenoptera: Agaonidae).

Description. Body habitus, pharynx, female gonad, male testis, and positions of ventral body openings are typical of *Pristionchus* nematodes, except for morph-specific characters as specified below (Fig. 1, E to I, and 2A). Adults consist of five morphs. Because homologies of morphs are uncertain with respect to the morphs of other *Pristionchus* species or with the five morphs of *P. borbonicus* sp. nov. and *P. sycomori* sp. nov., an independent nomenclature (that is, α to ε) is used here. Cuticle of morphs α to δ has annulation, as well as rings of punctations that form evenly spaced longitudinal striations; cuticle of morph ε is thick, with large annulations and no apparent punctation or longitudinal striation. Pharynx of morphs α to δ has a "fish-bone" or zipper-like lumen; pharyngeal lumen of morph ε is smooth. Adults consist of five adult morphs:

Morph α: Head wide, not tapering posterior to the labial region; with six similarly sized, rounded, slightly offset lips; pre-gymnostomatal cheilostom slightly taller than gymnostom, with tightly packed rugae originating from the anterior to posterior base of cheilostom; gymnostom with heavy punctations, anterior margin consisting of six "wave"-like projections radially offset from lips by 30°; pro-mesostegostom without apparent projecting lobes; metastegostom with claw-like dorsal tooth, claw-like right subventral tooth, and coarsely serrated left subventral ridge slightly overlapping the dorsal tooth; telostegostom deeper ventrally than dorsally, deeper than wide, sclerotized.

Morph β: Head narrow; lips indistinct; pre-gymnostomatal cheilostom shorter than gymnostom, with tightly packed rugae originating from the posterior base of cheilostom; gymnostom with fine punctation, anterior margin slightly wavy but without distinct projections; metastegostom with claw-like dorsal tooth, claw-like right subventral tooth, and coarsely serrated left subventral ridge not overlapping the dorsal tooth; telostegostom as in morph α.

Morph γ: Cheilostom vacuous, undivided; gymnostom thin, smooth, narrower than and barely overlapping cheilostom; stegostom simple, smooth, except for a small dorsal bulge with thickened cuticle.

Morph δ: Six lips of similar size, distinct only at the stomatal opening; cuticle thick distally and vacuolated medially (internally), separated into adradial bulges, the anterior margins of which form a ring of sharp anterior points; gymnostom short, barely overlapping cheilostom, narrower than cheilostom, distally thickened and medially vacuolated; metastegostom with a small, thin, triangular dorsal tooth and with two symmetrical, subventral, dagger-like teeth larger than the dorsal tooth; telostegostom shallow, weakly sclerotized.

Morph ε: Large morph of variable body size, often twice the length of other morphs; labial region expanded into a large (longer than one labial body width), umbrella-like flap, the left side of which is open as a slit with a round opening at the base, and with six ribs consisting of labial papillae within cuticle; amphids present as small pores near the tip of the umbrella-like structure; cheilostom smooth, anterior margin marked by per- and interradial notches; cheilostom and gymnostom dorsoventrally isometric, such that the ventral boundary between these regions projects inwardly like a tooth; gymnostom smooth; stegostom simple, smooth, except for a flat, triangular thickening of cuticle in place of the dorsal tooth; telostegostom not sclerotized, indistinct.

Nine pairs of male genital papillae are arranged as <v1, (v2d, v3), C, v4, (ad, Ph), (v5 to v7), pd>, such that v3 is closer to (⅓ of a cloacal body width anterior to) v1 than to v4, and v2d and v3 are at the same level. Manubrium is wide and longitudinally flat, with a ventral hook projecting posteriad behind the rest of the spicule; posterior part of the spicule has a distinct dorsal keel that is as deep as the spicule itself; gubernaculum is flared anteriorly, such that ventral and dorsal walls separate at an angle of 45°. Vagina is expanded into an axially "heart-shaped" recaptaculum seminis. Tails of both sexes are conical (ca. four to five cloacal/anal body widths).

Diagnosis. The new species is distinguished from all other Diplogastridae, except for *P. borbonicus* sp. nov. and *P. sycomori* sp. nov. by the presence of five morphs and by having morphs of laterally symmetrical and laterally asymmetrical stomatal structures in the same species. The new species is diagnosed from the latter two species by the presence of a form (morph δ) with a vacuolated cheilostom separated into adradial divisions and by the presence of a form (morph ε) with an umbrella-like labial flap that is open on the left side and that extends more than a labial body diameter anterior from the stomatal opening. It is further distinguished from all other nematode species by its unique 18*S* rRNA barcode (ca. 850-bp fragment defined by primers SSU18A and SSU26R; GenBank accession number KT188859).

MATERIALS AND METHODS

Nematode isolation

To sample nematodes, we collected figs from *F. mauritiana* (La Réunion), *F. sycomorus* (South Africa), and *F. racemosa* (Vietnam). Individual figs were dissected, and all nematodes that were present in the cavity of the fig were collected. Nematodes that were identified as *Pristionchus* were individually transferred into a sterile buffer, which was developed to allow short-term culture of fig-associated nematodes. The composition of the buffer approximated the fig environment and was based on the chemical composition of raw figs (*31*). We then screened *Pristionchus* nematodes for their mouth phenotypes using a light microscope or stereomicroscope before proceeding with further experiments.

Genome sequencing of individuals of *P. borbonicus*

We isolated adult individuals of *P. borbonicus* from freshly collected figs of *F. mauritiana*. Living nematode individuals were kept in a sterile buffer for 10 to 15 min to minimize possible surface contamination, after which the nematodes were individually transferred into a lysis solution and thereafter frozen until DNA extraction. The DNA of individual nematodes was isolated using the MasterPure DNA Purification Kit (Epicentre), following the manufacturer's protocol for DNA purification from tissue samples. The DNA was sheared using a S220 focused ultrasonicator (Covaris) under the following operation conditions: 10 dc, 4 i, 200 cpb, and 80 s. Genomic paired-end libraries were prepared using Low Input Library Preparation Kit (Clontech Laboratories). Size selection was performed on final libraries using BluePippin and 1.5%

Downloaded from http://advances.sciencemag.org/ on February 10, 2016

agarose gel cassettes (Sage Science). Paired-end libraries were sequenced using a HiSeq 2000 system (Illumina). mRNA libraries that were used for scaffolding (see below) were prepared from TRIzol-lysed individuals. Total RNA was isolated from single specimens using the PureLink RNA micro kit (Invitrogen), after which complementary DNA (cDNA) was prepared using the SMARTer Ultra Low Input cDNA synthesis kit (Clontech Laboratories). cDNA was sheared using the following operation conditions: 10 dc, 4 i, 200 cpb, 40 s. Paired-end libraries were prepared and sequenced as described above.

Genome assembly and analysis of the molecular diversity of *P. borbonicus*

A draft genome assembly for *P. borbonicus* was generated from the DNA-sequencing data of a single individual using the SOAPdenovo assembler (*32*). Genomic and transcriptomic data from other individuals were used for additional scaffolding and gap closing (*33*, *34*). After discarding contamination [contigs with more than half of the sequence showing a >95% identity to non-Diplogastrid sequences in the National Center for Biotechnology Information (NCBI) nucleotide database], the final assembly comprised 157,322 contigs spanning 155 Mb with an N50 contig size of 9.4 kb. Genomic data for 49 individuals were aligned to the *P. borbonicus* draft genome using a Burrows-Wheeler aligner (*35*). Single-nucleotide polymorphism (SNP) calling and diversity analysis were performed as previously described (*21*). Variable sites with coverage in all samples were extracted to reconstruct a TCS genotype network (that is, a phylogenetic network estimation using statistical parsimony) (*36*) using PopART 1.7 (http://popart.otago.ac.nz).

Haplotype diversity of *P. sycomori* and *P. racemosae*

We extracted DNA from living or DESS (a solution containing dimethyl sulfoxide, disodium EDTA, and saturated NaCl)–preserved individuals. Fragments of *ND1*, *Cytb*, and *COI* mitochondrial genes were amplified and sequenced for *P. sycomori*, and sequences of the *COI* gene were obtained for individuals of *P. racemosae*. The sequences were quality-checked and assembled using Geneious 6.1.4 and aligned using Muscle 3.8 (*37*). The concatenated alignment of *ND1*, *Cytb*, and *COI* genes for 77 individuals of *P. sycomori* contained 52 variable and 36 parsimony-informative sites. The alignment of the *COI* sequences of 104 individuals of *P. racemosae* had 98 variable and 54 parsimony-informative sites. Maximal mtDNA sequence divergence between isolates of the same species was estimated by *p* distance using MEGA 6 (*38*). For comparison, we estimated sequence divergence in corresponding regions of the mtDNA of 104 *P. pacificus* strains (*21*). TCS haplotype networks were inferred from those alignments using PopART 1.7.

Geometric morphometrics and analysis of disparity

To quantify the mouth morphology of different morphs and species of *Pristionchus*, we used a geometric morphometrics approach adapted from a previous study (*17*). Briefly, 13 two-dimensional landmarks were assigned to homologous structures of the nematode stoma (mouth), as informed by fine structural anatomy (*39*, *40*). In addition to 11 landmarks used previously (*17*), two landmarks that marked the position of dorsal and ventral labial sensilla were recorded (fig. S1). Landmark coordinates were identified twice for each specimen, digitalized using tpsDig2 (*41*), and averaged for each specimen using MorphoJ (*42*). In total, our data set included 18 species and 450 individuals of *Pristionchus*. PCA of shape was performed on Procrustes-superimposed landmark coordinates, and PCA of stomatal form was performed on superimposed landmark coordinates + logarithm-transformed centroid size (*18*, *19*). The proportion of total variance explained by the first three principal component axes for all analyses is given in table S4. Disparity between different morphs of polyphenic species of *Pristionchus* was calculated as the maximal Euclidean pairwise distance between morph means in Procrustes shape space using the MATLAB package MDA (*43*). Principal components that explained more than 10% of the total variance were included in the analysis.

Testing mode of transmission of nematodes

To confirm that *Pristionchus* nematodes were transmitted by wasps pollinating the figs, we brought ripe figs of *F. mauritiana* into the laboratory. The figs were kept at room temperature until a new generation of pollinator wasps (*C. coecus*) emerged from them. Emerging female wasps were collected in a trap and then preserved at −25°C until further examination. Ten wasps were placed in 2 ml of water with 0.1% Triton X and kept on a shaker for 1 hour to allow dispersal (dauer) juvenile nematodes to detach from the body surface of the wasp. Eighty-four nematode dauers were collected, and the DNA from individual dauers was extracted. We then amplified and sequenced a portion of the 18*S* rRNA gene, specifically an 830-bp diagnostic fragment developed for nematode identification (*44*, *45*). The sequences were compared to those of nematodes previously isolated from figs of *F. mauritiana*.

Induction of alternative phenotypes

We collected figs of *F. sycomorus* of early interfloral phase and confirmed that only males and females of morph V of *P. sycomori* were present. We then collected 20 gravid females from different figs, transferred them into a 3-cm Petri dish filled with the buffer described above, and provided them with a microbial food supply that enabled their reproduction on plates (that is, mixed bacteria extracted from host figs, 1 mg of *Escherichia coli* strain OP50, or 1 mg of *Erwinia typographi* strain P11-1, all of which resulted in the same induced phenotype). The females were allowed to lay eggs, which in 8 days developed into adult males and females. The mouth phenotypes of the offspring were then scored.

Metagenomic analysis of predation

Genomic data of 49 individuals of *P. borbonicus* were screened for 18*S* rRNA sequences using PhyloSift 1.0.1 (*46*). Paired reads that had similarity to eukaryotic 18*S* rRNA reference genes were extracted and assembled using Geneious 6.1.4. Resulting contigs were searched against the NCBI database using BLAST, and contigs that matched nematode 18*S* rRNA genes were identified. Those nematode 18*S* rRNA genes were used as references to which genomic reads of individual *P. borbonicus* nematodes were mapped, and the normalized coverage for non-*Pristionchus* nematode and *Pristionchus* 18*S* rRNA was estimated. Normalized coverage was calculated as follows: (coverage of non-*Pristionchus* 18*S* rRNA/coverage of *Pristionchus* 18*S* rRNA) × 3000, where 3000 is the average coverage of the 18*S* rRNA gene for *P. borbonicus* individuals.

Phylogeny of *Pristionchus*

We inferred the phylogeny of 28 described and 7 new species of *Pristionchus*. In addition to the three species described herein, we included species isolated from four other species or populations of *Ficus* (*Sycomorus*), section *Sycomorus* [*Ficus sur* in South Africa (*Pristionchus* sp. 35), *F. racemosa* in Australia (*Pristionchus* sp. 36), and *Ficus variegata* in

Downloaded from http://advances.sciencemag.org/ on February 10, 2016

Australia (*Pristionchus* sp. 37) and Okinawa, Japan (*Pristionchus* sp. 38)] in our phylogenetic analysis to test the monophyly of fig-associated *Pristionchus*. The diplogastrid nematodes *Parapristionchus giblindavisi*, *Micoletzkya masseyi*, and *Allodiplogaster sudhausi* were included as outgroups (*17*). The phylogeny was inferred from a concatenated alignment of 27 ribosomal protein genes and 18*S* and 28*S* rRNA genes. The ribosomal protein genes included in the analysis were *rpl-1*, *rpl-2*, *rpl-10*, *rpl-14*, *rpl-16*, *rpl-23*, *rpl-26*, *rpl-27*, *rpl-27a*, *rpl-28*, *rpl-29*, *rpl-30*, *rpl-31*, *rpl-32*, *rpl-34*, *rpl-35*, *rpl-38*, *rpl-39*, *rps-1*, *rps-8*, *rps-14*, *rps-20*, *rps-21*, *rps-24*, *rps-25*, *rps-27*, and *rps-28*, with conditions as described previously (*47*). Ribosomal protein gene sequences were individually aligned by predicted translation using default settings in Muscle 3.8, and rRNA genes were aligned using the G-INS-I algorithm and default settings in MAFFT 7.1 (*48*). The final alignment included 15,902 total and 3485 parsimony-informative sites. The fraction of missing data was less than 16%.

The phylogeny was inferred under the Bayesian optimality criterion, as implemented in MrBayes 3.2.2 (*49*). The inference was performed on the CIPRES Science Gateway (*50*). For the analyses, the data set was partitioned into three subsets: two for 18*S* and 28*S* rRNA genes, which were analyzed using a "mixed" + Γ model, and the third for the ribosomal protein genes, which was analyzed under a codon + Γ model. Model parameters were unlinked across partitions. Two independent analyses, each containing four chains, were run for 20 million generations, with chains sampled every 1000 generations. After confirming convergence of runs and mixing of chains using Tracer 1.6 (*51*), the first half of generations was discarded as burn-in, and the remaining tree topologies were summarized to generate a 50% majority-rule consensus tree.

Composition of buffer for short-term maintenance of fig nematodes

The buffer was composed of the following: potassium chloride, 55 mM; dipotassium phosphate, 3.6 mM; calcium chloride dihydrate, 8.7 mM; magnesium sulfate, 6.65 mM; ascorbic acid, 57 μM; sorbitol, 1.1 mM; ribitol, 1.3 mM; mannitol, 1.1 mM; citric acid, 0.5 mM; mallic acid, 0.75 mM; BME Vitamin Solution (100×) B 6891 (Sigma-Aldrich), 10 ml/liter; trace metals solution (1.86 g of disodium EDTA, 0.69 g of $FeSO_4{\cdot}7H_2O$, 0.2 g of $MnCl_2{\cdot}4H_2O$, 0.29 g of $ZnSO_4{\cdot}7H_2O$, and 0.025 g of $CuSO_4{\cdot}5H_2O$, in 1 liter of H_2O), 10 ml/liter. The pH of the buffer was adjusted to 7.5 with potassium hydroxide, and the buffer was sterilized by filtering (Nalgene 295-4545).

SUPPLEMENTARY MATERIALS

Supplementary material for this article is available at http://advances.sciencemag.org/cgi/content/full/2/1/e1501031/DC1

Fig. S1. Positions of 13 two-dimensional landmarks recorded for the stoma of fig-associated *Pristionchus* species.

Table S1. Nematode dauers transmitted by wasps (*C. coecus*) emerging from ripe figs of *F. mauritiana*.

Table S2. Ratio of morphs in a single fig sycone for males and females of *P. sycomori*.

Table S3. Nematode species isolated from sycones of *F. mauritiana*, *F. sycomorus*, and *F. racemosa*.

Table S4. Proportion of variance explained by the first three principal component axes in the PCA of mouth form and shape for fig-associated *Pristionchus* species.

REFERENCES AND NOTES

1. G. G. Simpson, *The Major Features of Evolution* (Columbia Univ. Press, New York, 1953), 434 pp.
2. D. Schluter, *The Ecology of Adaptive Radiations* (Oxford Univ. Press, Oxford, 2000), 288 pp.
3. S. Gavrilets, J. B. Losos, Adaptive radiation: Contrasting theory with data. *Science* **323**, 732–737 (2009).
4. D. Brawand, C. E. Wagner, Y. I. Li, M. Malinsky, I. Keller, S. Fan, O. Simakov, A. Y. Ng, Z. W. Lim, E. Bezault, J. Turner-Maier, J. Johnson, R. Alcazar, H. J. Noh, P. Russell, B. Aken, J. Alföldi, C. Amemiya, N. Azzouzi, J.-F. Baroiller, F. Barloy-Hubler, A. Berlin, R. Bloomquist, K. L. Carleton, M. A. Conte, H. D'Cotta, O. Eshel, L. Gaffney, F. Galibert, H. F. Gante, S. Gnerre, L. Greuter, R. Guyon, N. S. Haddad, W. Haerty, R. M. Harris, H. A. Hofmann, T. Hourlier, G. Hulata, D. B. Jaffe, M. Lara, A. P. Lee, I. MacCallum, S. Mwaiko, M. Nikaido, H. Nishihara, C. Ozouf-Costaz, D. J. Penman, D. Przybylski, M. Rakotomanga, S. C. P. Renn, F. J. Ribeiro, M. Ron, W. Salzburger, L. Sanchez-Pulido, M. E. Santos, S. Searle, T. Sharpe, R. Swofford, F. J. Tan, L. Williams, S. Young, S. Yin, N. Okada, T. D. Kocher, E. A. Miska, E. S. Lander, B. Venkatesh, R. D. Fernald, A. Meyer, C. P. Ponting, J. T. Streelman, K. Lindblad-Toh, O. Seehausen, F. Di Palma, The genomic substrate for adaptive radiation in African cichlid fish. *Nature* **513**, 375–381 (2014).
5. S. Lamichhaney, J. Berglund, M. S. Almén, K. Maqbool, M. Grabherr, A. Martinez-Barrio, M. Promerová, C.-J. Rubin, C. Wang, N. Zamani, B. R. Grant, P. R. Grant, M. T. Webster, L. Andersson, Evolution of Darwin's finches and their beaks revealed by genome sequencing. *Nature* **518**, 371–375 (2015).
6. M. J. West-Eberhard, *Developmental Plasticity and Evolution* (Oxford Univ. Press, Oxford, 2003), 816 pp.
7. E. O. Wilson, The origin and evolution of polymorphism in ants. *Q. Rev. Biol.* **28**, 136–156 (1953).
8. N. A. Moran, The evolution of aphid life cycles. *Annu. Rev. Entomol.* **37**, 321–348 (1992).
9. S. M. Shuster, Alternative reproductive behavior: Three discrete male morphs in *Paracerceis sculpta*, an intertidal isopod from the northern Gulf of California. *J. Crustacean Biol.* **7**, 318–327 (1987).
10. E. Gianoli, F. Carrasco-Urra, Leaf mimicry in a climbing plant protects against herbivory. *Curr. Biol.* **24**, 984–987 (2014).
11. G. C. Martin, A. M. Owen, J. I. Way, Nematodes, figs, and wasps. *J. Nematol.* **5**, 77–78 (1973).
12. N. Vovlas, R. N. Inserra, N. Greco, *Schistonchus caprifici* parasitizing caprifig (*Ficus carica sylvestris*) florets and the relationship with its fig wasp (*Blastophaga psenes*) vector. *Nematologica* **38**, 215–226 (1992).
13. E. A. Herre, Population structure and the evolution of virulence in nematode parasites of fig wasps. *Science* **259**, 1442–1445 (1993).
14. R. M. Giblin-Davis, K. A. Davies, G. S. Taylor, W. K. Thomas, Entomophilic nematode models for studying biodiversity and cospeciation, in *Nematology, Advances and Perspectives: Nematode Morphology, Physiology and Ecology*, Z. X. Chen, S. Y. Chen, D. W. Dickson, Eds. (CABI Publishing, Wallingford, Oxfordshire, 2004), pp. 493–540.
15. N. Kanzaki, R. M. Giblin-Davis, K. Davies, W. Ye, B. J. Center, W. K. Thomas, *Teratodiplogaster fignewmani* gen. nov., sp. nov. (Nematoda: Diplogastridae) from the syconia of *Ficus racemose* in Australia. *Zool. Sci.* **26**, 569–578 (2009).
16. A. Krishnan, S. Muralidharan, L. Sharma, R. M. Borges, A hitchhiker's guide to a crowded syconium: How do fig nematodes find the right ride? *Funct. Ecol.* **24**, 741–749 (2010).
17. V. Susoy, E. J. Ragsdale, N. Kanzaki, R. J. Sommer, Rapid diversification associated with a macroevolutionary pulse of developmental plasticity. *Elife* **4**, e05463 (2015).
18. I. L. Dryden, K. V. Mardia, *Statistical Shape Analysis* (Wiley, Chichester, 1998), 376 pp.
19. P. Mitteroecker, P. Gunz, M. Bernhard, K. Schaefer, F. L. Bookstein, Comparison of cranial ontogenetic trajectories among great apes and humans. *J. Hum. Evol.* **46**, 679–698 (2004).
20. R. I. Molnar, G. Bartelmes, I. Dinkelacker, H. Witte, R. J. Sommer, Mutation rates and intraspecific divergence of the mitochondrial genome of *Pristionchus pacificus*. *Mol. Biol. Evol.* **28**, 2317–2326 (2011).
21. C. Rödelsperger, R. A. Neher, A. M. Weller, G. Eberhardt, H. Witte, W. E. Mayer, C. Dieterich, R. J. Sommer, Characterization of genetic diversity in the nematode *Pristionchus pacificus* from population-scale resequencing data. *Genetics* **196**, 1153–1165 (2014).
22. E. J. Ragsdale, M. R. Müller, C. Rödelsperger, R. J. Sommer, A developmental switch coupled to the evolution of plasticity acts through a sulfatase. *Cell* **155**, 922–933 (2013).
23. A. Cruaud, N. Rønsted, B. Chantarasuwan, L. S. Chou, W. L. Clement, A. Couloux, B. Cousins, G. Genson, R. D. Harrison, P. E. Hanson, M. Hossaert-Mckey, R. Jabbour-Zahab, E. Jousselin, C. Kerdelhué, F. Kjellberg, C. Lopez-Vaamonde, J. Peebles, Y.-Q. Peng, R. A. S. Pereira, T. Schramm, R. Ubaidillah, S. van Noort, G. D. Weiblen, D.-R. Yang, A. Yodpinyanee, R. Libeskind-Hadas, J. M. Cook, J.-Y. Rasplus, V. Savolainen, An extreme case of plant–insect codiversification: Figs and fig-pollinating wasps. *Syst. Biol.* **61**, 1029–1047 (2012).
24. G. W. Yeates, T. Bongers, R. G. M. De Goede, D. W. Freckman, S. S. Georgieva, Feeding habits in soil nematode families and genera—An outline for soil ecologists. *J. Nematol.* **25**, 315–331 (1993).
25. T. Bongers, The Maturity Index, the evolution of nematode life history traits, adaptive radiation and cp-scaling. *Plant Soil* **212**, 13–22 (1999).
26. J. D. Van Dyken, M. J. Wade, The genetic signature of conditional expression. *Genetics* **184**, 557–570 (2010).
27. D. W. Pfennig, M. A. Wund, E. C. Snell-Rood, T. Cruickshank, C. D. Schlichting, A. P. Moczek, Phenotypic plasticity's impacts on diversification and speciation. *Trends Ecol. Evol.* **25**, 459–467 (2010).
28. S. R. Purandare, R. D. Bickel, J. Jaquiery, C. Rispe, J. A. Brisson, Accelerated evolution of morph-biased genes in pea aphids. *Mol. Biol. Evol.* **31**, 2073–2083 (2014).

Downloaded from http://advances.sciencemag.org/ on February 10, 2016

29. D. W. Pfennig, P. J. Murphy, How fluctuating competition and phenotypic plasticity mediate species divergence. *Evolution* **56**, 1217–1228 (2002).
30. M. R. Orr, T. B. Smith, Ecology and speciation. *Trends Ecol. Evol.* **13**, 502–506 (1998).
31. U.S. Department of Agriculture, Agricultural Research Service, *USDA National Nutrient Database for Standard Reference, Release 27. Nutrient Data Laboratory Home Page*, 2014; www.ars.usda.gov/nutrientdata
32. R. Li, H. Zhu, J. Ruan, W. Qian, X. Fang, Z. Shi, Y. Li, S. Li, G. Shan, K. Kristiansen, S. Li, H. Yang, J. Wang, J. Wang, De novo assembly of human genomes with massively parallel short read sequencing. *Genome Res.* **20**, 265–272 (2010).
33. M. Boetzer, C. V. Henkel, H. J. Jansen, D. Butler, W. Pirovano, Scaffolding pre-assembled contigs using SSPACE. *Bioinformatics* **27**, 578–579 (2011).
34. W. Xue, J.-T. Li, Y.-P. Zhu, G.-Y. Hou, X.-F. Kong, Y.-Y. Kuang, X.-W. Sun, L_RNA_scaffolder: Scaffolding genomes with transcripts. *BMC Genomics* **14**, 604 (2013).
35. H. Li, R. Durbin, Fast and accurate long-read alignment with Burrows–Wheeler transform. *Bioinformatics* **26**, 589–595 (2010).
36. M. Clement, Q. Snell, P. Walker, D. Posada, K. Crandall, TCS: Estimating gene genealogies. *Proc. 16th Int. Parallel. Distrib. Process Symp.* **2**, 184 (2002).
37. R. C. Edgar, MUSCLE: Multiple sequence alignment with high accuracy and high throughput. *Nucleic Acids Res.* **32**, 1792–1797 (2004).
38. K. Tamura, G. Stecher, D. Peterson, A. Filipski, S. Kumar, MEGA6: Molecular Evolutionary Genetics Analysis version 6.0. *Mol. Biol. Evol.* **30**, 2725–2729 (2013).
39. J. G. Baldwin, C. D. Eddleman, R. M. Giblin-Davis, D. S. Williams, J. T. Vida, W. K. Thomas, The buccal capsule of *Aduncospiculum halicti* (Nemata: Diplogasterina): An ultrastructural and molecular phylogenetic study. *Can. J. Zool.* **75**, 407–423 (1997).
40. E. J. Ragsdale, J. G. Baldwin, Resolving phylogenetic incongruence to articulate homology and phenotypic evolution: A case study from Nematoda. *Proc. Bio. Sci.* **277**, 1299–1307 (2010).
41. F. J. Rohlf, *TpsDig2: A Program for Landmark Development and Analysis* (Department of Ecology and Evolution, State University of New York at Stony Brook, Stony Brook, 2008); http://life.bio.sunysb.edu/morph/
42. C. P. Klingenberg, MorphoJ: An integrated software package for geometric morphometrics. *Mol. Ecol. Resour.* **11**, 353–357 (2011).
43. N. Navarro, MDA: A MATLAB-based program for morphospace-disparity analysis. *Comput. Geosci.* **29**, 655–664 (2003).
44. R. Floyd, E. Abebe, A. Papert, M. Blaxter, Molecular barcodes for soil nematode identification. *Mol. Ecol.* **11**, 839–850 (2002).
45. M. Herrmann, W. E. Mayer, R. J. Sommer, Nematodes of the genus *Pristionchus* are closely associated with scarab beetles and the Colorado potato beetle in Western Europe. *Zoology* **109**, 96–108 (2006).
46. A. E. Darling, G. Jospin, E. Lowe, F. A. Matsen IV, H. M. Bik, J. A. Eisen, PhyloSift: Phylogenetic analysis of genomes and metagenomes. *PeerJ* **2**, e243 (2014).
47. W. E. Mayer, M. Herrmann, R. J. Sommer, Phylogeny of the nematode genus *Pristionchus* and implications for biodiversity, biogeography and the evolution of hermaphroditism. *BMC Evol. Biol.* **7**, 104 (2007).
48. K. Katoh, D. M. Standley, MAFFT multiple sequence alignment software version 7: Improvements in performance and usability. *Mol. Biol. Evol.* **30**, 772–780 (2013).
49. F. Ronquist, M. Teslenko, P. van der Mark, D. L. Ayres, A. Darling, S. Höhna, B. Larget, L. Liu, M. A. Suchard, J. P. Huelsenbeck, MrBayes 3.2: Efficient Bayesian phylogenetic inference and model choice across a large model space. *Syst. Biol.* **61**, 539–542 (2012).
50. M. A. Miller, W. Pfeiffer, T. Schwarz, Creating the CIPRES Science Gateway for inference of large phylogenetic trees, in *Proceedings of the Gateway Computing Environments Workshop (GCE)*, 14 November 2006, New Orleans, pp. 1–8.
51. A. J. Drummond, A. Rambaut, BEAST: Bayesian Evolutionary Analysis by Sampling Trees. *BMC Evol. Biol.* **7**, 214 (2007).

Acknowledgments: We thank J. Berger for scanning electron microscopy analysis, M. Lalk for chemical analyses, and D. Strasberg, J. Rochat, J. M. Meyer, and the staff of the Office national des forêts (La Réunion) and Parc national de La Réunion for collecting permits and long-term support with sample collection. **Funding:** This work was funded by the Max Planck Society. C.N.N. was funded in part by the Vietnam National Foundation of Science and Technology (NAFOSTED) through project 106.12-2012.84. **Author contributions:** V.S., E.J.R., and R.J.S. conceived and designed the study. V.S., M.H., N.K., M.K., C.N.N., R.M.G.-D., and R.J.S. collected the samples. V.S. and N.K. acquired the data. V.S., W.R., and C.W. performed data sequencing. V.S. and C.R. analyzed the data. V.S., E.J.R., and R.J.S. wrote the manuscript. **Competing interests:** The authors declare that they have no competing interests. **Data and materials availability:** Sequences generated for this study have been deposited in GenBank under accession numbers KT188832 to KT188928. The genome assembly of *P. borbonicus* and a file with 10,509 concatenated SNPs from 49 individuals are available at www.pristionchus.org/borbonicus/. All other data needed to evaluate the conclusions in the paper are available in present in the paper and/or the Supplementary Materials. Additional data related to this paper may be requested from the authors.

Submitted 3 August 2015
Accepted 10 November 2015
Published 15 January 2016
10.1126/sciadv.1501031

Citation: V. Susoy, M. Herrmann, N. Kanzaki, M. Kruger, C. N. Nguyen, C. Rödelsperger, W. Röseler, C. Weiler, R. M. Giblin-Davis, E. J. Ragsdale, R. J. Sommer, Large-scale diversification without genetic isolation in nematode symbionts of figs. *Sci. Adv.* **2**, e1501031 (2016).

Downloaded from http://advances.sciencemag.org/ on February 10, 2016

Science Advances

AAAS

advances.sciencemag.org/cgi/content/full/2/1/e1501031/DC1

Supplementary Materials for

Large-scale diversification without genetic isolation in nematode symbionts of figs

Vladislav Susoy, Matthias Herrmann, Natsumi Kanzaki, Meike Kruger, Chau N. Nguyen, Christian Rödelsperger, Waltraud Röseler, Christian Weiler, Robin M. Giblin-Davis, Erik J. Ragsdale, Ralf J. Sommer

Published 15 January 2016, *Sci. Adv.* **2**, e1501031 (2016)
DOI: 10.1126/sciadv.1501031

The PDF file includes:

Fig. S1. Positions of 13 two-dimensional landmarks recorded for the stoma (mouth) of fig-associated *Pristionchus* species. Landmarks are shown here for three morphs of *P. sycomori*. Descriptions of mouth morphology as drawn follow Susoy *et al*. (*16*).

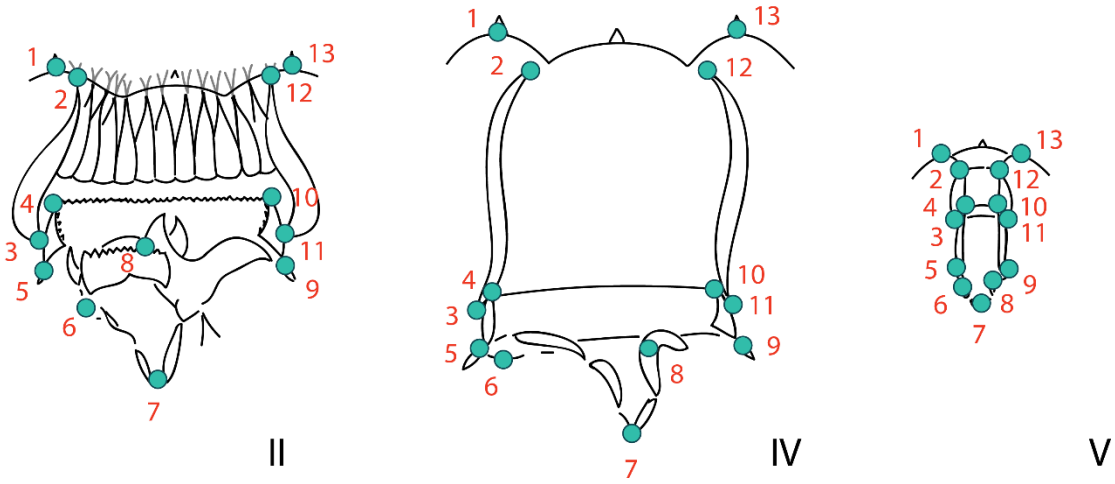

Table S1. Nematode dauers transmitted by wasps (*C. coecus*) emerging from ripe figs of *F. mauritiana*. Nematodes, collected from 10 female wasps, were individually identified by their 18S rRNA barcodes.

Teratodiplogaster sp.	*Pristionchus borbonicus*	*Acrostichus* sp.	*Schistonchus* sp.
70	6	5	3

Table S2. Ratio of morphs in a single fig sycone for males and females of *P. sycomori*. Data for syconia with more than 6 adults of *P. sycomori* are shown. Ratios given as percentage of total examined individuals per fig.

Females					males			n	fig stage
I	II	III	IV	V	II	IV	V		
0	0	0	0	100	0	0	100	9	early interfloral phase
0	0	0	0	100	0	0	100	11	early interfloral phase
0	0	0	0	100	0	0	100	12	early interfloral phase
0	0	0	0	100	0	0	100	9	early interfloral phase
0	0	0	0	100	0	0	100	11	early interfloral phase
0	0	0	0	100	0	0	100	15	early interfloral phase
0	0	0	0	100	0	0	100	14	early interfloral phase
0	0	0	0	100	0	0	100	7	early interfloral phase
0	0	0	0	100	0	0	100	16	early interfloral phase
42	29	0	29	0	100	0	0	12	late interfloral phase
33	50	0	17	0	100	0	0	10	late interfloral phase
25	75	0	0	0	100	0	0	8	late interfloral phase
24	60	0	16	0	100	0	0	39	late interfloral phase
0	80	0	20	0	100	0	0	8	late interfloral phase
0	75	0	25	0	100	0	0	8	late interfloral phase
0	50	0	50	0	0	100	0	8	late interfloral phase
0	28	0	72	0	29	71	0	32	late interfloral phase
0	20	0	80	0	100	0	0	8	late interfloral phase
0	0	50	50	0	67	33	0	7	late interfloral phase
0	0	100	0	0	100	0	0	9	late interfloral phase

Table S3. Nematode species isolated from sycones of *F. mauritiana*, *F. sycomorus*, and *F. racemosa*. "+" - present, "-" - not observed.

	F. mauritiana	*F. sycomorus*	*F. racemosa*
Pristionchus spp.	+	+	+
Teratodiplogaster spp.	+	+	+
Acrostichus spp.	+	+	-
Schistonchus spp.	+	-	+
Bursaphelenchus spp.	+	+	-
Parasitodiplogaster sp.	-	+	-
Caenorhabditis spp.*	+	-	-

* *Caenorhabditis briggsae* and an undescribed species of *Caenorhabditis* were found in syconia of *F. mauritiana* only rarely.

Table S4. Proportion of variance explained by the first three principal component axes in the PCA of mouth form and shape for fig-associated *Pristionchus* species.

	PC1	PC2	PC3
P. borbonicus, PCA of shape	59	26	7
P. borbonicus, PCA of form	92	6	1
P. sycomori, PCA of shape	59	26	8
P. sycomori, PCA of form	89	6	3
P. racemosae, PCA of shape	74	12	4
P. racemosae, PCA of form	77	15	2
Pristionchus spp. (individuals), PCA of shape	50	18	9
Pristionchus spp. (species morph means), PCA of shape	55	20	9

© 2015. Published by The Company of Biologists Ltd | The Journal of Experimental Biology (2015) 218, 1306-1313 doi:10.1242/jeb.118620

RESEARCH ARTICLE

Predatory feeding behaviour in *Pristionchus* nematodes is dependent on phenotypic plasticity and induced by serotonin

Martin Wilecki*, James W. Lightfoot*, Vladislav Susoy and Ralf J. Sommer‡

ABSTRACT

Behavioural innovation and morphological adaptation are intrinsically linked but their relationship is often poorly understood. In nematodes, a huge diversity of feeding morphologies and behaviours can be observed to meet their distinctive dietary and environmental demands. *Pristionchus* and their relatives show varied feeding activities, both consuming bacteria and also predating other nematodes. In addition, *Pristionchus* nematodes display dimorphic mouth structures triggered by an irreversible developmental switch, which generates a narrower mouthed form with a single tooth and a wider mouthed form with an additional tooth. However, little is known about the specific predatory adaptations of these mouth forms or the associated mechanisms and behaviours. Through a mechanistic analysis of predation behaviours, in particular in the model organism *Pristionchus pacificus*, we reveal multifaceted feeding modes characterised by dynamic rhythmic switching and tooth stimulation. This complex feeding mode switch is regulated by the neurotransmitter serotonin in a previously uncharacterised role, a process that appears conserved across several predatory nematode species. Furthermore, we investigated the effects of starvation, prey size and prey preference on *P. pacificus* predatory feeding kinetics, revealing predation to be a fundamental component of the *P. pacificus* feeding repertoire, thus providing an additional rich source of nutrition in addition to bacteria. Finally, we found that mouth form morphology also has a striking impact on predation, suppressing predatory behaviour in the narrow mouthed form. Our results therefore hint at the regulatory networks involved in controlling predatory feeding and underscore *P. pacificus* as a model for understanding the evolution of complex behaviours.

KEY WORDS: Predation behaviour, *Pristionchus pacificus*, Neurotransmitter, Developmental plasticity

INTRODUCTION

Animals have evolved different behaviours and morphological adaptations to meet their needs in exploiting different environments. Morphology and behaviour are intimately coupled as behaviour is restricted by morphological limits while also driving morphological diversity through the evolution of novel functions. Nematodes are a well-studied and abundant animal group in which to analyse the relationship between morphology and behaviour. Nematodes show a staggering array of morphological structures and behaviours including a vast spectrum of mouth adaptations that coincide with a great diversity in feeding behaviours and diets (De Ley et al., 1995; von Lieven, 2003; Baldwin et al., 2004; Ragsdale et al., 2008; Sato et al., 2008). In bacteriovorus species such as *Caenorhabditis elegans*, the buccal cavity is often composed of a simple tube with a more complex apparatus found in the terminal bulb where hardened discs of collagen form a grinder to aid in bacterial lysis (Straud et al., 2013). In contrast, parasitic species employ a host of specialised implements for penetrating their host tissue. This includes fine stylets observed in the commercially significant cyst nematodes of the genus *Heterodera* (Handoo, 2002), and sharpened teeth in the medically significant hookworm species *Ancylostoma duodenale* and *Necator americanus* (Hotez et al., 2004, 2010). Omnivorous nematodes including *Pristionchus* are capable of both microbial feeding and predatory feeding on other nematodes, and also have teeth for lacerating open the cuticle of their prey. Interestingly, this mouth specialisation is often dimorphic with one morph, the stenostomatous (St) form thought to be optimised for bacterial food sources and a second morph, the eurystomatous (Eu) form optimised for predation (Serobyan et al., 2013, 2014). *Pristionchus* therefore offers an ideal opportunity to study behaviour under both morphological and behavioural contexts.

The diplogastrid *Pristionchus pacificus* Sommer, Carta, Kim and Sternberg 1996 has been developed as a model organism for comparative and integrative evolutionary biology. It boasts an annotated genome (Dieterich et al., 2008), and phylogenetic and molecular tools (Schlager et al., 2009; Sommer and McGaughran, 2013), and much of its ecology is established, revealing a close necromenic association with scarab beetles (Fig. 1B) (Herrmann et al., 2007). Furthermore, recent mapping of the pharyngeal connectome has exposed fundamental wiring differences between *P. pacificus* and *C. elegans*, perhaps guiding behavioural changes between the species (Bumbarger et al., 2013). The mouth dimorphism in *P. pacificus* has also been intensely studied as a model for developmental (phenotypic) plasticity, thought to be a major process driving novelty in evolution (Susoy et al., 2015). The developmental pathways guiding the mouth dimorphism represent a complex regulatory network including small molecules (Bose et al., 2012). An endocrine signalling pathway consisting of the nuclear hormone receptor *Ppa-daf-12* and the steroid hormone dafachronic acid (DA) act further downstream (Bento et al., 2010). Recently, the sulphatase *eud-1* was identified as a developmental switch that not only has a key function during development but also guides microevolutionary and macroevolutionary patterns (Ragsdale et al., 2013). In contrast to these recently acquired insights into the molecular network regulating the mouth dimorphism in *P. pacificus* (Fig. 1J), very little of the behaviours associated with predatory feeding or the contribution from the differing mouth forms has been studied.

Here, we report a mechanistic analysis of predatory feeding in *P. pacificus*, revealing unique qualities not observable during bacterial feeding. This includes altered pharyngeal dynamics and stimulation of the dorsal tooth, which is used to eviscerate

Max-Planck Institute for Developmental Biology, Department for Evolutionary Biology, Spemannstrasse 37, Tuebingen 72076, Germany.
*Joint first authors

‡Author for correspondence (ralf.sommer@tuebingen.mpg.de)

Received 18 December 2014; Accepted 23 February 2015

The Journal of Experimental Biology

The Journal of Experimental Biology (2015) 218, 1306-1313 doi:10.1242/jeb.118620

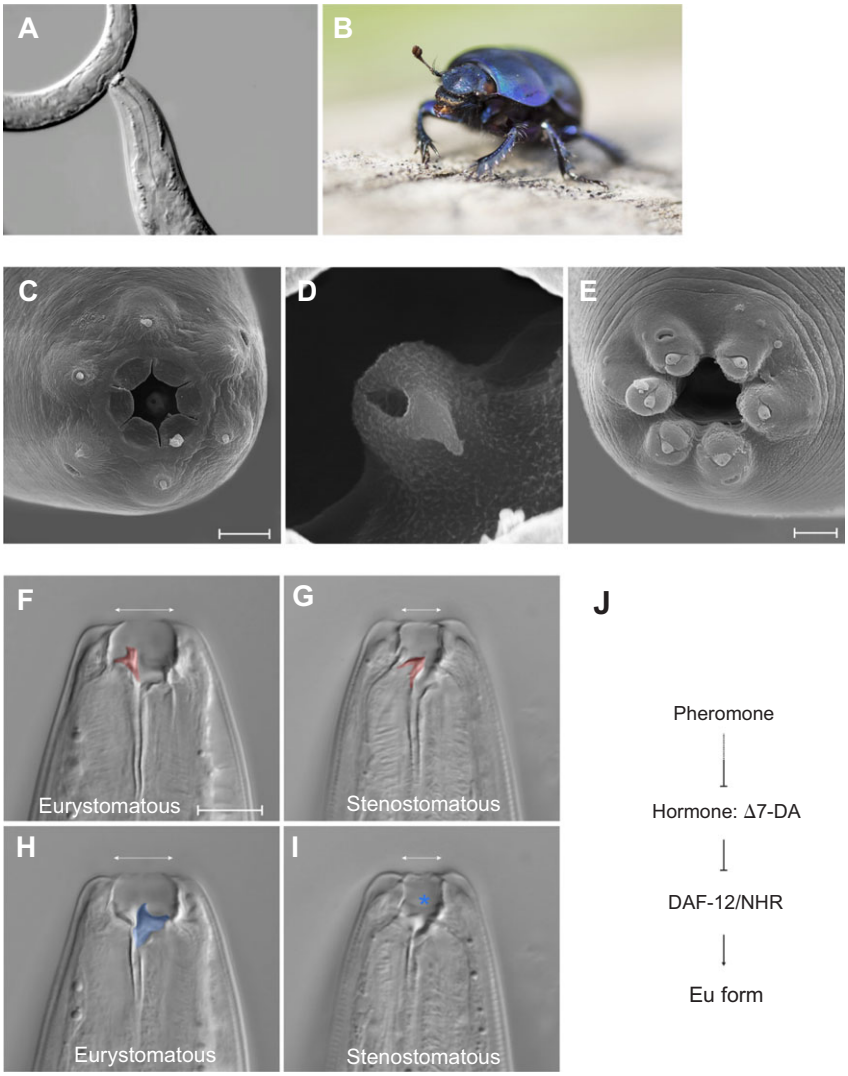

Fig. 1. Developmental plasticity in *Pristionchus pacificus* enables a predatory diet. (A) Image of killing behaviour in a *P. pacificus* eurystomatous (Eu) hermaphrodite feeding on a *Caenorhabditis elegans* larva. Image by Dr Dan Bumbarger. (B) *Pristionchus pacificus* lives in a necromenic association with scarab beetles. Photograph by Jan M. Meyer. (C) SEM images of an adult *P. pacificus* hermaphrodite with Eu mouth form revealing predatory adaptations. Scale bar, 3 µm. (D) Magnified images of the hook-shaped dorsal tooth and the large gland duct opening. (E) SEM image of an adult *C. elegans* hermaphrodite. Scale bar, 2 µm. (F,G) Nomarski image of the mouth dimorphism in *P. pacificus*. A single adult Eu and stenostomatous (St) hermaphrodite across two focal planes. The dorsal tooth, false coloured red, is larger and claw-like in the Eu form (F) compared with the flint-shaped St form (G). (H,I) The opposing subventral tooth, false coloured blue, is large and hook shaped in the Eu form (H), while absent in the St form (asterisk, I). Scale bar in F (applies to F–I), 10 µm. (J) Regulatory model for the mouth form decision pathway. Δ7-DA, Δ7-dafachronic acid; DAF-12 and NHR, nuclear hormone receptors.

prey. Through a pharmacological analysis of the effects of neurotransmitters, we identified a functional basis for regulating the behavioural switch between bacterial feeding and predatory feeding, and show this is conserved across several predatory nematode species. Furthermore, to understand predator and prey interactions, we investigated the impact of starvation, prey size and prey preference on *P. pacificus* predatory feeding. Finally, as the *Pristionchus* genus is well characterised, with most species revealing phenotypically plastic mouth structures falling into two distinct mouth types, we exploited this phenomenon to investigate the effects of mouth form morphology on predatory success and on predatory feeding behaviour itself.

RESULTS

Predatory feeding mode induces altered feeding rhythms

Pristionchus pacificus, like many diplogastrids, is capable of predatory feeding behaviour, supplementing its available food by feeding on other nematodes (Fig. 1A; supplementary material Movie 1). Accompanying this behaviour, a mouth dimorphism exists in *P. pacificus*, with the St bacteriovorus mouth comprising a single blunt dorsal tooth and the Eu predatory mouth form composed of a pair of opposing teeth including a flexible and enlarged dorsal tooth and a sizeable subventral tooth (Fig. 1C–I). Mouth forms can be readily identified based on these morphological differences. Furthermore, the pharynx of *P. pacificus* can be divided into three regions as in *C. elegans*, based on pharyngeal muscle groupings. These are the corpus, isthmus and terminal bulb. While in *C. elegans* pumping occurs anteriorly in the corpus and anterior isthmus and posteriorly in the terminal bulb, in *P. pacificus* pumping occurs only anteriorly in the corpus (Chiang et al., 2006). To explore predatory feeding behaviour in *P. pacificus*, we first analysed pharyngeal rhythms and the effect on tooth stimulation under different feeding conditions. We found that pumping rates during bacterial feeding were substantially higher than during predatory feeding (Fig. 2A). In contrast, the movement of the dorsal tooth could be observed only sporadically during bacterial feeding. However, tooth movement increased substantially during predatory feeding and appeared to be coupled to pharyngeal pumping in a 1:1 ratio (Fig. 2A). Thus, *P. pacificus* shows considerable differences in its feeding rhythms and dynamics during bacterial and predatory feeding.

Predatory feeding rhythms can be stimulated through serotonin exposure

To elucidate the neurobiological basis underlying the regulation of feeding behaviour, we conducted pharmacological experiments analysing the effects of the neurotransmitters serotonin, dopamine, octopamine and tyramine on pharyngeal pumping and tooth

The Journal of Experimental Biology (2015) 218, 1306-1313 doi:10.1242/jeb.118620

movement rate (Fig. 2B). Of these neurotransmitters, only serotonin triggered a predatory-like pumping and tooth movement response, causing a reduction in pharyngeal rhythms and stimulating tooth activity to levels similar to those observed while feeding on prey (supplementary material Movie 2). Despite lacking the opposing teeth of the Eu mouth form, St morph animals still possess a noticeable dorsal tooth although with very different morphology. Because of this evident difference in tooth morphology, we questioned whether it was controlled by a similar process. Wild-type *P. pacificus* (PS312) is mostly of the Eu morph with low numbers of St morph animals detectable. Fortunately, the recently characterised *eud-1* mutant (Ragsdale et al., 2013) is entirely St and therefore provided a means to acquire abundant St mouth form animals. Exposure of St animals to serotonin also elicited a strong predatory-like response, with tooth movement and pumping rates replicating those observed in Eu morph animals during predatory feeding (Fig. 2A). Thus, serotonin induces similar predatory-like feeding behaviour in both Eu and St morph animals.

Serotonin control of predatory feeding rhythms is evolutionarily conserved

As serotonin had such a profound effect on the feeding dynamics of *P. pacificus*, inducing predatory feeding rhythms, we speculated that this effect may be conserved among other predatory nematodes. In addition to *P. pacificus*, predation is a common feeding mechanism utilised by many other nematode species including other members of the genus *Pristionchus* but also many of its more distant relatives. Therefore, we tested three further *Pristionchus* species, including the closely related sister species *P. exspectatus*, as well as *P. entomophagus* and *P. fissidentatus* and a more distantly related representative outgroup *Allodiplogaster sudhausi*. In all assayed species, serotonin induced tooth stimulation in a 1:1 ratio with pharyngeal pumping, indicating a conserved mode of action (Fig. 2C). It is therefore conceivable that this mechanism of serotonin mediated predatory feeding mode switching may be conserved amongst diverse predatory nematodes.

Serotonin in *C. elegans* has long been associated with food signalling, increasing pharyngeal pumping rate while slowing locomotion. Consequently, the associated serotonergic neurons have been well characterised through numerous antibody and expression studies (Horvitz et al., 1982; Avery and Horvitz, 1990; Sze et al., 2000). In order to elucidate potential neurons associated with the modulation of predatory rhythms, we conducted serotonin immunostaining in *P. pacificus*. Antibody staining indicated several serotonergic neurons situated in the pharynx of *P. pacificus* as previously reported (Rivard et al., 2010). One pair of neurons appeared strongly serotonergic (Fig. 2D). These neurons were identified as the neurosecretory motor neurons (NSM), which are known to be strongly serotonergic in *C. elegans*. A second more anterior pair of neurons displayed weaker serotonin expression and, based on their position and form, they were identified as the pharyngeal interneurons, I1. Interestingly, the I1 neurons in *P. pacificus* were identified as a candidate regulator of predatory feeding in a recent connectomic study (Bumbarger et al., 2013).

Kinetics of predator–prey interactions

To study the interactions between *P. pacificus* predators and *C. elegans* prey, we initially focused on the Eu mouth morph because of its previous predatory associations (Serobyan et al., 2014). Predatory feeding behaviour was divided into three distinct categories. Firstly, 'bites', defined by a switch into predatory pumping rhythms and coinciding with a restriction in motility of the prey species. This was often accompanied by a strong touch response in the prey when the bite was unsuccessful. Secondly, 'kills', as indicated by an opening of the prey cuticle and leaking of pseudocoelomic fluid. Thirdly, 'feeding' events, categorised by the predator successfully opening the prey cuticle and remaining in close proximity to the laceration, consuming leaking innards. This was frequently accompanied by switching between bacterial and predatory pumping rhythms. Upon transferral and recovery of *P. pacificus* predators to biting assay plates (supplementary material Fig. S1), biting behaviour rapidly commenced, with an average of 15.3±6.2 bites per 10 min. Of these bites, 5.3±3.1 resulted in successful kills during the 10 min assay, an average killing efficiency of 35%. Surprisingly, not all bites were accompanied by feeding behaviour, with an average 2.6±2.2 feeding events per 10 min, corresponding to only 49% of successfully killed prey (Fig. 3A). This may be caused in part by prey being damaged as they escape or intriguingly may be evidence that *P. pacificus* predators eliminate potential competition.

To clarify whether the predatory feeding behaviour observed in *P. pacificus* is induced more or less strongly upon starvation, *P. pacificus* predators were starved for 4, 8, 24, 48 and 72 h before being placed with *C. elegans* larvae and repeating the previous assay (Fig. 3A). For each of the three feeding behaviour types quantified (i.e. biting, killing and feeding), a weak to moderate negative correlation was observed between the number of times the behaviour was expressed and starvation time (Pearson product-moment correlation, $r_{58}=-0.58$, $P<0.001$ for biting; $r_{58}=-0.39$, $P=0.002$ for killing; $r_{58}=-0.27$, $P=0.04$ for feeding). After a 4 h starvation, a minor increase in biting behaviour was elicited, possibly representing some predatory modulation of biting behaviour during early starvation. This was, however, absent at the later starvation time points. More noticeable was the decrease in biting events after severe starvation times such as after 72 h without food. Although these animals showed a reduction in biting activity, behaviourally animals spent prolonged periods feeding on killed individual prey, ensuring maximum uptake of nutrients and therefore reducing the total number of bites. Taken together, starvation is therefore not necessary to induce predatory feeding behaviour and, consequently, is likely to form part of the *P. pacificus* conventional feeding repertoire, probably supplementing its available bacterial nutrient intake with nematodes whenever possible.

Pristionchus has a preference for bacterial food

Next, we investigated aspects of *P. pacificus* predatory feeding resembling more closely the conditions found in nature, such as co-existence of food sources and differently staged prey items. It is highly likely that both bacteria and nematode larvae are represented in the regular diet of *P. pacificus* worms and it is also probable that *P. pacificus* may encounter the two food sources concurrently. Under such circumstances, food preference and choice may influence *P. pacificus* feeding behaviour. We therefore analysed which food source *P. pacificus* preferred through a chemoattraction assay between nematode larvae and a bacterial food source. As our laboratory *P. pacificus* strains are successfully raised on *Escherichia coli* OP50, we selected this as our bacterial food source and utilised immobilised *C. elegans* larvae as a counter-option. Under assay conditions, *P. pacificus* predators appeared to favour the bacterial food source with a chemoattraction index of 0.55. As *P. pacificus* appeared to have a preference for bacteria over nematode larvae, we next tested the impact of this on predatory feeding behaviour. *Pristionchus pacificus* predators were placed on an assay plate containing both a lawn of *E. coli* and *C. elegans* larvae and the

The Journal of Experimental Biology (2015) 218, 1306-1313 doi:10.1242/jeb.118620

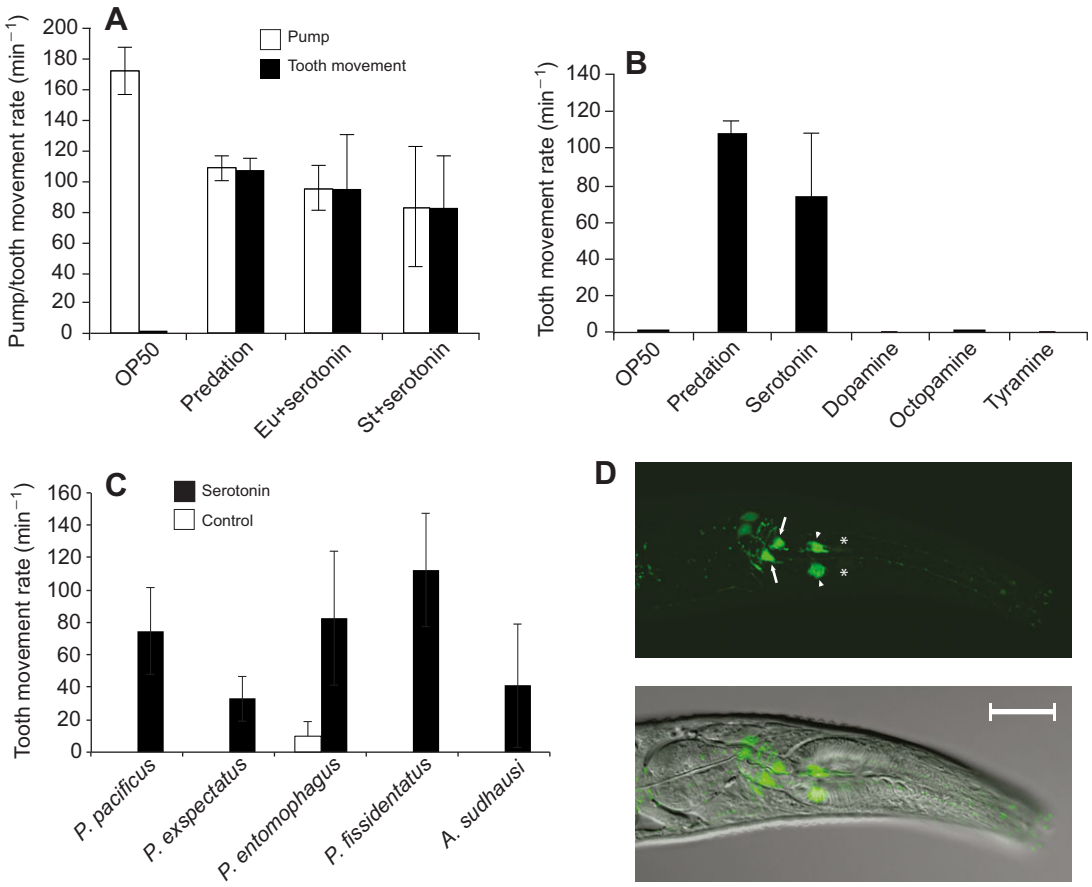

Fig. 2. Predatory feeding mode is regulated by the neurotransmitter serotonin. (A) Quantification of pharyngeal pumping and tooth movement rates reveals significant differences between bacterial and predatory feeding. Pumping rate is substantially lower during predatory feeding compared with bacterial feeding, while tooth movement rate increases dramatically. The neurotransmitter serotonin (10 mmol l^{-1}) triggers a predatory-like pumping and tooth movement response in both Eu (wild-type) and St (*eud-1* mutant) animals. OP50, *Escherichia coli* OP50. Error bars represent s.d. (B) Neurotransmitter effect on tooth movement rate. Treatment with 10 mmol l^{-1} serotonin triggers a predatory-like tooth movement response. The neurotransmitters dopamine (10 mmol l^{-1}), octopamine (10 mmol l^{-1}) and tyramine (10 mmol l^{-1}) do not affect tooth movement. Error bars represent s.d. (C) Serotonin (10 mmol l^{-1}) effect on tooth movement rate in Eu animals of selected *Pristionchus* species and the outgroup *Allodiplogaster sudhausi*. Serotonin triggers a predatory-like pumping and tooth movement response in all predatory nematodes tested. Error bars represent s.d. (D) Serotonin immunostaining merged with DIC image in whole-mount heads of adult nematodes. Anterior is to the right. Serotonergic neurons, probably corresponding to NSM (arrowheads), ADF (arrows) and I1 (asterisks), could be detected in the pharynx of *P. pacificus*. Scale bar, 20 µm.

number of biting events during a 10 min interval was observed. The number of biting events while *P. pacificus* predators were surrounded by bacteria was significantly lower (t_{18}=−4.183 P=0.0006) than when they were without bacteria, therefore reinforcing the preference for this bacterial food source over *C. elegans* nematode larvae (Fig. 3B). However, although the biting of larvae was lower, biting and killing events were still abundant. In its natural environment, *P. pacificus* is likely to encounter nematodes of all developmental stages. To understand the predatory capabilities of *P. pacificus*, we challenged *P. pacificus* predators with *C. elegans* prey of different developmental stages. *Pristionchus pacificus* predators were fed on *C. elegans* larvae immediately post-filtering, as well as after 24, 48 and 72 h of growth on OP50 (Fig. 3C). *Caenorhabditis elegans* larvae grown for 24 and 48 h were still in larval stages, whereas 72 h of growth results in gravid adults. Biting behaviour and successful kills were observed across all time points. *Pristionchus pacificus* predators were able to successfully bite all developmental stages of *C. elegans* with a consistent biting rate; no association between the number of bites and prey size was observed (Pearson product-moment correlation, r_{38}=−0.11, P=0.49). Killing efficiency, however, was negatively correlated with the prey size (r_{38}=−0.64, P<0.001) when the 72 h post-filter time point was included, and showed no correlation when only the first three time points were included in the analysis (r_{38}=−0.03, P<0.88). We hypothesise that at 72 h post-filtering, the *C. elegans* cuticle had probably reached a suitable thickness to prevent *P. pacificus* penetrating and successfully killing them. Despite this, *P. pacificus* bites still elicited a strong touch response in the 72 h *C. elegans* prey, inducing noticeable discomfort (supplementary material Movie 3).

Eu mouth form is required for predatory feeding behaviour in the genus *Pristionchus*

Nearly all members of the genus *Pristionchus* are dimorphic (*P. elegans* is fixed in the St morph while *P. triformis* has an additional extreme mouth morph, megastomatous, Mg), and so presented an ideal opportunity to study the influence of mouth morphology on predatory feeding behaviour within an evolutionary context. We selected 20 *Pristionchus* species and four additional diplogastrid species as comparative out-groups with which to analyse the influence of mouth form on predatory feeding behaviour (Fig. 4A). Animals were selected for mouth form, and corpse assays

The Journal of Experimental Biology (2015) 218, 1306-1313 doi:10.1242/jeb.118620

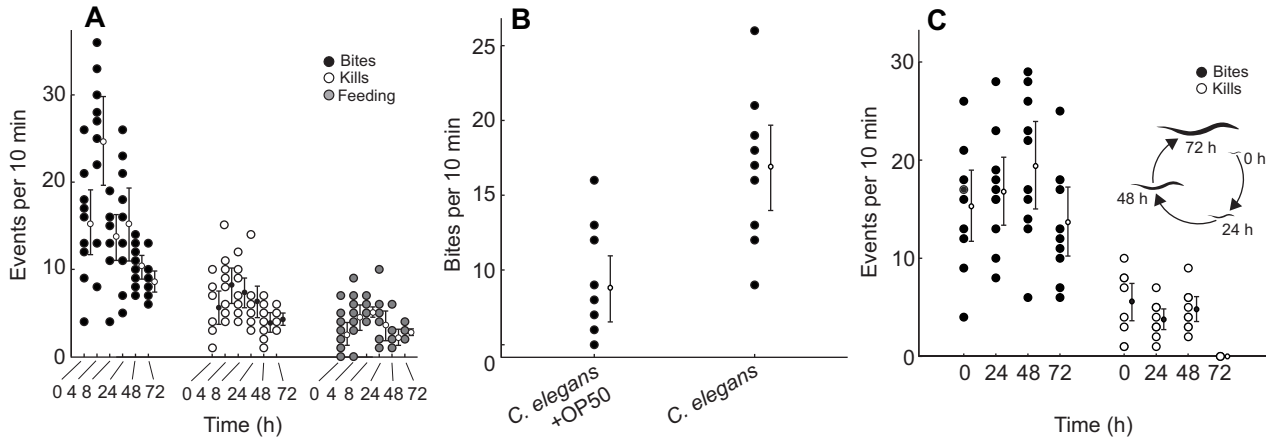

Fig. 3. Predator–prey interactions. (A) Biting assay investigating the effects of starvation upon *P. pacificus* predatory behaviour. *Pristionchus pacificus* predators were starved for 4, 8, 24, 48 h and subsequently fed on *C. elegans* prey. Bites, kills and feeding events were quantified (*N*=10). Starvation initially modulates an increase in biting activity, with severe starvation inducing prolonged feeding times that reduce the number of bites. Error bars represent 95% confidence interval of the mean. (B) Biting assay examining *P. pacificus* predators feeding on *C. elegans* larvae alone and also on *C. elegans* larvae in the presence of *E. coli* OP50. In the presence of additional bacterial food, *P. pacificus* biting rates decreased although biting of larvae was still abundant. (C) Biting assay examining the effects of prey size on predation success. *Pristionchus pacificus* were transferred to plates containing filtered *C. elegans* larvae fed for 0, 24, 48 and 72 h encompassing L1 to adult prey, and biting behaviour together with successful kills were quantified. *Pristionchus pacificus* bites all developmental stages of *C. elegans* prey with only adult animals protected (*N*=10). Each point represents a single replicate. If fewer than 10 circles are visible, they are hidden behind those displayed.

(supplementary material Fig. S1) were carried out on each species and mouth morph to detect successful predation events. Strikingly, corpses were not observed on any *Pristionchus* St assay plates while corpses were detected on nearly all Eu assay plates (Fig. 4B). *Pristionchus* St mouth forms were therefore unable to undertake predatory feeding, indicating a strong morphological influence on behaviour. In contrast, in all out-group species tested, St animals were still able to kill at a similar frequency to the other mouth morphs. It is important to note that all tested out-groups have St mouth forms that have a dorsal and subventral tooth, whereas the latter is absent in St animals of *Pristionchus* species.

Although *Pristionchus* St mouth forms were unable to kill prey, it was unclear whether this was caused by a mechanical deficiency, perhaps due to the much narrower mouth cavity in St animals, or if the killing behaviour itself was altered. Consequently, we selected four *Pristionchus* proficient killers and the out-group species *A. sudhausi* for further analysis via bite assay (Fig. 4C). As expected, both Eu and St mouth morphs of *A. sudhausi* frequently attacked prey. However, in all *Pristionchus* species tested, only the Eu mouth morph animals engaged in predatory feeding behaviour (supplementary material Movie 1). St mouth morphs appeared uninterested in the surrounding prey and no bites were detected (supplementary material Movie 4).

St mouth morphs are opportunistic scavengers

As we had previously demonstrated feeding mode switching in both *P. pacificus* Eu and St animals through exposure to serotonin (Fig. 2A), the finding that St morph animals failed to kill prey was somewhat surprising. In nature, Eu and St animals are likely to co-exist. As Eu mouth morphs kill abundantly, we speculated that St mouth morphs might be able to utilise a predatory feeding mode for scavenging on the corpses of killed nematodes. Consequently, we placed several adult *C. elegans* corpses amongst *P. pacificus* St animals. Indeed, predatory feeding behaviour was immediately stimulated upon contact with the opened *C. elegans* corpses (Fig. 4D). These findings indicate that predatory feeding behaviour is robustly suppressed in *Pristionchus* St animals; however, it is not entirely abolished, providing St animals with a mechanism for the opportunistic scavenging of nematode corpses.

DISCUSSION

This study is the first to characterise predatory feeding behaviour in nematodes, exposing fundamental differences between bacterial and predatory feeding dynamics and, most significantly, revealing a functional role for serotonin in this process as well as demonstrating the influence of mouth morphology on behaviour. We show that *P. pacificus* feeding dynamics are heavily influenced by diet, with distinct pumping rates and tooth stimulation corresponding directly with bacterial or predatory feeding. *Pristionchus pacificus* bacterial feeding is associated with rapid pharyngeal pumping (Kroetz et al., 2012) while we show predatory feeding necessitates slower, stronger pharyngeal rhythms coinciding with tooth activity in a 1:1 ratio. These differing feeding rhythms fall into discrete categories probably with differing genetic, muscular and neuronal contributions. As *P. pacificus* and *C. elegans* share identical numbers of pharyngeal neurons and mapped pharyngeal positions (Bumbarger et al., 2013), future cell-ablation experiments will help dissect the neuronal networks involved.

Feeding mode switching to predatory feeding behaviour appears to be driven by the neurotransmitter serotonin, although the genetic and neurobiological mechanisms behind this are as yet unknown. The effect of serotonin on nematode behaviour has been extensively studied in *C. elegans* by coupling food sensation to various neurological processes while identifying the neurons associated (Horvitz et al., 1982; Avery and Horvitz, 1990; Sze et al., 2000). Within the pharynx, only the NSM neurons are highly serotonergic in *C. elegans* and have a postulated role in food signalling. In the pharynx of *P. pacificus*, a pair of strongly serotonergic neurons was identified similar to the findings of a previous report (Rivard et al., 2010), corresponding to the NSM neurons, with a pair of weak serotonergic neurons anterior to this. These additional serotonergic neurons correspond to *P. pacificus* I1, which reinforces prior

The Journal of Experimental Biology (2015) 218, 1306-1313 doi:10.1242/jeb.118620

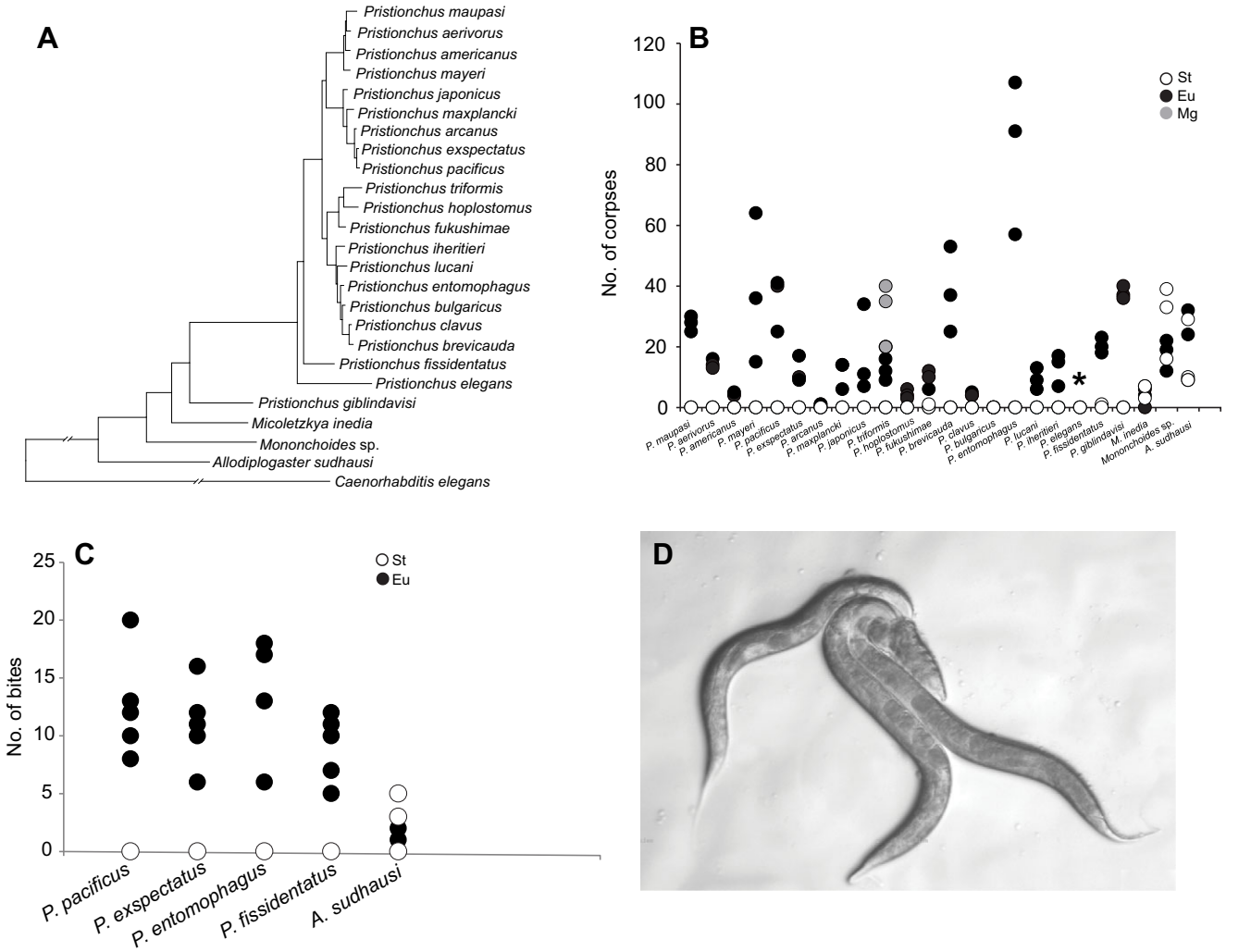

Fig. 4. Eu mouth form is required for predatory feeding behaviour in the genus *Pristionchus*. (A) Maximum likelihood tree of *Pristionchus* and outgroup species examined for predatory feeding behaviour on filtered *C. elegans* larvae, inferred using partial 18 S rRNA and 27 ribosomal protein genes. (B) Corpse assays investigating the effects of mouth form on predatory feeding success. Eu and St mouth forms for each species were analysed independently in triplicate for *N*=5 animals and the corpses counted after 2 h. Predatory feeding behaviour is prevalent in the majority of species analysed. No corpses were visible on St plates of any species. *The monomorphic *P. elegans* with a fixed St mouth form (*N*=3). Mg, megastomatous. (C) Bite assay of selected efficient predatory killing species in order to differentiate between a failure to successfully kill prey and a failure to engage in predatory feeding behaviour. Predatory behaviour appears suppressed in St mouth forms of *Pristionchus* species (*N*=5). Each point represents a single replicate. If fewer circles are visible than specified, they are hidden behind those displayed. (D) St mouth forms engage in predatory-like feeding rhythms, facilitating the scavenging of nematode corpses.

connectomic data speculating additional predatory functionality of this neuron pair based on graph theory analysis (Bumbarger et al., 2013). Furthermore, with recent advancements in methods for generating gene knockouts through CRISPR generated mutations (Lo et al., 2013; Witte et al., 2015), the analysis of genes involved in components of neurotransmitter synthesis and receptor genes can now be investigated.

While studies on the dimorphic properties of the *P. pacificus* mouth form have made great strides in elucidating the intricate developmental and chemical queues driving this process (Bento et al., 2010; Bose et al., 2012; Ragsdale et al., 2013), little was known of the influence of mouth form morphology on behaviour or its evolutionary conservation. Our study reveals a strong correlation between mouth morph and predatory feeding behaviour conserved within the *Pristionchus* genus. Animals with the smaller St mouth morph are unable to bite or kill live prey, indicating robust suppression of predatory killing behaviour. Despite the lack of killing behaviour in St morph animals, the predatory feeding mode was retained and still utilised for the opportunistic scavenging of previously killed nematodes. Our studies also show the importance of differentiating between predatory feeding behaviour and scavenging behaviour, perhaps explaining discrepancies with a previous finding (Serobyan et al., 2014). In this context, we would speculate that the observed killing without feeding behaviour of Eu and the scavenging behaviour of St morphs might be of significance under real environmental conditions. Additionally, the killing of nematodes by Eu morph animals leaves abundant carcasses, which are likely to stimulate the growth of more bacteria, thus providing additional nutritional benefits for the nematodes, while the elimination of competitors might represent a second function for the killing behaviour of Eu animals; support for such hypotheses will await testing in real ecological settings.

Taken together, our results characterised predatory feeding behaviour in *P. pacificus*, revealing novel functions for the well-described neurotransmitter serotonin. In addition, through our analysis of the mouth form dimorphism present in most

The Journal of Experimental Biology (2015) 218, 1306-1313 doi:10.1242/jeb.118620

Pristionchus species we also implicated this developmental decision in the control of predatory behaviour, indicating the existence of additional regulatory pathways feeding into this neuronal system. Therefore, further investigations into *P. pacificus* predatory feeding behaviour should provide a greater understanding of the mechanisms driving the evolution of complex behaviours within fixed neuronal networks.

MATERIALS AND METHODS

Nematode species

Nematode species were maintained at 20°C on NGM agar plates with *E. coli* OP50. Worm species and strains used were *C. elegans* (N2), *P. pacificus* (PS312), *P. maupasi* (RS0143), *P. aerivorus* (RS5106), *P. americanus* (RS0140), *P. mayeri* (RS5460), *P. exspectatus* (RS5522B), *P. arcanus* (RS5527), *P. maxplancki* (RS5594), *P. japonicus* (RS5528), *P. triformis* (ST5233), *P. hoplostomus* (JU1090), *P. fukishimae* (RS5595), *P. brevicauda* (RS5231), *P. clavus* (RS5284), *P. bulgaricus* (RS5283), *P. entomophagus* (RS0144), *P. lucani* (RS5050), *P. inheritieri* (SB245), *P. elegans* (RS5229), *P. fissidentatus* (RS5133), *P. giblindavisi* (RS5555), *Micoletzkya inedia* (RS5605), *Mononchoides* sp. 1 (RS5441) and *A. sudhausi* (B413).

Pumping and tooth rate

Pristionchus pacificus predators were maintained at 20°C until young adult stage. Animals were then transferred to an assay plate seeded with OP50 or filled with >5000 *C. elegans* larvae for observation via a Zeiss Axio Imager a1 microscope and high speed camera. Animals were left undisturbed for 15 min prior to assaying to allow for recovery. Pharyngeal pumping and tooth movements were observed for 15 s in at least 20 animals under each condition. *Caenorhabditis elegans* prey were prepared by growing cultures until newly starved and therefore contained an abundance of L1 and L2 larvae. These plates were washed with M9 and then passed through two 20 µm filters to remove larger animals. The filtered wash was centrifuged at 1500 rpm and 2 µl of the larval pellet added to each 6 cm NGM unseeded assay plate before the addition of any *P. pacificus* predators. For pharmacological assaying of neurotransmitters, animals were transferred to small (3 cm) assay plates containing 10 mmol l^{-1} of the appropriate neurotransmitter, and pharyngeal pumping and tooth movement were observed as described above.

Immunohistochemistry

Staining with anti-serotonin antibody was carried out as described by Desai et al. (1988). Briefly, worms were rinsed 3× in M9 and fixed overnight at 4°C in 500 µl of 4% paraformaldehyde/PBS. After being washed 3× in 0.5% Triton X-100/PBS, the animals were incubated overnight at 37°C in 500 µl of 5% β-mercaptoethanol/1% Triton X-100/0.1 mol l^{-1} Tris, pH 7.4. After incubation, worms were further washed 2× in 1% Triton X-100/0.1 mol l^{-1} Tris, pH 7.4, followed by a wash in 1× in collagenase buffer (1 mmol l^{-1} $CaCl_2$/1% Triton X-100/0.1 mol l^{-1} Tris, pH 7.4). They were then incubated for 2–8 h at 37°C in collagenase type IV in collagenase buffer. Animals were centrifuged at 1500 rpm and the pellet washed 3× in 0.5% Triton X-100/PBS before blocking for 1 h at room temperature in 100 µl of 1% BSA/0.5% Triton X-100/PBS. Processed animals were incubated overnight at room temperature in 1:100 anti-serotonin antibody in 1% BSA/0.5% Triton X-100/PBS before washing a further 2× in Triton X-100/PBS to remove unbound antibodies. A second blocking reaction for 1 h in 0.1% BSA/0.5% Triton X-100/PBS was carried out before incubation overnight at 4°C in 50 µl of 1:100 cy3 goat anti-rabbit secondary antibody. Finally, excess secondary antibody was removed by washing 3× in 0.5% Triton X-100/PBS and the worms mounted with Vectashield for imaging. Images were acquired on an Olympus FV 1000 confocal microscope.

Mouth form phenotyping

Mouth form phenotyping was attained through observation of the buccal cavity via a Zeiss SteREO Discovery V12 microscope. Morph identities were categorised based on previous described species characteristics and could be subsequently verified through mounting and ×40 Nomarski examination.

Biting assay

Biting assays provided more detailed behavioural analysis. Prey were maintained on bacteria until freshly starved, resulting in an abundance of young larvae. These plates were washed with M9, passed twice through a 20 µm filter, centrifuged and deposited on to the assay plate by pipetting 2 µl of worm pellet on to a 6 cm NGM unseeded plate. Predatory nematodes were screened for the required mouth morph and a single classified predator placed on to the assay plate and allowed to recover for 15 min. After recovery, the predatory animal was observed on a light stereo-microscope for 10 min and the number of bites/kills/feeding events quantified as appropriate. Bites were characterised by a switch in predator pumping mode coincident with a restriction in movement of the prey; kills were characterised by an opening of the prey cuticle; and feeding was characterised by the predator remaining adjacent to the successfully lacerated prey and observable consumption taking place (supplementary material Fig. S1A). Each assay was conducted 5–10 times depending on the experiment to ensure repeatability. The associations between different types of feeding behaviour and independent variables (i.e. starvation time and prey size) were tested using Pearson product-moment correlation. Size data for *C. elegans* were retrieved from Fernando et al. (2011).

Corpse assay

Corpse assays facilitated rapid quantification of predatory behaviour over a large number of species. Prey were maintained on bacteria until freshly starved, resulting in an abundance of young larvae. These plates were washed with M9, passed twice through a 20 µm filter, centrifuged and deposited on to the assay plate by pipetting 2 µl of worm pellet on to a 6 cm NGM unseeded plate. Five predatory nematodes were screened for the appropriate mouth morph and added to assay plates. Predators were permitted to feed on the prey for 2 h and the plate was subsequently screened for the presence of deflated corpses (supplementary material Fig. S1B). Each assay was conducted in triplicate to ensure repeatability.

Chemoattraction assay

Chemoattraction assays were carried out similar to previously described *Pristionchus* procedures with some modifications (Hong and Sommer, 2006). Briefly, standard nematode growth plates were seeded with a small spot of OP50 or with filtered *C. elegans* larvae at either side of the plate. To each attractant spot, 1.5 µl of 1 mol l^{-1} sodium azide was added in order to anaesthetise worms and prevent them from leaving the area upon attraction. Twenty *P. pacificus* adult worms were added equidistant between the two attractant sources and left for 16 h. The number of animals located at each source was quantified and a chemotaxis index scored by the following calculation: (no. of animals at attractant−no. of animals at control) / (total no. of nematodes at attractant and control). Three replicates were carried out and the mean chemoattraction index of the replicates was calculated.

Acknowledgements

We would like thank the *Caenorhabditis* Genetic Center for *C. elegans* strains, Jürgen Berger of the Electron Microscopy facility and Jan M. Meyer and Dr Dan Bumbarger for images.

Competing interests

The authors declare no competing or financial interests.

Author contributions

All experiments performed by M.W., J.W.L. and V.S. M.W., J.W.L. and R.J.S. designed the experiments and wrote the manuscript.

Funding

This work was funded by the Max Planck Society.

Supplementary material

Supplementary material available online at
http://jeb.biologists.org/lookup/suppl/doi:10.1242/jeb.118620/-/DC1

References

Avery, L. and Horvitz, H. R. (1990). Effects of starvation and neuroactive drugs on feeding in *Caenorhabditis elegans*. *J. Exp. Zool.* **253**, 263-270.

Baldwin, J. G., Ragsdale, E. J. and Bumbarger, D. (2004). Revised hypotheses for phylogenetic homology of the stomatostylet in tylenchid nematodes. *Nematology* **6**, 623-632.

Bento, G., Ogawa, A. and Sommer, R. J. (2010). Co-option of the hormone-signalling module dafachronic acid-DAF-12 in nematode evolution. *Nature* **466**, 494-497.

Bose, N., Ogawa, A., von Reuss, S. H., Yim, J. J., Ragsdale, E. J., Sommer, R. J. and Schroeder, F. C. (2012). Complex small-molecule architectures regulate phenotypic plasticity in a nematode. *Angew. Chem. Int. Edit.* **51**, 12438-12443.

Bumbarger, D. J., Riebesell, M., Rödelsperger, C. and Sommer, R. J. (2013). System-wide rewiring underlies behavioral differences in predatory and bacterial-feeding nematodes. *Cell* **152**, 109-119.

Chiang, J.-T. A., Steciuk, M., Shtonda, B. and Avery, L. (2006). Evolution of pharyngeal behaviors and neuronal functions in free-living soil nematodes. *J. Exp. Biol.* **209**, 1859-1873.

De Ley, P., Van De Velde, M. C., Mounport, D., Baujard, P. and Coomans, A. (1995). Ultrastructure of the stoma in Cephalobidae, Panagrolaimidae and Rhabditidae, with a proposal for a revised stoma terminology in Rhabditida (Nematoda). *Nematologica* **41**, 153-182.

Desai, C., Garriga, G., McIntire, S. L. and Horvitz, H. R. (1988). A genetic pathway for the development of the *Caenorhabditis elegans* HSN motor neurons. *Nature* **336**, 638-646.

Dieterich, C., Clifton, S. W., Schuster, L. N., Chinwalla, A., Delehaunty, K., Dinkelacker, I., Fulton, L., Fulton, R., Godfrey, J., Minx, P. et al. (2008). The *Pristionchus pacificus* genome provides a unique perspective on nematode lifestyle and parasitism. *Nat. Genet.* **40**, 1193-1198.

Fernando, T., Flibotte, S., Xiong, S., Yin, J., Yzeiraj, E., Moerman, D. G., Meléndez, A. and Savage-Dunn, C. (2011). *C. elegans* ADAMTS ADT-2 regulates body size by modulating TGFβ signaling and cuticle collagen organization. *Dev. Biol.* **352**, 92-103.

Handoo, Z. A. (2002). A key and compendium to species of the *Heterodera avenae* group (Nematoda : Heteroderidae). *J. Nematol.* **34**, 250-262.

Herrmann, M., Mayer, W. E., Hong, R. L., Kienle, S., Minasaki, R. and Sommer, R. J. (2007). The nematode *Pristionchus pacificus* (Nematoda: Diplogastridae) is associated with the oriental beetle *Exomala orientalis* (Coleoptera: Scarabaeidae) in Japan. *Zool. Sci.* **24**, 883-889.

Hong, R. L. and Sommer, R. J. (2006). Chemoattraction in *Pristionchus* nematodes and implications for insect recognition. *Curr. Biol.* **16**, 2359-2365.

Horvitz, H. R., Chalfie, M., Trent, C., Sulston, J. E. and Evans, P. D. (1982). Serotonin and octopamine in the nematode *Caenorhabditis elegans*. *Science* **216**, 1012-1014.

Hotez, P. J., Brooker, S., Bethony, J. M., Bottazzi, M. E., Loukas, A. and Xiao, S. H. (2004). Hookworm infection. *New. Engl. J. Med.* **351**, 799-807.

Hotez, P. J., Bethony, J. M., Diemert, D. J., Pearson, M. and Loukas, A. (2010). Developing vaccines to combat hookworm infection and intestinal schistosomiasis. *Nat. Rev. Microbiol.* **8**, 814-826.

Kroetz, S. M., Srinivasan, J., Yaghoobian, J., Sternberg, P. W. and Hong, R. L. (2012). The cGMP signaling pathway affects feeding behavior in the necromenic nematode *Pristionchus pacificus*. *PLoS ONE* **7**, e34464.

Lo, T.-W., Pickle, C. S., Lin, S., Ralston, E. J., Gurling, M., Schartner, C. M., Bian, Q., Doudna, J. A. and Meyer, B. J. (2013). Precise and heritable genome editing in evolutionarily diverse nematodes using TALENs and CRISPR/Cas9 to engineer insertions and deletions. *Genetics* **195**, 331-348.

Ragsdale, E. J., Crum, J., Ellisman, M. H. and Baldwin, J. G. (2008). Three-dimensional reconstruction of the stomatostylet and anterior epidermis in the nematode *Aphelenchus avenae* (Nematoda: Aphelenchidae) with implications for the evolution of plant parasitism. *J. Morphol.* **269**, 1181-1196.

Ragsdale, E. J., Müller, M. R., Rödelsperger, C. and Sommer, R. J. (2013). A developmental switch coupled to the evolution of plasticity acts through a sulfatase. *Cell* **155**, 922-933.

Rivard, L., Srinivasan, J., Stone, A., Ochoa, S., Sternberg, P. W. and Loer, C. M. (2010). A comparison of experience-dependent locomotory behaviors and biogenic amine neurons in nematode relatives of *Caenorhabditis elegans*. *BMC Neurosci.* **11**, 22.

Sato, H., Tanaka, S., Une, Y., Torii, H., Yokoyama, M., Suzuki, K., Amimoto, A. and Hasegawa, H. (2008). The stomal morphology of parasitic females of *Strongyloides spp*. by scanning electron microscopy. *Parasitol. Res.* **102**, 541-546.

Schlager, B., Wang, X., Braach, G. and Sommer, R. J. (2009). Molecular cloning of a dominant roller mutant and establishment of DNA-mediated transformation in the Nematode *Pristionchus pacificus*. *Genesis* **47**, 300-304.

Serobyan, V., Ragsdale, E. J., Müller, M. R. and Sommer, R. J. (2013). Feeding plasticity in the nematode *Pristionchus pacificus* is influenced by sex and social context and is linked to developmental speed. *Evol. Dev.* **15**, 161-170.

Serobyan, V., Ragsdale, E. J. and Sommer, R. J. (2014). Adaptive value of a predatory mouth-form in a dimorphic nematode. *Proc. R. Soc. B Biol. Sci.* **281**, 20141334.

Sommer, R. J. and McGaughran, A. (2013). The nematode *Pristionchus pacificus* as a model system for integrative studies in evolutionary biology. *Mol. Ecol.* **22**, 2380-2393.

Straud, S., Lee, I., Song, B., Avery, L. and You, Y.-J. (2013). The jaw of the worm: GTPase-activating protein EAT-17 regulates grinder formation in *Caenorhabditis elegans*. *Genetics* **195**, 115-125.

Susoy, V., Ragsdale, E. J., Kanzaki, N. and Sommer, R. J. (2015). Rapid diversification associated with a macroevolutionary pulse of developmental plasticity. *eLife* **4**,

Sze, J. Y., Victor, M., Loer, C., Shi, Y. and Ruvkun, G. (2000). Food and metabolic signalling defects in a *Caenorhabditis elegans* serotonin-synthesis mutant. *Nature* **403**, 560-564.

von Lieven, A. F. (2003). Functional morphology and evolutionary origin of the three-part pharynx in nematodes. *Zoology* **106**, 183-201.

Witte, H., Moreno, E., Rödelsperger, C., Kim, J., Kim, J.-S., Streit, A. and Sommer, R. J. (2015). Gene inactivation using the CRISPR/Cas9 system in the nematode *Pristionchus pacificus*. *Dev. Genes Evol.* **225**, 55-62.

JOURNAL OF Evolutionary Biology

doi: 10.1111/jeb.12367

Preferential host switching and codivergence shaped radiation of bark beetle symbionts, nematodes of *Micoletzkya* (Nematoda: Diplogastridae)

V. SUSOY & M. HERRMANN

Department of Evolutionary Biology, Max Planck Institute for Developmental Biology, Tübingen, Germany

Keywords:

coevolution;
cospeciation;
phylogeny;
speciation;
symbiosis.

Abstract

Host-symbiont systems are of particular interest to evolutionary biology because they allow testable inferences of diversification processes while also providing both a historical basis and an ecological context for studies of adaptation. Our investigations of bark beetle symbionts, predatory nematodes of the genus *Micoletzkya*, have revealed remarkable diversity of the group along with a high level of host specificity. Cophylogenetic analyses suggest that evolution of the nematodes was largely influenced by the evolutionary history of beetles. The diversification of the symbionts, however, could not be attributed to parallel divergence alone; our results indicate that adaptive radiation of the nematodes was shaped by preferential host shifts among closely related beetles along with codivergence. Whereas ecological and geographic isolation have played a major role in the diversification of *Micoletzkya* at shallow phylogenetic depths, adaptations towards related hosts have played a role in shaping cophylogenetic structure at a larger evolutionary scale.

Introduction

Reciprocal adaptations among interacting organisms shape patterns of biodiversity (Darwin, 1862; van der Heijden *et al.*, 1998; Bascompte *et al.*, 2003; Thompson, 2005). In host-symbiont systems (de Bary, 1879), a long history of intimate relationships can lead to codivergence, whereby the divergence of symbionts tracks that of the hosts. Series of consecutive codivergence events over evolutionary time eventually result in congruent phylogenies of interacting taxa (Hafner & Page, 1995; Hughes *et al.*, 2007; Cruaud *et al.*, 2012). Conversely, historical events such as host switches, duplications, failures to diverge, and losses disrupt phylogenetic congruence (Page, 1994). The degree of phylogenetic congruence is affected by several ecological factors that influence the distribution and abundance of the hosts and associates: (i) the vertical mode of symbiont transmission within host populations and limited abilities to disperse to a novel host enforce parallel divergence; (ii) sympatry and syntopy of the hosts facilitate host switching; (iii) patchiness of symbiont distributions and low infestation rates make duplications and losses more likely to happen (Clayton *et al.*, 2004). Ecological isolation, however, is not the only mechanism that shapes cophylogenetic patterns; adaptive specialization greatly contributes to phylogenetic congruence by reducing the probability of successful colonization of a novel host (Clayton *et al.*, 2003; Perlman & Jaenike, 2003). In the absence of symbiont adaptation to a particular host, even rare opportunities for host switching would obscure signals of parallel divergence over long evolutionary timeframes. Furthermore, preferential switching towards related hosts alone can give rise to a cophylogenetic structure (de Vienne *et al.*, 2007).

To fully understand how isolation and specialization affect diversification in host-symbiont systems, it is necessary to couple detailed knowledge about the evolutionary history of each interacting species with a comprehensive mechanistic understanding of adaptations between symbiotic partners. Beyond the simple description of cophylogenetic patterns, empirical studies

Correspondence: Matthias Herrmann, Department of Evolutionary Biology, Max Planck Institute for Developmental Biology, Spemannstraße 37, 72076 Tübingen, Germany.
Tel.: +49 7071 601 484; fax: +49 7071 601 498;
e-mail: matthias.herrmann@tuebingen.mpg.de

of coevolutionary associations can elucidate mechanistic bases of adaptation to a well-defined environment. Such studies are particularly feasible in systems where symbiotic associations are amenable to controlled, direct observation and experimental manipulation.

Nematodes are believed to represent the most species-rich group of multicellular organisms, and their evolutionary success is largely attributed to various symbioses with plants and animals (Lambshead, 1993; Blaxter *et al.*, 1998). Yet little is known about nematode biodiversity and the factors that shape their distribution and diversification. Studies have shown that host switching is very common among parasitic and pathogenic nematodes (Pozio *et al.*, 2009; Hasegawa *et al.*, 2010; Laetsch *et al.*, 2012; McFrederick *et al.*, 2013a), and codivergence might have occurred in nematodes that are symbiotic with specialized groups of insects, such as fig wasps, *Fergusonina* flies and sweat bees (Giblin-Davis *et al.*, 2004; McFrederick & Taylor, 2013b).

Nematodes of the genus *Micoletzkya* (Diplogastridae; Sudhaus & von Lieven, 2003) are found exclusively in association with bark beetles and their relatives, the wood-boring weevils of *Araucarius*. The host range of *Micoletzkya* nematodes includes several economically important bark beetles across North America and Europe; examples include the mountain pine beetle (*Dendroctonus ponderosae*), the spruce beetle (*D. rufipennis*), and the eight-toothed European spruce bark beetle (*Ips typographus*) (Rühm, 1956; Massey, 1974). Except for a short dispersal period, bark beetles spend most of their lives within tunnels that they build in bark or wood. The life history of *Micoletzkya* is tightly linked to that of the bark beetle hosts (Figs 1 and S1). *Micoletzkya* nematodes are transmitted by dispersing, adult bark beetles as dauer larvae; dauers are nonfeeding, developmentally arrested larvae that have heightened ability to withstand abiotic stresses. Adult bark beetles can each carry up to several hundred dauer larvae. By the time the male and female host beetles have established a breeding gallery and laid eggs, the nematodes resume development; they have a few free-living generations in the breeding galleries of the hosts where they feed on other bark beetle-associated organisms, including parasitic nematodes (Susoy *et al.*, 2013) and are thus potentially beneficial to the beetle hosts. As bark beetles reach adulthood, dauer juveniles again arise to infest their hosts. The vertical mode of *Micoletzkya* transmission in populations of beetles and the presumably high degree of host specificity (Rühm, 1956) foster the potential for parallel divergence and make *Micoletzkya* perfect candidates for studies of cospeciation. Moreover, the nematodes have a generation time of about 10 days and can be cultured on monoxenic bacteria, making them amenable to ecological and biological studies.

The nematodes of *Micoletzkya* have intimate, stable and highly specific associations with their hosts. Therefore, the beetle-*Micoletzkya* association is an ideal system for examining the role of isolation and adaptive specialization in determining host range and radiation of symbionts. In this study, we have demonstrated the diversity of nematodes using a molecular barcoding approach and have identified, by cophylogenetic analyses, forces that influence their diversification.

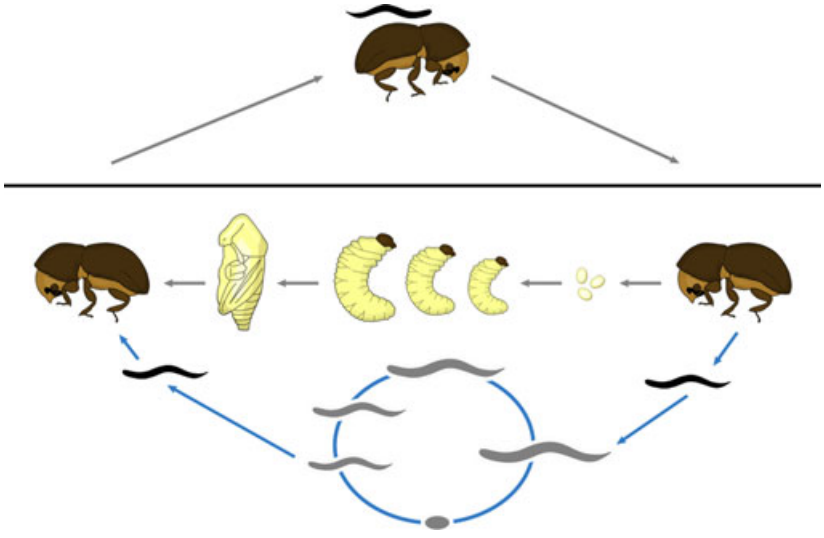

Fig. 1 Life cycle of *Micoletzkya* nematodes is tightly linked to that of their specific bark beetle hosts. Nematode dispersal larvae (dauers) locate onto the body surface of male and female beetles for transmission (shown above the solid line) and resume their development in breeding galleries of the hosts (below the line). After several free-living generations, the nematodes enter dauer arrest and infest emerging young beetles. Thus, *Micoletzkya* nematodes are transmitted vertically within a population of bark beetles.

Materials and methods

Sampling, isolation and culturing of nematodes

Live beetles were dissected and placed individually onto nematode growth medium (NGM) agar plates. We preserved samples of beetle tissue in ethanol for molecular analyses. The agar plates were screened for the presence of *Micoletzkya* nematodes after several days of incubation at room temperature. When possible, monoxenic cultures of nematodes were established using *Erwinia*-related bacterium isolate P11-1 as food (Susoy *et al.*, 2013); culturable species were used in subsequent molecular analyses and mating experiments. These isolates are being permanently maintained as living cultures and have been preserved in liquid nitrogen as previously described (Herrmann *et al.*, 2006a). For nematode strains not brought into culture, we used single adult worms or dauer juveniles from the original beetle plates for DNA extraction. The species *M. buetschlii* and *Micoletzkya* sp. 7 were cultured using plates that contained *C. elegans* larvae as food.

Species delimitation, mating tests and molecular analyses

Bark beetles were identified to genus and species levels based on morphology. For molecular analyses, we preferably used the same beetle specimens that yielded *Micoletzkya* nematodes; otherwise, we used beetles of the same species collected at the same locality and time. We obtained partial sequences of three nuclear genes (18s rRNA, 28s rRNA and *EF-1α*) from two specimens of each beetle species that tested positive for *Micoletzkya*. A wood-boring weevil *Rhyncolus* sp. (Coleoptera: Cossoninae) was included in the analyses as outgroup. Sequences were aligned using MUSCLE 3.8 with default settings (Edgar, 2004), *EF-1α* was realigned by translation, and ambiguously aligned regions were removed from the alignment manually.

Micoletzkya species delimitation was based on comparison of 18s rRNA partial sequences. For each nematode isolate, we sequenced a 1.6-kb fragment of the 18s rRNA gene. Isolates that had the same haplotype (showed no difference in 18s rRNA partial sequence) were considered (tentatively) the same putative species. We chose 18s marker because it was shown to be useful for species delimitation in *Pristionchus*, a genus of diplogastrid nematodes closely related to *Micoletzkya* (Mayer *et al.*, 2009). Studies on multiple species and strains of *Pristionchus* that involved mating tests demonstrated that (i) strains that had identical 18s rRNA haplotypes were always able to produce fertile F2 offspring, and (ii) even a small difference (i.e. one nucleotide) in the gene sequence provided evidence for existence of novel species (Herrmann *et al.*, 2006a,b, 2010; Kanzaki *et al.*, 2012, 2013).

We confirmed molecular-based species delimitation by performing mating tests within the most closely related pairs of culturable isolates of *Micoletzkya* as informed by our phylogenetic analysis (see Phylogenetic reconstruction). In each cross, one virgin female of one species was placed together with five males of the second species. All crosses were performed reciprocally. We screened the plates after 10 days for the presence of progeny; each test was repeated three times, and we performed positive controls using males and virgin females of the same isolate. If crosses yielded F1 worms, we then backcrossed the F1 to parental lines and checked for viable F2 progeny. Species names were assigned to those putative species that matched morphological descriptions of previously described *Micoletzkya* and that were isolated from the type host.

For phylogenetic analyses, we also amplified and sequenced an approximately 0.7-kb portion of *coxI* and a 3.3-kb fragment of 28s rRNA for one to two isolates of each putative *Micoletzkya* species and obtained sequences of ribosomal protein genes *rpl-2*, *rpl-9*, *rpl-10* and *rpl-23* using the reverse transcription polymerase chain reaction as previously described by Mayer *et al.* (2007). Combined ribosomal protein sequences were approximately 2.3 kb in length and available from 13 culturable putative species out of 26 total putative species of *Micoletzkya* included in the phylogenetic analyses (Table S1); most of the major *Micoletzkya* clades (seven of nine) contained at least one terminal taxon that had no missing data. Diplogastrid nematodes *Koerneria* sp. (RS1982), *Acrostichus* sp. (RS5083), *Pristionchus pacificus* (PS312) and *Parapristionchus giblindavisi* (RS5555) were used as outgroups; nucleotide sequences of these nematodes were retrieved from GenBank. 18s and 28s rRNA sequences were aligned with the help of MAFFT 6.9 (Katoh *et al.*,2002) using the G-INS-i method. Nucleotide sequences of *coxI* and ribosomal protein genes were aligned using MUSCLE 3.8 and realigned by translation. Regions that were ambiguously aligned for both ingroup (*Micoletzkya* spp.) and outgroup (*Koerneria*, *Acrostichus*, *Pristionchus* and *Parapristionchus*) taxa were completely removed manually. Characters that could not be unambiguously aligned only for the outgroup taxa were treated as missing data. The total amount of missing data in the concatenated alignment was 13%.

Primers used in this study are listed in Table S2. Nematode, and bark beetle sequences original for this study and obtained previously (Susoy *et al.*, 2013) are available in GenBank under Accession Numbers KJ530992–KJ531197 and JX163954–JX163992. Accession Numbers for *Koerneria* sp. (RS1982), *Acrostichus* sp. (RS5083), *P. pacificus* (PS312) and *P. giblindavisi* (RS5555) are listed in Table S3.

Phylogenetic reconstruction

Phylogenetic trees of beetles and nematodes were inferred from concatenated alignments under the maximum likelihood (ML) criterion as implemented in RAxML 7.3 (Stamatakis, 2006) and by Bayesian inference in MrBayes 3.2. (Ronquist *et al.*, 2012). For beetles, the sequence alignment contained 2755 characters, including 530 variable and 400 parsimony-informative sites. The alignment was divided into five partitions for ML search: 18s rRNA, 28s rRNA and *EF-1α* 1st, 2nd, and 3rd codon positions. We used the general time reversible (GTR) model of nucleotide substitutions with gamma-distributed rate heterogeneity across sites (GTRGAMMA) for all partitions, and carried out 50 ML searches on distinct starting trees. Support values for the best-scoring ML tree were obtained by performing 1000 bootstrap pseudoreplicates. For Bayesian analysis, the dataset was divided into three partitions: 18s rRNA, 28s rRNA and *EF-1α*. For the 18s and 28s rRNA partitions, reversible substitution model space was sampled during MrBayes runs by setting nst to 'mixed'. Among site rate heterogenetic was assumed to be gamma-distributed. We used the codon model for the partition containing *EF-1α*. Parameters were unlinked across partitions. We ran four independent MCMC analyses for 3×10^6 generations, sampling chains every 100th generation. We discarded as burn-in 33% of samples before summarizing parameters and trees. After confirming convergence of runs, a 50% majority-rule consensus tree was generated with clade probability values given as posterior probabilities (PP).

For nematodes, the concatenated alignment consisted of 7909 nucleotide positions, of which 2325 were variable and 1444 parsimony-informative. For Bayesian inference, the alignment was partitioned as follows: 18s rRNA, 28s rRNA, combined ribosomal protein genes and *coxI*; for ML analyses, the last two fractions were further partitioned according to codon position. Fifty ML searches were performed under a GTRGAMMA model for all partitions. Preliminary results revealed higher rates of divergence in *coxI* compared with the other genes (results not shown); we therefore performed additional analysis on a dataset excluding these sequences. Support values for best-scoring ML trees were estimated from 1000 bootstrap pseudoreplicates. In the Bayesian analysis, the first two partitions, which contained 18s rRNA and 28s rRNA sequences, were analysed using 'mixed' + Γ model, and the codon model was used for partitions that contained protein-coding genes. Parameters were unlinked across partitions. We ran four independent analyses for 7×10^6 generations, sampling chains every 100th generation. To account for burn-in, we discarded 33% of samples before summarizing parameters and 33% of samples before summarizing trees. A 50% majority-rule consensus tree was generated after confirming run convergence and burn-in assignment.

Cophylogenetic analyses

Degrees of phylogenetic congruence were assessed using reconciliation analyses. We performed topology- and distance-based tests both in Jane 4 (Conow *et al.*, 2010) and in AxParafit (Stamatakis *et al.*, 2007), a modified version of ParaFit (Legendre *et al.*, 2002) implemented in Copycat (Meier-Kolthoff *et al.*, 2007). Both methods efficiently handle large datasets and allow for instances where symbionts occur on multiple hosts.

Jane 4 uses host and associate phylogenies and an association map as inputs and performs heuristic searches to find the most parsimonious mapping solutions for a given dataset. The most parsimonious solutions are chosen according to the specified weight metrics of five different types of evolutionary events. In our analyses, we assigned costs of zero to codivergence events, one to duplications, losses and failures to diverge, and two for duplications with a host switch. A vertex-based cost model was used, and searches were run for 100 generations with the population size set to 1000. Randomization tests were performed by generating 100 samples of random-tip mappings using the same genetic algorithm parameters as used in the original analysis.

AxParafit tests the null hypothesis of independent evolution of interacting taxa. In contrast to Jane 4, the programme uses pairwise distances, rather than phylogenies, and a table of host-symbiont associations. Distances were estimated according to patristic distances calculated from the host and symbiont phylogenies, and the input matrices were transformed into a matrix of principal coordinates with the help of AxPcoords (Stamatakis *et al.*, 2007), from which a ParaFitGlobal statistic was calculated. Random permutations were performed on rows of the association matrix to assess statistical significance. AxParafit also evaluates significance of individual host-symbiont associations by estimating their contribution to the overall cophylogenetic structure. For tests of individual associations, we used patristic distances derived from the beetle and nematode phylogenies and employed the Lingoes method to correct for negative eigenvalues. Tests were performed with 9999 permutations.

To test for cophylogeny at three different phylogenetic scales, we used (i) complete beetle and nematode datasets; (ii) phylogenies of two crown groups of *Micoletzkya* (*buetschlii* and *palliati*) and their hosts; and (iii) pruned beetle and nematode phylogenies. In all reconciliation analyses, the Bayesian trees of beetles and of nematodes were used as inputs. Results of statistical tests were considered significant when $P < 0.05$.

Results

Beetle-nematode associations

Bark beetles were collected from several locations across Central and Eastern Europe, North America and Japan (Table 1). Of the 85 bark beetle species that we examined (more than 6000 individual beetles), 35 tested positive for *Micoletzkya* nematodes. For 14 beetle species, nematode associations are reported here for the first time. In total, bark beetles yielded more than 450 isolates of *Micoletzkya*. Isolates that showed no difference in the 18s rRNA gene were tentatively considered as belonging to the same species. By this criterion, *Micoletzkya* isolates fell into 26 different putative species. Mating tests confirmed reproductive isolation in six of seven pairs tested (Table 2), as these trials produced no fertile F1 progeny, although two species produced sterile F1 hybrids. Crosses between *M. buetschlii* and '*M.* sp. 7' resulted in fertile offspring, indicating that they might belong to the same biological species. Because mating tests could not be performed for unculturable isolates, reproductive isolation could not be ruled out for all closely related putative species pairs. Based on our comparative analysis of 18s rRNA sequences, however, we hypothesize that our putative species represent unique, separate evolutionary lineages (Wiley, 1978; Adams, 1998).

Putative species of *Micoletzkya* appeared to be remarkably host-specific (Fig. 2). Nineteen species were each found in an association with a single species of bark beetle. Six putative species of *Micoletzkya* were found on more than one host, although in all cases but one the hosts were closely related (i.e. the different hosts were members of the same genus; Fig. 3). An exception was the case of *M.* cf. *inedia*, which was the only nematode found on beetles belonging to different beetle subfamilies. The associations between bark beetles and the nematodes were also consistent; when collected from several different localities, beetles of the same species yielded nematodes belonging to the same putative species of *Micoletzkya* (Table 1). For example, the eight-toothed bark beetle *I. typographus* was repeatedly found in an association with *M. buetschlii* across many locations in Central and Eastern Europe. Similarly, individuals of the pine engraver beetle *I. pini* and the mountain pine beetle *D. ponderosae*, which were collected from several locations in Arizona and Canada, at all times yielded *M.* sp. 12 and *M.* cf. *inedia,* respectively. We never observed two closely related putative species of *Micoletzkya* in association with the same beetle species. However, *Dryocoetes autographus* and *Hylurgops reticulatus* each harboured two phylogenetically distant species of *Micoletzkya*. In *D. autographus*, we observed co-infestation by two *Micoletzkya* species, *M.* sp. 3 and *M.* sp. 5, although most individuals of this host carried only one of the two nematode species.

Table 1 Host beetles collected in this study and *Micoletzkya* nematodes isolated from them. Numbers in brackets indicate number of nematode isolates obtained from respective beetle species.

Beetle species	Location	Nematode putative species
Dendroctonus approximatus	AZ, USA	*M.* sp. 19 (1)
Dendroctonus ponderosae	BC, Canada	*M.* cf. *inedia* (4)
	AZ, USA	*M.* cf. *inedia* (16)
Dendroctonus rufipennis	AZ, USA	*M.* sp. 19 (5)
Dryocoetes affaber	Alberta, Canada	*M.* sp. 14 (3)
Dryocoetes autographus	Czech Republic	*M.* sp. 5 (3)
	Germany	*M.* sp. 3 (18), *M.* sp. 5 (9)
Dryocoetes uniseriatus	Japan	*M. japonica**
Hylastes ater	Germany	*M. hylurginophila* (9)
Hylastes attenuatus	Germany	*M. palliati* (5)
Hylastes brunneus	Germany	*M. hylurginophila* (18)
Hylastes gracilis	AZ, USA	*M.* sp. 26 (6)
Hylastes opacus	Germany	*M. palliati* (10)
Hylurgops palliatus	Czech Republic	*M. palliati* (8)
	Germany	*M. palliati* (82)
Hylurgops cf. *porosus*	AZ, USA	*M.* sp. 15 (2)
Hylurgops reticulatus	Alberta, Canada	*M.* sp. 13 (9), *M.* sp. 15 (1)
Hylurgops subcostulatus	AZ, USA	*M.* sp. 20 (24)
Hylurgus ligniperda	Germany	*M. hylurginophila* (3)
Ips acuminatus	Germany	*M.* sp. 8 (2)
	Italy	*M.* sp. 8 (2)
Ips amitinus	Czech Republic	*M. buetschlii* (12)
Ips bonanseai	AZ, USA	*M.* sp. 24 (4)
Ips calligraphus	AZ, USA	*M.* cf. *calligraphi* (4)
Ips cembrae	Germany	*M.* sp. 7 (20)
Ips confusus	AZ, USA	*M.* sp. 22 (9)
Ips duplicatus	Czech Republic	*M. buetschlii* (10)
Ips integer	AZ, USA	*M.* cf. *calligraphi* (8)
Ips knausi	AZ, USA	*M.* sp. 25 (3)
Ips lecontei	AZ, USA	*M.* cf. *calligraphi* (9)
Ips pilifrons	AZ, USA	*M.* sp. 23 (6)
Ips pini	Alberta, Canada	*M.* sp. 12 (16)
	BC, Canada	*M.* sp. 12 (8)
	AZ, USA	*M.* sp. 12 (15)
Ips sexdentatus	Austria	*M. sexdentati* (32)
Ips typographus	Austria	*M. buetschlii* (4)
	Belgium	*M. buetschlii* (2)
	Czech Republic	*M. buetschlii* (6)
	Estonia	*M. buetschlii* (13)
	Germany	*M. buetschlii* (70)
Orthotomicus caelatus	Alberta, Canada	*M. masseyi* (15)
Orthotomicus latidens	AZ, USA	*M.* cf. *inedia* (2)
Orthotomicus sp.	Japan	*M.* sp. 18*
Pityokteines curvidens	Germany	*M.* sp. 4 (11)
Scierus sp.	AZ, USA	*M.* sp. 27 (2)

**M. japonica* and *M.* sp. 18 were isolated by Natsumi Kanzaki.

In line with previous observations (Rühm, 1956; Massey, 1974), only those bark beetles associated with conifers harboured *Micoletzkya*. We isolated nematodes from all analysed species of *Ips, Hylastes* and *Hylurgops* but not all species of *Dendroctonus*, *Orthotomicus* and

Table 2 Results of mating tests between closely related *Micoletzkya* isolates.

Cross	F1 progeny	F2 progeny
M. buetschlii males × *M.* sp. 7 females	Yes	Yes
M. buetschlii females × *M.* sp. 7 males	Yes	Yes
M. buetschlii males × *M.* cf. *calligraphi* females	No	–
M. buetschlii females × *M.* cf. *calligraphi* males	No	–
M. sp. 7 males × *M.* cf. *calligraphi* females	No	–
M. sp. 7 females × *M.* cf. *calligraphi* males	No	–
M. buetschlii males × *M. masseyi* females	No	–
M. buetschlii females × *M. masseyi* males	No	–
M. hylurginophila males × *M. palliati* females	No	–
M. hylurginophila females × *M. palliati* males	Yes	No
M. sp. 26 males × *M. hylurginophila* females	No	–
M. sp. 26 females × *M. hylurginophila* males	Yes	No
M. palliati males × *M.* sp. 26 females	No	–
M. palliati females × *M.* sp. 26 males	No	–

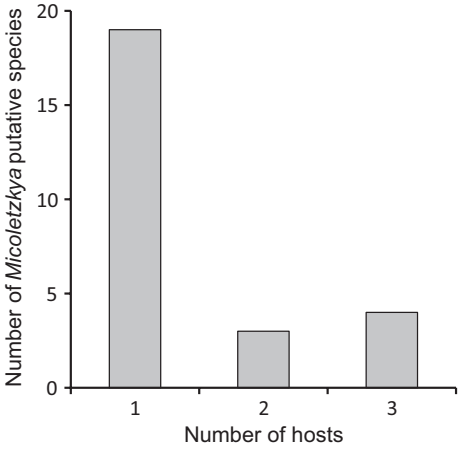

Fig. 2 Host specificity of *Micoletzkya* nematodes. The number of bark beetle species used as hosts by putative *Micoletzkya* species.

Pityokteines. For some species, the absence of *Micoletzkya* might be attributed to the small number of individual beetles available for examination or to biases introduced by procedures of nematode isolation. Namely, positive associations were scored only if developmental recovery from the dauer stage was successful, thereby allowing observation of adult nematodes on a plate. However, because dauer recovery rates were very low in some *Micoletzkya* species, high fractions of false negatives may have resulted from such samples. Therefore, we give no estimates of beetle infestation rates. Never-

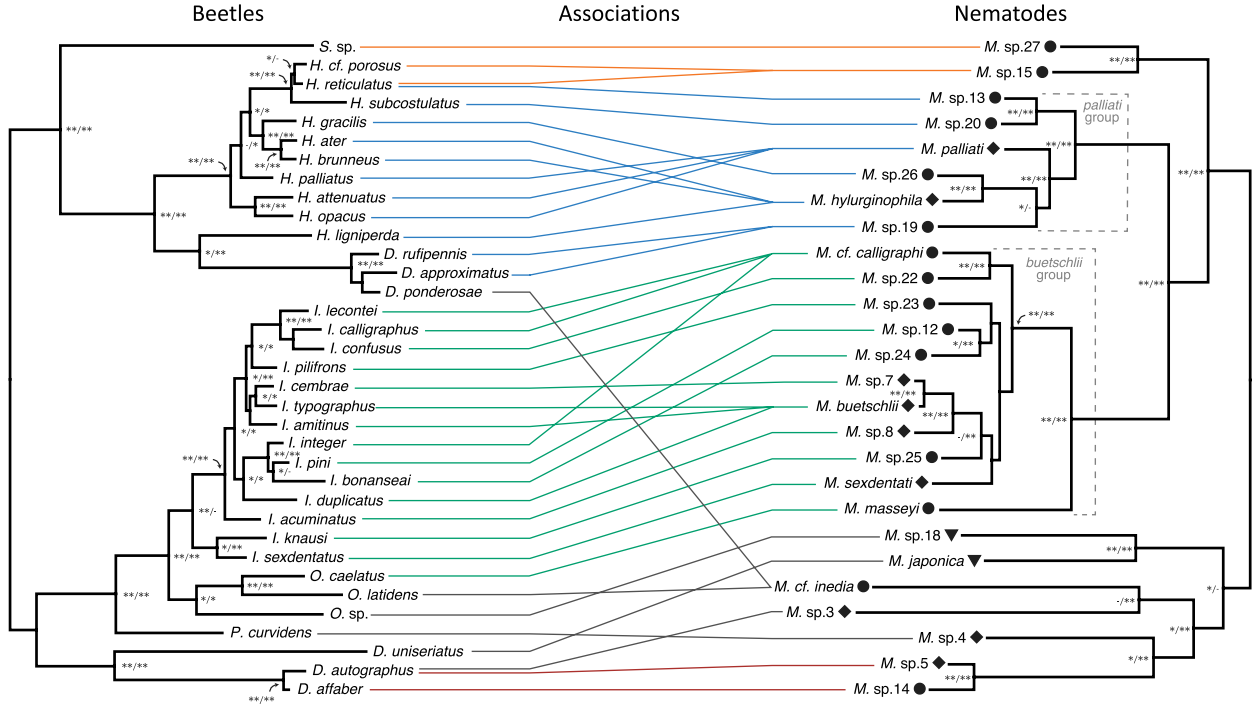

Fig. 3 Comparison of beetle and nematodes phylogenies. Bayesian trees of bark beetles and *Micoletzkya* are shown. Links between species indicate associations as observed in this study. Circles, diamonds and triangles mark species of American, European and Japanese origin, respectively. Different colours denote individual associations of four crown groups of *Micoletzkya*. Clades that received bootstrap support (BS) above 85% and had maximum (100%) Bayesian posterior probabilities (PP) are indicated with two asterisks, and values above 75% and 98% are indicated by at least one asterisk; values are given in the form BS/PP.

theless, it should be mentioned that infestation with *Micoletzkya* appears to be very high among *Ips* and Hilastini beetles, with rates approaching 100% in populations of some beetle species (also see Rühm, 1956).

Phylogenies of beetles and nematodes

Phylogenetic analyses yielded fully resolved and well-supported trees for the host beetles (Figs 3, S2 and S3). Phylogenies inferred by ML and Bayesian analyses had identical topologies. The trees contained 35 terminal nodes, and phylogenetic relationships among beetle taxa were consistent with those reported previously (Cognato & Sperling, 2000; Sequeira *et al.*, 2000; Jordal *et al.*, 2011; Reeve *et al.*, 2012).

The phylogeny of *Micoletzkya* included 26 terminal nodes. Bayesian and ML analyses resulted in topologically identical trees, except for the position of *M.* sp. 19, which differed among ML runs depending on whether the dataset included *coxI* sequences (Figs 3, S4–S6). Nine major lineages of *Micoletzkya* could be distinguished. The first clade, for convenience designated as the *buetschlii* group, consisted of eleven closely related putative species: *M.* cf. *calligraphi*, *M.* sp. 22, *M.* sp. 23, *M.* sp. 12, *M.* sp. 24, *M.* sp. 7, *M. buetschlii*, *M.* sp. 8, *M.* sp. 25, *M. sexdentati*, and *M. masseyi*. A second clade, designated as the *palliati* group, included six species: *M.* sp. 13, *M.* sp. 20, *M. palliati*, *M.* sp. 26, *M. hylurginophila*, and *M.* sp. 19. Two *Micoletzkya* clades contained two closely related putative species each: *M.* sp. 5 and *M.* sp. 14 in one, *M.* sp. 15 and *M.* sp. 27 in the other. The phylogenetically diverged *M. japonica* and *M.* sp. 18 formed a well-supported monophyletic group. Finally, three lineages were comprised of single species: *M.* cf. *inedia*, *M.* sp. 3 and *M.* sp. 4. Although the majority of the clades were highly supported, a few nodes at the base of the tree and in the *buetschlii* group received only low support.

Reconciliation analyses

To identify forces that drive the evolutionary radiation of *Micoletzkya*, we performed both topology- and distance-based analyses on various datasets. First, we tested for phylogenetic congruence using comprehensive beetle and nematode trees. Second, we tested for non-random host associations within two major, well-supported crown groups of *Micoletzkya* — the *buetschlii* and *palliati* clades. Third, to test for congruence of phylogenies at deeper levels, we performed the same analyses using pruned trees of beetle and nematodes. Here, a single representative of Hylastini and single representatives of each of the remaining beetle genera were retained (e.g. *I. typographus* as representative of the genus *Ips*). Similarly, a single member of each of the nine designated groups of *Micoletzkya* was selected for the analyses.

Both topology- and distance-based analyses on the comprehensive dataset of beetles and nematodes, which included 35 host species, 26 nematode lineages and 37 association links, rejected the null hypothesis of random associations between the beetles and their nematodes. The topology-based analysis, conducted using Jane 4, resulted in 14 equally parsimonious nonisomorphic solutions. Each of these solutions had a total cost of 64 given the selected event weight metrics; this cost was significantly lower ($P < 0.01$) than that derived from random tip mappings (mean: 140, standard deviation: 15). The analysis, however, introduced a high fraction of noncodivergence events; the least-cost solutions incurred nine codivergence events, two duplications, 14 duplications coupled with a host switch, 23 losses and 11 failures to diverge. Distance-based analysis of the complete beetle and nematode datasets, conducted using Global ParaFit, rejected the null hypothesis of independent evolution in the two groups ($P = 0.0001$). Moreover, tests of individual links indicated that 32 of the 37 associations (86%) significantly contributed to overall phylogenetic congruence.

Topology-based tests showed that the associations between members of the two major crown groups of *Micoletzkya* and their hosts differ from random ($P = 0.04$ in both instances). Similarly, crown-group analyses in AxParafit suggested a significant, global cophylogenetic structure for the *buetschlii* and *palliati* groups ($P = 0.01$ and $P = 0.01$, respectively). The test of individual associations, however, showed that only 1/15 and 2/12 association links were statistically significant for the *buetschlii* and *palliati* groups, respectively. This could be partially due to the decreased power of the distance-based test of individual associations when the number of associations is small (Legendre *et al.*, 2002; Gottschling *et al.*, 2011).

Topology- and distance-based analyses on pruned trees failed to reject the null hypotheses of random associations ($P = 0.20$ and $P = 0.43$), thus revealing no significant evidence for parallel divergence between beetles and nematodes at a deep phylogenetic level.

Discussion

In a phylum that is both species-rich and broadly characterized by host associations (Blaxter *et al.*, 1998; Hugot *et al.*, 2001), systems showing strong host specificity provide a model for how biodiversity of symbionts is generated. Here, we show that beetle relatedness plays a larger role in mediating nematodes' diversification patterns than does geographic proximity. Different nematode species collected from the same continent do not assemble monophyletic groups, except for two *Micoletzkya* species from Japan. Species of European and American origin are scattered across the phylogeny of the genus, and three of four crown groups of *Micoletzkya* that have more than one species have representatives from both continents. Instead, certain lineages of *Micoletzkya* tend to be associated with particular groups of bark beetles. Nematodes of the *buetschlii* clade are exclu-

sively associated with the members of the genus *Ips* and their close relatives, beetles of *Orthotomicus*. Conversely, members of the *palliati* group have been found only in an association with bark beetles of the subfamily Hylasininae, and the closely related *M.* sp. 5 and *M.* sp. 14 are associated with two closely related *Dryocoetes* species. Exceptions do exist, however; two putative *Micoletzkya* species were found on phylogenetically distantly related beetles each, and in two cases, individuals of the same beetle species harboured distantly related nematodes.

Topology- and distance-based statistical analyses of the complete beetle and nematode datasets confirm the general pattern described above: the *Micoletzkya* phylogeny has significant degree of accordance with that of beetles. The ParaFit test of individual links revealed nearly all of the documented nematode-beetle associations contribute significantly to the global cophylogenetic structure. Separate topology- and distance-based tests on crown groups suggest nonrandom associations between hosts and members of both major crown groups of *Micoletzkya*, indicating that radiation of the nematodes has been shaped by the evolutionary history of their hosts. However, contemporary associations cannot be attributed to parallel divergence alone. When the comprehensive dataset was used, cophylogeny mapping incurred a high fraction of noncodivergence events, with most of the putative codivergence events being assigned to shallow nodes in the beetle and nematode phylogenies. Furthermore, reconciliation analyses on pruned beetle and nematode trees revealed little cophylogenetic structure at deep phylogenetic levels.

Some incongruence between phylogenies might result from sampling gaps, which could have obscured the inference of cophylogenetic history by affecting both the phylogenetic analyses and the power of reconciliation methods. Indeed, some discrepancies between beetle and nematode phylogenies were associated with weakly supported nodes in the *Micoletzkya* tree. A few major mismatches, however, are likely the result of historical events. For example, the *buetschlii* and *palliati* clades, which appear to be sister taxa in our analyses, are associated with *Ips* and Hylasininae beetles, respectively, the two of which diverge at the base of the beetle tree, whereas beetles of *Dryocoetes*, the group that is sister to Ipini harbour nematodes that belong to basal *Micoletzkya* clades. Overall, the data indicate that congruence between comprehensive beetle and nematode phylogenies might be a consequence of preferential host shifts on related hosts accompanied by parallel divergence events rather than the result of consecutive, strict codivergence events.

Considering the above, our results point to a mechanism of speciation in *Micoletzkya* symbionts. Namely, bark beetle speciation, which often occurs in sympatry and in association with the colonization of new tree species (Avtzis *et al.*, 2012), is probably the main factor driving speciation of *Micoletzkya* nematodes. As populations of emerging beetle species become more separated, gene flow between populations of their vertically transmitted symbionts decreases, eventually leading to reproductive isolation and speciation. However, if the contact between related host species were to occur again, nematodes might readily switch between them, and competition between these symbionts may lead to extinction of the original, thereby obscuring signals of parallel divergence at shallow evolutionary depths. Indeed, our results suggest that *Micoletzkya* have the potential to switch between phylogenetically related bark beetles. We observed a few cases when nematodes were shared by related syntopic hosts. In particular, three European *Ips* beetles (*I. typographus*, *I. amitinus* and *I. duplicatus*) that have the same primary host tree (Pfeffer, 1994) are infested with the same putative species of *Micoletzkya* (*M. buetschlii*). In contrast, three other European *Ips* species, *I. cembrae*, *I. acuminatus* and *I. sexdentatus*, which infest different coniferous trees, each have a unique nematode associate. In addition to ecological isolation, host specificity is further facilitated by geographic isolation; beetles that were collected from different continents never carried nematodes belonging to the same putative species of *Micoletzkya*. Thus, the possibility for contact among related hosts is an important determinant of the nematodes' host range, and ecological and geographic isolation are crucial factors that influence diversification and speciation in *Micoletzkya*. The absence of host contact facilitates cophylogenetic structure at shallow evolutionary depths.

Conversely, instances of sharing the same nematodes by phylogenetically distantly related beetles are rare, even if the beetles are both sympatric and syntopic. For example, bark beetles *I. typographus*, *H. palliatus* and *D. autographus* frequently infest the same tree (Pfeffer, 1994). Nevertheless, each of these beetles has unique *Micoletzkya* associates, and we observed no cases of host switching. It might be expected then that adaptations of nematodes to one beetle host or particular group of hosts are maladaptive on other beetle species and limit the abilities of *Micoletzkya* to expand their niche by colonizing new beetle lineages. Preferential host switching towards related hosts has probably played a role in emergence and maintenance of cophylogenetic structure at large evolutionary scale.

Our examination of a wide range of *Micoletzkya* associates and beetle hosts from different geographic localities and various host trees has indicated broad phylogenetic congruence of the symbiotic lineages. However, our taxon sampling was presumably far from complete. We could not examine all bark beetle species that were already known to carry *Micoletzkya*. Furthermore, the true diversity of the nematode genus might have been obscured by the sampling bias towards hosts in Central Europe and North America. Examining of *Micoletzkya* symbionts of basal scolytid groups such as *Hylurgonotus* and *Xylechinosomus* would be of particular

interest for elucidating ancestral beetle-nematode associations. These beetles are hypothesized to have been associated with *Araucaria* trees since the Mesozoic, and these trees have been suggested to be the ancestral host of bark beetles (Sequeira *et al.*, 2000). Therefore, determining the phylogenetic position of the *Micoletzkya* symbionts of *Aracucaria*-feeding Tomicini might shed light on the evolution and timing of the most ancient beetle-nematode associations.

Finally, our study has implications for empirical research on coadaptation, particularly questions that can be addressed in a tractable laboratory setting. Interaction with host beetles is a crucial part of *Micoletzkya* ecology. Many aspects of these interactions could be mediated through chemical cues, for example host recognition behaviour and the regulation of the nematode developmental switches, such as dauer entry and dauer exit. This work provides the essential historical context and ecological basis for future mechanistic studies of adaptations between symbiotic partners. Furthermore, a historical framework for host associations enables studies of adaptation to include other species in the system, including bacteria, fungi and presumptive nematode parasites of the beetles. For example, knowing interactions among the beetles, *Micoletzkya* nematodes, and other species could give insight into whether and how *Micoletzkya* benefit their carriers, and whether such interactions have any impact on the diversity of the hosts.

Acknowledgments

We thank Matthias Dobbertin, Gerhard Elsner, Monica Gaylord, Heiko Gebhardt, Šárka Grucmanová, Rich Hofstetter, Francois Mayer, Joel McMillin, Matt Paulsen, Mary Reid, John Reinhold, Kaljo Voolma and Rudolf Wegensteiner for collecting beetles, Natsumi Kanzaki for two nematode isolates, Heike Haussmann for nematode strain freezing, Erik Ragsdale, Cameron Weadick, and Ralf Sommer for discussions and valuable comments on the manuscript. The work was supported by the Max Planck Society. The authors declare that there is no conflict of interest.

References

Adams, B.J. 1998. Species concepts and the evolutionary paradigm in modern nematology. *J. Nematol.* **30**: 1–21.

Avtzis, D.N., Bertheau, C. & Stauffer, C. 2012. What is next in bark beetle phylogeography? *Insects* **3**: 453–472.

de Bary, A. 1879. *Die Erscheinung der Symbiose*. Verlag Trubner, Straßburg.

Bascompte, J., Jordano, P., Melian, C.J. & Olesen, J.M. 2003. The nested assembly of plant-animal mutualistic networks. *Proc. Natl. Acad. Sci. USA* **100**: 9383–9387.

Blaxter, M.L., De Ley, P., Garey, J.R., Liu, L.X., Scheldeman, P., Vierstraete, A. *et al.* 1998. A molecular evolutionary framework for the phylum Nematoda. *Nature* **392**: 71–75.

Clayton, D.H., Bush, S.E., Goates, B.M. & Johnson, K.P. 2003. Host defense reinforces host-parasite cospeciation. *Proc. Natl. Acad. Sci. USA* **100**: 15694–15699.

Clayton, D.H., Bush, S.E. & Johnson, K.P. 2004. Ecology of congruence: past meets present. *Syst. Biol.* **53**: 165–173.

Cognato, A.I. & Sperling, F.A.H. 2000. Phylogeny of *Ips* DeGeer species (Coleoptera: Scolytidae) inferred from mitochondrial cytochrome oxidase I DNA sequence. *Mol. Phylogenet. Evol.* **14**: 445–460.

Conow, C., Fielder, D., Ovadia, Y. & Libeskind-Hadas, R. 2010. Jane: a new tool for the cophylogeny reconstruction problem. *Algorithms Mol. Biol.* **5**: 16.

Cruaud, A., Ronsted, N., Chantarasuwan, B., Chou, L.S., Clement, W.L., Couloux, A. *et al.* 2012. An extreme case of plant-insect codiversification: figs and fig-Pollinating wasps. *Syst. Biol.* **61**: 1029–1047.

Darwin, C. 1862. *On the Various Contrivances by Which British and Foreign Orchids are Fertilised by Insects, and on the Good Effects of Intercrossing*. John Murray, London.

Edgar, R.C. 2004. MUSCLE: multiple sequence alignment with high accuracy and high throughput. *Nucleic Acids Res.* **32**: 1792–1797.

Giblin-Davis, R.M., Davies, K.A., Taylor, G.S. & Thomas, W.K., 2004. *Entomophilic Nematode Models for Studying Biodiversity and Cospeciation*. CABI Publishing, Wallingford.

Gottschling, M., Goeker, M., Stamatakis, A., Bininda-Emonds, O.R.P., Nindl, I. & Bravo, I.G. 2011. Quantifying the phylodynamic forces driving papillomavirus evolution. *Mol. Biol. Evol.* **28**: 2101–2113.

Hafner, M.S. & Page, R.D.M. 1995. Molecular phylogenies and host-parasite cospeciation: gophers and lice as a model system. *Philos. Trans. R. Soc. Lond. B Biol. Sci.* **349**: 77–83.

Hasegawa, H., Sato, H., Fujita, S., Nguema, P.P.M., Nobusue, K., Miyagi, K. *et al.* 2010. Molecular identification of the causative agent of human strongyloidiasis acquired in Tanzania: dispersal and diversity of *Strongyloides* spp. and their hosts. *Parasitol. Int.* **59**: 407–413.

van der Heijden, M.G.A., Klironomos, J.N., Ursic, M., Moutoglis, P., Streitwolf-Engel, R., Boller, T. *et al.* 1998. Mycorrhizal fungal diversity determines plant biodiversity, ecosystem variability and productivity. *Nature* **396**: 69–72.

Herrmann, M., Mayer, W.E. & Sommer, R.J. 2006a. Nematodes of the genus *Pristionchus* are closely associated with scarab beetles and the Colorado potato beetle in Western Europe. *Zoology (Jena)* **109**: 96–108.

Herrmann, M., Mayer, W.E. & Sommer, R.J. 2006b. Sex, bugs and Haldane's rule: the nematode genus *Pristionchus* in the United States. *Front. Zool.* **3**: 14.

Herrmann, M., Kienle, S., Mayer, W.E., Rochat, J. & Sommer, R.J. 2010. Haplotype diversity of the nematode *Pristionchus pacificus* on Réunion in the Indian Ocean suggests multiple independent invasions. *Biol. J. Linn. Soc.* **100**: 170–179.

Hughes, J., Kennedy, M., Johnson, K.P., Palma, R.L. & Page, R.D.M. 2007. Multiple cophylogenetic analyses reveal frequent cospeciation between pelecaniform birds and *Pectinopygus* lice. *Syst. Biol.* **56**: 232–251.

Hugot, J.P., Baujard, P. & Morand, S. 2001. Biodiversity in helminths and nematodes as a field of study: an overview. *Nematology* **3**: 199–208.

Jordal, B.H., Sequeira, A.S. & Cognato, A.I. 2011. The age and phylogeny of wood boring weevils and the origin of subsociality. *Mol. Phylogenet. Evol.* **59**: 708–724.

Kanzaki, N., Ragsdale, E., Herrmann, M., Mayer, W.E. & Sommer, R.J. 2012. Description of three *Pristionchus* species (Nematoda: Diplogastridae) from Japan that form a cryptic species complex with the model organism *P. pacificus*. *Zoolog. Sci.* **29**: 403–417.

Kanzaki, N., Ragsdale, E.J., Herrmann, M., Susoy, V. & Sommer, R.J. 2013. Two androdioecious and one dioecious new species of *Pristionchus* (Nematoda: Diplogastridae): new reference points for the evolution of reproductive mode. *J. Nematol.* **45**: 172–194.

Katoh, K., Misawa, K., Kuma, K. & Miyata, T. 2002. MAFFT: a novel method for rapid multiple sequence alignment based on fast Fourier transform. *Nucleic Acids Res.* **30**: 3059–3066.

Laetsch, D.R., Heitlinger, E.G., Taraschewski, H., Nadler, S.A. & Blaxter, M.L. 2012. The phylogenetics of Anguillicolidae (Nematoda: Anguillicoloidea), swimbladder parasites of eels. *BMC Evol. Biol.* **12**: 60.

Lambshead, P.J.D. 1993. Recent developments in marine benthic biodiversity research. *Oceanis* **19**: 5–24.

Legendre, P., Desdevises, Y. & Bazin, E. 2002. A statistical test for host-parasite coevolution. *Syst. Biol.* **51**: 217–234.

Massey, C.L. 1974. Biology and taxonomy of nematode parasites and associates of bark beetles in the United States. Agriculture Handb U S Dep Agric No. 446: 1–233.

Mayer, W.E., Herrmann, M. & Sommer, R.J. 2007. Phylogeny of the nematode genus *Pristionchus* and implications for biodiversity, biogeography and the evolution of hermaphroditism. *BMC Evol. Biol.* **7**: 104.

Mayer, W.E., Herrmann, M. & Sommer, R.J. 2009. Molecular phylogeny of beetle associated diplogastrid nematodes suggests host switching rather than nematode-beetle coevolution. *BMC Evol. Biol.* **9**: 212.

McFrederick, Q.S. & Taylor, D.R. 2013b. Evolutionary history of nematodes associated with sweat bees. *Mol. Phylogenet. Evol.* **66**: 847–856.

McFrederick, Q.S., Haselkorn, T.S., Verocai, G.G. & Jaenike, J. 2013a. Cryptic *Onchocerca* species infecting North American cervids, with implications for the evolutionary history of host associations in *Onchocerca*. *Parasitology* **140**: 1201–1210.

Meier-Kolthoff, J.P., Auch, A.F., Huson, D.H. & Goeker, M. 2007. CopyCat: cophylogenetic analysis tool. *Bioinformatics* **23**: 898–900.

Page, R.D.M. 1994. Parallel phylogenies: reconstructing the history of host-parasite assemblages. *Cladistics* **10**: 155–173.

Perlman, S.J. & Jaenike, J. 2003. Infection success in novel hosts: an experimental and phylogenetic study of *Drosophila*-parasitic nematodes. *Evolution* **57**: 544–557.

Pfeffer, A. 1994. Zentral- und westpaläarktische Borken- und Kernkäfer. *Entomol. Basiliensia* **17**: 5–310.

Pozio, E., Hoberg, E., La Rosa, G. & Zarlenga, D.S. 2009. Molecular taxonomy, phylogeny and biogeography of nematodes belonging to the *Trichinella* genus. *Infect. Genet. Evol.* **9**: 606–616.

Reeve, J.D., Anderson, F.E. & Kelley, S.T. 2012. Ancestral state reconstruction for *Dendroctonus* bark beetles: evolution of a tree killer. *Environ. Entomol.* **41**: 723–730.

Ronquist, F., Teslenko, M., van der Mark, P., Ayres, D.L., Darling, A., Hohna, S. *et al.* 2012. MrBayes 3.2: efficient Bayesian phylogenetic inference and model choice across a large model space. *Syst. Biol.* **61**: 539–542.

Rühm, W. 1956. Die Nematoden der Ipiden. Parasitologische Schriftenreihe No. 6: 1–437.

Sequeira, A.S., Normark, B.B. & Farrell, B.D. 2000. Evolutionary assembly of the conifer fauna: distinguishing ancient from recent associations in bark beetles. *Proc. Biol. Sci.* **267**: 2359–2366.

Stamatakis, A. 2006. RAxML-VI-HPC: maximum likelihood-based phylogenetic analyses with thousands of taxa and mixed models. *Bioinformatics* **22**: 2688–2690.

Stamatakis, A., Auch, A.F., Meier-Kolthoff, J. & Goeker, M. 2007. AxPcoords & parallel AxParafit: statistical co-phylogenetic analyses on thousands of taxa. *BMC Bioinformatics* **8**: 405.

Sudhaus, W. & von Lieven, A.F. 2003. A phylogenetic classification and catalogue of the Diplogastridae (Secernentea, Nematoda). *J. Nematode Morphol. System.* **6**: 43–89.

Susoy, V., Kanzaki, N. & Herrmann, M. 2013. Description of the bark beetle associated nematodes *Micoletzkya masseyi* n. sp and *M. japonica* n. sp (Nematoda: Diplogastridae). *Nematology* **15**: 213–231.

Thompson, J.N. 2005. *The Geographic Mosaic of Coevolution*. University of Chicago Press, Chicago & London.

de Vienne, D.M., Giraud, T. & Shykoff, J.A. 2007. When can host shifts produce congruent host and parasite phylogenies? A simulation approach. *J. Evol. Biol.* **20**: 1428–1438.

Wiley, E.O. 1978. Evolutionary species concept reconsidered. *Syst. Zool.* **27**: 17–26.

Supporting information

Additional Supporting Information may be found in the online version of this article:

Figure S1 Dauer juveniles of *Micoletzkya sexdentati* (shown with white arrows) are located on the surface of a bark beetle *Ips sexdentatus;* beetle elytrae have been removed.

Figure S2 Bayesian phylogeny of beetles.

Figure S3 ML phylogeny of beetles.

Figure S4 Bayesian phylogeny of nematodes.

Figure S5 ML phylogeny of nematodes.

Figure S6 ML phylogeny of nematodes.

Table S1 Molecular markers used in phylogenetic analyses.

Table S2 Oligonucleotides used in the study.

Table S3 GenBank accession numbers for outgroup nematode taxa.

Received 21 January 2014; accepted 25 February 2014

Journal of Nematology 46(1):50–59. 2014.
© The Society of Nematologists 2014.

Leptojacobus dorci n. gen., n. sp. (Nematoda: Diplogastridae), an Associate of *Dorcus* Stag Beetles (Coleoptera: Lucanidae)

Natsumi Kanzaki,[1] Erik J. Ragsdale,[2] Vladislav Susoy,[2] Ralf J. Sommer[2]

Abstract: A new species of diplogastrid nematode, *Leptojacobus dorci* n. gen., n. sp., was isolated from adults of the stag beetle *Dorcus ritsemae* (Coleoptera: Lucanidae) that were purchased from a pet shop in Japan. *Leptojacobus* n. gen. is circumscribed by a very thin, delicate body and by a small stoma with minute armature. A combination of other stomatal characters, namely the division of the cheilostom into adradial plates, the symmetry of the subventral stegostomatal sectors, and the presence of a thin, conical dorsal tooth, further distinguishes *Leptojacobus* n. gen. from other genera of Diplogastridae. Phylogenetic analysis of nearly full-length SSU rRNA sequences support the new species, together with an isolate identified previously as *Koerneria luziae*, to be excluded from a clade including all other molecularly characterized diplogastrids with teeth and stomatal dimorphism. Therefore, the new species will be of importance for reconstruction of ancestral character histories in Diplogastridae, a family circumscribed by a suite of feeding-related novelties.

Key words: dimorphism, evolution, morphology, new genus, new species, novelty, stoma, taxonomy, phylogeny.

The nematodes of Diplogastridae Micoletzky, 1922 are widely found in phoretic, necromenic, and parasitic associations with insects (Sudhaus and Fürst von Lieven, 2003). Targeting potential host insects for sampling is therefore likely to be a source of undocumented diversity in the family. Attention to stag beetles (Coleoptera: Lucanidae) in particular has recently revealed several new species of nematode associates, including two species of *Pristionchus* Kreis, 1932 (Kanzaki et al., 2011, 2012a, 2013) and a previously undescribed genus, *Parapristionchus* Kanzaki, Ragsdale, Herrmann, Mayer, Tanaka, and Sommer, 2012b. By continuing such collecting efforts, we have discovered a new diplogastrid species and report it in this article. We currently recognize 33 valid genera of Diplogastridae (Sudhaus and Fürst von Lieven, 2003; Kanzaki et al., 2009, 2012b; Fürst von Lieven et al., 2011; Susoy and Herrmann, 2012; Herrmann et al., 2013), and we assign the new species, based on morphological and molecular evidence, to an additional, new genus in the family.

Besides improving our understanding of the phylogenetic diversity and life histories in Diplogastridae, records of distinct new morphotypes, including new taxonomic "genera," facilitate inferences of character evolution. Diplogastrid nematodes are characterized by a suite of feeding-related evolutionary novelties, including teeth, stomatal dimorphism, and predatory behavior. Because the family is represented by an advanced model system for genetics and developmental biology, *Pristionchus pacificus* Sommer, Carta, Kim, and Sternberg, 1996 (Sommer and McGaughran, 2013), detailed mechanisms for these traits are now being revealed, including the rewiring of conserved neurons to enable predation (Bumbarger et al., 2013) and the regulation of the dimorphism by hormones (Bento et al., 2010), novel pheromones (Bose et al., 2012), and a novel developmental switch (Ragsdale et al., 2013). However, determining the order of evolutionary events still requires rigorous inference of ancestral character states. Therefore, the analysis of new taxa, particularly those representing ancient divergences relative to previously sampled diplogastrid species, will allow more accurate polarization of character transformations. Here, we show by a phylogenetic analysis of nearly full-length SSU rRNA gene sequences that the new species we describe is excluded from a clade of almost all other sequenced diplogastrids with teeth and a dimorphism. To complement this finding, we present a morphological description of the new species, the analysis of which will be essential for reconstructing the histories of novelties in the family.

Materials and Methods

Nematode isolation and cultivation: The new species was isolated from *Dorcus ritsemae* Oberthür and Houlbert, 1914 (Coleoptera: Lucanidae) by first placing adult beetles on fermented wood flakes, a common substrate for rearing stag beetles. Before introducing beetles, food flakes were sterilized by drying at 80°C for 2 d. After 2 wk of keeping beetles on this medium, beetles were removed from the substrate, after which wood flakes were kept at 25°C for 6 mon. About 5 g of subsamples were taken occasionally to be soaked in water or placed on a Baermann funnel, both methods of which yielded individuals of the new species. Alternatively, wood flakes from the beetle substrate were also placed directly on plates with of 2% water agar or NGM agar without peptone or cholesterol, with chunks of NGM agar (with peptone and cholesterol) placed on top. Approximately 3 ml of tap water were added to each culture plate, and plates were sealed with Parafilm to prevent desiccation. Microbiota originating from

Received for publication October 31, 2013.
[1]Forest Pathology Laboratory, Forestry and Forest Products Research Institute, 1 Matsunosato, Tsukuba, Ibaraki 305-8687 Japan.
[2]Max Planck Institute for Developmental Biology, Department of Evolutionary Biology, Spemannstraße 37, 72076 Tübingen, Germany.
Natsumi Kanzaki and Erik J. Ragsdale contributed equally to this work.
We thank Jürgen Berger for SEM, and we are grateful to Matthias Herrmann for his ideas and advice on our work with "Slim Jim," the new species described herein.
E-mail: ralf.sommer@tuebingen.mpg.de
This paper was edited by David Shapiro-Ilan.

the nematode body surface, gut, or both propagated voluntarily on this medium and were used as the sole food source for the nematodes.

Morphological observation and preparation of type material: Material for morphological observation was provided by 2- to 3-wk-old cultures of the new species. Observations by light microscopy (LM) and differential interference contrast (DIC) microscopy were conducted using live nematodes, which were transferred by mouth pipette from culture plates to slides. For line drawings, specimens were mounted into water on slides with silicone grease and then relaxed by applying gentle heat (Kanzaki, 2013). For morphometrics, specimens were mounted on slides with pads of 5% noble agar and 0.15% sodium azide and were additionally relaxed by heat when necessary. To prepare type material, nematodes were isolated from type strain cultures, rinsed in distilled water to remove bacteria, heat-killed at 95°C, fixed in 5% formalin, and processed through a glycerol and ethanol series using Seinhorst's method (Hooper, 1986). Nomarski micrographs were taken using a Zeiss Axio Imager Z.1 microscope and a Spot RT-SE camera supported by the program MetaMorph v.7.1.3 (Molecular Devices, Sunnyvale, CA).

Scanning electron microscopy: Nematodes were prepared for scanning electron microscopy (SEM) by fixation in 2.5% glutaraldehyde in PBS buffer and then postfixed with 1% osmium tetroxide. After several rinses with water, samples were dehydrated through a graded ethanol series, followed by critical point drying from liquid carbon dioxide. Specimens were mounted on polylysine-coated cover slips, sputter-coated with 20-nm gold/palladium, and then imaged with a Hitachi S-800 field emission scanning electron microscope operating at 20 kV.

Molecular characterization and phylogenetic analysis: We amplified a nearly full-length sequence of the SSU rRNA gene of the new species, using the forward primer SSU18A (AAA GAT TAA GCC ATG CAT G) (Eyualem and Blaxter, 2003) and reverse primer VL26346 (GGT TCA AGC CAC TGC GAT) (Susoy et al., 2013). The gene was sequenced using the above amplification primers as well as forward primer VL26345 (GCG AAA GCA TTT GCC AAG A) (Susoy et al., 2013) and reverse primer SSU26R (CAT TCT TGG CAA ATG CTT TCG) (Eyualem and Blaxter, 2003). PCR conditions were as described by Mayer et al. (2007). The sequence was assembled using the program SeqMan Pro 7.2.2 (DNASTAR) and has been deposited in the GenBank database under the accession number KF924399.

Phylogenetic analysis was performed on an alignment of sequences of the SSU rRNA gene. Homologous sequences for all other taxa included in the analysis were retrieved from GenBank. Nearly full-length SSU rRNA sequences were aligned using MAFFT version v. 7.0 (Katoh et al., 2002), followed by manual improvement of the alignment in Geneious version 6.1, including deletion of ambiguously aligned positions. The phylogeny was inferred under maximum likelihood (ML) and Bayesian criteria, as implemented in RAxML v.7.2.8 (Stamatakis, 2006) and MrBayes 3.2 (Ronquist et al., 2012), respectively. For the ML analysis, which invoked a general time reversible model with a gamma-shaped distribution of rates across sites, 50 independent runs with different starting trees were performed. Bootstrap support (BS) was evaluated by 1,000 pseudoreplicates. Bayesian analyses were initiated with random starting trees and were run with four chains for 4 million generations. Markov chains were sampled at intervals of 100 generations. The analysis was performed four times. After confirming convergence of runs, the first 25% generations were discarded as burn-in and the remaining topologies used to generate a 50% majority-rule consensus tree with clade credibility values given as posterior probabilities (PP). Bayesian analysis invoked a mixed model of substitution with a gamma-shaped distribution across sites. Model parameters were unlinked across character partitions in all analyses.

Results

*Leptojacobus** n. gen.

Description: Diplogastridae. The body is cylindrical, very thin, and delicate. The cuticle is finely annulated, although annulations are less distinct when cuticle detaches from body, as is common in the type species. The proclivity for the cuticle to detach from the body and become "baggy" is tentatively considered a diagnostic character for the genus. The cuticle also has fine longitudinal striations, lending a cross-hatched appearance to the body surface where the cuticle is tightly bound to the body. Six lips are present but are not clearly separated from each other or from the rest of the body. Six setiform labial sensilla are present in both sexes. Four additional cephalic papillae are present in males, as typical for diplogastrid nematodes. The stoma is small and stomatal armature minute. Collectively, the cheilostom and gymnostom are at least as wide as long, such that the stoma is not tube-shaped (i.e., "rhabditiform"). The cheilostom is apically divided into six adradial plates, which extend into minute flaps. Divisions of the cheilostom within the stoma cannot be distinguished with certainty by DIC microscopy. The cheilostom overlaps the gymnostom to give the appearance of a ring around the stoma. The stegostom is dorsoventrally anisomorphic, as typical for diplogastrid nematodes. A moveable dorsal tooth, which is thin and conical, is present. The left and right subventral sectors of the stegostom are symmetrical and form thinly cuticularized ridges. The postdental telostegostom is cup-shaped. Stegostomatal

* Derived from the Greek λεπτός ("slim") + *Ιάκωβος* ("Jim") and refers to the unusually thin bodies of these diplogastrid nematodes.

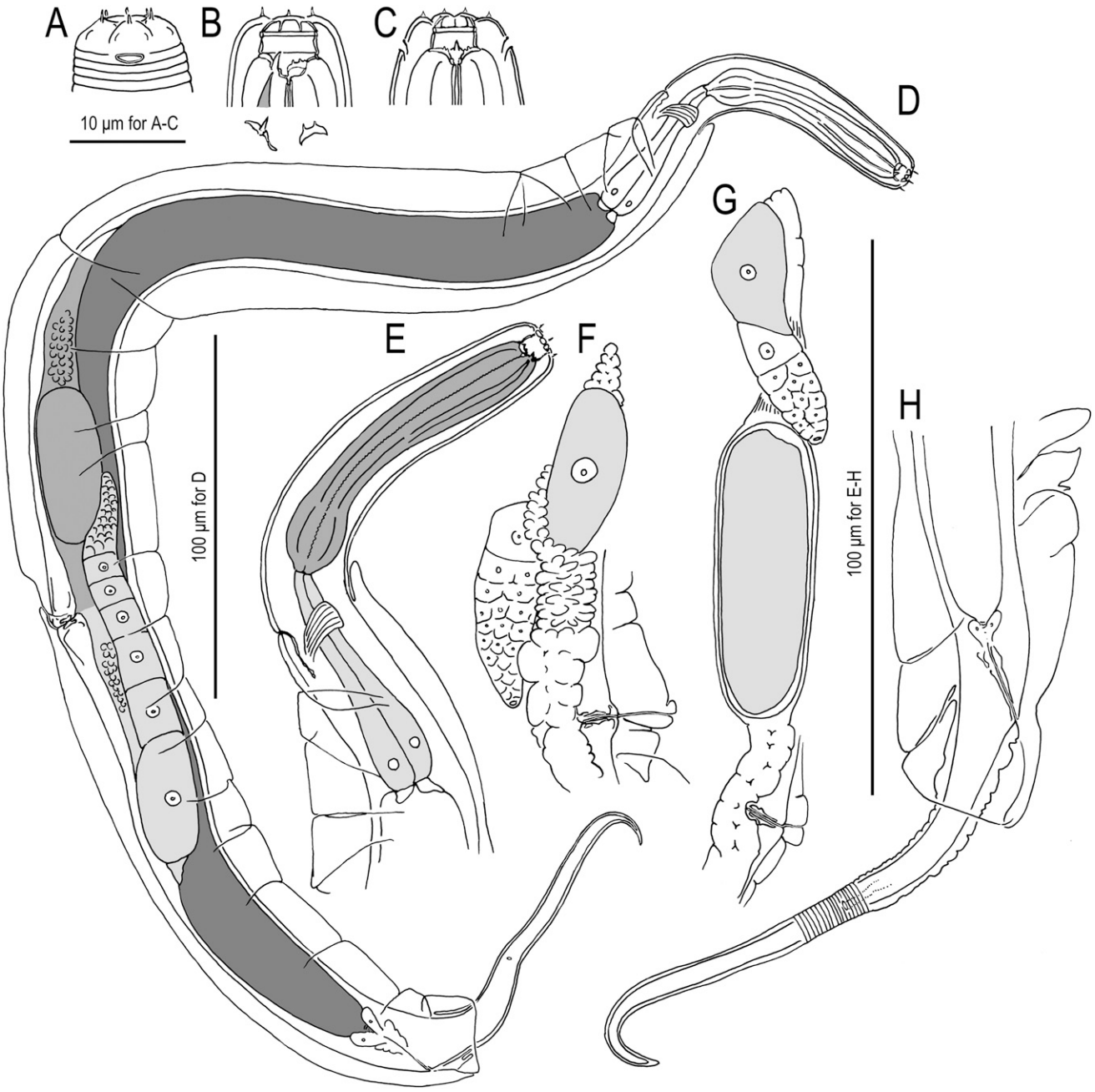

Fig. 1. *Leptojacobus dorci* n. gen., n. sp. A. Surface of anterior region of adult male. B. Left lateral view of stomatal region. C. Ventral view of stomatal region. D. Adult female whole body. E. Anterior region of adult female in left lateral view. F,G. Anterior gonad of female in right lateral view. H. Female tail in right lateral view.

apodemes are absent. Dimorphism of the typically small stoma was not observed. The dorsal gland is large and distinct, and the dorsal musculature of the procorpus is more developed than the subventral musculature, both as typical for diplogastrids. The metacorpus is muscular, forming a well-developed median bulb. The isthmus is narrow and not muscular, and the basal bulb is glandular. In both sexes, the gonads occupy most of or the entire small body diameter. Female gonads are didelphic, amphidelphic, and reflexed. The testis is not reflexed. Males have nine pairs of genital papillae as well as one small, unpaired, ventral genital papilla on the anterior cloacal lip. A bursa or bursal flap is absent. The life cycle consists of one molt inside of the egg and three molts after hatching, as typical for diplogastrid nematodes.

Type and only species: Leptojacobus dorci n. gen., n. sp.

Relationships: Leptojacobus n. gen. is distinguished from all other diplogastrids (Fürst von Lieven and Sudhaus, 2000; Sudhaus and Fürst von Lieven, 2003) by its very thin, delicate body, which is atypical of diplogastrids and other rhabditids, and by its minute stomatal structures. Although these characters clearly distinguish the new genus, *Leptojacobus* n. gen. is further diagnosed by a combination of several stomatal characters in particular,

namely the apical division of the cheilostom into adradial plates and flaps, the symmetry of left and right subventral sectors, the presence of a thin, conical dorsal tooth. The presence of adradial plates (i.e., per- and interradial cheilostomatal divisions) distinguishes the new genus from all other Diplogastridae except for *Acrostichus* Rahm, 1928, *Diplogasteriana* Meyl, 1960, and some species of *Paroigolaimella* Paramonov, 1952, but it is distinguished from the former two by the lack of subventral teeth or projections and is distinguished from all of them by its thin, conical dorsal tooth and the small size of its stoma. Although symmetry of the subventral sectors is also present in several diplogastrid genera without a tube-shaped stoma, namely the above three genera and *Sachsia* Meyl, 1960, *Leptojacobus* n. gen. is distinguished from all four genera as described above. The new genus is distinguished from all other taxa with symmetrical subventral sectors, namely *Demaniella* Steiner, 1914, *Diplogasteroides* de Man, 1912, *Diplogastrellus* Paramonov, 1952, *Goffartia* Hirschmann, 1952, *Mehdinema* Farooqui, 1967, *Pseudodiplogasteroides* Körner, 1954, *Rhabditidoides* Rahm, 1928, *Rhabditolaimus* Fuchs, 1914, and *Sudhausia* Herrmann, Ragsdale, Kanzaki, and Sommer, 2013, by the absence of a tube-shaped gymnostom. All of the generic characters above distinguish the new genus from *Koerneria* Meyl, 1960, including a Japanese strain tentatively identified as *Koerneria luziae* (Körner, 1954) Meyl, 1960 (Kanzaki et al., 2011), which is a possible sister taxon to *Leptojacobus* n. gen. (see below). Bearing a superficial resemblance to the new genus is *Deleyia* Holovachov and Boström, 2006, which like the type host of the type species of *Leptojacobus* n. gen. lives in rotting wood and has a small and slender body, baggy cuticle, a pharynx without a grinder, and a small stoma. However, *Leptojacobus* n. gen. is clearly distinguished from *Deleyia* by a stoma with teeth and other armature vs. a reduced stoma, one vs. two circles of labial papilla, and a well-developed muscular corpus.

*Leptojacobus dorci** n. sp.
(Figs. 1–4)

Measurements: See Table 1.

Adults. Outer layers of cuticle often detach from the rest of the body wall. When the cuticle separates from the rest of the body, it consistently detaches between the excretory pore and cloaca/anus. Annulation, but not the longitudinal striation, is most apparent in the neck and tail of the nematodes, i.e., where the cuticle does not detach. Conversely, striation is the predominantly visible pattern in areas of detached cuticle. Where the cuticle has detached, horizontal striations can also be observed in the layer of cuticle still attached to the body wall. The head does not narrow relative to

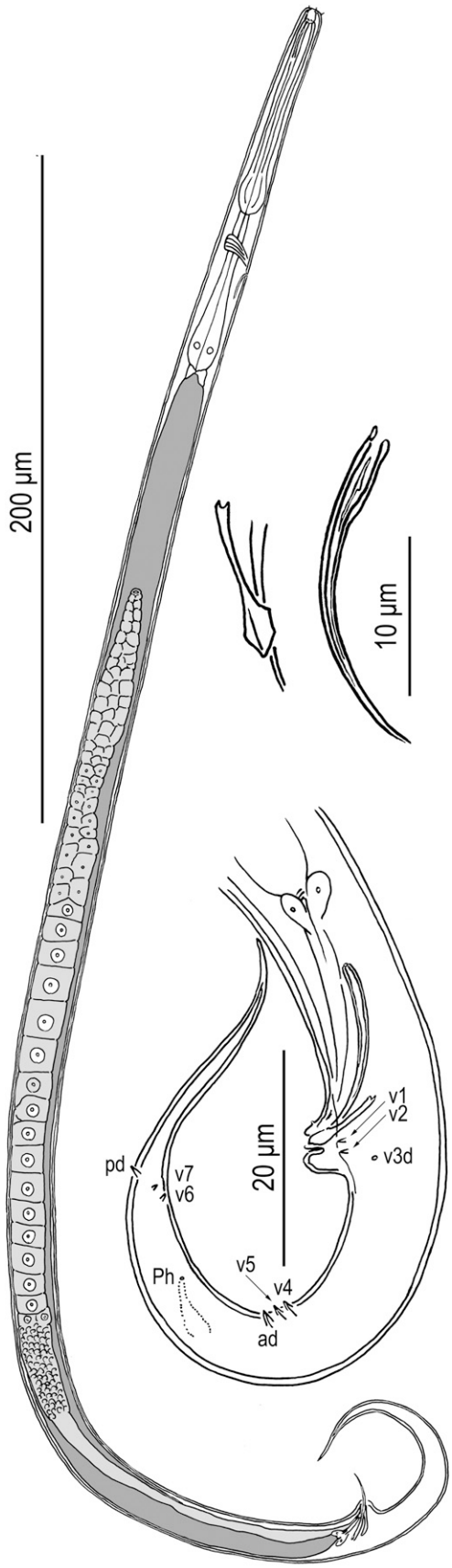

Fig. 2. *Leptojacobus dorci* n. gen., n. sp. A. Whole body of adult male. B: Spicule and gubernaculum in right lateral view. C. Male tail in left lateral view.

* The species epithet is the Latin genitive of *Dorcus*, the type host genus for the new species.

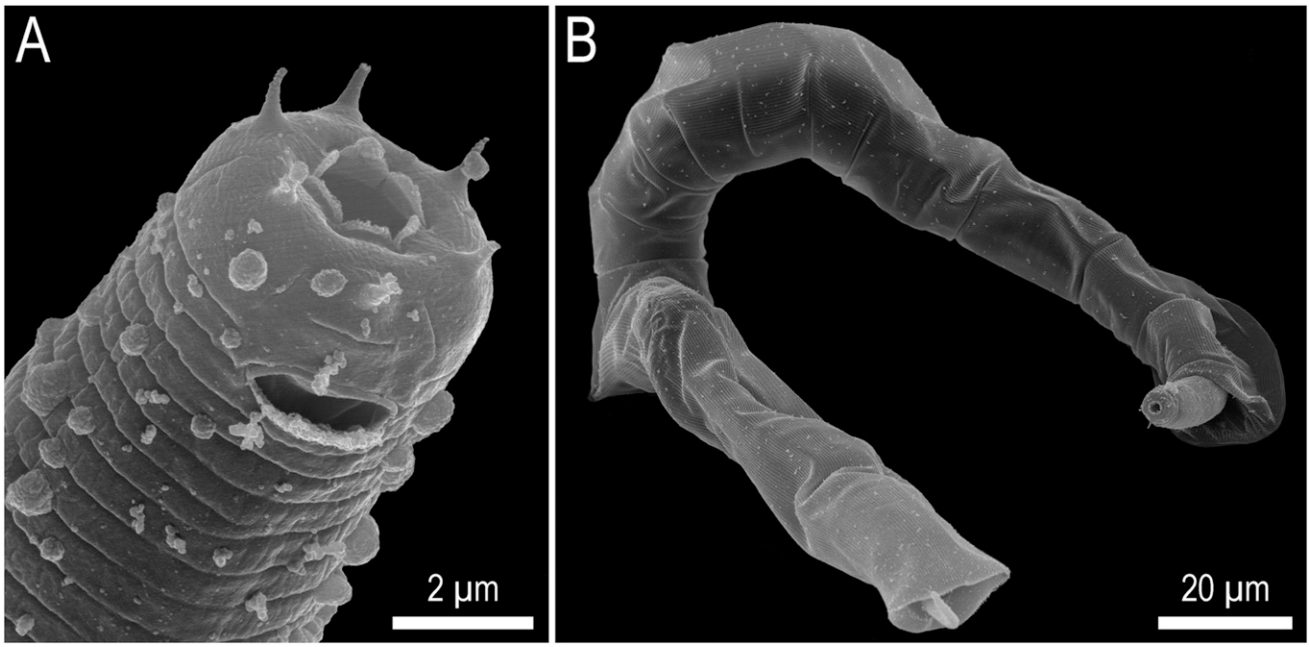

FIG. 3. Scanning electron micrographs of *Leptojacobus dorci* n. gen., n. sp. A. Female, oblique lateral and en face view. Lips are only slightly separated, and cheilostomatal flaps are adradial. Globules or contaminants on body surface, observed on several specimens, are of unknown origin. B. Whole body of female, showing detached, "baggy" body-wall cuticle.

width of neck or the rest of the body, and the apex of the lip region is almost perpendicular to the body wall at the region of the anterior neck. Body annulation extends anteriad to the amphid apertures and posteriad almost to the tail tip. Amphidial apertures are lateral, are positioned at the level of the gymnostom, and are large relative to the size of the lip region, being almost as wide as individual lips. In addition to stomatal characters as described for the genus, the stegostom anterior to the tooth forms a sclerotized ridge, and the two subventral ridges of the stegostom each bear two minute denticles. The pharyngeal corpus (procorpus and median bulb) is about 1.2 times as long as the postcorpus (isthmus and basal bulb). The pharyngointestinal junction is well developed. The hemizonid was not observed. Deirids were not easily observed, presumably because of the common detachment of the body-wall cuticle, but in at least one individual they were localized to the region of the basal bulb.

Male. The excretory pore is usually posterior to the nerve ring. The testis is to the right of the intestine, stretches about half of the body length, and occupies almost the entire body diameter and so does not run either ventrally or dorsally. Spermatogonia are arranged in two to three rows for the distal third of gonad and in a single row for the middle third. The vas deferens is long, comprising the proximal third of the gonad, and is wide only distally, where it contains mature, amoeboid spermatids. Three cloacal glands, two subventral and one dorsal, are present but not obvious. Spicules are paired and separate, and they are simple and slender. In lateral view, spicules are smoothly ventrally arcuate, giving spicules a curve of about 100°. The manubrium is long, being almost a fourth of the spicule length, and is not set off from the rest of the spicule, and the spicule shaft and blade (i.e., calomus and lamina complex) gradually thins posteriorly, being only slightly expanded at the anterior fourth of its length. The gubernaculum is also slender, about or slightly less than half of the length of spicules, possessing small ventral and dorsal peaks at its posterior end, thinning midway along its length, forming a ventral tube enclosing spicules at posterior fourth of its length, and expanding into a small ventral keel at its anterior tip. When the body cuticle is detached, the cuticle extending posteriad overlaps the cloaca. The phasmid (Ph) is difficult to observe by DIC microscopy and is located at about half of the tail length. Nine pairs of genital papillae and a pair of phasmids are arranged as <(v1, C, v2, v3d), (v4, v5, ad), Ph, (v6, v7), pd> in the nomenclature of Sudhaus and Fürst von Lieven (2000), or <(P1, C, P2, P3d), (P4, P5, P6d), Ph, (P7, P8), P9d)> in the homology-agnostic nomenclature of Kanzaki et al. (2012a). Papilla v1 is thus very close to v2, which is at about the same level as v3d; putative v4 is unusually posterior, being closely anterior to ad; putative v6 is unusually far anterior, even anterior to ad; Ph is midway between ad and v6; pd is clearly posterior to v6 and v7. The tail is conical, strongly ventrally curved when killed by heat, about five cloacal body widths in length, and it has a thinly pointed, hyaline tip.

Female. The excretory pore is usually at the level of or anterior to the nerve ring. The ovary, oviduct, and uterus are distinct in each genital system. Gonads are reflexed. The anterior gonadal branch in young individuals extends along the right of the intestine, with the reflexion to the right of the proximal part; however,

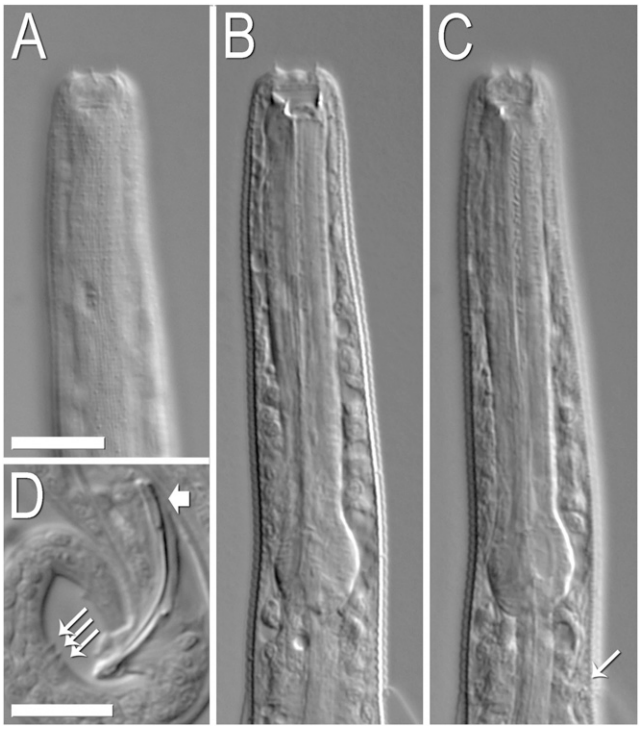

FIG. 4. DIC micrographs of *Leptojacobus dorci* n. gen., n. sp. Scale bars are 10 μm. A–C, which are at the same scale, show the neck of a single adult female in right lateral view and at several focal planes. A. Body surface, including amphid aperture. Plane is right lateral. B. Stomatal characters shown are the small, conical dorsal tooth, a subventral ridge with two minute denticles, and the ring of overlap of cheilostom and gymnostom. The cuticle is detached posteriorly, as shown at the bottom of image. Plane is sagittal at stoma. C. Cuticle detaches immediately posterior to the excretory pore (arrow). D. Male genitalia in left lateral view. The cluster of three genital papillae (putative v4, v5, and pd; long arrows) is unusual among diplogastrids. Shown are the long, slender manubrium (short arrow) of spicule and the distal (posterior) keel of the distinctively thin gubernaculum. Plane is sagittal at excretory pore.

when a large oocyte is in the uterus, the proximal part of the gonad is sometimes forced to the left of the intestine, in addition to pushing the intestine to the dorsal wall. The posterior branch is consistently to the left of the intestine, the reflexion being to the left of the proximal part. The reflexed part of each gonadal branch comprises the ovary, in which oocytes are arranged in two to three rows for the distal half or less of the reflexion, and has a single row of oocytes in the remainder of the ovary. The flexure of each gonad is usually twisted 180° around the axis of the gonad, except for when a fully developed oocyte in the oviduct or uterus stretches the ovary longitudinally, thereby untwisting the flexure (Fig. 2F,G). The oviduct, which comprises most of the length of the proximal part of the gonad, has a bunched appearance, similar to a crustaformeria, but can be stretched smooth by the internal passage of an oocyte. Sperm are stored throughout the oviduct, and a distinct spermatheca is absent. The uterus is short and consists of flattened, diamond-shaped cells. Up to a single egg is observed in the oviduct or uterus at one time. A distinct receptaculum seminis is absent. The vagina is perpendicular to the body surface and is thinly but distinctly sclerotized. In lateral view, the vulva is slightly protuberant where the cuticle adheres to the body wall; the vulva extends as a canal through the detached body cuticle, when it is detached, and apart from this canal the cuticle surrounding the vulva is completely detached from the rest of the body wall. The rectum is about one anal body width long, and the intestinal-rectal junction is surrounded by well-developed sphincter muscle. Three rectal glands, two subventral and one dorsal, are present. When the body cuticle is detached, the cuticle extending posteriad overlaps the cloaca. The phasmid is difficult to observe by DIC microscopy and is located at about midtail length. The tail is conical, about eight anal body widths in length, and has a conical tip.

Type host (carrier) and locality: The culture from which the type specimens were obtained was originally isolated by N. Kanzaki from adults of the stag beetle *Dorcus ritsemae* as described above. The beetles were purchased from a pet shop in Aichi Prefecture, Japan, and were marketed as wild-collected individuals, purportedly from their native range in Indonesia, presumably Java. Nematodes were not isolated directly from the beetles, although failure to isolate them from the bodies of beetles may have been because of procedural artifact. Specifically, dissecting beetles on agar plates is a method typically successful for isolating larger species in other diplogastrid genera, as well as other rhabditids, from their beetle carriers (Herrmann et al., 2006). As a consequence, these larger nematodes develop and proliferate quickly and could have easily obscured the small, more slowly developing individuals of *L. dorci* n. gen., n. sp. Therefore, although *D. ritsemae* is considered to be the type carrier of the new species, the nature of the nematode's association with the host is still unknown.

Type material, type strain, and nomenclatural registration: A holotype male (accession 31368), three paratype males, and seven paratype females (31369-31372) have been deposited in the University of California Riverside Nematode Collection (UCRNC), CA. Two paratype males and four paratype females have been deposited in the Swedish Natural History Museum, Stockholm, Sweden. The type strain is available in living culture from the Department of Evolutionary Biology, Max Planck Institute (MPI) for Developmental Biology, Tübingen, Germany and can be provided to other researchers upon request. Attempts to achieve frozen stocks of this species have been unsuccessful. The new genus has been registered in the ZooBank database (zoobank.org) under the identifier 0978210B-FD0C-4553-A425-0B684CA44D8C, and the new species binomial under the identifier CEFC571F-72EC-484B-92D2-59C483EF6B7C.

Molecular characterization and phylogenetic analysis: The alignment comprised 1,605 sites, 872 of which were variable and 699 parsimony informative. Only the ML tree is shown (Fig. 5). Monophyly of the family

TABLE 1. Morphometrics of male holotype (in glycerin) and male and female specimens (temporary water mounts) of *Leptojacobus dorci* n. gen., n. sp. All measurements are in μm and in the form: mean ± sd (range).

Character	Male		Female
	Holotype	Temporary water mounts	Temporary water mounts
n	–	12	10
L	475	546 ± 62 (455-664)	658 ± 68 (534-737)
L'	417	480 ± 56 (401-590)	558 ± 66 (445-634)
a	43	43 ± 5.9 (35-57)	29 ± 4.1 (22-36)
b	5.5	5.3 ± 0.4 (4.8-6.2)	6.0 ± 0.7 (4.9-6.7)
c	8.2	8.4 ± 0.6 (7.1-9.0)	6.6 ± 0.6 (5.6-7.5)
c'	6.9	5.3 ± 1.1 (4.2-7.7)	7.8 ± 1.1 (6.5-9.4)
V or T	47	54 ± 3.7 (46-58)	50 ± 4.4 (42-55)
Maximum body diam. (not detached cuticle)	11	13 ± 2.0 (8.0-15)	23 ± 1.8 (20-26)
Stoma diam.	2.3	2.9 ± 0.5 (2.0-3.8)	4.6 ± 0.6 (3.5-5.3)
Stoma length	3.1	4.1 ± 0.3 (3.6-4.6)	4.7 ± 0.5 (4.1-5.4)
Anterior end to amphidial aperture	2.0	2.4 ± 0.2 (2.0-2.8)	2.2 ± 0.5 (1.3-3.0)
Corpus length	42	52 ± 4.7 (39-55)	60 ± 2.8 (53-63)
Pharynx length	79	99 ± 7.4 (79-107)	106 ± 3.7 (97-112)
Corpus as % pharynx length	53	52 ± 1.5 (49-55)	56 ± 1.4 (54-58)
Neck length	86	102 ± 7.5 (82-110)	109 ± 3.9 (62-72)
Median bulb diam.	6.5	6.7 ± 0.3 (6.0-7.2)	10 ± 0.9 (8.0-11)
Basal bulb diam.	5.3	6.1 ± 1.0 (4.7-8.3)	10 ± 0.7 (9.1-12)
Excretory pore from anterior end	60	70 ± 8.2 (51-82)	70 ± 3.5 (66-78)
Nerve ring from anterior end	57	66 ± 7.5 (47-75)	72 ± 6.4 (63-81)
Vulva from anterior end	–	–	329 ± 58 (223-381)
Vulva to anus distance	–	–	230 ± 14 (210-256)
Length of anterior gonad branch	–	–	95 ± 16 (72-116)
Length of anterior flexure	–	–	80 ± 17 (61-116)
Length of posterior gonad branch	–	–	100 ± 12 (85-127)
Length of posterior flexure	–		85 ± 14 (67-108)
Testis length	223	294 ± 47 (213-379)	–
Cloacal or anal body diam.	8.4	13 ± 2.8 (7.0-16)	13 ± 2.0 (10-16)
Tail length	58	65 ± 7.7 (54-74)	99 ± 5.6 (89-105)
Spicule length (curve)	23	25 ± 1.6 (23-27)	–
Spicule length (chord)	20	22 ± 1.7 (18-25)	–
Gubernaculum length	10	11 ± 1.2 (9.0-13)	–

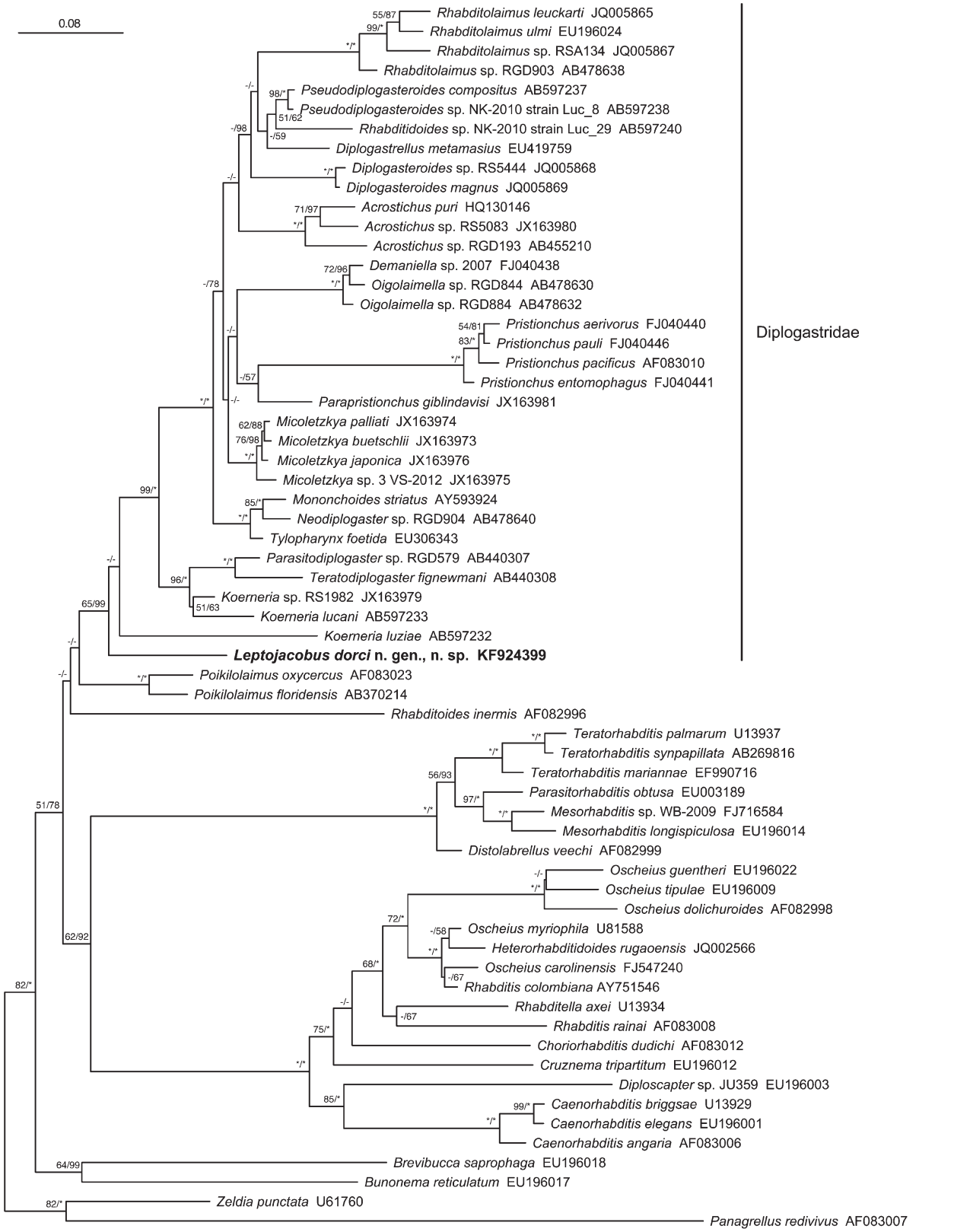

FIG. 5. Phylogenetic relationships of Diplogastridae and outgroups, as inferred by maximum likelihood (ML) of nearly full-length SSU rRNA sequences. The tree with the highest log likelihood is shown. For nodes that were present in the topology inferred by Bayesian analysis, posterior probabilities (PP) are also given. Support values are shown next to the nodes: left value is the proportion of trees in which the associated taxa clustered together in 1,000 bootstrap pseudoreplicates in the ML analysis; right value, PP of that node according to Bayesian inference. Support values above 50% are shown. Asterisks indicate 100% support; dashes indicate < 50% BS (left value) or the absence of the node in the Bayesian tree (right value). Tree is drawn to scale, with branch lengths measured in the number of substitutions per site. GenBank accession numbers are given to right of taxon names.

Diplogastridae, including *L. dorci* n. gen., n. sp., was recovered in both ML and Bayesian analyses, albeit with variable support (65% BS, 99% PP). The new species was excluded from a highly supported clade (99% BS, 100% PP) that includes all but one other diplogastrid species analyzed in this study. The Japanese isolate of *K. luziae* was the other species excluded from this clade, consistent with a previous study that included this isolate (Kanzaki et al., 2011). The phylogenetic position of *L. dorci* n. gen., n. sp. relative to that of *K. luziae* differed between the ML and Bayesian analyses, and was poorly supported in both: in the ML tree, the new species was sister to all other analyzed Diplogastridae (< 50% BS); in the Bayesian tree, it was the sister of *K. luziae* (73% PP). Finally, the inclusion of *L. dorci* n. gen., n. sp. in our analysis yielded poorly supported and conflicting results regarding the closest outgroup to all sampled diplogastrid taxa: whereas the closest clade was *Poikilolaimus* spp. Fuchs, 1930 in the ML analysis (< 50% BS), the outgroup was predicted to be *Rhabditoides inermis* (Schneider, 1866) Dougherty, 1955 in the Bayesian analysis (58% PP). Therefore, *L. dorci* n. gen., n. sp. is clearly basal to most or all of the Diplogastridae included in this study, although the precise position of the new species and the identity of the nearest outgroup to the family remain ambiguous.

Discussion

Leptojacobus dorci n. gen., n. sp. has been shown by an analysis of nearly full-length SSU rRNA sequences to represent an ancient divergence from other taxa in the family (as defined by Sudhaus and Fürst von Lieven, 2003). Specifically, *L. dorci* n. gen., n. sp. is excluded from a well-supported monophyletic clade that includes all other diplogastrid taxa so characterized to date, with the exception of *K. luziae*. The new species therefore provides a basis for reconstructing ancient character histories in Diplogastridae, a group characterized by a number of novelties relative to outgroup rhabditids. Although the phylogenetic positions of *L. dorci* n. gen., n. sp. and *K. luziae* were not well supported in our analyses, the relatively basal divergence of *L. dorci* n. gen., n. sp. in the family directs the search for possible plesiomorphic or intermediate states for diplogastrid-specific characters. The new species clearly shows characters diagnostic of diplogastrids: the first molt inside the egg (Fürst von Lieven, 2005), as well as a glandular pharyngeal postcorpus, anisomorphy of the anterior pharynx, and a moveable dorsal tooth (Sudhaus and Fürst von Lieven, 2003). Based on only these characters, *L. dorci* n. gen., n. sp. is not an obvious morphological intermediate between diplogastrids and outgroups.

In contrast to the above traits, stomatal dimorphism was not observed in the new species. This trait, although absent in many diplogastrid genera, is unique to the family. The apparent absence of dimorphism in *L. dorci* n. gen., n. sp., however, might have been observational artifact. For example, particular environmental cues triggering the development of an alternative mouthform may not have been met. Alternatively, the small size of stoma structures in *L. dorci* n. gen., n. sp., which are at the limit of what is accessible by LM and DIC microscopy, might have confounded interpretation of the trait. On the other hand, a true absence of dimorphism in *L. dorci* n. gen., n. sp., if this species were the sister to a clade including all dimorphic diplogastrids, would suggest that this trait was gained only after the evolution of a moveable tooth. Clearly, better phylogenetic resolution, deeper sampling of taxa and characters, and perhaps more intensive morphological analysis of *L. dorci* n. gen., n. sp., will be required to address the question of which trait came first in the evolution of Diplogastridae. Knowing this will be necessary to determine the role, if any, of plasticity in the evolution of moveable teeth as well as other mouth armature, as might be predicted by theory (e.g., West-Eberhard, 2003; Moczek, 2007).

In addition to the interesting morphological questions our discovery of *L. dorci* n. gen., n. sp. poses, the new species provides further evidence for unknown diversity to be discovered in association with beetles. With increased taxon sampling, it may be possible to infer ancient ecological associations in Diplogastridae. As with *L. dorci* n. gen., n. sp., *K. luziae* has also been reported from *Dorcus* stag beetles (Körner, 1954; Kanzaki et al., 2011), while the potentially close outgroup *Rhabditoides inermis* is known from carrion beetles (Coleoptera: Silphidae) (Völk, 1950). Notwithstanding a possible sampling bias toward beetle hosts, these observations support an ancestral association with them. Corroborating this is our discovery of a morphologically close but genetically distinct isolate of *Leptojacobus* n. gen. from rearing substrate of *Dorcus rectus* (N.K., unpubl. data), although we unfortunately lost that strain. Thus the continued sampling of stag beetles, including by the isolation strategy herein, holds promise for the discovery of more undescribed diversity in anciently divergent diplogastrid lineages.

Literature Cited

Bento, G., Ogawa, A., and Sommer, R. J. 2010. Co-option of the hormone-signalling module dafachronic acid-DAF-12 in nematode evolution. Nature 466:494–497.

Bose, N., Ogawa, A., von Reuss, S. H., Yim, J. J., Ragsdale, E. J., Sommer, R. J., and Schroeder, F. C. 2012. Complex small-molecule architectures regulate phenotypic plasticity in a nematode. Angewandte Chemie 51:12438–12443.

Bumbarger, D. J., Riebesell, M., Rödelsperger, C., and Sommer, R. J. 2013. System-wide rewiring underlies behavioral differences in predatory and bacterial-feeding nematodes. Cell 152:109–119.

de Man, J. G. 1912. Helminthologische Beiträge. Zoologische Jahrbücher. Abteilung für Systematik 15 (Suppl.):439–464.

Dougherty, E. C. 1955. The genera and species of the subfamily Rhabditinae Micoletzky, 1922 (Nematoda). A nomenclatorial

analysis—including an addendum on the composition of the family Rhabditidae Örley, 1880. Journal of Helminthology 29:105–152.

Eyualem, A., and Blaxter, M. 2003. Comparison of biological, molecular, and morphological methods of species identification in a set of cultured *Panagrolaimus* isolates. Journal of Nematology 35:119–128.

Farooqui, M. N. 1967. On a new family Mehdinematidae fam. nov. from *Gryllus domesticus*. Zoologischer Anzeiger 178:322–326.

Fuchs, G. 1914. Über Parasiten und andere biologisch an die Borkenkäfer gebundene Nematoden. 85. Verhandlung der Gesellschaft Deutscher Naturforscher und Ärzte 2:688–692.

Fuchs, G. 1930. Neue an Borken- und Rüsselkäfer gebundene Nematoden, halbparasitische und Wohnungseinmieter. Zoologische Jahrbücher. Abteilung für Systematik 59:505–646.

Fürst von Lieven, A. 2005. The embryonic moult in diplogastrids (Nematoda)—homology of developmental stages and heterochrony as a prerequisite for morphological diversity. Zoologischer Anzeiger 244:79–91.

Fürst von Lieven, A., Uni, S., Ueda, K., Barbuto, M., and Bain, O. 2011. *Cutidiplogaster manati* n. gen., n. sp. (Nematoda: Diplogastridae) from skin lesions of a West Indian manatee (Sirenia) from the Okinawa Churaumi Aquarium. Nematology 13:51–59.

Fürst von Lieven, A., and Sudhaus, W. 2000. Comparative and functional morphology of the buccal cavity of Diplogastrina (Nematoda) and a first outline of the phylogeny of this taxon. Journal of Zoological Systematics and Evolutionary Research 38:37–63.

Herrmann, M., Mayer, W. E., and Sommer, R. J. 2006. Nematodes of the genus *Pristionchus* are closely associated with scarab beetles and the Colorado potato beetle in Western Europe. Zoology 109:96–108.

Herrmann, M., Ragsdale, E. J., Kanzaki, N., and Sommer, R. J. 2013. *Sudhausia aristotokia* n. gen., n. sp. and *S. crassa* n. gen., n. sp. (Nematoda: Diplogastridae): Viviparous new species with precocious gonad development. Nematology 15:1001–1020.

Hirschmann, H. 1952. Die Nematoden der Wassergrenze mittelfränkischer Gewässer. Zoologische Jahrbücher. Abteilung für Systematik 81:313–407.

Hooper, D. J. 1986. Handling, fixing, staining and mounting nematodes. Pp. 59–80 *in* Southey, J. F., ed. Methods for work with plant and soil nematodes. London: Her Majesty's Stationary Office.

Holovachov, O., and Boström, S. 2006. *Deleyia* gen. n. with a discussion of its phylogenetic relationships to the genera *Daubaylia* Chitwood & Chitwood, 1934 and *Myolaimus* Cobb, 1920 (Nematoda: Rhabditida). Nematology 8:223–233.

Kanzaki, N. 2013. Simple methods for morphological observation of nematodes. Nematological Research 43:9–13.

Kanzaki, N., Giblin-Davis, R. M., Davies, K., Ye, W., Center, B. J., and Thomas, W. K. 2009. *Teratodiplogaster fignewmani* gen. nov., sp. nov. (Nematoda: Diplogastridae) from the syconia of *Ficus racemosa* in Australia. Zoological Science 26:569–578.

Kanzaki, N., Ragsdale, E. J., Herrmann, M., Mayer, W. E., and Sommer, R. J. 2012a. Description of three *Pristionchus* species (Nematoda: Diplogastridae) from Japan that form a cryptic species complex with the model organism *P. pacificus*. Zoological Science 29:403–417.

Kanzaki, N., Ragsdale, E. J., Herrmann, M., Mayer, W. E., Tanaka, R., and Sommer, R. J. 2012b. *Parapristionchus giblindavisi* n. gen., n. sp. (Rhabditida: Diplogastridae) isolated from stag beetles (Coleoptera: Lucanidae) in Japan. Nematology 14:933–947.

Kanzaki, N., Ragsdale, E. J., Herrmann, M., Röseler, W., and Sommer, R. J. 2013. Two new species of *Pristionchus* (Nematoda: Diplogastridae) support the biogeographic importance of Japan for the evolution of the genus *Pristionchus* and the model system *P. pacificus*. Zoological Science 30:680–692.

Kanzaki, N., Taki, H., Masuya, H., Okabe, K., Tanaka, R., and Abe, F. 2011. Diversity of stag beetle-associated nematodes in Japan. Environmental Entomology 40:281–288.

Katoh, K., Misawa, K., Kuma, K., and Miyata, T. 2002. MAFFT: A novel method for rapid multiple sequence alignment based on fast Fourier transform. Nucleic Acids Research 30:3059–3066.

Körner, H. 1954. Die Nematodenfauna des vergehenden Holzes und ihre Beziehungen zu den Insekten. Zoologische Jahrbücher. Abteilung für Systematik 82:245–353.

Kreis, H. A. 1932. Beiträge zur Kenntnis pflanzenparasitischer Nematoden. Zeitschrift für Parasitenkunde 5:184–194.

Mayer, W. E., Herrmann, M., and Sommer, R. J. 2007. Phylogeny of the nematode genus *Pristionchus* and implications for biodiversity, biogeography and the evolution of hermaphroditism. BMC Evolutionary Biology 7:104.

Meyl, A. H. 1960. Freilebende Nematoden. *In* P. Brohmer, P. Ehrmann, and G. Ulmer, eds. Die Tierwelt Mitteleuropas: Freilebende Nematoden. Leipzig, Germany: Quelle & Meyer.

Micoletzky, H. 1922. Die freilebenden Erd-Nematoden. Archiv für Naturgeschichte. Abteiliung A 87:1–650.

Moczek, A. P. 2007. Developmental capacitance, genetic accommodation, and adaptive evolution. Evolution and Development 9:299–305.

Oberthür, R., and Houlbert, C. 1914. Lucanides de Java. Insecta: Revue Illustrée d'Entomologie (Rennes) 4:155–163.

Paramonov, A. A. 1952. Opyt ekologicheskoi klassifikatsii fitonematod. Trudy Gelmintologicheskoi Laboratorii. Akademia Nauk SSSR (Moskva) 6:338–369.

Ragsdale, E. J., Müller, M. R., Rödelsperger, C., and Sommer, R. J. 2013. A developmental switch coupled to the evolution of plasticity acts through a sulfatase. Cell 155:922–933.

Rahm, G. 1928. Alguns nematodes parasitas e semiparasitas das plantas culturães do Brasil. Archivos do Instituto de Biológico de Defesa Agricola e Animal (São Paolo) 1:239–251.

Ronquist, F., Teslenko, M., van der Mark, P., Ayres, D. L., Darling, A., Höhna, S., Larget, B., Liu, L., Suchard, M. A., and Huelsenbeck, J. P. 2012. MrBayes 3.2: Efficient Bayesian phylogenetic inference and model choice across a large model space. Systematic Biology 61:539–542.

Schneider, A. 1866. Monographie der Nematoden. Berlin, Germany: Reimer.

Sommer, R. J., Carta, L. K., Kim, S. Y., and Sternberg, P. W. 1996. Morphological, genetic and molecular description of *Pristionchus pacificus* n. sp. (Nematoda: Neodiplogastridae). Fundamental and Applied Nematology 19:511–521.

Sommer, R. J., and McGaughran, A. 2013. The nematode *Pristionchus pacificus* as a model system for integrative studies in evolutionary biology. Molecular Ecology 22:2380–2393.

Stamatakis, A. 2006. RAxML-VI-HPC: Maximum likelihood-based analyses with thousands of taxa and mixed models. Bioinformatics 22:2688–2690.

Steiner, G. 1914. Freilebende Nematoden aus der Schweiz. 1.+ 2. Teil. Archiv für Hydrobiologie und Planktonkunde 9:259–276, 420–438.

Sudhaus, W., and Fürst von Lieven, A. 2003. A phylogenetic classification and catalogue of the Diplogastridae (Secernentea, Nematoda). Journal of Nematode Morphology and Systematics 6:43–90.

Susoy, V., and Herrmann, M. 2012. Validation of *Rhabditolaimus* Fuchs, 1914 (Nematoda: Diplogastridae) supported by integrative taxonomic evidence. Nematology 14:595–604.

Susoy, V., Kanzaki, N., and Herrmann, M. 2013. Description of the bark beetle associated nematodes *Micoletzkya masseyi* n. sp. and *M. japonica* n. sp. (Nematoda: Diplogastridae). Nematology 15:213–231.

Völk, J. 1950. Die Nematoden der Regenwürmer und aasbesuchenden Käfer. Zoologische Jahrbücher. Abteilung für Systematik 79:1–70.

West-Eberhard, M. J. 2003. Developmental plasticity and evolution. Oxford, UK: Oxford University Press.

BRILL

Nematology 15 (2013) 213-231

Nematology
brill.com/nemy

Description of the bark beetle associated nematodes *Micoletzkya masseyi* n. sp. and *M. japonica* n. sp. (Nematoda: Diplogastridae)

Vladislav SUSOY [1], Natsumi KANZAKI [2] and Matthias HERRMANN [1,*]

[1] *Max Planck Institute for Developmental Biology, Department of Evolutionary Biology, Spemannstraße 37, Tübingen, Germany*
[2] *Forest Pathology Laboratory, Forestry and Forest Products Research Institute, 1 Matsunosato, Tsukuba, Ibaraki 305-8687, Japan*

Received: 12 March 2012; revised: 16 June 2012
Accepted for publication: 16 June 2012; available online: 22 August 2012

Summary – *Micoletzkya masseyi* n. sp. and *M. japonica* n. sp. from bark beetles *Orthotomicus caelatus* and *Dryocoetes uniseriatus*, respectively, are described based on morphology and molecular data. Both species are gonochoristic and can be cultured monoxenically on bacteria. *Micoletzkya masseyi* n. sp. is differentiated from other species of the genus by a very short male tail, P6-P8 genital papillae arranged in a triangle and with P7 being closer to P8 than to P6, and a conoid female tail to a sharp terminus. *Micoletzkya japonica* n. sp. is distinct from other *Micoletzkya* species by the arrangement of its male papillae such that P6 and P7 are close to each other and P8 is positioned apart from them, a conoid male tail with a spicate terminus, and a small gubernaculum (*ca* 11 μm in length). Phylogeny of the genus was inferred using nucleotide sequences of 18S rRNA, 28S rRNA, COI, and two ribosomal protein genes. Biological data for the new species are presented and the associations between *Micoletzkya* species and bark beetles are discussed.

Keywords – *Dryocoetes uniseriatus*, mating tests, molecular, morphology, morphometrics, mouth dimorphism, new species, *Orthotomicus caelatus*, phoresy, phylogeny, Scolytidae, taxonomy.

Nematodes of the Diplogastridae Micoletzky, 1922 are commonly associated with insects (Poinar, 1975). Types of associations are diverse among various diplogastrid genera. For example, nematodes of *Pristionchus* Kreis, 1932 have a necromenic association mostly with scarab beetles (Herrmann *et al*., 2006a, b), *Koerneria* spp. are frequently associated with stag and dung beetles (Sachs, 1950; Körner, 1954; Kanzaki *et al*., 2011a), and *Parasitodiplogaster* spp. parasitise fig wasps (Giblin-Davis *et al*., 2006). Nematodes of the diplogastrid genera *Fuchsnema* Andrássy, 1984 and *Micoletzkya* Weingärtner, 1955 are known to be symbionts of bark beetles (Coleoptera: Scolytidae) and some closely related wood-boring weevils (Coleoptera: Curculionidae) (Fuchs, 1915; Rühm, 1956, 1965; Massey, 1974).

Dauer juveniles of *Micoletzkya* nematodes disperse onto the body surface of a host beetle for transmission and resume their development in breeding galleries of the host (Rühm, 1956). After several free-living generations, dispersal juveniles develop to infest emerging young beetles. Many species of Scolytidae, including economically important members of *Dendroctonus* Erichson and *Ips* de Geer, are known to have *Micoletzkya* symbionts. However, the ecology of these associations is poorly understood. Given the possibility of cryptic speciation in diplogastrids (*e.g.*, Kanzaki *et al*., 2012a) and the sampling bias toward hosts in central Europe and the western United States, the diversity of the genus might be underestimated. Comprehensive studies on the biology and ecology of *Micoletzkya* have been limited, in part due to the difficulties in culturing these nematodes continuously under laboratory conditions (Rühm, 1956; Vosilite, 1990).

The genus includes 23 previously described nominal species (Sudhaus & Fürst von Lieven, 2003; Huang *et al*., 2010). Monophyly of the taxon is well supported by apomorphies as given by Sudhaus & Fürst von Lieven (2003). Apomorphic characters are the arrangement of male genital papillae such that P1 and P2 are closely associated, a long postdental part of the stegostom and a tight ecological association with wood-boring weevils. However, the phylogenetic position of *Micoletzkya* within the Diplogastridae is still uncertain. In one study on the molecu-

* Corresponding author, e-mail: Matthias.herrmann@tuebingen.mpg.de

© Koninklijke Brill NV, Leiden, 2013
DOI:10.1163/15685411-00002672

lar phylogeny of beetle-associated diplogastrids (Mayer *et al*., 2009), *Micoletzkya* sp. formed a group together with members of *Pristionchus*, *Acrostichus* Rahm, 1928, and *Diplogasteriana* Meyl, 1960, although this grouping showed only low statistical support.

Over the course of a long-term survey of bark beetles for the presence of associated nematodes of the Diplogastridae, more than 200 isolates of *Micoletzkya* species were obtained from several beetle species. Some of these nematodes could not be assigned to any described species of the genus. In the present study we describe two new species of *Micoletzkya*, both isolated from bark beetles, based on their morphology and molecular sequences. These two new gonochoristic species can be readily cultured on agar plates seeded with bacteria and have a relatively short generation time, making them amenable to biological and ecological studies.

Materials and methods

Nematode isolation and culturing

Living adult bark beetles were dissected and put individually onto nematode growth medium (NGM) agar or 2% water agar plates. After several days of incubation at room temperature, the samples were screened for presence of diplogastrid nematodes. To generate isofemale lines, single gravid females were transferred individually from positive plates onto NGM agar plates seeded with bacteria. An isolate of *Erwinia*-related bacterium P11-1 was used as food for culturing of *Micoletzkya masseyi* n. sp. *Escherichia coli* strain OP50 was used for culturing of *M. japonica* n. sp. The bacterial isolate P11-1 was obtained from the gut of the nematode *M. buetschlii* Fuchs, 1915 during a study on the trophic behaviour of the species (Susoy & Herrmann, unpubl.). The bacterium is characterised by its 16s rRNA sequence, which can be retrieved from the GenBank database under accession number JX163953. Selected nematode isolates were maintained as living laboratory cultures and preserved in liquid nitrogen following the protocol described by Herrmann *et al*. (2006a). For morphological examination, nematodes from 2-week-old cultures were used. Eurystomatous forms were obtained from about 1-month-old cultures where nematodes had been subjected to starvation conditions.

Morphological observations

Morphological observations and measurements were made from formalin-fixed type specimens and from heat-inactivated nematodes placed in 7 μl of M9 buffer on an agar pad. Type material was fixed according to the protocol of Ryss (2003), followed by processing through a glycerin-ethanol series using Seinhorst's method (Hooper, 1986). Drawings were made using a Zeiss microscope equipped with Nomarski optics and camera lucida. Measurements were done with the help of MetaMorph imaging software.

Scanning electron microscopy

For SEM observations, nematodes were collected from cultures and cleaned by washing three times in PBS buffer. Samples were fixed using 2.5% glutaraldehyde and post-fixed in 1% osmium tetroxide, rinsed with water several times, dehydrated through a graded ethanol series, critical point dried from carbon dioxide, and sputter-coated with 20 nm gold-palladium.

Molecular characterisation and phylogeny

For molecular characterisation of nematode isolates and strains (Table 1), partial fragments of the 18S rRNA, 28S rRNA and COI genes were amplified and sequenced from nuclear and mitochondrial DNA using primers given in Table 2. In addition, sequences of two ribosomal protein genes, *rpl-2* and *rpl-9*, were obtained using the reverse transcription polymerase chain reaction (RT-PCR). Total RNA was isolated from worms using TRIzol method (Chomczynski & Sacchi, 1987) and Absolutely RNA Nanoprep Kit (Agilent Technologies). cDNA synthesis was done with the help of SuperScript II Reverse Transcriptase kit (Invitrogen) and the primer RH5620 (5′-GAA GAT CTA GAG CGG CCG CCC TTT TTT TTT TTT TTT-3′). Complete transcripts were obtained following the protocol of Mayer *et al*. (2007). Gene-specific oligonucleotides used were WM16739, WM18611, WM15359 and WM16152 (Mayer *et al*., 2009) to target *rpl-2* and *rpl-9* and VL26353 (5′-CTG GTG GTT WCC TCC TCC GTG RGG AT-3′), targeting the *rpl-2* gene (present study).

Sequences were assembled using the program SeqMan Pro 7.2.2 (DNASTAR) and aligned using MUSCLE (Edgar, 2004), followed by manual improvement of the alignment in Mega 5.05 (Tamura *et al*., 2007). Phylogeny was inferred using Bayesian analysis as implemented in MrBayes 3.1.2 (Huelsenbeck & Ronquist, 2001). A con-

Table 1. Origin of nematode isolates used in the study.

Nematode taxon	Strain	Host/habitat	Location	Reference
Acrostichus sp.	RS5083	Soil	Breitenholz, Germany	Mayer *et al.* (2009)
Koerneria sp.	RS1982	*Melolontha melolontha*	Usedom, Germany	Mayer *et al.* (2009)
Micoletzkya masseyi n. sp.	RS5540	*Orthotomicus caelatus*	Alberta, Canada	This study
Micoletzkya buetschlii	–	*Ips typographus*	Tübingen, Germany	This study
Micoletzkya japonica n. sp.	RS5524	*Dryocoetes uniseriatus*	Ibaraki, Japan	This study
Micoletzkya palliati	–	*Hylurgops palliatus*	Tübingen, Germany	This study
Micoletzkya sp. 3	RS5562	*Dryocoetes autographus*	Tübingen, Germany	This study
Micoletzkya sp. 14	RS5541	*Dryocoetes affaber*	Alberta, Canada	This study
Pristionchus pacificus	PS312	Soil	Pasadena, USA	Sommer *et al.* (1996)
Parapristionchus giblindavisi	RS5555	*Dorcus rubrofemoratus*	Iwaizumi, Japan	Kanzaki *et al.* (2012b)
Rhabditoides inermis	SB328	*Nicrophorus* sp.	Berlin, Germany	

Table 2. Oligonucleotides employed in the study.

Primer name	Gene	Orientation	Sequence ($5' \rightarrow 3'$)	Reference
VL26341	COI	Sense	CCTACTATGATTGGTGGTTTTGGTAATTG	This study
VL26342	COI	Antisense	GTAGCAGCAGTAAAATAAGCACG	This study
VL26343	COI	Sense	GGTGGTTTTGGTAATTGAATRTTAC	This study
VL26344	COI	Antisense	TAAGCACGWGAATCTAAATCYATWCC	This study
SSU18A	18SrRNA	Sense	AAAGATTAAGCCATGCATG	Eyualem & Blaxter (2003)
SSU26R	18SrRNA	Antisense	CATTCTTGGCAAATGCTTTCG	Eyualem & Blaxter (2003)
VL26345	18SrRNA	Sense	GCGAAAGCATTTGCCAAGA	This study
VL26346	18SrRNA	Antisense	GGTTCAAGCCACTGCGAT	This study
KK28S-1	28SrRNA	Sense	AAGGATTCCCTTAGTAACGGCGAGTG	Kiontke *et al.* (2004)
KK28S-16	28SrRNA	Antisense	TCAATCAAAGGATAGTCTCAACAGATCGC	Kiontke *et al.* (2004)
VL26347	28SrRNA	Sense	CGCTAAGGAGTGTGTAACAACTCACCT	This study
VL26348	28SrRNA	Sense	CTGATTTCTGCCCAGTGCTCTGAATG	This study
VL26349	28SrRNA	Sense	GTCTTAAGTTCGCTGGAAGGCAACT	This study
VL26350	28SrRNA	Antisense	GGTGAGTTGTTACACACTCCTTAG	This study
VL26351	28SrRNA	Antisense	CACCAAGATCTGCACCGACGGAA	This study
VL26352	28SrRNA	Antisense	CCTTGGCTGTGGTTTCGCTAGATAGT	This study

catenated alignment of COI, 18S, 28S, *rpl-2* and *rpl-9* was divided into eight partitions: COI 1st, 2nd and 3rd positions, ribosomal protein genes 1st, 2nd and 3rd positions, 18S and 28S. A general time reversible (GTR) model with a proportion of invariable sites and a gamma-shaped distribution of rates across sites was invoked. Model parameters were unlinked across partitions. A Markov chain Monte Carlo search was run for 2 000 000 generations with sampling every 100th generation and excluding the first 500 000 generations as burn-in.

Nucleotide sequences obtained in the present study were deposited in the GenBank database under accession numbers JX163954-JX163992. Sequences of the following nematode isolates were retrieved from GenBank for inclusion in phylogenetic analysis: *Acrostichus* sp. *rpl-2* (GQ422215), *rpl-9* (GQ422185); *Koerneria* sp. *rpl-2* (EF634530) and *rpl-9* (GQ422183); *M. buetschlii rpl-2* (GQ422210) and *rpl-9* (GQ422177); *Pristionchus pacificus* Sommer, Carta, Kim & Sternberg, 1996 COI (JF414117), 18S rRNA (AF083010), 28S rRNA (EU195982), *rpl-2* (EF634512) and *rpl-9* (GQ422181); *Parapristionchus giblindavisi* Kanzaki, Ragsdale, Herrmann, Mayer, Tanaka & Sommer, 2012 *rpl-2* (JQ677914); *Rhabditoides inermis* 18S rRNA (AF082996), 28S rRNA (EU195981), *rpl-2* (GQ422218) and *rpl-9* (GQ422188).

Mating experiments

Micoletzkya buetschlii specimens were isolated from a laboratory culture of *Ips typographus* L. and cultured

using *Caenorhabditis elegans* N2 strain as food. Five males of *M. buetschlii* were placed together with five J4 females of *M. masseyi* n. sp. and *vice versa* on NGM agar plates seeded with several thousands of *C. elegans* L1 and L2. Plates without added cholesterol and peptone were used to prevent bacterial and fungal growth. After 10 days the plates were screened for the presence of progeny. Each test was repeated at least five times. Positive controls were performed using males and virgin females of the same species. To confirm the identity of *M. buetschlii* isolates used for the mating tests, parent worms were lysed after each experiment and their partial 18S rRNA sequences were compared to the reference 18S rRNA gene sequence of *M. buetschlii*.

Results

Micoletzkya masseyi[*] n. sp.
(Figs 1, 2)

Measurements

See Table 3.

Description

Adults

Body of medium size, cylindrical. Cuticle *ca* 1 μm thick with fine annulation and moderately prominent longitudinal striation. Each stria underlain by a double row of dots. Lateral fields consisting of two lines weakly distinguishable from cuticle striation when observed using light microscopy (LM). Deirid located laterally, posterior to pharyngo-intestinal junction, inconspicuous. Six faint lip sectors present, each bearing a single, short, apical papilla. Deviation from hexaradiate symmetry observed, such that lateral papillae are situated much further from mouth opening than subdorsal and subventral papillae. A circle of four cephalic papillae present in males only. Amphidial apertures small, located at cheilostom level. Mouth dimorphism observed with stenostomatous (narrow mouth) and eurystomatous (wide mouth) forms occurring in females and only stenostomatous form appearing in males. Pharynx typical diplogastroid, its anterior part very muscular, composed of procorpus and metacorpus forming median bulb. Ridges of pharyngeal cuticular lining strongly developed. Isthmus slender, not muscular. Terminal bulb glandular, almost as broad as median bulb. Isthmus and terminal bulb slightly longer than combined procorpus and metacorpus, such that posterior to anterior pharynx ratio is *ca* 1.2. Nerve ring at middle of isthmus. Pharyngo-intestinal junction clearly observed. Hemizonid not discernible.

Stenostomatous form

Head narrowly rounded. Stoma from anterior end of cheilostom to base of stegostom deeper than broad. Cheilostom broader than long, divided into six plates. Gymnostom almost as long as broad, its anterior part internally overlapping with cheilostom. Stegostom bearing conspicuous, movable, dorsal claw-like tooth and pointed right subventral tooth. Left subventral side of stegostom bearing ventrally located blunt cusp, more dorsally located peak with pointed tip, and ventrally located conspicuous adventitious pointed denticle. Postdental part of stegostom appreciably extended and sclerotised. Duct of dorsal pharyngeal gland clearly penetrating dorsal tooth. Excretory pore located ventrally near pharynx end or posterior to it.

Eurystomatous form

Head broadly rounded. Stoma from anterior end of cheilostom to base of stegostom as broad as deep. Cheilostom consisting of six broad plates, anterior margin of these plates notched. Gymnostom less than half as long as broad, its anterior edge serrated. Stegostom bearing large dorsal claw-like tooth and large pointed right subventral denticle. Left subventral side of stegostom bearing two conspicuous peaks and adventitious denticle. Postdental part of stegostom sclerotised and noticeably long. Duct of dorsal gland very prominent, penetrating dorsal tooth. Excretory pore near anterior part of terminal bulb.

Male

Testis single, ventrally located, reflexed to right side. Reflexed and distal unreflexed parts of gonad containing spermatogonia. Spermatocytes large, arranged in a single row. Spicules paired, separate, smoothly ventrally arcuate, proximally cephalated, distally pointed. Gubernaculum conspicuous, encompassing spicules on both sides, its anterior ventral part heavily sclerotised. Dorsal surface of gubernaculum bearing two pairs of anteriorly directed processes. Nine pairs of genital papillae, a single precloacal sensillum, and phasmids present and arranged as ⟨(P1, P2), P3d, C, P4, P5d, Ph, (P6, P7, P8), P9d⟩. Papillae

[*] The species is named after Calvin L. Massey, in honour of his contributions to revealing and describing a diversity of nematodes of the genus *Micoletzkya* in the USA.

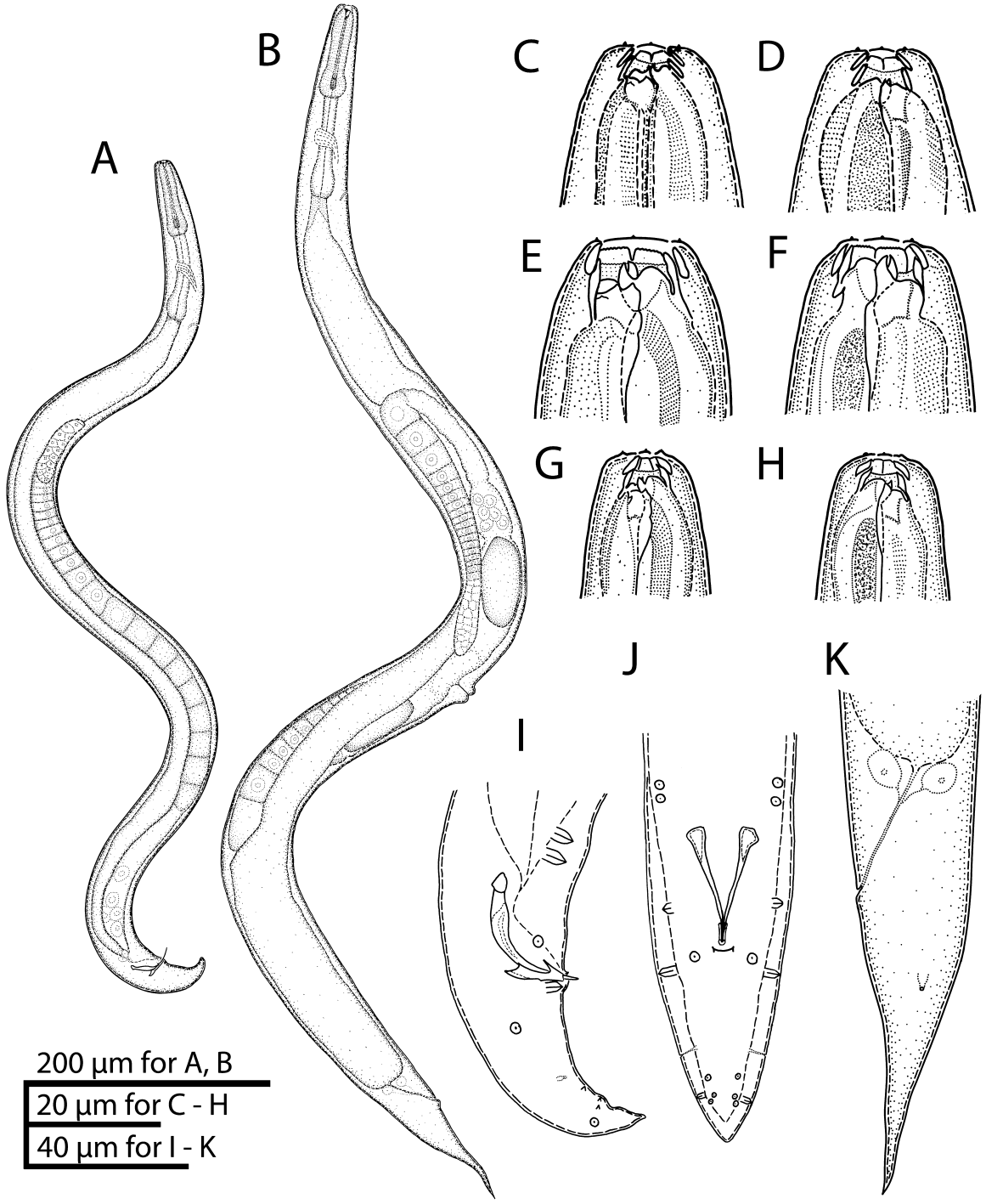

Fig. 1. *Micoletzkya masseyi* n. sp. A: Male, right lateral view; B: Entire stenostomatous female, right lateral view; C: Stomatal region of stenostomatous female, left lateral view; D: Stomatal region of stenostomatous female, right lateral view; E: Stomatal region of eurystomatous female, left lateral view; F: Stomatal region of eurystomatous female, right lateral view; G: Stomatal region of stenostomatous male, left lateral view; H: Stomatal region of stenostomatous male, right lateral view; I: Posterior region of male, right lateral view; J: Posterior region of male, ventral view; K: Posterior region of female, left lateral view.

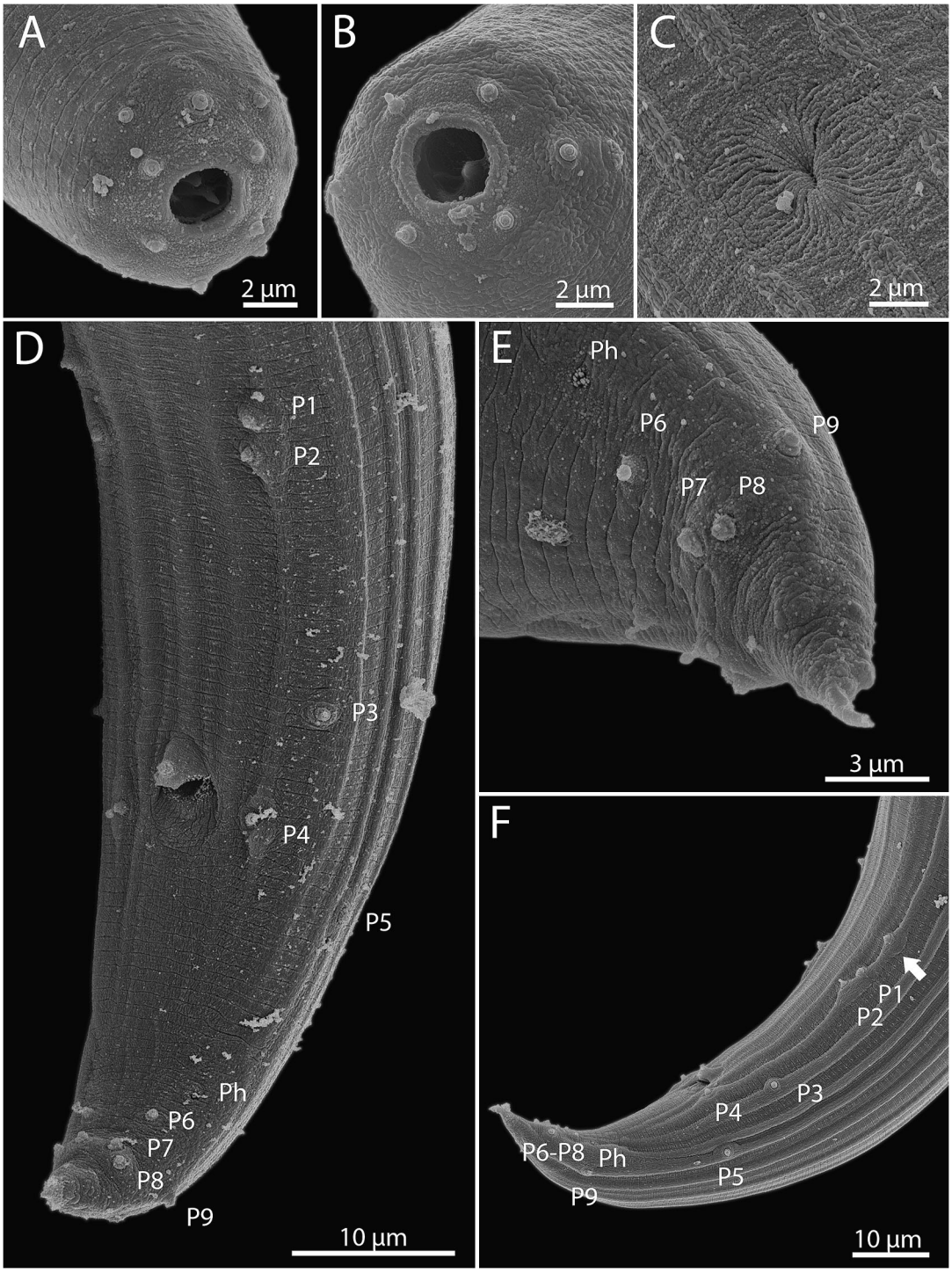

Fig. 2. Scanning electron micrographs of *Micoletzkya masseyi* n. sp. A: Anterior region of stenostomatous male; B: Anterior region of stenostomatous female; C: Female vulva; D: Posterior region of male; E: Tail region of male; F: Posterior region of male. White arrow indicates extra papilla, only present in some specimens, and located anterior to P1. (Abbreviations: P1-P9 = male papillae; Ph = phasmid.)

Table 3. Morphometrics of formalin-fixed holotype male, heat-relaxed male and female specimens of *Micoletzkya masseyi* n. sp. All measurements are in μm and in the form: mean ± s.d. (range).

Character	Male		Stenostomatous female	Eurystomatous female
	Holotype	Temporary water mounts	Temporary water mounts	Temporary water mounts
n	–	10	10	10
L	693	784 ± 82 (639-872)	1164 ± 51 (1059-1226)	867 ± 63 (797-976)
L′	659	740 ± 81 (598-831)	1079 ± 52 (973-1142)	797 ± 61 (734-906)
a	21.0	20.8 ± 1.0 (19.2-22.6)	20.6 ± 0.7 (19.5-21.5)	18.2 ± 1.1 (17.2-20.8)
b	5.8	5.8 ± 0.6 (4.7-6.3)	7.5 ± 0.4 (7.0-8.0)	5.0 ± 0.3 (4.7-5.7)
c	20.2	17.9 ± 2.3 (15.4-21.5)	13.7 ± 1.1 (12.3-16.2)	12.4 ± 0.9 (10.8-13.9)
c′	19.2	16.9 ± 2.3 (14.4-20.5)	12.7 ± 1.1 (11.3-15.2)	11.4 ± 0.9 (9.8-12.9)
T or V	66	58 ± 6 (48-64)	52 ± 1 (51-55)	55 ± 1 (54-56)
Max. body diam.	33	38 ± 4.6 (28-44)	57 ± 3.6 (50-61)	47 ± 1.9 (45-52)
Stoma length	6.8	8.2 ± 0.7 (6.7-9.3)	10.2 ± 0.6 (9.3-11.1)	9.7 ± 0.6 (8.4-10.4)
Stoma diam.	4.3	5.3 ± 0.6 (4.1-6.4)	6.1 ± 0.7 (5.4-7.6)	9.9 ± 0.4 (9.4-10.4)
Pharynx length (head to base of pharynx)	119	136 ± 3.7 (130-143)	155 ± 8.4 (147-169)	173.6 ± 3.7 (166-179)
Anterior pharynx (pro- + metacorpus)	54	61 ± 1.9 (59-65)	69 ± 2.4 (66-73)	80 ± 3.2 (75-85)
Posterior pharynx (ithmus + basal bulb)	59	71 ± 2.7 (68-77)	81 ± 6.3 (75-92)	85 ± 3.4 (80-90)
Post./ant. pharynx ratio	1.1	1.2 ± 0.0 (1.1-1.2)	1.2 ± 0.1 (1.1-1.3)	1.1 ± 0.1 (1.0-1.2)
Median bulb diam.	15	16.0 ± 1.3 (13.8-18.1)	20.8 ± 1.1 (19.5-22.8)	25.1 ± 1.2 (23.7-28.0)
Terminal bulb diam.	13	15.1 ± 1.5 (12.3-16.8)	19.3 ± 1.3 (17.2-20.7)	24.6 ± 1.1 (23.0-26.7)
Ant. end to nerve ring	78	91 ± 6 (85-104)	102 ± 6 (93-111)	106 ± 5 (100-116)
Ant. end to excretory pore	116	130 ± 11 (112-144)	159 ± 9 (144-171)	141 ± 8.4 (133-159)
Testis length	462	459 ± 74 (331-526)	–	–
Ant. gonad length (vulva to reflex)	–	–	264 ± 29 (216-300)	203 ± 25 (169-244)

Table 3. (Continued.)

Character	Male		Stenostomatous female	Eurystomatous female
	Holotype	Temporary water mounts	Temporary water mounts	Temporary water mounts
Post. gonad length (vulva to reflex)	–	–	229 ± 22 (201-259)	181 ± 17 (157-204)
Ant. end to vulva	–	–	613 ± 33 (552-647)	479 ± 37 (432-548)
Vulva to anus distance	–	–	467 ± 24 (421-499)	318 ± 26 (289-363)
Cloacal or anal body diam.	21	26 ± 2.6 (21-30)	35 ± 2.3 (32-39)	28 ± 3.1 (25-36)
Tail length	40	44 ± 4 (39-51)	85 ± 5 (75-92)	70 ± 6 (61-78)
Spicule length (curve)	38	38 ± 2.2 (34-40)	–	–
Spicule length (chord)	31	33 ± 1.9 (29-35)	–	–
Gubernaculum length	14.6	15.9 ± 0.8 (14.6-16.8)	–	–

P1 and P2 located close to each other as typical for nematodes of the genus, *ca* 1.5 cloacal body diam. anterior to cloacal opening, P3d slightly anterior to cloaca, P4 positioned immediately posterior to cloaca, P5d located slightly posterior to P4, P6 situated ca one cloacal body diam. posterior to cloaca, P6, P7 and P8 close to each other and arranged in a triangle with P7 being most ventral and P7 located closer to P8 than to P6, P9d located at level of P7 or P8. P6, P7, P8 and P9d disposed just anterior of tail terminus. P1, P2, P3d, P4 and P5d rather large and conspicuous. P9d small but larger than P6, P7, and P8. P6, P7 and P8 very small, not easily observed by LM. In some specimens, an additional, conspicuous pair of papillae present anterior to P1. Bursa absent. Tail short, conical, ventrally arcuate possessing a very short terminal mucro.

Female

Vulva located at mid-body, transverse. Lips of vulva appearing protuberant when observed using LM, vulva opening circular. Amphidelphic, ovaries dorsally reflexed, extending beyond vulva in some specimens. Anterior gonad branch positioned to right of intestine, posterior to left. Anterior gonad branch from vulva to reflex longer than posterior branch. Oocytes arranged in two or three rows in distal end of ovaries and in one row in proximal part. Spermatheca located halfway between reflex and vulva, usually filled with sperm, separated from ovary and uterus by a restriction. Oviparous, up to two eggs present in spermatheca or uterus. In some specimens, egg laying compromised and as many as 14 eggs may be retained. Rectal gland cells faint. Posterior anal lip slightly protuberant. Phasmids moderately conspicuous, located at *ca* one anal body diam. posterior to anus. Tail relatively short, conoid to a sharp terminus.

Type host and locality

The type strain of *M. masseyi* n. sp. was isolated from the bark beetle *Orthotomicus caelatus* Eichhoff. The beetle was collected in Kananaskis valley, Alberta, Canada, in August 2011 and obtained by courtesy of Dr Mary Reid, Biogeoscience Institute, Alberta, Canada.

Type material

Holotype male, six paratype males, six paratype stenostomatous females and six paratype eurystomatous females deposited at University of California Riverside Nematode Collection (UCRNC), Riverside, CA, USA. Six paratype males, six paratype stenostomatous females and six paratype eurystomatous females deposited in the collection of the Natural History Museum Karlsruhe, Germany.

Type strain culture

The type strain is maintained as living culture and frozen stocks under the strain number RS5540 at the Department of Evolutionary Biology, Max Planck Institute for Developmental Biology, Tübingen, Germany, and is available upon request.

Diagnosis and relationships

Micoletzkya masseyi n. sp. is characterised by a very short conical male tail, a relatively short conoid female tail to a sharp terminus, and the arrangement of P6-P8 caudal papilla in a triangle immediately anterior to terminus, with P7 being located closer to P8 than to P6.

Micoletzkya masseyi n. sp. is readily distinguished from most described nematodes of the genus by the tail shape of the male. A short conical male tail also characterises *M. bandelieri* Massey, 1960, *M. cervicula* Massey, 1966 and some specimens of *M. sexdentati* Blinova & Vosilite, 1978. *Micoletzkya masseyi* n. sp. is distinguished from *M. bandelieri* by a spicule length of 34-40 μm (curved median line) *vs* 42-47 μm, female tail conoid with a sharp terminus *vs* conical with a rounded terminus, and by P6-P8 caudal papilla being arranged in a triangle *vs* in series. *Micoletzkya masseyi* n. sp. differs from *M. cervicula* by a spicule length of 34-40 *vs* 50 μm, P6-P8 caudal papilla arranged in a triangle *vs* in series, and P9 positioned at P7 or P8 *vs* located at P6 level; and from *M. sexdentati* by arrangement of its genital papilla, by stomatal morphology, such that the left subventral part of the stegostom bears two cusps *vs* one pointed peak, by a spicule length of 34-40 *vs* 36-48 μm and by gubernaculum length of 14.8-16.8 *vs* 17-22 μm. Unlike *M. masseyi* n. sp., *M. sexdentati* males have a tail that is conoid to a spicate terminus, the latter being absent in some specimens.

***Micoletzkya japonica*[*] n. sp.**
(Figs 3, 4)

Measurements

See Table 4.

[*] The species epithet refers to the type locality of the species.

Description

Adults

Body cylindrical, of medium size. Cuticle *ca* 1 μm thick with faint annulation and conspicuous striation. Each stria underlain by a double row of small dots. Lateral fields formed of two moderately prominent lines. Deirid inconspicuous, laterally situated, located posterior to end of pharynx. Six faint lip sectors present, each bearing a single, short, apical papilla. Subdorsal and subventral papillae located closer to mouth opening than lateral papillae. Four small cephalic papillae present in males. Amphidial apertures small, inconspicuous, located at level of cheilostom. Both stenostomatous and eurystomatous forms occurring in females. Only stenostomatous form occurring in males. Ridges of pharyngeal circular lining well developed. Procorpus and median bulb of pharynx very muscular. Isthmus slender, not muscular. Terminal bulb glandular. Procorpus and metacorpus shorter than isthmus and terminal bulb combined such that posterior to anterior pharynx ratio *ca* 1.2. Nerve ring encircling middle of isthmus. Pharyngo-intestinal junction clearly observed. Hemizonid not discernible.

Stenostomatous form

Head narrowly rounded. Stoma narrow, twice as deep as broad when measured from anterior end of cheilostom to base of stegostom. Cheilostom divided into six plates. Gymnostom nearly as long as broad, its anterior part internally overlapping with posterior part of cheilostom. Stegostom bearing small, movable, dorsal claw-like tooth and small, pointed, right subventral tooth. Left subventral side of stegostom bearing two small peaks with pointed tips and inconspicuous adventitious denticle. Postdental region of stegostom twice as long as broad. Duct of dorsal pharyngeal gland penetrating dorsal tooth. Excretory pore conspicuous, located ventrally near pharynx end or more posterior.

Eurystomatous form

Head broadly rounded. Six lip sectors present, each bearing a single, short, apical papilla. Buccal cavity broad, almost as broad as deep. Cheilostom composed of six plates. Gymnostom at least twice as broad as long. Anterior edge of gymnostom serrated. Stegostom bearing large dorsal claw-like tooth and large pointed right subventral tooth. Left subventral side of stegostom bearing two conspicuous peaks with pointed tips and adventitious denticle. Postdental part of stegostom extended and sclerotised. Duct of dorsal pharyngeal gland clearly penetrating dorsal

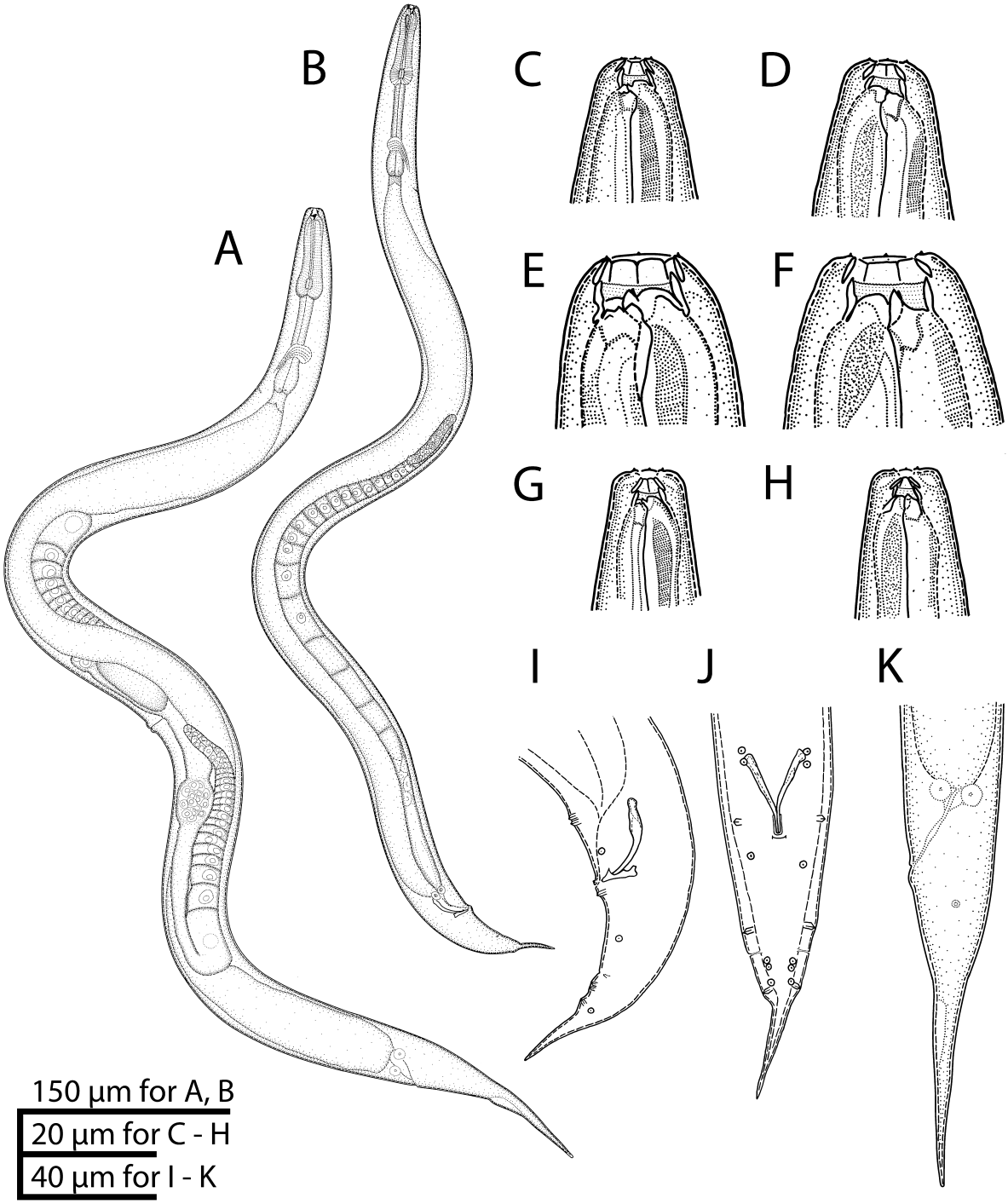

Fig. 3. *Micoletzkya japonica* n. sp. A: Entire stenostomatous female, left lateral view; B: Entire male (stenostomatous), right lateral view; C: Stomatal region of stenostomatous female, left lateral view; D: Stomatal region of stenostomatous female, right lateral view; E: Stomatal region of eurystomatous female, left lateral view; F: Stomatal region of eurystomatous female, right lateral view; G: Stomatal region of male, left lateral view; H: Stomatal region of male, right lateral view; I: Posterior region of male, left lateral view; J: Posterior region of male, ventral view; K: Posterior region of female, left lateral view.

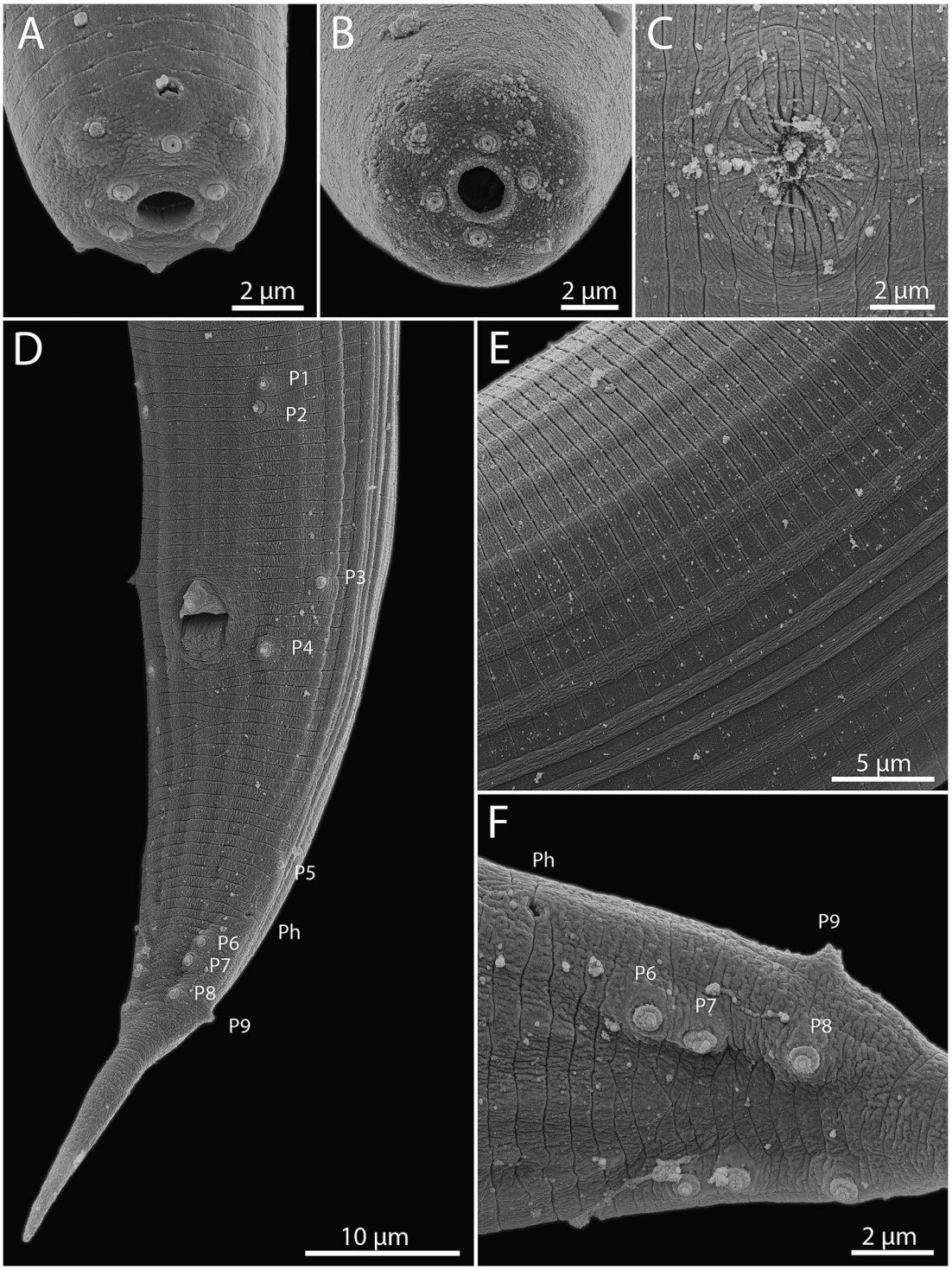

Fig. 4. Scanning electron micrographs of *Micoletzkya japonica* n. sp. A: Anterior region of stenostomatous male; B: Anterior region of stenostomatous female; C: Female vulva; D: Posterior region of male; E: Cuticular surface; F: Tail region of male. (Abbreviations: P1-P9 = male papillae; Ph = phasmid.)

Table 4. Morphometrics of formalin-fixed holotype male, heat-relaxed male and female specimens of *Micoletzkya japonica* n. sp. All measurements are in μm and in the form: mean ± s.d. (range).

Character	Male		Stenostomatous female	Eurystomatous female
	Holotype	Temporary water mounts	Temporary water mounts	Temporary water mounts
n	–	10	10	10
L	659	808 ± 45 (713-860)	982 ± 76 (853-1127)	827 ± 76 (701-937)
L′	604	734 ± 43 (651-787)	869 ± 70 (754-997)	729 ± 67 (620-821)
a	24.0	22.4 ± 1.3 (20.2-24.4)	22.5 ± 1.2 (20.7-24.1)	20.6 ± 1.1 (18.5-22.3)
b	6.3	6.5 ± 0.4 (5.9-6.9)	7.2 ± 0.4 (6.5-7.8)	5.2 ± 0.4 (4.5-5.8)
c	12.0	11.1 ± 0.7 (10.1-12.4)	8.6 ± 0.5 (8.1-9.5)	8.5 ± 0.6 (7.8-9.7)
c′	11.0	10.1 ± 0.7 (9.1-11.4)	7.6 ± 0.5 (7.1-8.5)	7.5 ± 0.6 (6.8-8.7)
T or V	56	52 ± 3 (47-55)	52 ± 1 (51-54)	55 ± 0.5 (54-55)
Max. body diam.	27	36 ± 3 (31-41)	44 ± 3.6 (38-50)	40 ± 3.8 (34-46)
Stoma length	6.5	8.1 ± 0.5 (7.4-9.2)	7.9 ± 1.0 (6.3-9.5)	12.6 ± 0.5 (11.9-13.4)
Stoma diam.	2.4	2.7 ± 0.2 (2.3-3.0)	3.3 ± 0.4 (2.6-3.9)	9.7 ± 0.5 (8.9-10.3)
Pharynx length (head to base of pharynx)	104	124 ± 1.5 (121-126)	137 ± 4.2 (132-147)	159 ± 6.6 (153-173)
Anterior pharynx (pro- + metacorpus)	49	54 ± 0.8 (53-56)	61 ± 2.1 (57-65)	70 ± 2.4 (67-75)
Posterior pharynx (ithmus + basal bulb)	52	65 ± 1.5 (62-67)	72 ± 2.6 (69-77)	83 ± 4.3 (79-91)
Post./ant. pharynx ratio	1.1	1.2 ± 0.0 (1.1-1.2)	1.2 ± 0.0 (1.1-1.2)	1.2 ± 0.1 (1.1-1.3)
Median bulb diam.	13.3	15.3 ± 0.6 (14.3-16.6)	17.2 ± 0.6 (16.2-18-2)	24.1 ± 1.4 (22.4-26.7)
Terminal bulb diam.	10.4	11.4 ± 0.6 (10.6-12.2)	13.9 ± 0.9 (12.1-15.4)	23.9 ± 1.8 (21.3-27.0)
Ant. end to nerve ring	103	95 ± 4 (87-101)	102 ± 5 (94-111)	100 ± 3 (97-105)
Ant. end to excretory pore	120	129 ± 6 (116-135)	135 ± 8 (125-154)	132 ± 7.3 (121-144)
Testis length	373	425 ± 43 (354-469)	–	–
Ant. gonad length (vulva to reflex)	–	–	176 ± 24 (136-213)	144 ± 29 (91-187)

Table 4. (Continued.)

Character	Male		Stenostomatous female	Eurystomatous female
	Holotype	Temporary water mounts	Temporary water mounts	Temporary water mounts
Post. gonad length (vulva to reflex)	–	–	167 ± 19 (134-193)	124 ± 23 (81-153)
Ant. end to vulva	–	–	513 ± 36 (455-570)	451 ± 42 (386-518)
Vulva to anus distance	–	–	356 ± 36 (300-427)	279 ± 26 (234-310)
Cloacal or anal body diam.	20	27 ± 1.8 (22-28)	29 ± 3.9 (25-39)	27 ± 2.4 (23-31)
Tail length	55	73 ± 5 (62-78)	114 ± 8 (99-130)	98 ± 11 (81-116)
Spicule length (curve)	28	29 ± 0.6 (28-30)	–	–
Spicule length (chord)	23	26 ± 0.8 (25-28)	–	–
Gubernaculum length	11.6	11.1 ± 0.3 (10.6-11.6)	–	–

tooth. Excretory pore located near anterior part of terminal bulb.

Male

Testis single, ventrally located, reflexed to right side. Reflexed and distal unreflexed parts containing spermatogonia arranged in two or three rows, more proximal part containing large spermatocytes arranged in a single row. Spicules paired, separate, smoothly ventrally arcuate, proximally cephalated, distally pointed. Gubernaculum conspicuous, small, *ca* 11 μm long, encompassing spicules on both sides, its dorsal surface possessing two pairs of anteriorly directed processes. Nine pairs of genital papillae, a single precloacal sensillum, and phasmids present and arranged as ⟨(P1, P2), P3d, C, P4, P5d, ph, (P6, P7, P8), P9d⟩. Papillae P1 and P2 closely associated, *ca* one anal body diam. anterior to cloacal opening, P3d anterior to cloaca, P4 positioned immediately posterior to cloaca, P5 situated *ca* one anal body diam. posterior to cloaca, relatively close to phasmid, P6, P7 and P8 close to each other and arranged linearly, with P6 and P7 closely associated and P8 more distant from the former two, P9d located at the level of P8. P1, P2, P3d and P4 rather large and conspicuous. P5d, P6, P7, P8 and P9d also prominent but smaller than P1-P4. Bursa absent. Tail moderately long, ventrally arcuate, conoid with spicate terminus.

Female

Vulva located at mid-body, transverse. Lips of vulva protuberant, vulva opening circular. Amphidelphic, ovaries reflexed, distal gonad not crossing plane of vulva. Anterior gonad branch positioned to right of intestine, posterior to left. Anterior gonad branch from vulva to reflex as long as posterior branch. Oocytes arranged in two or three rows in distal end of ovaries and in one row in proximal part. Spermatheca approximately midway from vulva to reflex, usually filled with sperm, separated from ovary and uterus by regions of narrower diam. Oviparous, up to two eggs present in spermatheca or uterus. Rectal gland cells present but not obvious. Posterior anal lip slightly protuberant. Phasmids moderately conspicuous. Tail conoid to a pointed terminus.

TYPE HOST AND LOCALITY

The type strain of *M. japonica* n. sp. was isolated from the bark beetle *Dryocoetes uniseriatus* Eggers that had just emerged from a dead log of *Pinus thunbergii* Parl. in early spring 2010. The beetle was collected in the Chiyoda Experimental Station of the Forestry and Forest Products Research Institute, Kasumigaura, Ibaraki, Japan.

Type material

Holotype male, six paratype males, six paratype stenostomatous females and six paratype eurystomatous females deposited at UCRNC. Six paratype males, six paratype stenostomatous females and six paratype eurystomatous females deposited in the collection of the Natural History Museum Karlsruhe.

Type strain culture

The strain from which the type material was obtained is maintained as living culture and frozen stocks under strain number RS5524 at the Department of Evolutionary Biology, Max Planck Institute for Developmental Biology, Tübingen, Germany, and is available upon request.

Diagnosis and relationships

Micoletzkya japonica n. sp. is characterised by the arrangement of the caudal papillae such that P6 and P7 are associated and P8 is positioned far apart from them, a conoid male tail with spicate terminus and a small gubernaculum *ca* 11 μm long.

The arrangement of genital papillae in *M. japonica* n. sp. is shared with *M. hylurginophila* Rühm, 1956. These two species are distinguished by the following morphometric values, respectively: male pharynx length of 104-126 *vs* 168-172 μm; spicule length of 28-30 *vs* 39-43 μm; gubernaculum length of *ca* 11 *vs* 15-18 μm; male tail 62-78 *vs* 88-101 μm, and female tail 81-130 *vs* 133-137 μm. *Micoletzkya japonica* n. sp. differs from the morphologically very similar *M. diluta* Massey, 1966 by arrangement of the P6-P8 genital papillae, such that in *M. japonica* n. sp., P8 is positioned apart from P6 and P7, whereas in *M. diluta* the distance between P6, P7 and P8 is equal, and by the number of the lateral processes on the dorsal surface of the gubernaculum.

Molecular characterisation and phylogeny

A Bayesian tree was inferred from a dataset containing 6030 characters, of which 1680 sites were variable and 921 sites were parsimony informative (Fig. 5). The tree was rooted with *R. inermis* as an outgroup (Kiontke *et al*., 2007). *Koerneria* sp. occupied the most basal position among the diplogastrid isolates which is consistent with previous studies (Mayer *et al*., 2009; Susoy & Hermann, 2012). *Micoletzkya* is supported as monophyletic with maximal posterior probability. Within this group two subclades are present, one containing *M. japonica* n. sp., *M.* sp. 14 and *M.* sp. 3, and a second one containing *M. palliati*, *M. masseyi* n. sp. and *M. buetschlii*. Within the second subclade, *M. palliati* is basal and *M. masseyi* n. sp. is a sister taxon to *M. buetschlii*. Of the remaining diplogastrids included in the analysis, *Micoletzkya* is the sister to a group containing *Parapristionchus giblindavisi* and *Pristionchus pacificus* with posterior probability of 93, the latter two species being sister taxa with posterior probability of 1. *Acrostichus* sp. is a sister taxon to a group containing *Micoletzkya* spp., *Parapristionchus giblindavisi* and *Pristionchus pacificus*.

Mating experiments

All crosses between the phylogenetically closely related *M. masseyi* n. sp. and *M. buetschlii* were negative. In a few cases, egg laying was observed, although these eggs did not develop. Intraspecific crosses, serving as a positive control, always resulted in numerous progeny.

Biological data

The generation time from egg laying to egg laying of *M. masseyi* n. sp. is approximately 10 days when cultured on bacterium isolate P 11-1 at room temperature. *Micoletzkya japonica* n. sp. completes its life cycle in 7 days when OP50 is used as food. Both species display predatory behaviour when bacterial food is limited. They can predate on another bark-beetle-associated nematode, *Parasitorhabditis obtusa* Fuchs, 1915, and on *C. elegans* eggs, juveniles and adults, and they can successfully reproduce using nematode prey as a food source. Cannibalism was also observed, but only when no other food was available. Under harsh conditions (high population density, limited food) juveniles of *M. masseyi* n. sp. can undergo dauer arrest. In *M. japonica* n. sp. dauer formation has not been observed under laboratory conditions.

Discussion

Buccal cavity dimorphism has been observed in several diplogastrid genera (Fürst von Lieven & Sudhaus, 2000). Occurring at high frequencies under harsh conditions, the eurystomatous form is thought to be associated with omnivory and predation, in contrast to the presumed bacterial-feeding stenostomatous form. Although the mouth dimorphism in *Micoletzkya* was observed by Rühm (1956), Blinova & Vosilite (1978) and Huang *et al*. (2010), in most species only one mouth form (either eury- or stenostomatous) has been described. In *M.*

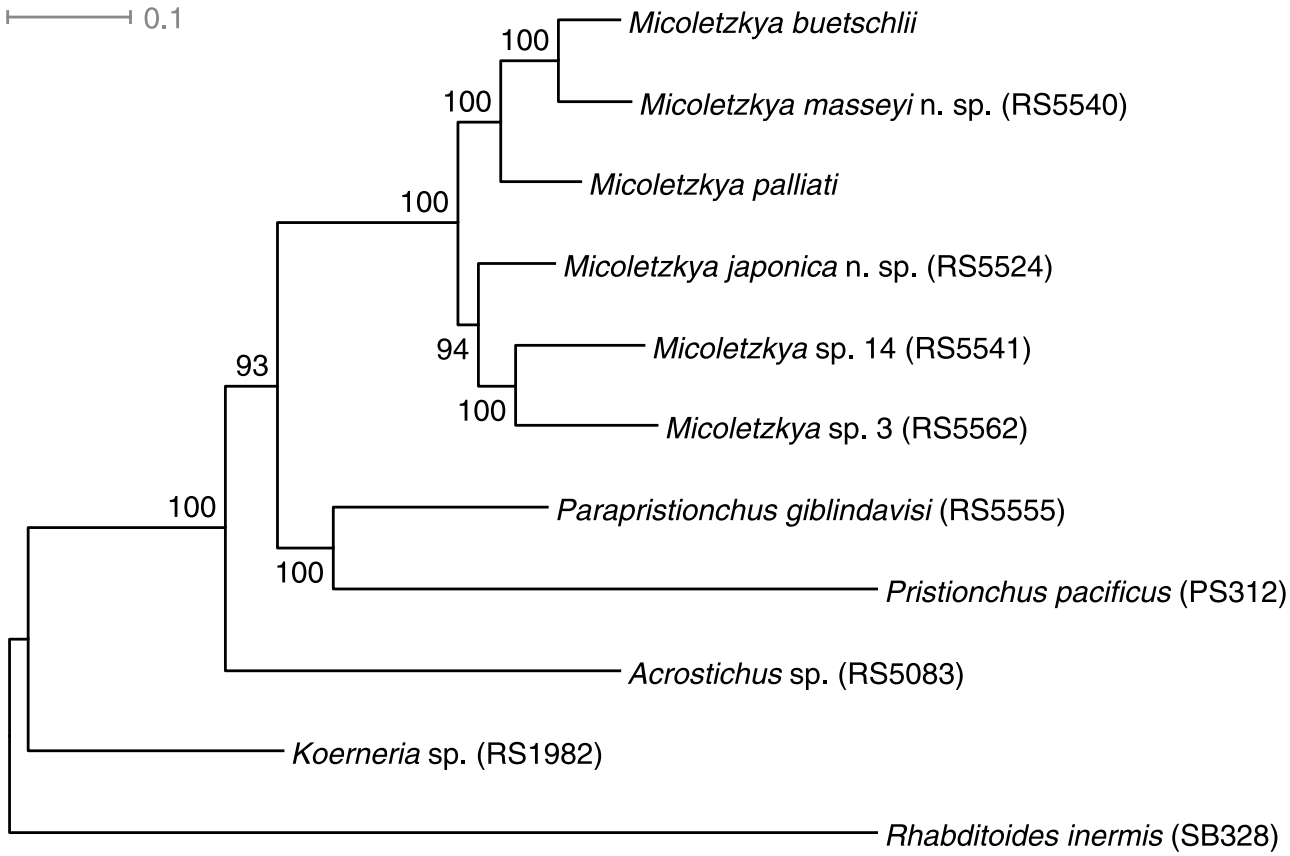

Fig. 5. Bayesian tree of Diplogastridae species rooted with *Rhabditoides inermis* as outgroup. Phylogeny was inferred from 6030 bp of concatenated alignment of COI, 18S rRNA, 28S rRNA, *rpl-2*, and *rpl-9*. Posterior probabilities are indicated at nodes.

masseyi n. sp. and *M. japonica* n. sp., only stenostomatous males and females were observed when grown under standard conditions with sufficient food supply. Eurystomatous females were observed from about 4-week-old cultures, when bacterial food was apparently exhausted. Eurystomatous females show typical characters such as a broad buccal cavity with a large dorsal tooth, a prominent subventral tooth, and conspicuous denticles on the left subventral side. Differences between the two mouth forms appear to be mostly quantitative, such that in stenostomatous worms the buccal cavity is narrow and all denticles are small. This is in contrast to the qualitative dimorphism of *Pristionchus pacificus*, in which the stenostomatous form completely lacks a tooth on the right subventral side (Fürst von Lieven & Sudhaus, 2000). Additionally, eury- and stenostomatous animals of both *Micoletzkya* species show previously unreported differences in pharynx size and relative position of the excretory pore (in heat-inactivated worms) such that in stenostomatous specimens the pharynx is smaller and excretory pore positioned near the end of, or posterior to, the terminal bulb, whereas in eurystomatous animals the pharynx is bigger and the pore is at the anterior part of the terminal bulb.

A characteristic arrangement of labial papillae was observed in the stenostomatous form of both *Micoletzkya* species described here and in *M. palliati* (Rühm, 1956), namely the subdorsal and subventral papillae being located closer to the mouth opening than the lateral papillae (Fig. 6). When we examined previously published SEMs and our unpublished observations of rhabditids and diplogastrids, this, or a similar arrangement, was found only in some diplogastrids: *Acrostichus* spp. (Kanzaki *et al.*, 2009b, 2010a, b), *Pristionchus* spp. (Kanzaki *et al.*, 2012a) and *Diplogastrellus metamasius* (Kanzaki *et al.*, 2008). *Rhabditolaimus* sp. showed a similar pattern, albeit not clear in this case (Susoy *et al.*, unpubl. obs.). On the other hand, all six labial papillae are located at the same distance from the stomatal opening in *Para-*

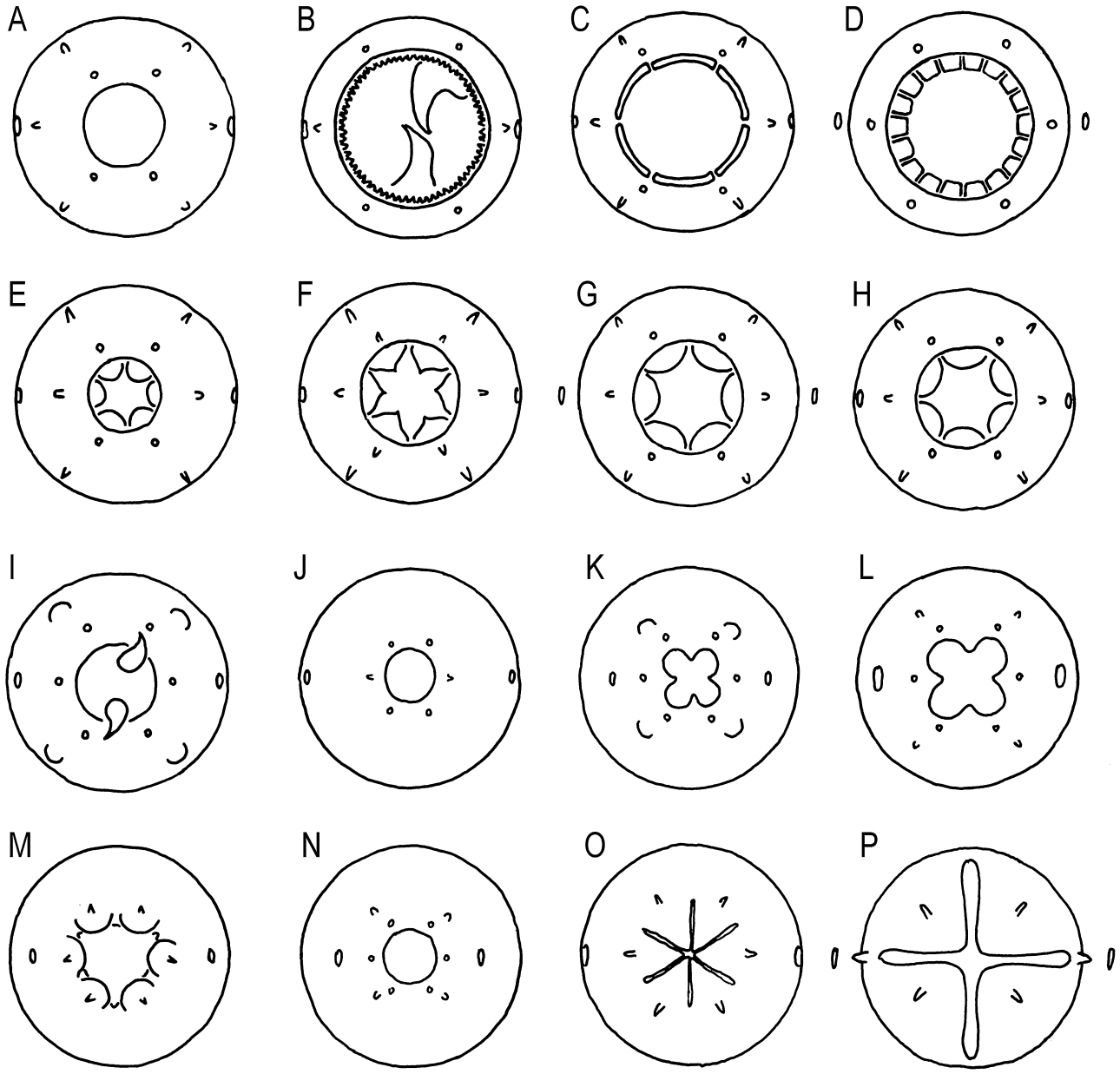

Fig. 6. Schematic drawing of *en face* view of several diplogastrids and rhabditids. A: *Micoletzkya* spp. stenostomatous male; B: *Micoletzkya* spp. eurystomatous female; C: *Acrostichus puri* stenostomatous male; D: *Acrostichus puri* eurystomatous female; E: *Acrostichus rhynchophori* stenostomatous male; F: *Acrostichus megaloptae* stenostomatous male; G: *Diplogastrellus metamasius* male; H: *Pristionchus pacificus* species complex stenostomatous male; I: *Parasitodiplogaster laevigatae* male; J: *Rhabditolaimus* sp. (RS5514) female; K: *Rhabditolaimus* sp. (RS5514) male; L: *Rhabditolaimus anoplophorae* male; M: Generalised rhabditid (*Caenorhabditis elegans*); N: *Halicephalobus mephisto*; O: *Poikilolaimus floridensis*; P: *Poikilolaimus carsiops*.

sitodiplogaster laevigatae (Giblin-Davis *et al.*, 2006), two species of *Rhabditidoides* spp. (Kanzaki, unpubl. obs.; Susoy *et al.*, unpubl. obs.), *C. elegans* (Ward, 1975), *Halicephalobus mephisto* Borgonie, García-Moyano, Litthauer, Bert, Bester, van Heerden, Möller, Erasmus & Onstott, 2011 and *Poikilolaimus floridensis* Kanzaki, Giblin-

Davis, Scheffrahn & Center, 2009 (Kanzaki *et al.*, 2009a). Although lateral papillae of *Poikilolaimus carsiops* Kanzaki, Li & Giblin-Davis, 2011 are relatively far posterior, this is probably due to degradation of the lateral lips (Kanzaki *et al.*, 2011b). Sensilla ultrastructure of papillae as studied in *C. elegans*, shows, however, connectivity differences between inner labial lateral neurons and inner labial quadrant neurons, suggesting different functions for the quadrant and lateral sensilla (White *et al*., 1986).

The arrangement observed in *Micoletzkya* spp., which is very conspicuous even compared to that of other diplogastrid genera, is, based on present evidence, considered to be an apomorphy of the genus. All three examined *Micoletzkya* spp., belonging to separate subclades, have this character in common. Close observation of more species and genera in diplogastrids will be necessary to properly map the character of labial papillae arrangement. Nevertheless, present analysis suggests that this character, which has hitherto not received attention, will be taxonomically useful with respect to related genera.

Micoletzkya species form a monophyletic group within the Diplogastridae. These nematodes are known to live in symbiosis with bark beetles and closely related beetles in the Curculionidae. The association seems to be very specific and obligatory for the nematodes. 24 out of 25 nominal species now included in *Micoletzkya* were isolated directly from the wood-boring weevils or from their breeding galleries. One species, *M. chinaae* Huang *et al*., 2010, was isolated from the xylem of dead pine. There is no report of *Micoletzkya* found in any other habitat. The question of whether *Micoletzkya* nematodes are host-specific and codiverged together with their beetle hosts, however, is still elusive. While Rühm (1956) insisted on a high degree of host-specificity of *Micoletzkya* species, other authors reported the same nematode species being associated with a few beetle hosts that belong to unrelated lineages within Scolytidae (Massey, 1974; Blinova & Vosilite, 1978). Lack of morphological characters useful for species delineation in Diplogastridae has already been pointed out by several authors (Blinova & Vosilite, 1978; Herrmann *et al*., 2006a; Kanzaki *et al*., 2012c). Along with incompleteness and incorrectness of some *Micoletzkya* descriptions, such a paucity of characters could have resulted in some cryptic species not being recognised or some species currently included in the genus being synonymous. A molecular barcoding approach, complemented by mating tests between closely related nematode isolates, may help to reveal the true diversity of the group, as has been possible for *Pristionchus* (Herrmann *et al*., 2006b; Kanzaki *et al*., 2012a). Moreover, further development of a robust phylogenetic framework will give insight into the evolutionary history and mechanisms driving speciation within *Micoletzkya*.

Micoletzkya spp. are specialised to inhabit bark beetle galleries and many of them fail to be permanently kept in laboratory culture (Rühm, 1956; Susoy & Herrmann, unpubl. obs.). The ability readily to culture *M. masseyi* n. sp. and *M. japonica* n. sp. on a monoxenic bacterial food source, together with their relatively short generation times of 10 and 7 days, respectively, make them useful for studying various aspects of nematode-insect interactions. For example, regulation of developmental switches such as dauer entry and dauer exit, processes linked to the infective stages of some parasitic nematodes (Sommer & Ogawa, 2011), is of particular interest as it might play an important role in synchronising life history of the nematodes with that of their beetle hosts. Several bark beetle species also can be successfully cultured under laboratory conditions. Many have short generation times and are known to have *Micoletzkya* symbionts (for example, *Ips* spp.) allowing for *in situ* studies of nematode-beetle ecology.

Acknowledgements

We thank Erik Ragsdale for valuable comments on the manuscript and great nematological discussions, Heike Haussmann for strain freezing, Jürgen Berger for help with SEM, Mary Reid for sending bark beetles and Ai Shimizu, University of Tokyo, for nematode strains and insect material.

References

Andrássy, I. (1984). *Klasse Nematoda (Ordnungen Monhysterida, Desmoscolecida, Araeolaimida, Chromadorida, Rhabditida)*. Stuttgart, Germany, Gustav Fischer Verlag.

Blinova, S.L. & Vosilite, B.S. (1978). An ecologo-morphological study of the nematode *Mikoletzkya sexdentati* n. sp. (Diplogasteridae) and a taxonomic analysis of the genus *Mikoletzkya* Weingaertner, 1955. *Trudy Gel'mintologicheskoi Laboratorii* 28, 58-67.

Borgonie, G., García-Moyano, A., Litthauer, D., Bert, W., Bester, A., van Heerden, E., Möller, C., Erasmus, M. & Onstott, T.C. (2011). Nematoda from the terrestrial deep subsurface of South Africa. *Nature* 474, 79-82.

Chomczynski, P. & Sacchi, N. (1987). Single-step method of RNA isolation by acid guanidinium thiocyanate-phenol-

chlrophorm extraction. *Analytical Biochemistry* 162, 156-159.

Edgar, R.C. (2004). MUSCLE: multiple sequence alignment with high accuracy and high throughput. *Nucleic Acids Research* 32, 1792-1797.

Eyualem, A. & Blaxter, M. (2003). Comparison of biological, molecular, and morphological methods of species identification in a set of cultured *Panagrolaimus* isolates. *Journal of Nematology* 35, 119-128.

Fuchs, G. (1915). Die Naturgeschichte der Nematoden und einiger anderer Parasiten: 1. des *Ips typographus* L. 2. des *Hylobius abietis* L. *Zoologische Jahrbücher* 38, 109-222.

Fürst von Lieven, A. & Sudhaus, W. (2000). Comparative and functional morphology of the buccal cavity of Diplogastrina (Nematoda) and a first outline of the phylogeny of this taxon. *Journal of Zoological Systematics and Evolutionary Research* 38, 37-63.

Giblin-Davis, R.M., Ye, W., Kanzaki, N., Williams, D., Morris, K. & Thomas, W.K. (2006). Stomatal ultrastructure, molecular phylogeny, and description of *Parasitodiplogaster laevigata* n. sp. (Nematoda: Diplogastridae), a parasite of fig wasps. *Journal of Nematology* 38, 137-149.

Herrmann, M., Mayer, W.E. & Sommer, R.J. (2006a). Nematodes of the genus *Pristionchus* are closely associated with scarab beetles and the Colorado potato beetle in Western Europe. *Zoology* 109, 96-108.

Herrmann, M., Mayer, W.E. & Sommer, R.J. (2006b). Sex, bugs and Haldane's rule: the nematode genus *Pristionchus* in the United States. *Frontiers in Zoology* 3, 14.

Hooper, D.J. (1986). Handling, fixing, staining and mounting nematodes. In: Southey, J.F. (Ed.). *Laboratory methods for work with plant and soil nematodes*. London, UK, Her Majesty's Stationery Office, pp. 59-80.

Huang, R., Liang, J., Lu, Q. & Zhang, X. (2010). *Micoletzkya chinaae* n. sp. (Nematoda: Diplogastridae), a potential predacious nematode and *Ektaphelenchus macrobulbosus* (Nematoda: Ektaphelenchinae) isolated from Simao pine in Southwestern China. *Journal of Nematology* 42, 298-306.

Huelsenbeck, J.P. & Ronquist, F. (2001). MRBAYES: Bayesian inference of phylogenetic trees. *Bioinformatics* 17, 754-755.

Kanzaki, N., Giblin-Davis, R.M., Zeng, Y., Ye, W. & Center, B.J. (2008). *Diplogastrellus metamasius* n. sp. (Rhabditida: Diplogastridae) isolated from *Metamasius hemipterus* (Olivier) (Coleoptera: Dryophthoridae) in southern Florida and Costa Rica. *Nematology* 10, 853-868.

Kanzaki, N., Giblin-Davis, R.M., Scheffrahn, R.H. & Center, B.J. (2009a). *Poikilolaimus floridensis* n. sp. (Rhabditida: Rhabditidae) associated with termite (Kalotermitidae). *Nematology* 11, 203-216.

Kanzaki, N., Giblin-Davis, R.M., Zeng, Y., Ye, W. & Center, B.J. (2009b). *Acrostichus rhynchophori* n. sp. (Rhabditida: Diplogastridae): a phoretic associate of *Rhynchophorus cruentatus* Fabricius and *R. palmarum* L. (Coleoptera: Curculionidae) in the Americas. *Nematology* 11, 669-688.

Kanzaki, N., Giblin-Davis, R.M., Zeng, Y., Ye, W., Center, B.J. & Thomas, W.K. (2010a). *Acrostichus puri* n. sp. (Nematoda: Diplogastridae), a phoretic associate of *Augochlora pura mosieri* Cockerell (Hymenoptera: Halictidae). *Nematology* 12, 49-64.

Kanzaki, N., Giblin-Davis, R.M., Wcislo, W.T., Zeng, Y., Ye, W., Center, B.J., Esquivel, A. & Thomas, W.K. (2010b). *Acrostichus megaloptae* n. sp. (Nematoda: Diplogastridae), a phoretic associate of *Megalopta* spp. (Hymenoptera: Halictidae) in Central America. *Nematology* 12, 453-468.

Kanzaki, N., Taki, H., Masuya, H., Okabe, K., Tanaka, R. & Abe, F. (2011a). Diversity of stag beetle-associated nematodes in Japan. *Environmental Entomology* 40, 281-288.

Kanzaki, N., Li, H.-F., Lan, Y.-C., Kosaka, H., Giblin-Davis, R.M. & Center, B.J. (2011b). *Poikilolaimus carsiops* n. sp. (Rhabditida: Rhabditidae) associated with *Neotermes koshunensis* (Kalotermitidae) in Kenting National Park, Taiwan. *Nematology* 13, 155-164.

Kanzaki, N., Ragsdale, E.J., Herrmann, M., Mayer, W.E. & Sommer, R.J. (2012a). Description of three *Pristionchus* species (Nematoda: Diplogastridae) from Japan that form a cryptic species complex with the model organism *P. pacificus*. *Zoological Science*, in press.

Kanzaki, N., Ragsdale, E.J., Herrmann, M., Mayer, W.E., Tanaka, R. & Sommer, R.J. (2012b). *Parapristionchus giblindavisi* n. gen., n. sp. (Rhabditida: Diplogastridae) isolated from stag beetles (Coleoptera: Lucanidae) in Japan. *Nematology* 14, 933-947.

Kanzaki, N., Ragsdale, E.J., Herrmann, M. & Sommer, R.J. (2012c). Two new species of *Pristionchus* (Rhabditida: Diplogastridae): *Pristionchus fissidentatus* n. sp. from Nepal and La Réunion Island and *Pristionchus elegans* n. sp. from Japan. *Journal of Nematology* 44, 80-90.

Kiontke, K., Gavin, N.P., Raynes, Y., Roehrig, C., Piano, F. & Fitch, D.H.A. (2004). *Caenorhabditis* phylogeny predicts convergence of hermaphroditism and extensive intron loss. *Proceedings of the National Academy of Sciences of the United States of America* 101, 9003-9008.

Kiontke, K., Barriere, A., Kolotuev, I., Podbilewicz, B., Sommer, R., Fitch, D.H.A. & Felix, M.A. (2007). Trends, stasis, and drift in the evolution of nematode vulva development. *Current Biology* 17, 1925-1937.

Körner, H. (1954). Die Nematodenfauna des vergehenden Holzes und ihre Beziehungen zu den Insekten. *Zoologische Jahrbücher (Systematik)* 82, 245-353.

Kreis, H.A. (1932). Beiträge zur Kenntnis pflanzenparasitischer Nematoden. *Zeitschrift für Parasitenkunde* 5, 184-194.

Massey, C.L. (1960). Nematode parasites and associates of the California five-spined engraver, *Ips confusus* (Lee). *Proceedings of the Helminthological Society of Washington* 27, 14-22.

Massey, C.L. (1966). Genus *Mikoletzkya* (Nematoda) in the United States. *Proceedings of the Helminthological Society of Washington* 33, 13-19.

Massey, C.L. (1974). *Biology and taxonomy of nematodes parasites and associates of bark beetles in the United States*, Agricultural Handbook 446. Washington, US Department Agricultural Forestry Service.

Mayer, W.E., Herrmann, M. & Sommer, R.J. (2007). Phylogeny of the nematode genus *Pristionchus* and implications for biodiversity, biogeography and the evolution of hermaphroditism. *BMC Evolutionary Biology* 7, 1-13.

Mayer, W.E., Herrmann, M. & Sommer, R.J. (2009). Molecular phylogeny of beetle associated diplogastrid nematodes suggests host switching rather than nematode-beetle coevolution. *BMC Evolutionary Biology* 9, 212-222.

Meyl, A.H. (1960). Die freilebenden Erd- und Süßwassernematoden (Fadenwürmer). In: Brohmer, P., Ehrmann, P. & Ulmer, G. (Eds). *Die Tierwelt Mitteleuropas*, 1 (5a). Leipzig, Germany, Quelle & Meyer.

Poinar Jr, G.O. (1975). *Entomogenous nematodes, a manual and host list of insect-nematode associations*. Leiden, The Netherlands, Brill.

Rahm, G. (1928). Alguns Nematodes parasitas e semi-parasitas das plantas culturães do Brasil. *Archivos do Instituto Biológico São Paulo* 1, 239-251.

Rühm, W. (1956). Die Nematoden der Ipiden. *Parasitologische Schriftenreihe* 6, 1-437.

Rühm, W. (1965). Zur "Wirtskreiserweiterung" einer mit Borkenkäfern (Scolytoidea, Col.) vergesellschafteten Nematodenart. *Zeitschrift für Parasitenkunde* 26, 230-253.

Ryss, A.Y. (2003). Express technique to prepare permanent collection slides of nematodes. *Zooystematica Rossica* 11, 257-260.

Sachs, H. (1950). Die Nematodenfauna der Rinderexkremente. Eine Ökologisch-systematische Studie. *Zoologische Jahrbücher (Systematik)* 79, 209-272.

Sommer, R.J. & Ogawa, A. (2011). Hormone signaling and phenotypic plasticity in nematode development and evolution. *Current Biology* 21, R758-R766.

Sommer, R.J., Carta, L.K., Kim, S.Y. & Sternberg, P.W. (1996). Morphological, genetic and molecular description of *Pristionchus pacificus* sp. n. (Nematoda: Neodiplogastridae). *Fundamental and Applied Nematology* 19, 511-521.

Sudhaus, W. & Fürst von Lieven, A. (2003). A phylogenetic classification and catalogue of the Diplogastridae (Secernentea, Nematoda). *Journal of Nematode Morphology and Systematics* 6, 43-89.

Susoy, V. & Herrmann, M. (2012). Validation of *Rhabditolaimus* Fuchs, 1914 (Nematoda: Diplogastridae) supported by integrative taxonomic evidence. *Nematology* 14, 595-604.

Tamura, K., Dudley, J., Nei, M. & Kumar, S. (2007). MEGA4: Molecular evolutionary genetics analysis (MEGA) software version 4.0. *Molecular Biology and Evolution* 24, 1596-1599.

Vosilite, B. (1990). A new nematode species, *Diplogasteroides sexdentati* sp. n., and some biological data on the ectonematodes of the stenograph bark beetle. In: Sonin, M. (Ed.). *Helminths of insects*. Leiden, New York, København, Köln, pp. 27-36.

Ward, S., Thomson, N., White, J.G. & Brenner, S. (1975). Electron microscopical reconstruction of the anterior sensory anatomy of the nematode *Caenorhabditis elegans*. *Journal of Comparative Neurology* 160, 313-337.

White, J.G., Southgate, E., Thomson, J.N. & Brenner, S. (1986). The structure of the nervous system of the nematode *Caenorhabditis elegans*. *Philosophical Transactions of the Royal Society of London B* 314, 1-340.

Weingärtner, I. (1955). Versuch einer Neuordnung der Gattung Diplogaster Schulze 1857 (Nematoda). *Zoologische Jahrbuecher (Systematik)* 83, 248-317.

Nematology, 2012, Vol. 14(5), 595-604

Validation of *Rhabditolaimus* Fuchs, 1914 (Nematoda: Diplogastridae) supported by integrative taxonomic evidence

Vladislav SUSOY and Matthias HERRMANN *

Max Planck Institute for Developmental Biology, Department Evolutionary Biology, Spemannstr. 37-39, 72076 Tübingen, Germany

Received: 12 August 2011; revised: 15 November 2011
Accepted for publication: 15 November 2011; available online: 23 February 2012

Summary – *Rhabditolaimus leuckarti*, type species of *Rhabditolaimus*, was isolated from its type host, *Hylobius abietis* (Coleoptera: Curculionidae), at several locations in central Europe. The position of the species among other diplogastrid nematodes was revised using morphological characters and molecular phylogenetic analysis. The revealed common apomorphic features and the inferred evolutionary tree strongly indicates a close relationship between *R. leuckarti* and *Myctolaimus*. Our findings suggest that the historical classifications do not reflect the natural relationships of some diplogastrid taxa. Therefore, we reject all previous synonymisations of *Rhabditolaimus* and consider it to be valid within the Diplogastridae. Five species are transferred from *Diplogasteroides* to *Rhabditolaimus*. *Myctolaimus sensu lato* is regarded as a junior synonym of *Rhabditolaimus* and the following new combinations are proposed: *R. anoplophorae* comb. n., *R. carolinensis* comb. n., *R. curzii* comb. n., *R. dendrophilus* comb. n., *R. erectus* comb. n., *R. goodeyi* comb. n., *R. inevectus*, comb. n., *R. kishtwarensis* comb. n., *R. macrolaimus* comb. n., *R. nacogdochensis* comb. n., *R. neolongistoma* comb. n., *R. pellucidus* comb. n., *R. platypi* comb. n., *R. rifflei* comb. n., *R. robiniae* comb. n., *R. ulmi* comb. n., *R. vitautasi* comb. n., *R. walkeri* comb. n. and *R. zamithi* comb. n.

Keywords – *Cylindrocorpus* syn. nov., *Diplogasteroides*, *Goodeyus* syn. nov., molecular, *Myctolaimellus* syn. nov., *Myctolaimus* syn. nov., new combination, new synonymy, phylogeny, *Protocylindrocorpus* syn. nov., *Rhabditolaimus leuckarti*, taxonomy.

The Diplogastridae (Nematoda: Secernentea) is known to have insect associations of many kinds, for example *Parasitodiplogaster* spp. with fig wasps (Giblin-Davis *et al*., 2006), *Micoletzkya* spp. with bark beetles (Rühm, 1956), and *Pristionchus* spp. with scarab beetles (Herrmann *et al*., 2006a, b).

There is an ongoing debate on the number of accepted genera and nomenclature of the Diplogastridae. Andrássy (1984) listed 42 genera in eight families and three superfamilies. Sudhaus and Fürst von Lieven (2003) published a catalogue of Diplogastridae synonymising many names and considered 28 genera with 312 species to be valid. Several studies show good agreement between molecular and morphological phylogenies (Mayer *et al*., 2009; Kiontke & Fitch, 2010) and we generally accept the taxonomical view and nomenclature of Sudhaus and Fürst von Lieven (2003).

However, Sudhaus and Fürst von Lieven (2003) were unable to show apomorphies for several diplogastrid genera, namely *Diplogasteroides* de Man, 1912, *Diplogastrellus* Paramonov, 1952, *Fictor* Paramonov, 1952, *Mononchoides* Rahm, 1928, and *Pseudodiplogasteroides* Körner, 1954, suggesting these genera might be paraphyletic and should therefore be studied in greater detail.

Diplogasteroides (*sensu* Sudhaus & Fürst von Lieven, 2003) is the second largest of these genera in doubt, with 27 described species. *Diplogasteroides* (= *Rhabditolaimus*) *leuckarti* (Fuchs, 1914) Rühm, 1956 has been isolated several times by different investigators, always from the same beetle species, the weevil *Hylobius abietis* (L., 1758). It had been described as *Rhabditolaimus leuckarti* by Fuchs (1914) and was then erroneously synonymised with *Dirhabdilaimus* Paramonov & Turlygina, 1955 by Paramonov and Turlygina (1955) and later with *Diplogasteroides* by Rühm (1956). Sudhaus and Fürst von

* Corresponding author, e-mail: matthias.herrmann@tuebingen.mpg.de

© *Koninklijke Brill NV, Leiden, 2012*
DOI:10.1163/156854111X617419

Lieven (2003) accepted this, while Andrássy (1984) considered *Rhabditolaimus* to be valid and listed two other species, *R. pini* Fuchs, 1931 and *R. picei* Fuchs, 1931, as belonging to the same genus.

As part of a long-term screen for new strains and species of diplogastrids we have investigated nematodes of wood-inhabiting insects. Screening *H. abietis* from different locations we consistently isolated the same nematode species. Comparing the strains from the different locations with each other and with the original description of *R. leuckarti* (Fuchs, 1914, 1915) it became evident that we had re-isolated the species. Some morphological features apparent in our isolate cast doubt on the placement of *R. leuckarti* in *Diplogasteroides*. Specimens had a very long gymnostom and an enlarged muscular procorpus, which are characters circumscribing the genus *Myctolaimus* (*sensu* Sudhaus & Lieven, 2003). As a further test of its identity we used molecular markers to infer its phylogenetic position.

Materials and methods

Beetles and nematode isolates

Adult individuals of *H. abietis* were collected from four localities in Germany (Göttingen, Kiebingen, Tübingen, Ülzen) and from Völkermarkt, Austria, during 2010-2011 (Table 1). The beetles were transferred alive to the laboratory, killed, and individually placed on nematode growth medium (NGM) agar plates. The samples were left to develop at room temperature for several days and screened at least three times for the presence of adult nematodes. Isogenic lines of emerging nematodes were produced by transferring single gravid females on to new plates seeded with *Escherichia coli* strain OP50. Selected isolates were maintained as laboratory cultures. From one isolate a reference strain was generated which also was preserved in liquid nitrogen according to the protocol described by Herrmann *et al*. (2006a).

Morphological identification and morphometrics

For morphological observation, nematodes were placed on microscope slides covered with a thin agar layer and inactivated with sodium azide. Measurements were taken using a Zeiss Axio Imager Z1 light microscope equipped with Nomarski optics and MetaMorph imaging software.

Molecular analysis and phylogenetic reconstruction

Genomic DNA was prepared from individual nematodes. For initial molecular typing of isolates, a *ca* 900 bp fragment of SSU was amplified by PCR and sequenced using primers listed by Herrmann *et al*. (2006a). For phylogenetic analysis, we additionally sequenced a second portion of 800 bp SSU using forward primer SSUF2 GC GAAAGCATTTGCCAAGA and reverse primer SSUR2 GGTTCAAGCCACTGCGAT and a 950 bp fragment of LSU with forward primer LSUF1 ACAAGTACCGT GAGGGAAAGTTG and reverse primer LSUR1 GGT GAGTTGTTACACACTCCTTAG. Nucleotide sequences determined for this study were deposited in the GenBank database under accession numbers JQ005865-JQ005869 for the SSU and JQ005870-JQ005874 for the LSU.

The sequences were assembled in the SeqMan Pro 7.2.2 (DNASTAR) program and aligned using ClustalX 2.0.12 (Larkin *et al*., 2007). Ambiguous regions were manually removed from the alignment. For phylogenetic analysis, LSU and SSU sequences were combined into a single dataset. Selection of an appropriate nucleotide substitution model and phylogeny reconstruction was done with the help of MEGA 5.01 software (Tamura *et al*., 2007). The tree was inferred by a heuristic search under the maximum likelihood (ML) criterion. To evaluate support for tree nodes, we performed 1000 pseudoreplicates of non-parametric bootstrap analysis.

Table 1. *Beetle and nematode collection data.*

Locality	Date	No. of *Hylobius abietis* examined	No. of beetles positive for *Rhabditolaimus leuckarti*
Göttingen, Germany	28/6/2010	10	2
Ülzen, Germany	2/8/2010	14	0
Kiebingen, Germany	26/4/2011; 24/5/2011	2	1
Völkermarkt, Austria	1/6/2011	46	18
Tübingen, Germany	7/6/2011; 26/6/2011	2	0

Results

To re-isolate *R. leuckarti*, we examined 74 specimens of its type host, *H. abietis*. Of those, 21 beetles from three different localities (Göttingen, Kiebingen, Völkermarkt) yielded diplogastrid nematodes that morphologically matched the descriptions of *R. leuckarti* by Fuchs (1915) and Rühm (1956). The identity of obtained isolates was confirmed by comparative analysis of 400 bp of the SSU fragment, which had been shown previously to be a useful marker for species delineation in *Pristionchus* Kreis, 1932 (Herrmann *et al*., 2006b). Strains of all locations were identical in their molecular sequences. The average observed infestation rate was 28%. The actual infestation rate, however, might be higher, as we only counted beetles as positive when dauer recovery was observed and adult nematodes developed on the plate. We chose one nematode isolate from Göttingen, Germany, to be a reference strain with the designated strain number RS5525.

Comparison of morphometric characters between individuals of the generated reference strain and the species described by Fuchs and re-described by Rühm did not reveal any major discrepancies (see Table 2; Fig. 1A, B).

To determine the molecular phylogenetic position of the *R. leuckarti* strain RS5525, its partial SSU and LSU sequences were obtained and aligned together with those of *Diplogasteroides magnus* (Völk, 1950) Weingärtner, 1953 (RS1983), *Diplogasteroides* sp. RS544, *Myctolaimus ulmi* (T. Goodey, 1930) Sudhaus & Fürst von Lieven, 2003 (PDL20), *Myctolaimus* sp. RGD808, *Myctolaimus* sp. RS5514, *Myctolaimus* sp. RSA134, *Koerneria* sp. SB110, and *Rhabditoides inermis* (Schneider, 1866) Dougherty, 1955 (see Table 3). An ML tree was inferred from a final dataset of 1999 nucleotides. The GTR + Γ model was selected with a shape parameter set to 0.46. The tree was rooted with *R. inermis* as the outgroup, as suggested by Kiontke *et al*. (2007).

The analysis yielded a well resolved and robust evolutionary tree of the selected diplogastrid strains (Fig. 2). Five out of six clades were recovered in over 95% of bootstrap pseudoreplicates. Three major branches could be discriminated. First, *Myctolaimus* spp. RGD808, RS5514 and RSA134, *M. ulmi* (PDL20) and *R. leuckarti* (RS5525) form a monophyletic clade with a bootstrap value of 100%. Second, *D. magnus* (RS1983) and *Diplogasteroides* sp. RS544 cluster together and formed a phylogenetically well separated sister group. A third branch includes *Koerneria* sp. SB110, which shows a basal position to all diplogastrid nematodes included in the analysis, which was consistent with a previous study by Mayer *et al*. (2009).

Discussion

Molecular phylogenetic reconstruction distinctly shows that *R. leuckarti* is not closely related to the two investigated members of *Diplogasteroides*. Instead, it is found in a group of *Myctolaimus* species that form a separate monophyletic clade.

Morphological evidence also suggests a close relationship of *R. leuckarti* and *Myctolaimus*. We found clear anatomical similarities between these two taxa in stoma and pharynx morphology. As already emphasised by several authors (*e.g*., Fuchs, 1915, 1931; Rühm, 1956; Andrássy, 1984, 2005), *R. leuckarti* has: *i*) a very long and narrow tube-shaped gymnostom, which is nine times as long as its diameter; and *ii*) a wide, muscular pharyngeal procorpus. Thus it shares all common apomorphic features of *Myctolaimus* given by Sudhaus and Fürst von Lieven (2003). However, the gymnostom is only one-fifth

Table 2. *Species names and GenBank accession numbers.*

Species	SSU	LSU
Rhabditolaimus leuckarti (RS5525)	JQ005865	JQ005870
Myctolaimus sp. RS5514	JQ005866	JQ005871
Myctolaimus sp. RSA134	JQ005867	JQ005872
Myctolaimus sp. RGD808	AB478635	AB478636
Myctolaimus ulmi (PDL20)	EU196024	EU195998
Diplogasteroides sp. RS5444	JQ005868	JQ005873
Diplogasteroides magnus (RS1983)	JQ005869	JQ005874
Koerneria sp. SB110	EU196025	EU195999
Rhabditoides inermis (DF5001, SB328)	AF082996	EU195981

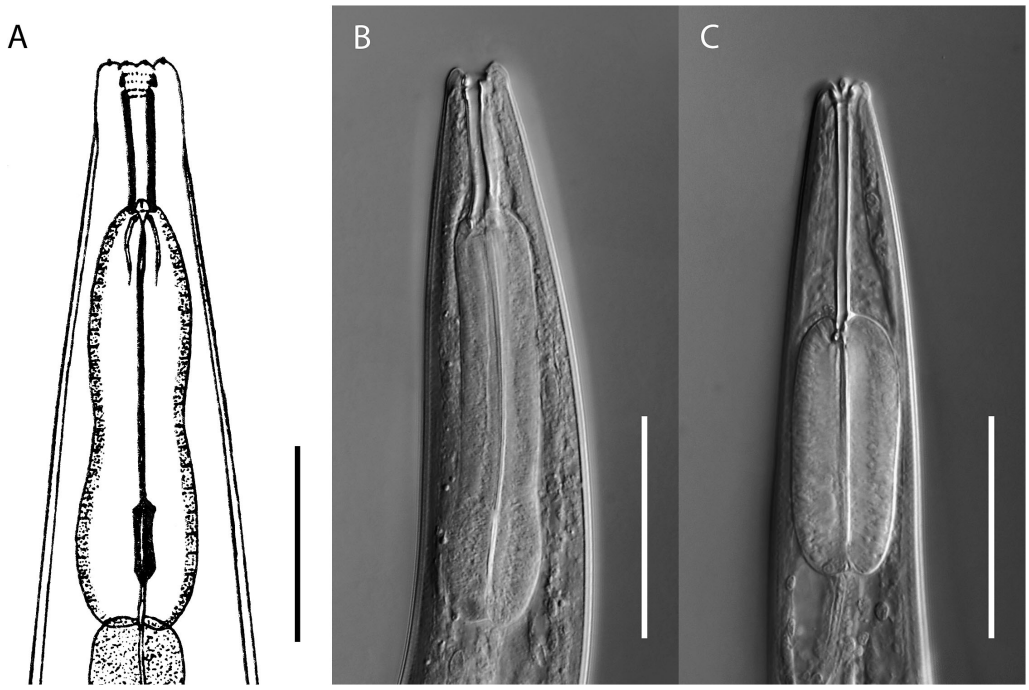

Fig. 1. *A: Anterior region of* Rhabditolaimus leuckarti *in Rühm (1956). B:* Rhabditolaimus leuckarti *strain RS5525; C:* Myctolaimus *sp. (RS5514); Note that* Myctolaimus *strain RS5514 has an anterior morphology that is characteristic for* Myctolaimus*, being genetically closely related to* R. leuckarti*. (Scale bars = 40 μm.)*

of the pharynx length instead of one-fourth as in *Myctolaimus*. Furthermore, the procorpus is not as short and strongly developed as is typical for *Myctolaimus* nematodes. We assume that this could be the reason why none of the historical classifications suggested a close relationship between *R. leuckarti* and *Myctolaimus*. The main differentiating characters for *Myctolaimus* were quantitative and appeared to vary a lot even among closely related nematode lineages (Fig. 1B, C). Whereas *R. leuckarti* has a stoma/corpus/postcorpus ratio of *ca* 1 : 2.5 : 2, the very closely related strain *Myctolaimus* sp. (RS5514) has a ratio of *ca* 1 : 1 : 1.

Based on both morphological and molecular data we conclude that: *i*) *Rhabditolaimus* was erroneously synonymised with *Diplogasteroides* by Rühm (1956) and by Sudhaus and Fürst von Lieven (2003), and therefore *Rhabditolaimus* must be re-erected and regarded as a separate genus within the Diplogastridae with its type species *R. leuckarti*; *ii*) *R. picei*, *R. pini*, *Diplogasteroides* (= *Dirhabdilaimus*) *carolinensis* (Massey, 1967) Sudhaus & Fürst von Lieven, 2003 and *Diplogasteroides* (= *Dirhabdilaimus*) *nacogdochensis* (Massey, 1974) Sudhaus & Fürst von Lieven, 2003, which have a morphology very similar to *R. leuckarti*, should be considered as valid species of *Rhabditolaimus*; and *iii*) *Myctolaimus* in the broad sense (*i.e.*, as in Sudhaus & Fürst von Lieven, 2003) must be regarded as a junior synonym of *Rhabditolaimus*.

We would like to state that, in our opinion, after removing five species the remaining genus, *Diplogasteroides* (*sensu* Sudhaus & Fürst von Lieven, 2003), probably remains polyphyletic and a detailed revision is needed.

We contend that our study demonstrates the power of combining morphological and molecular methods to identify nematode species and to get a more detailed idea about their position in the phylogeny. We would like to encourage nematologists to add molecular markers to their species descriptions whenever possible. Special attention should be on the choice of markers as some of them have already been frequently chosen by other nematologists and have proven to be informative (such as the full length SSU and to a minor extent LSU). Only with commonly used markers will it be possible to obtain sequences of other species from databanks.

Table 3. *Comparison of morphometric characters of* Rhabditolaimus leuckarti *and sodium azide inactivated specimens of RS5525. All measurements are in μm and in the form: (range) or mean ± s.d. (range).*

Character	*Rhabditolaimus leuckart* (*apud* Rühm, 1956)		*Rhabditolaimus leuckart* RS5525	
	Female	Male	Female	Male
n	n/a	n/a	10	10
L	(870-1260)	(825-1210)	1325 ± 137 (1069-1599)	991 ± 71 (845-1090)
L′	–	–	1223 ± 130 (980-1485)	948 ± 72 (798-1041)
a	(19.1-21.1)	(18.3-21.6)	22.1 ± 1.3 (20.5-24.2)	21.3 ± 1.0 (20.2-23.0)
b	(6.1-9.2)	(6.2-9.3)	8.7 ± 0.7 (7.2-10.0)	7.1 ± 0.5 (6.2-7.9)
c	(9.2-12.4)	(18.3-24.6)	13.1 ± 0.7 (12.0-14.0)	19.7 ± 2.6 (16.0-23.4)
c′	–	–	12.1 ± 0.7 (11.0-13.0)	18.7 ± 2.6 (15.0-22.4)
V	(49.5-58.6)	–	50.7 ± 1.3 (48.6-52.8)	–
Max. body diam.	(45-60)	(45-56)	60 ± 6.6 (47-67)	47 ± 3.0 (42-53)
Labial diam.	–	–	13.0 ± 1.0 (11.2-14.7)	13.8 ± 1.8 (9.0-15.3)
Stoma length	(35-38)	(30-35)	31.4 ± 2.5 (26.9-34.1)	31.6 ± 2.0 (27.7-34.2)
Stoma diam.	–	–	3.6 ± 0.4 (3.2-4.3)	3.5 ± 0.4 (3.0-4.1)
Pharynx length	(137-144)	(130-133)	152 ± 5.2 (146-161)	140 ± 5.7 (130-150)
Anterior pharynx	–	–	85 ± 3.6 (79-90)	79 ± 3.6 (73-86)
Posterior pharynx	–	–	67 ± 3.2 (63-72)	60 ± 3.2 (56-65)
Post./ant. pharynx ratio	–	–	0.8 ± 0.0 (0.7-0.8)	0.8 ± 0.0 (0.7-0.8)
Median bulb diam.	–	–	24.2 ± 1.6 (21.9-27.5)	20.3 ± 1.5 (18.8-23.7)
Terminal bulb diam.	–	–	15.9 ± 0.8 (15.0-17.4)	12.8 ± 1.9 (8.1-14.7)
Ant. end to nerve ring	–	–	148 ± 6.3 (138-155)	137 ± 7.2 (129-146)
Head to vulva	–	–	671 ± 62 (554-777)	–
Gonad length	–	–	573 ± 97 (373-726)	584 ± 60 (475-715)
Length of anterior gonad branch	–	–	280 ± 50 (164-335)	–
Anterior flexure	–	–	215 ± 47 (113-289)	69 ± 17 (38-88)

Table 3. *(Continued.)*

Character	*Rhabditolaimus leuckart* (*apud* Rühm, 1956)		*Rhabditolaimus leuckart* RS5525	
	Female	Male	Female	Male
Length of posterior gonad branch	–	–	294 ± 54 (209-391)	–
Posterior flexure	–	–	226 ± 40 (150-298)	–
Vulva to anus	(350-420)	–	552 ± 71 (426-708)	–
Anal body diam.	–	–	28.8 ± 2.6 (24.7-32.7)	30.1 ± 2.2 (24.4-32.7)
Rectum length	–	–	33.9 ± 3.9 (29.0-42.7)	38.4 ± 7.3 (27.0-50.0)
Spicule	–	(30-36)	–	31.8 ± 2.2 (28.4-34.4)
Gubernaculum	–	(15-17)	–	15.5 ± 0.7 (14.8-16.8)
Tail length	(88-102)	(46-59)	101 ± 7.5 (89-114)	51 ± 5.3 (45-60)

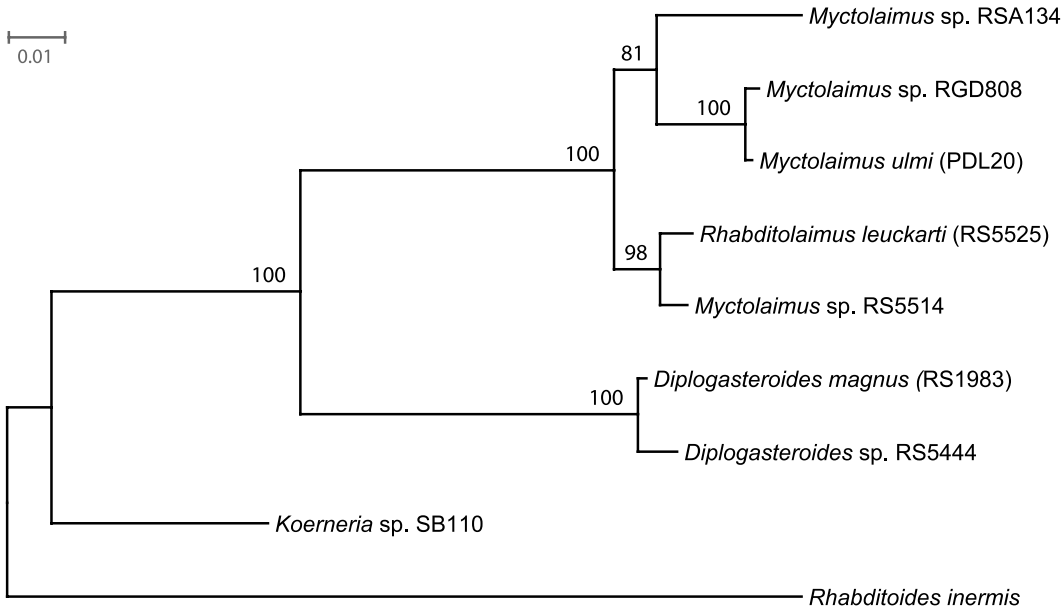

Fig. 2. *Phylogeny of eight strains of Diplogastridae, rooted with* Rhabditoides inermis *as outgroup. Maximum likelihood tree is based on combined dataset of 1999 characters acquired from partial sequences of SSU and LSU. Bootstrap support values are indicated above branches.*

Giving molecular information about nematode species will facilitate identification in the future even for non-experts – even if only eggs or juvenile stages are present. Our work also suggests that careful description of the substrate (duff, frass, decomposing organic matter) can be helpful for identifying otherwise absent insect hosts of collected nematodes. Thus we recommend that the future of the science increasingly takes such an integrative approach.

With the results from this study, *Rhabditolaimus* needs to be re-diagnosed and the valid species listed:

***Rhabditolaimus* Fuchs, 1914**
= *Diplogasteroides* (*Neodiplogasteroides*) de Man, 1912 (Rühm *in* Körner, 1954)
= *Myctolaimus* Cobb, 1920 syn. nov.
= *Cylindrogaster* T. Goodey, 1927 syn. nov. (*nec Cylindrogaster* Stal, 1855)
= *Goodeyus* Chitwood, 1933 syn. nov.
= *Cylindrocorpus* T. Goodey, 1939 syn. nov.
= *Protocylindrocorpus* Rühm, 1959 syn. nov.
= *Dirhabdilaimus* Paramonov & Turlygina, 1955
= *Neodiplogasteroides* Rühm *in* Körner, 1954 (Meyl, 1960)
= *Myctolaimellus* Andrássy, 1984 syn. nov.

Comment

There has been a lot of confusion as to which species is the type for *Rhabditolaimus*. In their 2003 publication, Sudhaus and Fürst von Lieven state "... when Sudhaus (1995) tried to clarify which species is the type for *Rhabditolaimus*, he overlooked that Fuchs (1914: 690) gave an unambiguous bibliographic reference for his new name *Rhabditolaimus leuckarti*: the "Rhabditisform" (Leuckart) described and depicted by Leuckart (1887, figs 9-13) in his paper on *Allantonema mirabile*. Thus, the name *Rhabditolaimus leuckarti* Fuchs, 1914 is valid, contrary to *Rhabditolaimus halleri* published in the same paper without an indication (Fuchs, 1914: 689). Therefore, *Rhabditolaimus* Fuchs, 1914 was monotypic and *R. leuckarti* is its type species". We fully agree with this opinion. In the 1915 paper, however, Fuchs gave additional information about *R. leuckarti* and we also used this publication for re-identification.

Diagnosis (emended)

Diplogastridae. Commonly associated with wood-inhabiting beetles, occasionally found in decomposing organic substances such as dung and compost. Cuticle finely to strongly striated, gymnostom forming a long and narrow tube, at least one-fifth of pharynx length, procorpus strongly developed, broad, vulva equatorial, located at 40-60% of body length.

Type species

Rhabditolaimus leuckarti Fuchs, 1914
= *Diplogaster* (*Fuchsia*) *leuckarti* (Fuchs, 1914) Micoletzky, 1922
= *Dirhabdilaimus leuckarti* (Fuchs, 1914) Paramonov & Turlygina, 1955
= *Diplogasteroides* (*Neodiplogasteroides*) *leuckarti* (Fuchs, 1914) Rühm *in* Körner, 1954
= *Neodiplogasteroides leuckarti* Rühm *in* Körner, 1954 (Meyl, 1960)

Other species

R. anoplophorae (Kanzaki & Futai, 2004) comb. n.
= *Cylindrocorpus anoplophorae* Kanzaki & Futai, 2004
= *Myctolaimus anoplophorae* (Kanzaki & Futai, 2004) Kanzaki, Kobayashi, Nozaki & Futai, 2006 [associated with a male of *Anoplophora malasiaca* (Coleoptera: Cerambycidae), Kyoto, Japan]
R. carolinensis (Massey, 1967) comb. n.
= *Dirhabdilaimus carolinensis* Massey, 1967
= *Diplogasteroides carolinensis* (Massey, 1967) Sudhaus & Fürst von Lieven, 2003 [associated with *Hylobius pales* and *Pachylobius picivorus* (Coleoptera: Curculionidae), Durham, NC, USA]
R. curzii (T. Goodey, 1935) comb. n.
= *Cylindrogaster curzii* T. Goodey, 1935
= *Myctolaimus curzii* (T. Goodey, 1935) Andrássy, 1984 [rotting *Manihot ulilissima* graft, Somalia]
R. dendrophilus (Kinn, 1984) comb. n.
= *Protocylindrocorpus dendrophilus* Kinn, 1984
= *Myctolaimus dendrophilus* (Kinn, 1984) Sudhaus & Fürst von Lieven, 2003 [duff of *Pinus elliottii* with *Platypus flavicornis* (Coleoptera: Platypodidae), Bentley, LA, USA]
R. erectus (Massey, 1960) comb. n.
= *Cylindrocorpus erectus* Massey, 1960
= *Myctolaimus erectus* (Massey, 1960) Andrássy, 1984 [associated with *Scolytus multistriatus* (Coleoptera: Scolytidae) in *Ulmus americana*, Albuquerque, NM, USA and Fort Collins, CO, USA]
R. goodeyi (Rühm, 1959) comb. n.

= *Cylindrocorpus* (*Protocylindrocorpus*) *goodeyi* Rühm, 1959
= *Goodeyus goodeyi* (Rühm, 1959) J.B. Goodey, 1963
= *Protocylindrocorpus goodeyi* Rühm, 1959 (Paramonov, 1964)
= *Myctolaimus goodeyi* (Rühm, 1959) Sudhaus & Fürst von Lieven, 2003 [slime under bark of a *Ceiba petandra* tree, Basel, Switzerland]
R. inevectus (Poinar, Jackson, Bell & Wahid, 2003) comb. n.
= *Cylindrocorpus inevectus* Poinar, Jackson, Bell & Wahid, 2003
= *Myctolaimus inevectus* (Poinar, Jackson, Bell & Wahid, 2003) Kanzaki, Kobayashi, Nozaki & Futai, 2006 [associated with *Elaeidobius kamerunicus* (Coleoptera: Cerambycidae), Baru Bangi, Malaysia]
R. kishtwarensis (Hussain, Tahseen, Khan & Jairajpuri, 2004) comb. n.
= *Myctolaimus kishtwarensis* Hussain, Tahseen, Khan & Jairajpuri, 2004 [slurry samples of ditches, Kishtwar, Jammu and Kashmir, India]
R. macrolaimus (A. Schneider, 1866) comb. n.
= *Leptodera macrolaimus* A. Schneider, 1866
= *Rhabditis macrolaimus* (A. Schneider, 1866) Örley, 1880
= *Cylindrogaster macrolaimus* (A. Schneider, 1866) Chitwood, 1933
= *Cylindrocorpus macrolaimus* (A. Schneider, 1866) Goodey, 1939
= *Myctolaimus macrolaimus* (A. Schneider, 1866) Andrássy, 1984
= *Rhabditis paraelongata* Mickoletzky, 1915
= *Rhabditis longistoma* Stefanski, 1922
= *Cylindrogaster coprophaga* T. Goodey, 1927 [dung and decaying substance]
R. nacogdochensis (Massey, 1974) comb. n.
= *Dirhabdilaimus nacogdochensis* Massey, 1974
= *Diplogasteroides nacogdochensis* (Massey, 1974) Sudhaus & Fürst von Lieven, 2003 [associated with *Dendroctonus terebrans* (Coleoptera: Scolytidae) Nacogdoches, TX, USA]
R. neolongistoma (Hussain, Tahseen, Khan & Jairajpuri, 2004) comb. n.
= *Myctolaimus neolongistoma* Hussain, Tahseen, Khan & Jairajpuri, 2004 [slurry samples of ditches, Srinagar, Jammu and Kashmir, India]
R. pellucidus (Cobb, 1920) comb. n.
= *Myctolaimus pellucidus* Cobb, 1920 [sheep dung, Moss Vale, NSW, Australia]
R. picei Fuchs, 1931
= *Diplogasteroides* (*Neodiplogasteroides*) *picei* (Fuchs, 1931) Rühm, 1956
= *Neodiplogasteroides picei* (Fuchs, 1931) Rühm, 1956 (Meyl, 1960)
= *Dirhabdilaimus picei* (Fuchs, 1931) Baker, 1962
= *Diplogasteroides picei* (Fuchs, 1931) Sudhaus & Fürst von Lieven, 2003 [associated with *Hylobius piceus* (Coleoptera: Curculionidae) in *Larix* sp., Karawanken mountains, Slovenia/Austria]
R. pini Fuchs, 1931
= *Dirhabdilaimus pini* (Fuchs, 1931) Paramonov & Turlygina, 1955
= *Diplogasteroides pini* (Fuchs, 1931) Sudhaus & Fürst von Lieven, 2003 [associated with *Pissodes pini* (Coleoptera: Curculionidae) under bark of *Pinus sylvestris*, near Ossiacher See, Karinthia, Austria]
R. platypi (Kanzaki, Kobayashi, Nozaki & Futai, 2006) comb. n.
= *Myctolaimus platypi* Kanzaki, Kobayashi, Nozaki & Futai, 2006 [associated with *Platypus quercivorus* (Coleoptera: Platypodidae), Kyoto, Japan]
R. rifflei (Massey & Hinds, 1970) comb. n.
= *Cylindrocorpus rifflei* Massey & Hinds, 1970
= *Myctolaimus rifflei* (Massey & Hinds, 1970) Andrássy, 1984 [*Cenangium* cankers on *Populus tremuloides* in Sandia Mountains, Cibola National Forest, NM, USA]
R. robiniae (Harman, Winter & Harman, 2000) comb. n.
= *Myctolaimellus robiniae* Harman, Winter & Harman, 2000
= *Myctolaimus robiniae* (Harman, Winter & Harman, 2000) Sudhaus & Fürst von Lieven, 2003 [associated with *Megacyllene robiniae* (Coleoptera: Cerambycidae) in *Robinia pseudoacacia*, Frostberg State University campus and Garrett County, MD, USA]
R. ulmi (T. Goodey, 1930) comb. n.
= *Cylindrogaster ulmi* T. Goodey, 1930
= *Rhabditolaimus schuurmansi* Fuchs, 1933
= *Goodeyus ulmi scolytus* Rühm, 1956
= *Myctolaimus ulmi* (T. Goodey, 1930) Sudhaus & Fürst von Lieven, 2003 [associated with *Scolytus* sp. (Coleoptera: Scolytidae)]
R. vitautasi (Korenchenko, 1975) comb. n.
= *Cylindrocorpus vitautasi* Korenchenko, 1975
= *Myctolaimus vitautasi* (Korenchenko, 1975) Sudhaus & Fürst von Lieven, 2003 [associated with *Ips subelongatus* (Coleoptera: Scolytidae) and *Hylobius albosparsus* (Coleoptera: Curculionidae) Russia]
R. walkeri (Hunt, 1980) comb. n.

= *Cylindrocorpus walkeri* Hunt, 1980
= *Myctolaimellus walkeri* (Hunt, 1980) Andrássy, 1984
= *Myctolaimus walkeri* (Hunt, 1980) Sudhaus & Fürst von Lieven, 2003 [associated with *Lagochirus araneiformis* (Coleoptera: Cerambycidae), St Lucia, West Indies]

R. zamithi (Lordello *in* Andrássy, 1984) comb. n.
= *Myctolaimus zamithi* Lordello *in* Andrássy, 1984 [decaying potatoes, Brazil]

INCERTAE SEDIS

Anand (2005, 2006) described two species in a new genus, *Ceratosolenus* Anand, 2005, that were found in association with fig wasps. Although pharynx morphology and shape of the gymnostom lend support for their position within *Rhabditolaimus*, we cannot unambiguously place them there, and therefore treat them as *species incertae sedis* pending further examination of the specimens.

Acknowledgements

We would like to thank Rudolf Wegensteiner, Universität für Bodenkultur, Wien and Gerhard Elsner, Nordwestdeutsche Versuchsanstalt, Abteilung Waldschutz Göttingen, for collecting and sending *Hylobius abietis*. Thanks go to Erik Ragsdale for critically reading the manuscript and giving valuable comments.

References

ANAND, L.R. (2005). Association of a nematode *Ceratosolenus racemosa* gen. n. sp. n. (Cylindrocorporidae: Rhabditida, Goodey, 1939) a wasp (*Ceratosolen* sp. n.) and fig *Ficus racemosa*. *Uttar Pradesh Journal of Zoology* 25, 59-62.

ANAND, L.R. (2006). *Ceratosolenus hyderabadensis* sp. n. (Cylindrocorporidae: Rhabditida, Goodey, 1939) association with wasp, *Ceratosolen* sp. and fig, *Ficus racemosa*. *Uttar Pradesh Journal of Zoology* 26, 115-117.

ANDRÁSSY, I. (1984). *Klasse Nematoda (Ordnungen Monhysterida, Desmoscolecida, Araeolaimida, Chromadorida, Rhabditida)*. Stuttgart, Germany, Gustav Fischer Verlag, 509 pp.

ANDRÁSSY, I. (2005). *Free-living nematodes of Hungary, I (Nematoda errantia)*. *Pedozoologica Hungarica 3* (Csuzdi, C. & Mahunka, S. (Eds)). Budapest, Hungary, Hungarian Natural History Museum and Systematic Zoology Research Group of the Hungarian Academy of Sciences, 518 pp.

BAKER, A.D. (1962). *Check lists of the nematode superfamilies Dorylaimoidea, Rhabditoidea, Tylenchoidea and Aphelenchoidea*. Leiden, The Netherlands, Brill, 261 pp.

CHITWOOD, B.G. (1933). On some nematodes of the superfamily Rhabditoidea and their status as parasites of reptiles and amphibians. *Journal of the Washington Academy of Sciences* 23, 508-520.

COBB, N.A. (1920). One hundred new nemas (type-species of 100 new genera). *Contributions to a Science of Nematology* 9, 217-343.

FUCHS, G. (1914). Über Parasiten und andere biologisch an die Borkenkäfer gebundene Nematoden. *Verhandlungen der Gesellschaft Deutscher Naturforscher und Ärzte* 2, 688-692.

FUCHS, G. (1915). Die Naturgeschichte der Nematoden und einiger anderer Parasiten: 1. des *Ips typographus* L. 2. des *Hylobius abietis* L. *Zoologische Jahrbücher* 38, 109-222.

FUCHS, G. (1931). Die Genera: 1. *Rhabditolaimus* Fuchs, 2. *Neodiplogaster* Cobb, 3. *Tylenchodon* Fuchs. *Centralblatt für das gesamte Forstwesen (Wien)* 57, 177-194.

GIBLIN-DAVIS, R.M., YE, W., KANZAKI, N., WILLIAMS, D., MORRIS, K. & THOMAS, W.K. (2006). Stomatal ultrastructure, molecular phylogeny and description of *Parasitodiplogaster laevigata* n. sp. (Nematode: Diplogastridae), a parasite of fig wasps. *Journal of Nematology* 38, 137-149.

GOODEY, T. (1927). *Cylindrogaster coprophaga* gen. et sp. nov. A nematode found in a culture of faeces from a wild brown rat. *Journal of Helminthology* 5, 25-32.

GOODEY, T. (1930). A new species of the nematode genus *Cylindrogaster*. *Journal of Helminthology* 8, 89-92.

GOODEY, T. (1935). On *Cylindrogaster curzii* n. sp., a saprophagous nematode. *Journal of Helminthology* 13, 19-24.

GOODEY, T. (1939). *Cylindrocorpus* nom. nov. for *Cylindrogaster* Goodey, 1927 (Nematoda). *Journal of Helminthology* 17, 149-150.

HARMAN, A., WINTER, J. & HARMAN, D. (2000). *Myctolaimellus robiniae* n. sp. (Diplogasterida: Cylindrocorporidae) from larval cavities of the locust borer, *Megacyllene robiniae* Forster. *Journal of Nematology* 32, 389-395.

HERRMANN, M., MAYER, W.E. & SOMMER, R.J. (2006a). Nematodes of the genus *Pristionchus* are closely associated with scarab beetles and the Colorado potato beetle in Western Europe. *Zoology* 109, 96-108.

HERRMANN, M., MAYER, W.E. & SOMMER, R.J. (2006b). Sex, bugs and Haldane's rule: the nematode genus *Pristionchus* in the United States. *Frontiers in Zoology* 3, 14.

HUNT, D.J. (1980). *Butlerius macrospiculum* n. sp. and *Cylindrocorpus walkeri* n. sp. (Nematoda: Diplogastroidea) from St Lucia, West Indies. *Revue de Nématologie* 3, 155-160.

HUSSAIN, A., TAHSEEN, Q., KHAN, R. & JAIRAJPURI, M.S. (2004). Description of two new species of *Myctolaimus* Cobb, 1920 (Nematoda: Cylindrocorporidae) from northern India. *Journal of Nematode Morphology and Systematics* 6, 95-102.

KANAZKI, N. & FUTAI, K. (2004). *Cylindrocorpus anoplophorae* n. sp. (Nematoda: Cylindrocorporidae) isolated from the white-spotted longicorn beetle, *Anoplophora*

malasiana (Coleoptera: Cerambycidae). *Japanese Journal of Nematology* 34, 11-19.

KANZAKI, N., KOBAYASHI, M., NOZAKI, A. & FUTAI, K. (2006). *Myctolaimus platypi* sp. n. (Nematoda: Cylindrocorporidae) isolated from the oak borer, *Platypus quercivorus* (Coleoptera: Platypodidae). *Nematology* 8, 717-725.

KINN, D.N. (1984). *Protocylindrocorpus dendrophilus* n. sp. (Nematoda, Cylindrocorporidae) associated with pine wood borings. *Journal of Nematology* 16, 131-134.

KIONTKE, K. & FITCH, D.H.A. (2010). Phenotypic plasticity. Different teeth for different feasts. *Current Biology* 20, 710-712.

KIONTKE, K., BARRIERE, A., KOLOTUEV, I., PODBILEWICZ, B., SOMMER, R.J., FITCH, D.H.A. & FELIX, M.A. (2007). Trends, stasis, and drift in the evolution of nematode vulva development. *Current Biology* 17, 1925-1937.

KORENCHENKO, E.A. (1975). [A new nematode species, *Cylindrocorpus vitautasi* n. sp. (Rhabditida, Cylindrocorporidae) from the tunnels of *Ips subelongatus* Motsch and *Hylobius albosparsus* Bon (Coleoptera) on *Larix daurica*.] In: *Paraziticheskie organizmy severo vostoka Azii*, pp. 190-198.

KÖRNER, H. (1954). Die Nematodenfauna des vergehenden Holzes und ihre Beziehungen zu den Insekten. *Zoologische Jahrbücher (Systematik)* 82, 245-353.

KREIS, H.A. (1932). Beiträge zur Kenntnis pflanzenparasitischer Nematoden. *Zeitschrift für Parasitenkunde* 5, 184-194.

LARKIN, M.A., BLACKSHIELDS, G., BROWN, N.P., CHENNA, R., MCGETTIGAN, P.A., MCWILLIAM, H., VALENTIN, F., WALLACE, I.M., WILM, A., LOPEZ, R., *ET AL.* (2007). Clustal W and Clustal X version 2.0. *Bioinformatics* 23, 2947-2948.

LEUCKART, R. (1887). Neue Beiträge zur Kenntniss des Baues und der Lebensgeschichte der Nematoden. *Abhandlungen der königlich sächsischen Gesellschaft der Wissenschaften, mathematisch-physikalische Klasse* 22, 565-704.

DE MAN, J.G. (1912). Helminthologische Beiträge. *Zoologische Jahrbücher, Supplement* 15, 439-464.

MASSEY, C.L. (1960). A new species of Nematoda, *Cylindrocorpus erectus*, associated with *Scolytus multistriatus* Marsh, in American elm. *Proceedings of the Helminthological Society of Washington* 27, 42-44.

MASSEY, C.L. (1967). Nematodes associated with tree-infecting insects: Paurodontidae new family and Misticiinae new subfamily with a description of one new genus and four new species. *Canadian Journal of Zoology* 45, 779-786.

MASSEY, C.L. (1974). *Biology and taxonomy of nematodes parasites and associates of bark beetles in the United States*. Agricultural handbook 446. Washington, DC, USA, US Department Agricultural Forestry Service, 233 pp.

MASSEY, C.L. & HINDS, T.E. (1970). Nematodes from aspen cankers in Colorado and New Mexico. *Canadian Journal of Zoology* 48, 97-108.

MAYER, W.E., HERRMANN, M. & SOMMER, R.J. (2009). Molecular phylogeny of beetle associated diplogastrid nematodes suggests host switching rather than nematode-beetle coevolution. *BMC Evolutionary Biology* 9, 212-222.

MEYL, A.H. (1960). *Die freilebenden Erd- und Süßwassernematoden (Fadenwürmer)*. Leipzig, Germany, Quelle & Meyer, 164 pp.

MICOLETZKY, H. (1915). Süßwasser-Nematoden aus Südafrika. *Denkschrift der kaiserlichen Akademie der Wissenschaften Wien, math.-nat. Klasse* 92, 149-171.

MICOLETZKY, H. (1922). Die freilebenden Erd-Nematoden. *Archiv für Naturgeschichte* 87A, 1-650.

ÖRLEY, L. (1880). Az Anguilluidák magánrajza. *Természetrajzi füzetek (Budapest)* 4, 1-165.

PARAMONOV, A.A. (1952). [Ecological classification of plant nematodes.] *Trudy Gelminthologicheskoi Laboratorii* 6, 338-369.

PARAMONOV, A.A. (1964). [*Fundamentals of phytonematology*.] Moscow, USSR, Trudy Gelminthologicheskoi Laboratorii, Akademia Nauk, 446 pp.

PARAMONOV, A.A. & TURLYGINA, E.C. (1955). [A revision of the family Diplogasteroididae Paramonov, 1952 (Phasmidia: Diplogasterata).] *Zoologichesky Zhurnal* 34, 522-531.

POINAR JR, G.O., JACKSON, T.A., BELL, N.L. & WAHID, M.B. (2003). *Cylindrocorpus inevectus* sp. n. associated with the oil palm weevil, *Elaeidobius kamerunicus* (Faust) (Coleoptera: Curculionidae), with a synopsis of the family Cylindrocorporidae and establishment of Longibuccidae n. fam. (Diplogastroidea: Nematoda). *Nematology* 5, 183-190.

RAHM, G. (1928). Alguns nematodes parasitas e semiparasitas das plantas culturaes do Brasil. *Archivo do Instituto de Biológico de Defensa Agricola e Animal (Sao Paulo)* 1, 239-251.

RÜHM, W. (1956). Die Nematoden der Ipiden. *Parasitologische Schriftenreihe* 6, 1-437.

RÜHM, W. (1959). *Cylindrocorpus* subg. nov., und *Protocylindrocorpus* subg. nov., zwei Untergattungen der Gattung *Cylindrocorpus* Goodey 1939. *Nematologica* 4, 76-82.

SCHNEIDER, A. (1866). *Monographie der Nematoden*. Berlin, Germany, Druck und Verlag von Georg Reimer, 357 pp.

STEFANSKI, W. (1922). Excrétion chez les nématodes libres. *Archivum Nauk Biologicznych Towarzystwa Naukowego Warszawaskiego* 1, 1-33.

SUDHAUS, W. (1995). What is the type species of *Rhabitolaimus*? *Nematologica* 41, 641.

SUDHAUS, W. & FÜRST VON LIEVEN, A. (2003). A phylogenetic classification and catalogue of the Diplogastridae (Secernentea, Nematoda). *Journal of Nematode Morphology and Systematics* 6, 43-89.

TAMURA, K., DUDLEY, J., NEI, M. & KUMAR, S. (2007). MEGA4: molecular evolutionary genetics analysis (MEGA) software version 4.0. *Molecular Biology and Evolution* 24, 1596-1599.

VÖLK, J. (1950). Die Nematoden der Regenwürmer und aasbesuchenden Käfer. *Zoologische Jahrbücher (Systematik)* 79, 1-70.

Journal of Nematology 45(3):172–194. 2013.
© The Society of Nematologists 2013.

Two Androdioecious and One Dioecious New Species of *Pristionchus* (Nematoda: Diplogastridae): New Reference Points for the Evolution of Reproductive Mode

Natsumi Kanzaki,[1,†] Erik J. Ragsdale,[2,†] Matthias Herrmann,[2] Vladislav Susoy,[2] Ralf J. Sommer[2]

Abstract: Rhabditid nematodes are one of a few animal taxa in which androdioecious reproduction, involving hermaphrodites and males, is found. In the genus *Pristionchus*, several cases of androdioecy are known, including the model species *P. pacificus*. A comprehensive understanding of the evolution of reproductive mode depends on dense taxon sampling and careful morphological and phylogenetic reconstruction. In this article, two new androdioecious species, *P. boliviae* n. sp. and *P. mayeri* n. sp., and one gonochoristic outgroup, *P. atlanticus* n. sp., are described on morphological, molecular, and biological evidence. Their phylogenetic relationships are inferred from 26 ribosomal protein genes and a partial SSU rRNA gene. Based on current representation, the new androdioecious species are sister taxa, indicating either speciation from an androdioecious ancestor or rapid convergent evolution in closely related species. Male sexual characters distinguish the new species, and new characters for six closely related *Pristionchus* species are presented. Male papillae are unusually variable in *P. boliviae* n. sp. and *P. mayeri* n. sp., consistent with the predictions of "selfing syndrome." Description and phylogeny of new androdioecious species, supported by fuller outgroup representation, establish new reference points for mechanistic studies in the *Pristionchus* system by expanding its comparative context.

Key words: gonochorism, hermaphroditism, morphology, *P. boliviae* n. sp., *P. mayeri* n. sp., phylogeny, *Pristionchus atlanticus* n. sp., selfing syndrome, taxonomy.

Androdioecy, a reproductive mode involving both hermaphrodites and males, has been considered an unlikely or rare phenomenon, given the improbable conditions theoretically necessary to give rise to and maintain it (Darwin, 1877; Charlesworth, 1984). Few cases of true androdioecy have been convincingly demonstrated in the animal kingdom and include rhabditid nematodes (for review, see Weeks, 2012). Of androdioecious nematodes, the most intensively studied belong to the model genus *Caenorhabditis*, although androdioecious species have been confirmed or inferred for the genera *Oscheius* (Félix et al., 2001) and *Panagrolaimus* (Lewis et al., 2009). Perhaps most striking is the number of cases that have been documented in the family Diplogastridae Micoletzky, 1922, including *Diplogasteroides magnus* (Völk, 1950), Weingärtner, 1955 (Kiontke et al., 2001), *Koerneria sudhausi* Fürst von Lieven, 2008, and several species of *Pristionchus* Kreis, 1932 (Mayer et al., 2007).

Intensive sampling efforts have now revealed that androdioecy has arisen at least six times independently in *Pristionchus* (Mayer et al., 2007, 2009). Of the four previously described self-fertilizing species of *Pristionchus*, at least three are androdioecious: *P. fissidentatus* Kanzaki, Ragsdale, Herrmann, and Sommer, 2012; *P. maupasi* (Potts, 1910) Paramonov, 1952; and *P. pacificus* Sommer, Carta, Kim, and Sternberg, 1996. In the fourth species, *P. entomophagus* (Steiner, 1929) Sudhaus and Fürst von Lieven, 2003, males have been observed in only a few strains, although those males found can successfully outcross (D'Anna and Sommer, unpubl. data).

Dense taxon sampling, a sound phylogenetic framework, and the presence of multiple reproductive modes in a single nematode group are essential for gaining insight into the evolution of reproductive mode (Denver et al., 2011). Consequently, *Pristionchus* is particularly well suited for reconstructing the events leading to androdioecy. In addition, the laboratory tractability of *Pristionchus* nematodes offers the potential to uncover specific genetic mechanisms underlying evolution. As a satellite model to *Caenorhabditis elegans*, *P. pacificus* is supported by an analytical toolkit including extensive genetic and genomic resources (Sommer, 2009). For example, work in this system previously demonstrated the global sex-determination gene *tra-1* to be functionally conserved in *C. elegans* and *P. pacificus* (Pires-da Silva and Sommer, 2004). Expanding the functional studies of derived reproductive modes will be made possible by the availability of closely related androdioecious species. Considerable advancements in understanding the evolution of sex determination in the androdioecious species *C. elegans* and *C. briggsae* (Haag, 2009; Thomas et al., 2012) demonstrate the power of such an approach. The establishment of a comparative context therefore awaits proper characterization of new potential models.

In the present study, we describe two new androdioecious species, *P. boliviae* n. sp. and *P. mayeri* n. sp., as well as a gonochoristic outgroup species, *P. atlanticus* n. sp. A molecular phylogenetic context, which had previously been inferred from several loci for the gonochoristic new species (Mayer et al., 2007), is extended to the other two new species and includes 26 ribosomal

Received for publication May 31, 2013.
[1]Forest Pathology Laboratory, Forestry and Forest Products Research Institute, 1 Matsunosato, Tsukuba, Ibaraki 305-8687 Japan.
[2]Max Planck Institute for Developmental Biology, Department of Evolutionary Biology, Spemannstraße 37, 72076 Tübingen, Germany.
[†]These authors contributed equally to this work.
We are grateful to the Alexander von Humboldt Foundation for the support of fellowship to EJR. We thank Heike Haussmann, Waltraud Röseler, and Gabi Eberhardt for maintaining live cultures and frozen stocks of *Pristionchus* species, and we are thankful to Andrew Chisholm for providing the latter strain. Roles of authors: NK and EJR made morphological observations; NK produced line drawings; EJR performed phylogenetic analyses; EJR and MH collected morphometric data; EJR, MH, and VS performed biological experiments; MH isolated nematode strains; and EJR and RJS wrote the manuscript.
E-mail: ralf.sommer@tuebingen.mpg.de
This paper was edited by Zafar Handoo.

protein genes. Additionally, new comparative morphological data are presented for six species phylogenetically close to the newly described species. Besides providing reference points for studies of the evolution of sex, description of these species will expand the potential for more general comparative biology in the *Pristionchus* system.

Materials and Methods

Nematode isolation and cultivation: Pristionchus boliviae n. sp. was isolated from an adult *Cyclocephala amazonica* (Coleoptera: Scarabaeidae) collected near Buena Vista, Bolivia. Host beetles were dissected on a 2.0% agar plate, after which the plate was kept at room temperature for several weeks. Nematodes proliferated on bacteria associated with the host beetle cadavers. Individuals were thereafter transferred to nematode growth medium (NGM) agar plates seeded with *Escherichia coli* OP50, and have been since kept in laboratory culture on this medium. This medium was also used to maintain strains of *P. mayeri* n. sp. and *P. atlanticus* n. sp., which were isolated as described in Herrmann et al. (2010) and Mayer et al. (2007), respectively.

Molecular characterization and phylogenetic analysis: For species diagnosis and phylogenetic analysis, we amplified an approximately 1-kb fragment of the SSU rRNA gene using the primers SSU18A (5'-AAAGATTAAGCC ATGCATG-3') and SSU26R (5'-CATTCTTGGCAAATG CTTTCG-3') (Floyd et al., 2002). The diagnostic fragment was approximately 500 bp of the 5' terminal end and was sequenced using the primer SSU9R (5'-AGCTGGAAT TACCGCGGCTG-3'). The partial SSU rRNA sequences of *P. boliviae* n. sp. and the type strain of *P. mayeri* n. sp. (RS5460) were original in this study and have been deposited in the GenBank database (Table 1). The diagnostic 472-bp fragment of the SSU rRNA gene was identical for all isolates of *P. mayeri* n. sp. except at one unambiguous nucleotide position (Fig. 1). This alternate sequence was found in several strains from La Réunion (RSA035), Mauritius, and Madagascar, and it has been deposited in GenBank (Table 1).

Phylogenetic analysis was performed on the partial SSU rRNA gene and 26 ribosomal protein genes. The aligned SSU rRNA fragment consisted of 851 positions. Ribosomal protein genes analyzed were those developed by Mayer et al. (2007) as marker loci based on their consistent presence in expressed sequence tag libraries of *Pristionchus* species. The dataset of ribosomal protein genes comprised a total of 10,758 aligned coding nucleotides. Genes included in the analysis were: *rpl-1*, *rpl-2*, *rpl-10*, *rpl-14*, *rpl-16*, *rpl-23*, *rpl-26*, *rpl-27*, *rpl-27a*, *rpl-28*, *rpl-30*, *rpl-31*, *rpl-32*, *rpl-34*, *rpl-35*, *rpl-38*, *rpl-39*, *rps-1*, *rps-8*, *rps-14*, *rps-20*, *rps-21*, *rps-24*, *rps-25*, *rps-27*, and *rps-28*. Ribosomal protein gene sequences for *P. boliviae* n. sp. and *P. mayeri* n. sp. are original in this study. All ribosomal protein gene sequences, except those for *rpl-38* and *rpl-39*, which were less than 200 nucleotides in length, have been deposited in GenBank (Table 1). All information regarding genes, primers, and PCR conditions is given in Mayer et al. (2007).

Table 1. GenBank accession numbers for gene sequences obtained in this study.

Gene	*Pristionchus boliviae* n. sp.	*Pristionchus mayeri* n. sp.
SSU rRNA	KC491629	KC491630 (RS5460) KC491631 (RSA035)
rpl-1	KC491632	KC491656
rpl-2	KC491633	KC491657
rpl-10	KC491634	KC491658
rpl-14	KC491635	KC491659
rpl-16	KC491636	KC491660
rpl-23	KC491637	KC491661
rpl-26	KC491638	KC491662
rpl-27	KC491639	KC491663
rpl-27a	KC491641	KC491664
rpl-28	KC491640	KC491665
rpl-30	KC491642	KC491666
rpl-31	KC491643	KC491667
rpl-32	KC491644	KC491679
rpl-34	KC491645	KC491668
rpl-35	KC491646	KC491669
rps-1	KC491654	KC491670
rps-8	KC491655	KC491671
rps-14	KC491647	KC491672
rps-20	KC491648	KC491673
rps-21	KC491653	KC491674
rps-24	KC491648	KC491675
rps-25	KC491650	KC491676
rps-27	KC491651	KC491677
rps-28	KC491652	KC491678

The concatenated dataset of the partial SSU rRNA and ribosomal protein genes was aligned using MUSCLE (Edgar, 2004), followed by manual alignment in MEGA5.05 (Tamura et al., 2011) and by deletion of ambiguously aligned positions. The alignment was partitioned into four subsets: one for the partial SSU rRNA gene and three according to codon position for the concatenated set of ribosomal protein genes. The phylogeny was inferred under maximum likelihood (ML) and Bayesian optimality criteria, as implemented in RAxML v.7.2.8 (Stamatakis, 2006) and MrBayes 3.2 (Ronquist et al., 2012), respectively. The ML analysis invoked a general time reversible model with a gamma-shaped distribution of rates across sites. Bayesian analyses were initiated with random starting trees and were run with four chains for 2×10^6 generations. Markov chains were sampled at intervals of 100 generations. Two runs were performed for the analysis. After confirming convergence of runs and discarding the first 5×10^5 generations as burn-in, remaining topologies were used to generate a 50% majority-rule consensus tree with clade credibility values given as posterior probabilities (PP). Bayesian analysis allowed a mixed model of substitution with a gamma-shaped distribution and specified *Koerneria* sp. (RS1982) as outgroup. Model parameters

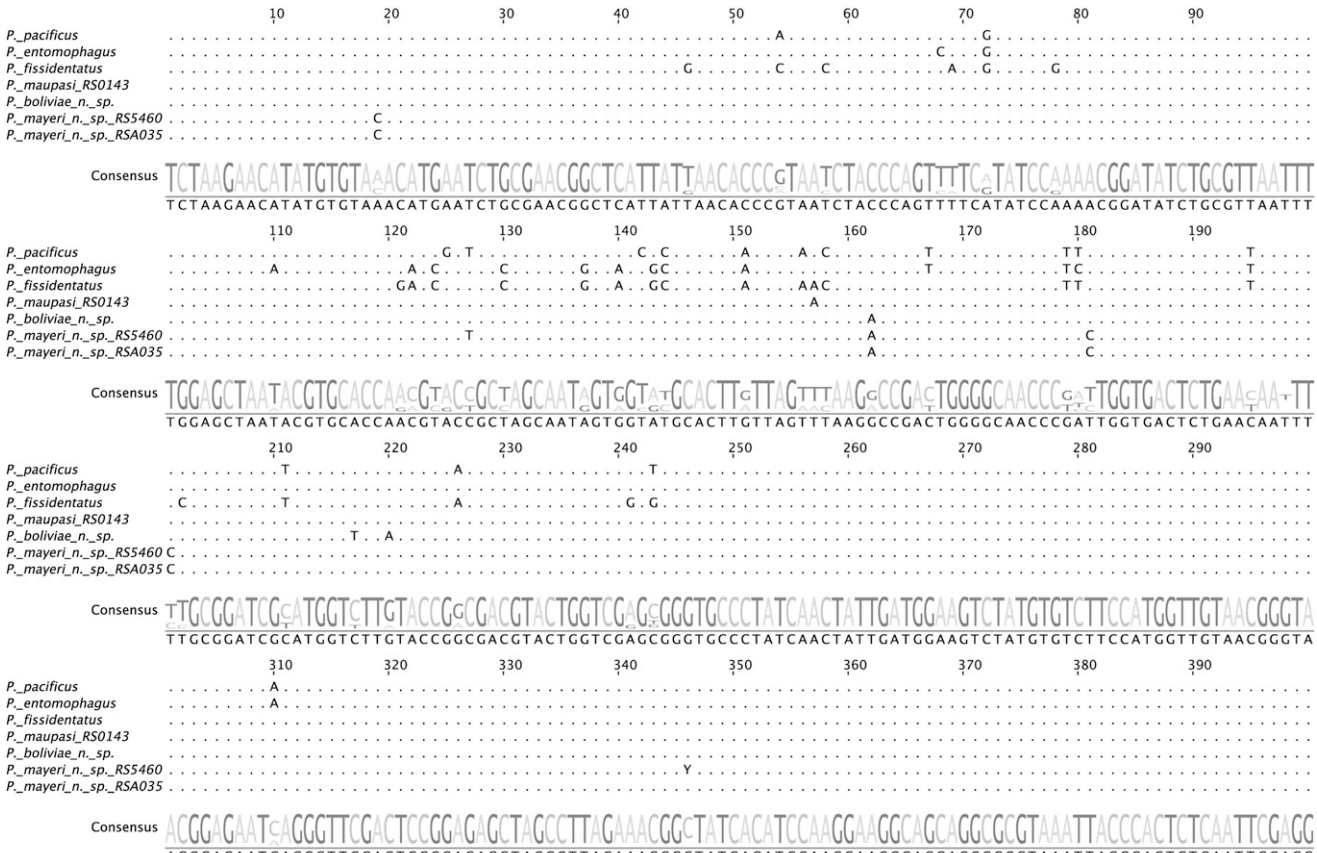

FIG. 1. Alignment of a 400-bp diagnostic fragment of the SSU rRNA gene for nominal hermaphroditic species of *Pristionchus*. Sequences were aligned manually. Points indicate nucleotides identical with consensus sequence. Numbering refers to base positions. Differences in sequences for newly described species are considered diagnostic of those species. Sequences for *P. boliviae* n. sp. and *P. mayeri* n. sp. are original in this study and have been deposited in GenBank as described in text. Other sequences were previously published and available in GenBank.

were unlinked across character partitions in the analyses. Bootstrap support (BS) in the ML tree was evaluated by 1,000 pseudoreplicates.

Presence and reproductive function of males: For *P. boliviae* n. sp. and *P. mayeri* n. sp., males were isolated from culture populations, after which crosses were set up between two males and one virgin (J4) hermaphrodite on plates seeded with a small bacterial lawn (25 µL *E. coli* OP50 in L-broth). Mating plates were maintained at 23°C. Because of the XX:X0 sex-determination system in *Pristionchus*, reproductive function of males was preliminarily considered successful if at least two males were present in the offspring of a single cross. For comparison, the frequency of meiotic X-chromosome nondisjunction was determined for nonmated hermaphrodites by allowing one J4 hermaphrodite per plate to produce progeny by selfing. Three replicates were performed per cross type. For *P. boliviae* n. sp., crosses were performed within the type strain (RS5262). For *P. mayeri* n. sp., crosses were performed within the type strain (RS5460), within the strain RSA035, which differed from the type strain by one nucleotide position in the diagnostic 472-bp SSU rRNA fragment described above, and between the type and RSA035 strains in both directions. In cases where crosses produced two or more F1 males, F1 males were sequenced to confirm their parentage, namely by detection of polymorphisms at known diagnostic sites in their SSU rRNA sequences. Crosses of all types were performed in triplicate.

Because of the limited success of crosses between strains of *P. mayeri* n. sp., especially in RSA035, additional crosses were performed between RSA035 and another isolate of *P. mayeri* n. sp., RSA138. Crosses each included five males and one J4 hermaphrodite placed on plates seeded with a bacterial lawn from 100 ml. In each of these crosses, the P0 strains differed at one nucleotide polymorphism in the SSU rRNA sequence (Fig. 1), such that parentage of offspring could be confirmed by sequencing. Additionally, F1 males resulting from these crosses were backcrossed to both P0 lines to test for reproductive isolation between P0 strains. Replicates were performed for each cross type as made possible by the availability of males.

Hybrid mating tests: To test whether *P. boliviae* n. sp. and *P. mayeri* n. sp. are reproductively isolated from each other, hybrid crosses between these two putative species were performed. Each cross, set up on plates as

described above, consisted of one J4 hermaphrodite from one species and two males of the opposite species. Crosses were performed reciprocally and in at least three replicates for each direction. All F1 males were sequenced to confirm their parentage.

Morphological observation and preparation of type material: One- to two-week-old cultures of *P. boliviae* n. sp. (RS5262, RS5518), *P. mayeri* n. sp. (RS5460, RSA035), and *P. atlanticus* n. sp. (CZ3975) provided material for morphological observation. Observations by light microscopy (LM) and differential interference contrast (DIC) microscopy were conducted using live nematodes, which were hand-picked from culture plates. For line drawings, specimens were mounted into water on slides and then relaxed by applying gentle heat. For morphometrics, specimens were mounted on slides with pads of 5% agar noble and 0.15% sodium azide and were additionally relaxed by heat when necessary. To prepare type material, nematodes were isolated from type strain cultures, rinsed in distilled water to remove bacteria, heat killed at 65°C, fixed in TAF to a final concentration of 5% formalin and 1.5% triethanolamine, and processed through a glycerol and ethanol series using Seinhorst's method (see Hooper et al., 1986). Nomarski micrographs were taken using a Zeiss Axio Imager Z.1 microscope and a Spot RT-SE camera supported by the program MetaMorph v.7.1.3 (Molecular Devices, Sunnyvale, CA). For comparison with the newly described species, original LM observations were also made on live specimens of the following species: *P. aerviorus* (Cobb in Merrill and Ford, 1916) Chitwood, 1937; *P. americanus* Herrmann, Mayer, and Sommer, 2006; *P. marianneae* Herrmann, Mayer, and Sommer, 2006; *P. maupasi* (strain RS0143); *P. pauli* Herrmann, Mayer, and Sommer, 2006; and *P. pseudaerivorus* Herrmann, Mayer, and Sommer, 2006.

Ancestral state reconstruction of papillae characters: To establish a set of diagnostic characters for a clade of *Pristionchus* including the three new species, male papillae arrangements were determined for species in the clade and reported in ventral view. These data were then used to map the evolution of male sexual characters in a clade including several self-fertilizing species. We reconstructed ancestral states of papilla characters by mapping them onto the phylogeny inferred from molecular sequences. Characters were mapped by simple parsimony, as implemented in Mesquite v.2.75 (Maddison and Maddison, 2011). The species *P. japonicus* Kanzaki, Ragsdale, Herrmann, Mayer, and Sommer, 2012 was selected as outgroup for character polarization. All other taxa were pruned from the tree prior to ancestral state reconstruction.

Results

Molecular characterization and phylogenetic analysis: Sequences of a 472-bp fragment of the small subunit (SSU) rRNA gene were unique for each new species described herein (Fig. 1). Beyond diagnostics, a resolved phylogenetic infrastructure is essential to track character evolution, including the events leading to hermaphroditism. To accomplish this, we employed a dataset of 26 ribosomal protein genes and the partial SSU rRNA gene to infer relationships among *Pristionchus* species. The total concatenated alignment comprised 11,609 sites, 1881 of which were parsimony informative. This dataset provided high resolution for most relationships in the genus, including all nodes immediately preceding the mapped origins of hermaphroditism (Fig. 2).

Tree topologies from ML and Bayesian analyses were identical. Only the ML tree is shown, along with support values from both analyses (Fig. 2). Results of the analysis show that *P. boliviae* n. sp. and *P. mayeri* n. sp. are sister taxa based on current taxon representation. Therefore, hermaphroditism in these two species is presently considered to have evolved once in their common ancestor. Consistent with previous phylogenetic analyses (Mayer et al., 2007, 2009; Kanzaki et al., 2012a, 2012b), three major clades of *Pristionchus* were strongly supported (100% BS and PP). One such clade included *P. pauli*, *P. atlanticus* n. sp., *P. marianneae*, *P. americanus*, *P. boliviae* n. sp., *P. mayeri* n. sp., *P. aerivorus*, *P. pseudaerivorus*, and *P. maupasi* and is designated herein as the "*maupasi*" group. Another strongly supported clade, including *P. japonicus*, *P. arcanus* Kanzaki, Ragsdale, Herrmann, Mayer, and Sommer, 2012; *P. exspectatus* Kanzaki, Ragsdale, Herrmann, Mayer, and Sommer, 2012; and *P. pacificus*, is designated as the "*pacificus*" group. The strongly supported clade referred to as the "*lheritieri*" group includes *P. lheritieri* (Maupas, 1919) Paramonov, 1952, *P. entomophagus*, and *P. uniformis* Fedorko and Stanuszek, 1971. Group designations indicate mutually exclusive clades and are unranked. Moreover, several species of *Pristionchus*, notably the putatively basal species *P. elegans* Kanzaki, Ragsdale, Herrmann, and Sommer, 2012 and *P. fissidentatus*, remain outside of this nomenclature.

Reproductive function of males: To assess the reproductive function of males, we performed laboratory tests in the form of intraspecific and hybrid crosses (Table 2). All males obtained as a result of these crossing experiments had their SSU rRNA gene sequenced, where informative, to determine their genotype. Crosses of males to conspecific hermaphrodites resulted in multiple male progeny in *P. boliviae* n. sp., although virgin hermaphrodites also produced high numbers of males. Mating experiments could thus not definitively demonstrate the ability of *P. boliviae* n. sp. to outcross. Because hermaphrodites produce high numbers of males with or without outcrossing, we consider the species to be androdioecious, as defined in Weeks (2012). Crosses within *P. mayeri* n. sp. initially resulted in few or no F1 male progeny. Furthermore, crosses producing males in

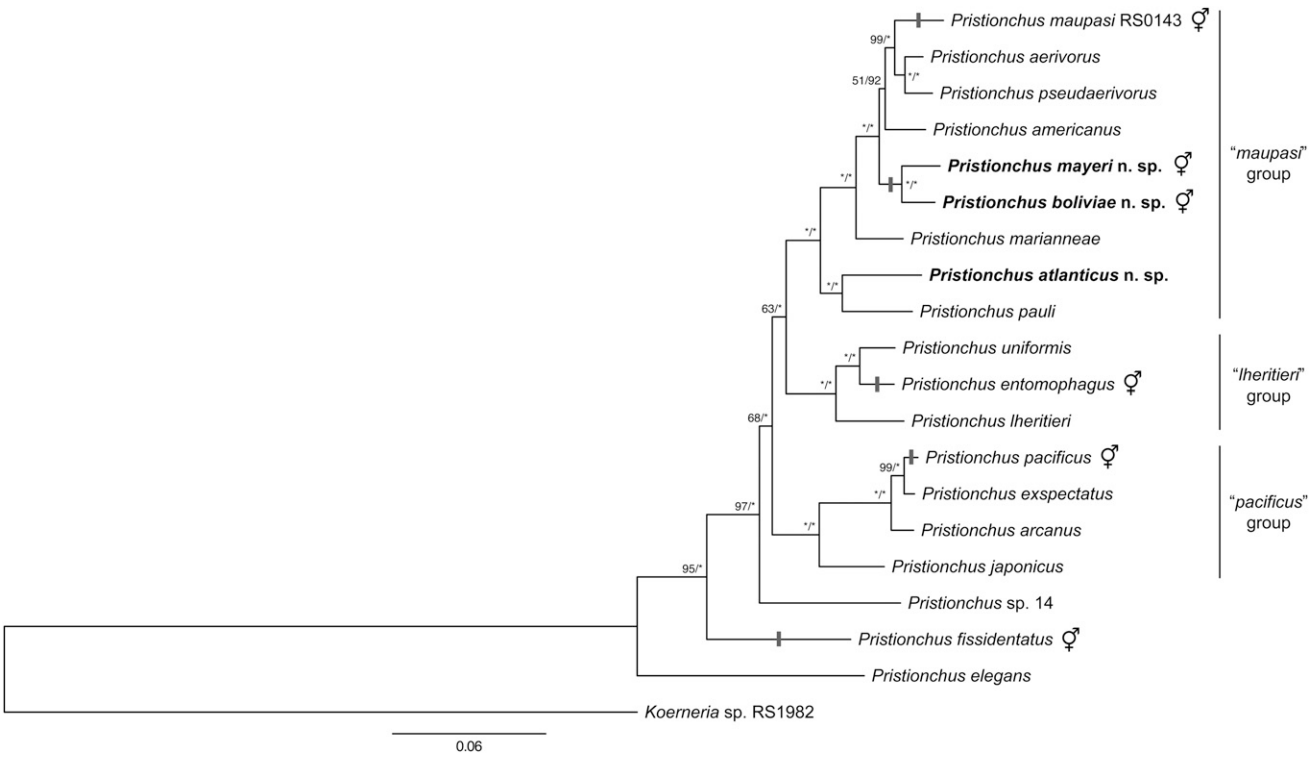

Fig. 2. Phylogenetic relationships of *Pristionchus* species inferred by maximum likelihood (ML) from a partial SSU rRNA fragment and 26 ribosomal protein-coding genes. Independent evolutionary origins of hermaphroditism (steps indicated by gray bars) were mapped by simple parsimony. The ML tree with the highest log likelihood is shown. The proportion of trees in which the associated taxa clustered together in 1,000 bootstrap pseudoreplicates is shown next to the nodes (left value). Tree topology is identical with that from Bayesian inference, and posterior probabilities for corresponding nodes are also displayed (right value) on tree. Bootstrap support values above 50% are shown. Asterisks indicate 100% support. Tree is drawn to scale, with branch lengths measured in the number of substitutions per site.

P. mayeri n. sp. always involved RSA035 mothers, and virgin RSA035 hermaphrodites also produced a strikingly high number of spontaneous males (Table 2). Therefore, to further test the ability of *P. mayeri* n. sp. to outcross, intraspecific crosses were performed using more (five) P0 males per cross and employed P0 strains that had distinct SSU rRNA sequences (Fig. 1), namely strains RSA035 and RSA138, allowing the genotyping of offspring to confirm paternity. Fathers sired males in at least one replicate in all attempted crosses of the latter strains (Table 2). Additionally, these F1 males could successfully cross to either P0 line, confirming that RSA035 and RSA138 belong to the same biological species (Table 2). Thus, *P. mayeri* n. sp. is functionally androdioecious.

Hybrid mating tests: Interspecific crosses between *P. boliviae* n. sp. hermaphrodites and *P. mayeri* n. sp. males were followed by multiple male progeny, although these males were confirmed by sequencing to be from selfing rather than crossing (Table 2). One replicate of the reciprocal cross resulted in two males, which were also confirmed to be spontaneous. Therefore, *P. boliviae* n. sp. and *P. mayeri* n. sp. showed prezygotic reproductive isolation and are considered to be unique biological species. Additionally, when compared with the reciprocal hybrid cross and intraspecific crosses, crosses between *P. boliviae* n. sp. males and *P. mayeri* n. sp. hermaphrodites showed a dramatic reduction in brood size, in one case consisting of as few as three hermaphrodite progeny (Table 2).

Morphology of the three new species: Reflecting the close relationships among *P. boliviae* n. sp., *P. mayeri* n. sp., and *P. atlanticus* n. sp., as inferred from molecular phylogeny, is a general similarity in the morphology of these three species. To avoid redundancy, morphology common to all three new species is described first, followed by species-specific characters and diagnoses for each species.

Description of characters common to the three new species: Adults. Body cylindrical, stout. Cuticle thick, with fine annulation and clear longitudinal striations. Lateral field consisting of two lines, only weakly distinguishable from body striation. Head without apparent lips, and with six short and papilliform labial sensilla. Four small, papilliform cephalic papillae present in males, as typical for diplogastrid nematodes. Amphidial apertures located at level of posterior end of cheilostomatal plates. Stomatal dimorphism present, with stenostomatous (narrow mouthed) and eurystomatous (wide mouthed) forms occurring in both males and hermaphrodites/females. Dorsal pharyngeal gland clearly observed, penetrating dorsal tooth to gland opening. Anterior part of pharynx (= pro- and metacorpus) 1.5 times as long as posterior part (isthmus and basal bulb). Procorpus very muscular, stout, occupying one-half to

TABLE 2. Intraspecific and hybrid crosses of *Pristionchus boliviae* n. sp. and three strains of *P. mayeri* n. sp. Crosses within strains were performed to test the reproductive function of males. Crosses between strains were performed to test for reproductive isolation. To estimate the frequency of meiotic X-chromosome nondisjunction, all F1 hermaprodites and males were counted. All crosses were performed with a single virgin P0 hermaphrodite. Where parent strains had unique SSU rRNA sequences, including within *P. mayeri* n. sp., the parentage of male offspring was confirmed by sequencing and is indicated in the far-right column. Following crosses between RSA035 and RSA138, F1 males were backcrossed to both P0 lines to test for reproductive isolation between P0 strains. The genotypes of F1 males used in crosses are shown in the "cross type" column as maternal/paternal. Crosses between RSA035, RSA138, and their F1 offspring resulted in sired males, confirming that *P. mayeri* n. sp. is functionally androdioecious and that the parent strains, which differ in their SSU rRNA sequence, belong to the same biological species.

			Offspring (n)	
Cross type (hermaphrodite x male)	Replicate	P0 males (n)	Hermaphrodites	Males from selfing/crossing
P. boliviae n. sp. RS5262 x	1	2	125	7/0
P. mayeri n. sp. RS5460	2	2	106	3/0
	3	2	148	8/0
P. mayeri n. sp. RS5460 x	1	2	25	0
P. boliviae n. sp. RS5262	2	2	9	0
	3	2	3	0
	4	2	6	2/0
P. boliviae n. sp. RS5262 x	1	2	133	6
P. boliviae n. sp. RS5262	2	2	149	13
	3	2	154	3
	4	2	134	2
P. boliviae n. sp. RS5262	1	0	126	6
(selfing only)	2	0	130	1
	3	0	135	5
	4	0	125	4
P. mayeri n. sp. RS5460 x	1	2	121	0
P. mayeri n. sp. RS5460	2	2	76	0
	3	2	43	0
P. mayeri n. sp. RS5460	1	2	86	0
(selfing only)	2	2	92	0
	3	2	103	0
P. mayeri n. sp. RSA035 x	1	2	142	2
P. mayeri n. sp. RSA035	2	2	147	1
	3	2	135	0
P. mayeri n. sp. RSA035	1	0	127	1
(selfing only)	2	0	117	3
	3	0	92	2
P. mayeri n. sp. RS5460 x	1	2	87	0
P. mayeri n. sp. RSA035	2	2	153	0
	3	2	63	0
P. mayeri n. sp. RSA035 x	1	2	35	0
P. mayeri n. sp. RS5460	2	2	30	0/1
	3	2	97	5/0
P. mayeri n. sp. RSA035 x	1	5	161	6/2
P. mayeri n. sp. RSA138	2	5	75	0/2
	3	5	64	0
P. mayeri n. sp. RSA138 x	1	5	139	3/3
P. mayeri n. sp. RSA035	2	5	194	2/3
	3	5	218	4/0
P. mayeri n. sp. RSA138 x	1	1	-	6/3
P. mayeri n. sp. RSA138/RSA035	2	1	-	6/1
	3	1	-	3/0
	4	1	-	2/0
P. mayeri n. sp. RSA138 x	1	1	-	2/0
P. mayeri n. sp. RSA035/RSA138	2	1	-	1/1
P. mayeri n. sp. RSA035 x	1	1	-	2/2
P. mayeri n. sp. RSA138/RSA035	2	1	-	3/0
P. mayeri n. sp. RSA035 x	1	1	-	1/0
P. mayeri n. sp. RSA035/RSA138	2	1	-	2/2

two-thirds of corresponding body width. Metacorpus very muscular, forming well-developed median bulb. Isthmus narrow, not muscular. Basal bulb glandular. Pharyngo-intestinal junction clearly observed, well developed. Nerve ring usually surrounding middle or slightly more anterior part of isthmus. Excretory pore not conspicuous, ventrally located with variable position, between slightly anterior to basal bulb and pharyngo-intestinal junction or sometimes farther posterior, excretory duct extending anteriad and reflexed back to position of pore. Hemizonid not clearly observed. Deirid observed laterally, slightly posterior to pharyngo-intestinal junction.

"Postdeirid" pores present and observed laterally, with positions inconsistent among individuals, five to eight for males and nine to 10 for females being confirmed by LM observation.

Stenostomatous form: Cheilostom consisting of six per- and interradial plates. Incisions between plates not easily distinguished by LM observation. Anterior end of each plate rounded and elongated to stick out from stomatal opening and form a small flap. Gymnostom short, cuticular ring-like anterior end overlapping cheilostom internally. Dorsal gymnostomatal wall slightly thickened compared with ventral side.

Eurystomatous form: Cheilostom divided into six distinct per- and interradial plates. Anterior end of each plate rounded and elongated to stick out from stomatal opening and form a small flap. Gymnostom with thick cuticle, forming a short, ring-like tube. Anterior end of gymnostom internally overlapping posterior end of cheilostomatal plates.

Male: Ventrally arcuate, strongly ventrally curved at tail region when killed by heat. Testis single, along ventral side of body, anterior part reflexed to right side. Vas deferens not clearly separated from other parts of gonad. Three (two subventral and one dorsal) cloacal gland cells observed at distal end of testis and intestine. Spicules paired, separate. Thick cuticle around tail region, falsely appearing as a narrow leptoderan bursa in ventral view. Dorsal side of gubernaculum possessing a single, membranous, anteriorly directed process and a lateral pair of more sclerotized anteriorly and ventrally directed processes. Cloacal opening slit-like in ventral view. One small, ventral, single genital papilla (vs) on anterior cloacal lip. Papilla nomenclature follows Sudhaus and Fürst von Lieven (2003): all ventral papillae and the most anterior dorsal papilla are numbered by absolute position along the body axis, whereby the dorsal papilla is appended with a "d" (i.e., v2d or v3d); remaining dorsal papillae are designated as anterior (ad) or posterior (pd). Papillae v1-ad of almost equal size, rather large and conspicuous, v5 and v6 very small, sometimes difficult to observe by LM, v7, and pd small but larger than v5 and v6, i.e., intermediate between v1-ad and v5/v6 in size. Tip of v6 papillae split into two small papilla-like projections. v1-ad, v7, and pd papilliform and cone-shaped, borne directly from body, v5 and v6 each shrouded at base by a socket-like structure. Excluding terminal spike, tail about two cloacal body widths long. Bursa or bursal flap absent. Tail conical, with long spike, which has filiform distal end.

Hermaphrodite/female: Relaxed or slightly ventrally arcuate when killed by heat. Gonad didelphic, amphidelphic. Each gonadal system arranged from vulva and vagina as uterus, oviduct, and ovotestis/ovary. Anterior gonad right of intestine, with uterus and oviduct extending ventrally and anteriorly on right of intestine and with a totally reflexed (= antidromous reflexion) ovotestis/ovary extending dorsally on left of intestine. Oocytes mostly arranged in multiple, sometimes more than five rows in distal two-thirds of ovotestis/ovary and in single row in remaining third of ovotestis/ovary, distal tips of each ovotestis/ovary reaching the oviduct of opposite gonad branch. Middle part of oviduct serving as spermatheca, sperm observed in distal part of oviduct, close to ovotestis/ovary. Eggs in single- to multiple-cell stage or even further developed at proximal part of oviduct (= uterus). Receptaculum seminis not observed. Dorsal wall of uterus at the level of vulva thickened and appears dark in LM observation. Four vaginal glands present but obscure. Vagina perpendicular to body surface, surrounded by sclerotized tissue. Vulva slightly protuberant in lateral view, pore-like in ventral view. Rectum about one anal body width long, intestinal-rectal junction surrounded by well-developed sphincter muscle. Three (two subventral and one dorsal) anal glands present at the intestinal/rectal junction, but not obvious. Anus in form of dome-shaped slit, posterior anal lip slightly protuberant. Phasmid about two anal body width posterior to anus. Tail long, distal end variable from filiform to long and conical.

Pristionchus boliviae n. sp.[*]

= *Pristionchus* sp. 16 *apud* Mayer et al. (2009)

(Figs. 3-6)

Measurements: See Table 3.

Description of species-specific characters: Adults. Species androdioecious, consisting of males and self-fertile hermaphrodites.

Stenostomatous form: Stegostom bearing: a large, conspicuous, flint-shaped (or inverted "V"-shaped) dorsal tooth; in the right subventral sector, a crescent-shaped or half-circular ridge with one or two small cusps that vary in position from internally directed to apex of ridge; a crescent-shaped left subventral ridge with two to three small peaks, often with apparent cleavage between two main peaks. Dorsal tooth sclerotized at surface.

Eurystomatous form: In type strain, typically smaller than stenostomatous form, possibly as a result of starvation. Stegostom bearing: a large claw-like dorsal tooth, with large base of varying size; a large claw-like right subventral tooth, occasionally with a split cusp; in the left subventral sector, a row of four to eight small- to medium-sized triangular subventral peaks projecting from a common cuticular plate that appears split midway along its length. Dorsal and right subventral teeth movable. Left subventral denticles immovable.

Male: Spontaneous males relatively common, often more than 5% of brood (strain RS5262). Spermatogonia arranged in about 10 rows in reflexed part, then well-developed spermatocytes arranged as eight to 10 rows in anterior two-thirds of main branch, then mature amoeboid spermatids arranged in multiple rows in remaining,

[*] The species epithet is the Latin genitive of Bolivia, the country of the type locality of this species.

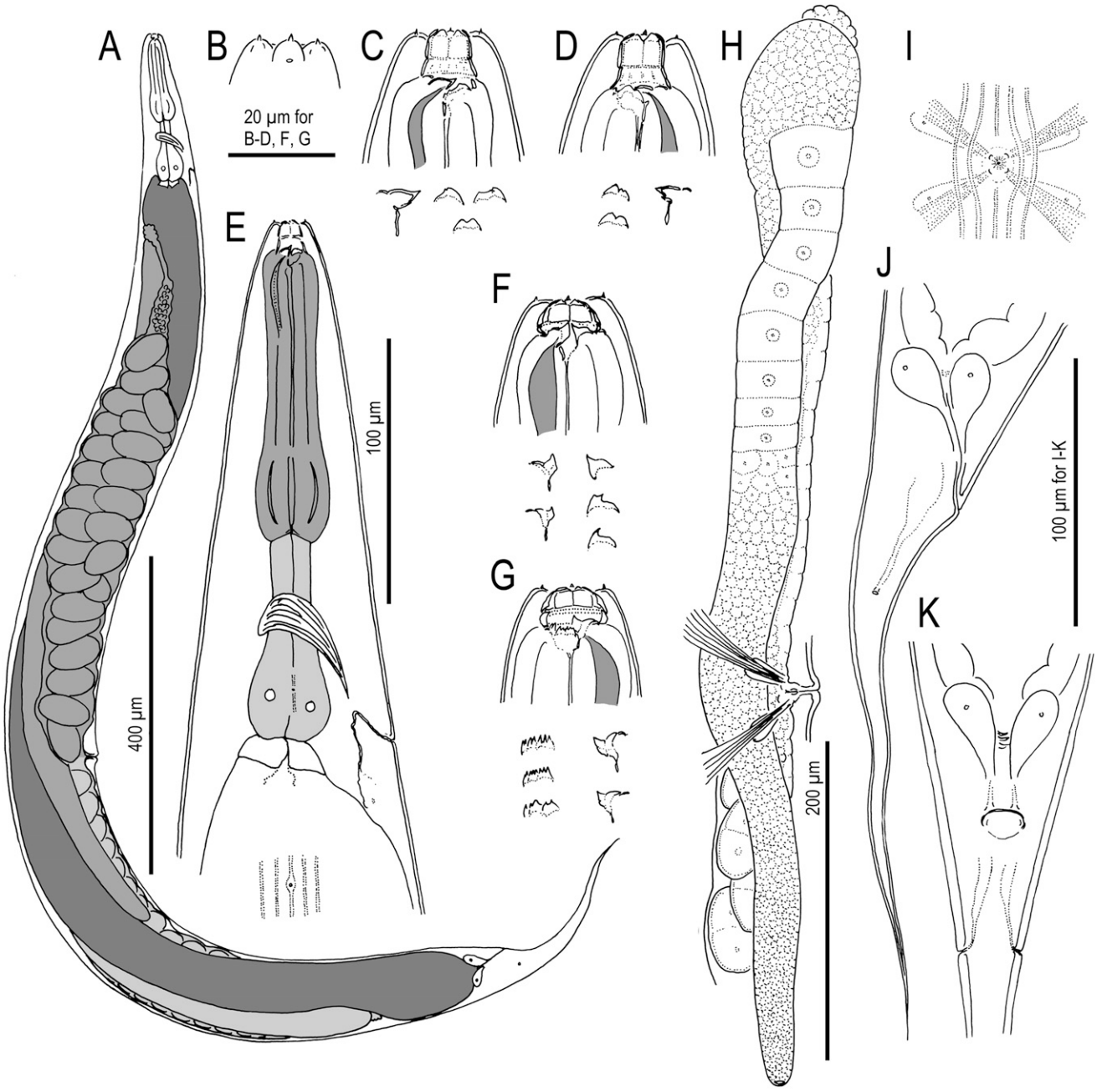

Fig. 3. Adult hermaphrodite of *Pristionchus boliviae* n. sp.: A. Whole body of stenostomatous individual in right lateral view. B. Lip region in lateral view. C. Stenostomatous form in right lateral view, showing dorsal tooth (below, left) and three variants of right subventral ridge with two cusps (below, right). D. Stenostomatous form in left lateral view, showing two variants of left subventral ridge (below, left) and dorsal tooth (below, right). E. Neck region of stenostomatous form in right lateral view. F. Eurystomatous hermaphrodite in right lateral view, showing two variants of dorsal tooth (below, left) and three variants of right subventral tooth (below, right). G. Eurystomatous hermaphrodite in left lateral view, showing three variants of left subventral ridge (below, left) and two variants of dorsal tooth (below, right). H. Anterior gonadal branch in right lateral view. I. Vulva in ventral view. J. Tail in right lateral view. K. Anus in ventral view.

proximal part of gonad. Spicules slender, smoothly curved in ventral view, adjacent to each other for distal third of their length, each smoothly tapering to pointed distal end. Spicule in lateral view smoothly ventrally arcuate, giving spicule about 100° curvature, slender oval manubrium, sometimes three times longer than wide, present at anterior end; lamina-calomus complex not ventrally expanded, such that anterior end of calomus is not offset from lamina, lamina smoothly tapering to pointed distal end. In one individual, spicules were grossly protracted with flattened manubria. Gubernaculum conspicuous, stout, less than one-third of spicule in length, broad anteriorly such that dorsal wall is recurved and dorsal and ventral walls separate at a 45° angle at posterior end. In lateral view, anterior part of gubernaculum with two serial curves separated by an acute, anteriorly directed process, with open anterior curvature and a deep terminal curvature about a third of

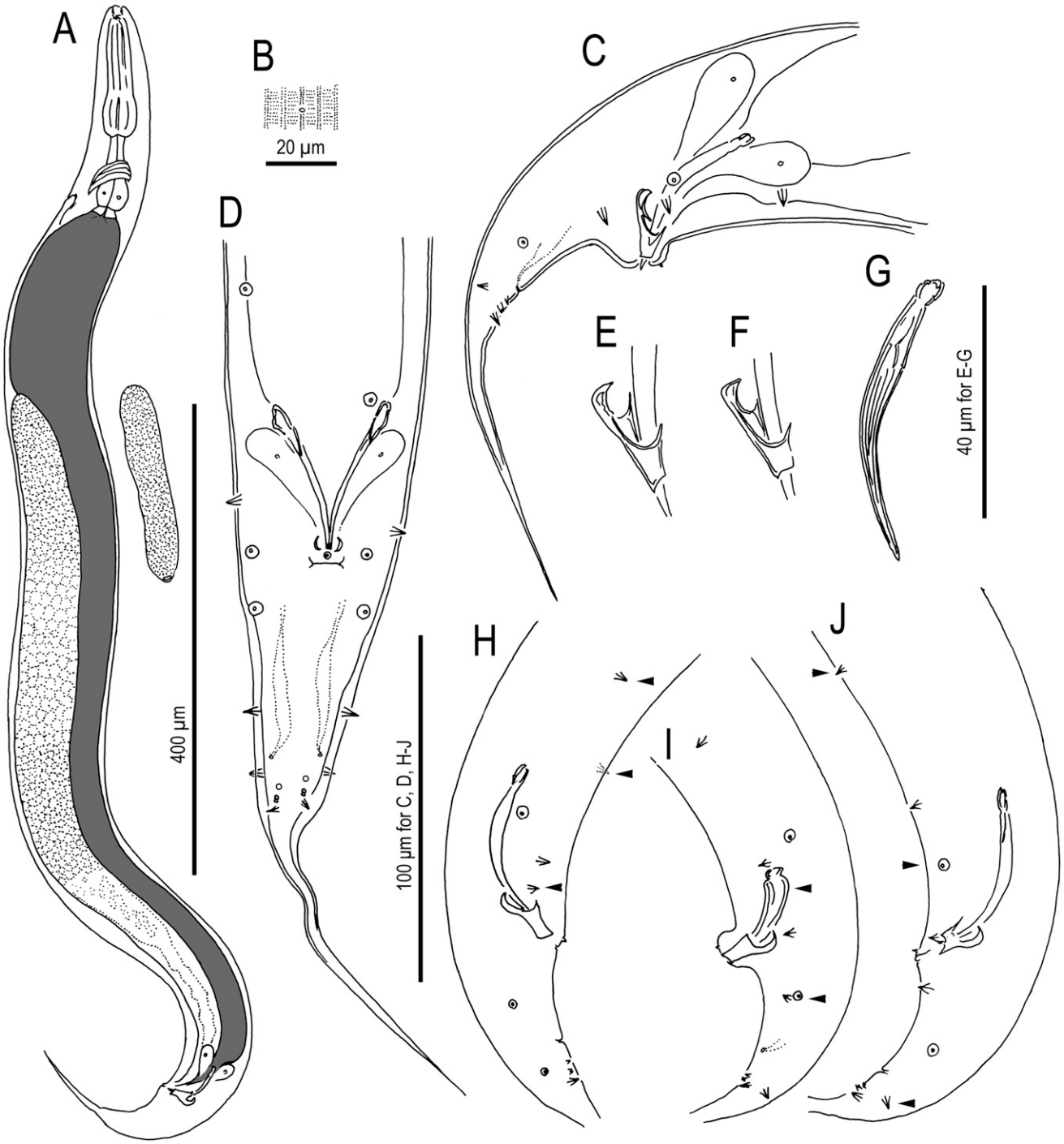

FIG. 4. Adult male of *Pristionchus boliviae* n. sp.: A. Whole body in left lateral view, in addition to reflexed part of testis (right). B. Excretory pore in ventral view. C. Tail in right lateral view. D. Tail in ventral view. E,F. Two variants of gubernaculum in right lateral view. G. Spicule in right lateral view of spicule. H–J. Variation of male tail observed in strain RS5518. H. Arrowheads indicate asymmetry of v1 pair (right v1 is far anterior to left v1) and anterior position of v4. I. Arrowheads indicate malformed spicule and duplicated ad papilla. J. Arrowheads indicate extra anterior ("v0") papilla and anterior positions of v2d and pd.

gubernaculum length; posterior part forming a short tube, about one-third of gubernaculum length, enveloping spicules. Nine pairs of genital papillae and a pair of phasmids present and arranged as <v1, (v2d, v3), C, v4, ad, Ph, (v5, v6, v7, pd)> (= <P1, (P2d, P3), C, P4, P5d, Ph, (P6, P7, P8, P9d)> in nomenclature of Kanzaki et al., 2012a, 2012b). Absolute positions of papillae, particularly v1–v4, highly variable (Figs. 4H–4J,5). Position of v1 papillae variable and asymmetrical, being from level of manubrium to much farther anterior, v2d slightly anterior to more than one cloacal body width anterior to C, v3 more consistent, usually within one-half cloacal body width anterior to v4, C and v4 clustered within two-thirds cloacal body width, ad closer to v4 than to v5 or a half

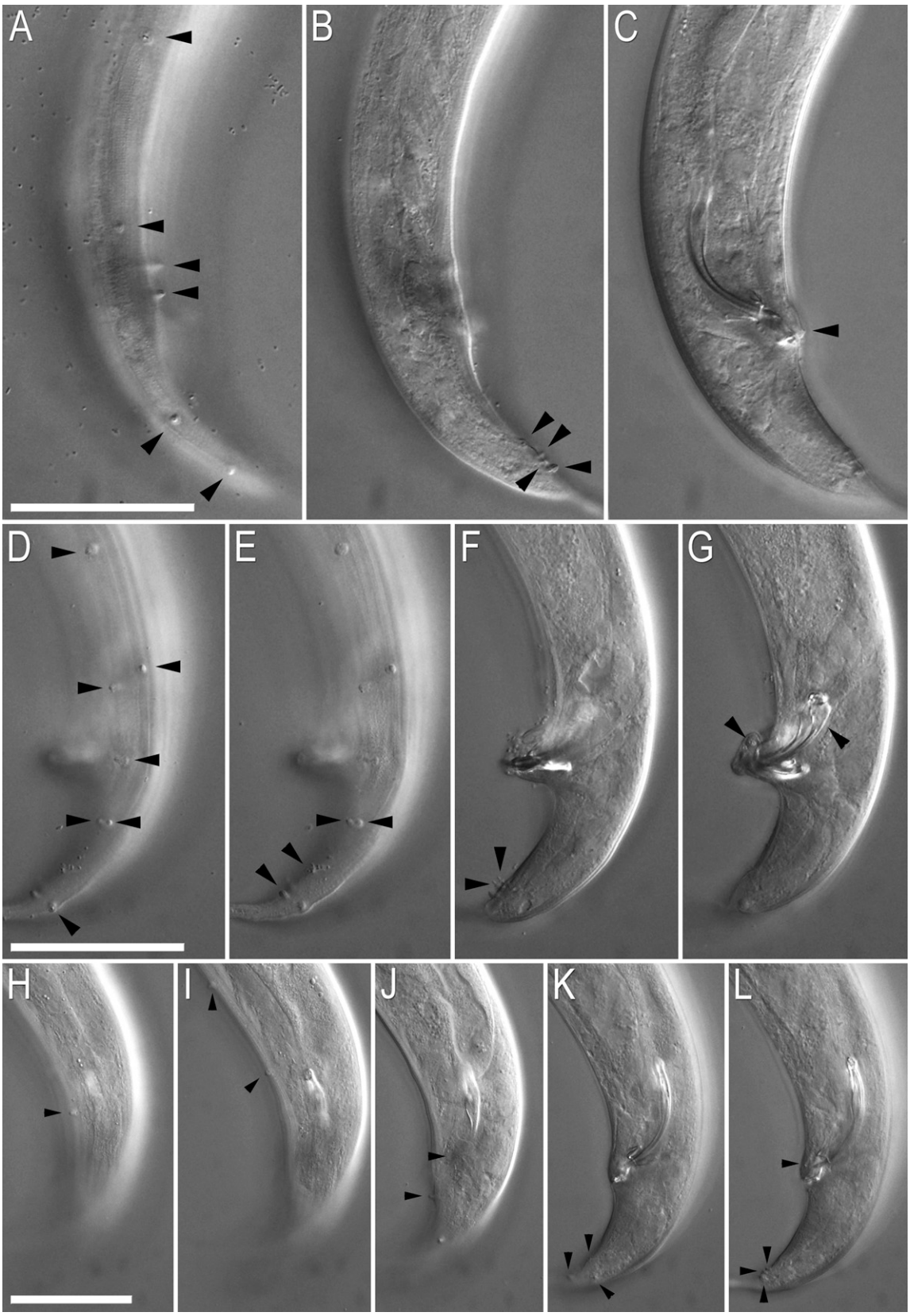

FIG. 5. Variation in male sexual morphology in *Pristionchus boliviae* n. sp. (strain RS5518) (scale bars are 50 μm): A–C. DIC micrographs of a single individual, summarized in Fig. 4H, in different focal planes and at the same scale. Arrowheads from top to bottom indicate: v1, v2d, v3, v4, ad, and pd in (A); phasmid, v5, v6, and v7 in (B); unpaired ventral papilla (vs) in (C). D–G. A second individual, summarized in Fig. 4I. Arrowheads from top to bottom indicate: v1, v2d, v3, v4, ad (duplicated), and pd in (A); ad (duplicated), phasmid, and P8 in (B); v5 and v6 in (C); malformed spicule and vs in (D). H–L. A third individual, summarized in Fig. 4J. Arrowheads from top to bottom indicate: v2d in (A); "v0" (extra anterior papilla) and v1 in (B); v3, v4, and ad in (C); phasmid, v7, and pd in (D); and vs, v5, v6, and v7 in (E).

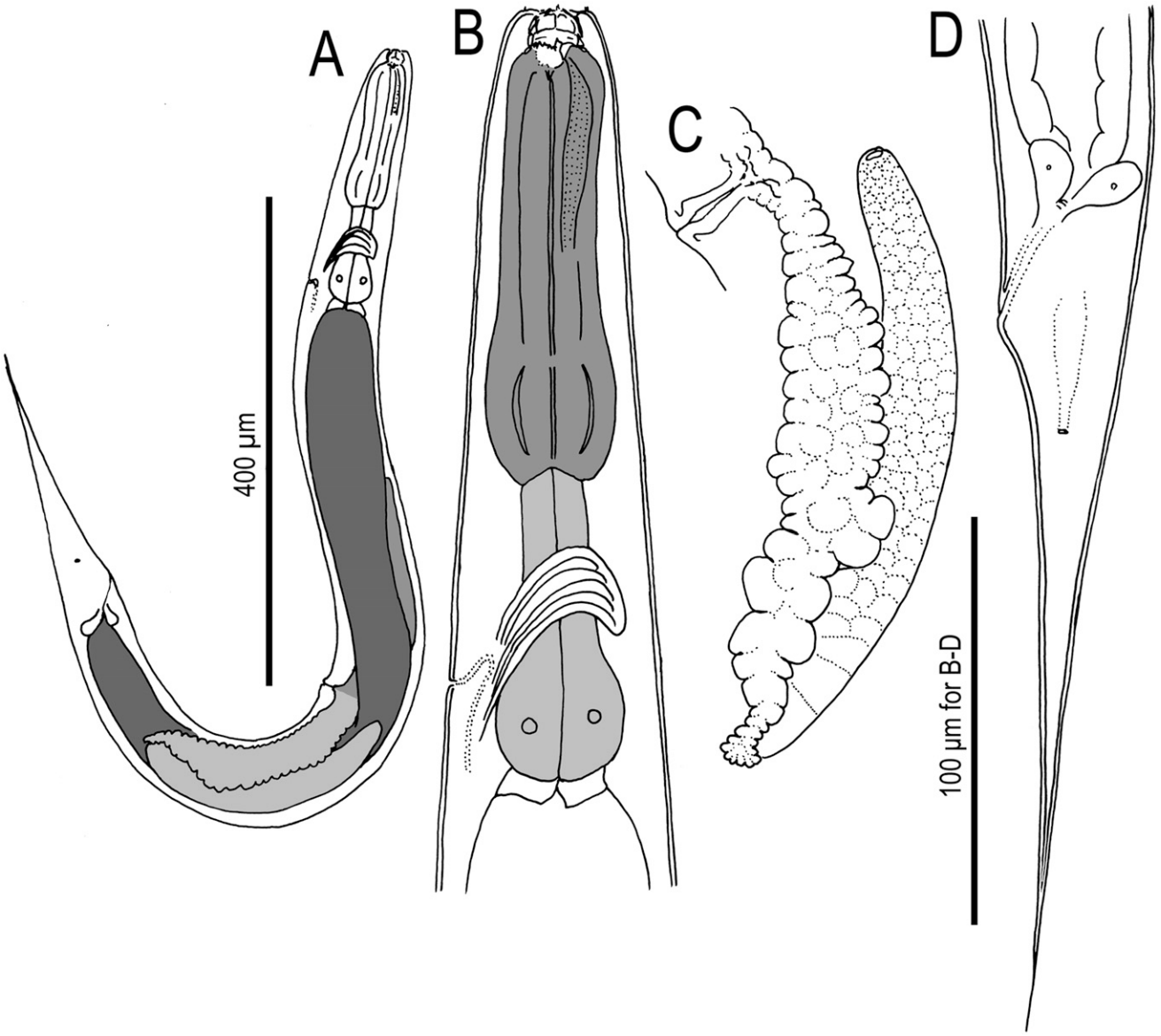

Fig. 6. Young adult eurystomatous hermaphrodite of *P. boliviae* n. sp. (RS5262): A. Whole body in left lateral view. B. Neck region in left lateral view. C. Posterior gonadal branch in left lateral view. D. Tail in left lateral view.

cloacal width posterior to v4, Ph at about same level of or just anterior to v5, v7 lateral to v5 and v6, such that v5–v7 form a triangle, and pd anterior, from level of v5/v6 to just posterior to phasmid. Additional papillae sometimes observed: one individual had a single papilla ("v0") far anterior to v1, and another individual had a duplicated ad (P5d) papilla on one side.

Diagnosis and relationships: Besides its generic characters, *P. boliviae* n. sp. is diagnosed by male genital papillae arranged as <v1, (v2d, v3), C, v4, ad, Ph, (v5, v6, v7, pd)>, whereby v1–v4 are highly variable in absolute position, particularly v1, positions of which are also often asymmetrical, v7 is lateral to v5/v6, v9 is at level of v5/v6 to just posterior of phasmid, and with occasional additional papillae, including "v0" and duplicated papillae (e.g., ad). *Pristionchus boliviae* n. sp. is distinguished from the closest known hermaphroditic species, *P. mayeri* n. sp., by a slender (up to three times longer than wide) vs. rounded (up to twice as long as wide) manubrium, although character states overlap in these two species; the posterior tube of gubernaculum being short (one-third gubernaculum length) vs. long (one-half length), and with the anterior opening of the tube being open, i.e., ventral and dorsal walls separating at 45° angle vs. narrow, i.e., walls separating at 30°; lamina-calomus complex not vs. distinctly ventrally expanded; papilla v7 consistently lateral to vs. in line with v5/v6; its unique SSU rRNA sequence, which differs from that of *P. mayeri* n. sp. in five to six nucleotide positions in a diagnostic 472-bp fragment of the gene. It is further distinguished from *P. mayeri* n. sp. by prezygotic reproductive isolation, namely the inability to form F1 hybrids. The species is

TABLE 3. Morphometrics of eurystomatous male holotype (in glycerin) and male and hermaphrodite specimens of *Pristionchus boliviae* n. sp. (temporary water mounts). All measurements made in μm and given in the form: mean ± sd (range).

Character	Eurystomatous male		Stenostomatous male Temporary water mounts	Eurystomatous hermaphrodite Temporary water mount	Stenotomatous hermaphrodite Temporary water mounts
	Holotype	Temporary water mounts			
n	-	5	10	5	10
L	904	993 ± 14 (975-1009)	988 ± 36 (907-1027)	996 ± 152 (916-1266)	1389 ± 259 (1115-1977)
L′	776	878 ± 15 (854-895)	867 ± 27 (829-920)	809 ± 135 (727-1048)	1172 ± 242 (931-1719)
a	18	14 ± 1.2 (13-15)	15 ± 1.0 (13-16)	16 ± 0.8 (15-17)	15 ± 2.2 (12-17)
b	6.5	6.1 ± 0.1 (5.9-6.2)	6.0 ± 0.3 (5.7-6.6)	5.5 ± 0.7 (5.0-6.7)	7.3 ± 1.2 (6.2-9.9)
c	7.1	8.7 ± 0.6 (8.1-9.7)	8.4 ± 1.5 (6.7-12)	5.3 ± 0.5 (4.8-5.8)	6.4 ± 0.8 (5.2-7.7)
c′	3.8	3.0 ± 0.3 (2.6-3.3)	3.0 ± 0.4 (2.4-3.7)	6.6 ± 0.9 (5.6-8.0)	5.6 ± 1.0 (4.1-7.3)
T or V	65	62 ± 2.1 (60-64)	61 ± 2.7 (58-66)	47 ± 1.9 (44-50)	47 ± 2.1 (42-50)
Maximum body diam.	50	73 ± 5.4 (65-78)	67 ± 4.5 (62-75)	61 ± 8.4 (54-75)	95 ± 34 (66-169)
Stoma width	10.5	9.4 ± 0.5 (8.7-10.0)	6.9 ± 0.5 (6.3-7.6)	10.8 ± 0.4 (10.2-11.2)	6.7 ± 0.6 (6.0-7.5)
Stoma height (cheilo- + gymnostom)	5.8	5.9 ± 0.8 (4.6-6.6)	6.8 ± 0.8 (6.1-8.8)	7.6 ± 0.8 (6.2-8.2)	8.8 ± 0.9 (7.4-10.2)
Stoma height (to base of stegostom)	10.8	9.3 ± 1.5 (6.9-10.7)	10.7 ± 0.7 (9.9-11.6)	11.0 ± 0.4 (10.6-11.5)	12.6 ± 1.0 (11.1-14.1)
Neck length (head to base of pharynx)	140	163 ± 4.0 (158-169)	166 ± 7.4 (156-175)	181 ± 5.7 (175-190)	192 ± 5.3 (181-200)
Anterior pharynx (pro- + metacorpus)	78	95 ± 2.2 (93-98)	95 ± 3.1 (91-99)	108 ± 4.8 (103-114)	115 ± 3.6 (108-119)
Posterior pharynx (isthmus + basal bulb)	56	62 ± 4.5 (58-69)	64 ± 4.2 (59-69)	65 ± 3.3 (63-70)	69 ± 4.0 (64-76)
Post./ant. pharynx ratio	72	65 ± 5.8 (59-73)	68 ± 3.1 (63-73)	61 ± 4.4 (57-68)	60 ± 4.3 (54-69)
Excretory pore from ant. end	127	127 ± 3.5 (123-133)	128 ± 6.7 (115-138)	143 ± 9.6 (135-159)	154 ± 9.5 (137-170)
Testis length	65	613 ± 14 (596-633)	606 ± 29 (582-659)	-	-
Ant. female gonad	-	-	-	225 ± 86 (179-378)	356 ± 70 (247-499)
Post. female gonad	-	-	-	200 ± 49 (171-287)	381 ± 101 (228-529)
Vulva to anus distance	-	-	-	342 ± 54 (309-438)	528 ± 132 (368-775)
Cloacal or anal body diam.	34	38 ± 2.0 (35-40)	40 ± 3.9 (32-46)	29 ± 5.8 (22-37)	40 ± 9.5 (31-62)
Tail length	128	115 ± 8.1 (102-121)	121 ± 20 (78-151)	187 ± 22 (157-218)	218 ± 25 (184-258)
Spicule length (curve)	58	53 ± 12 (33-63)	58 ± 5.5 (50-67)	-	-
Spicule length (chord)	48	43 ± 8.9 (27-49)	45 ± 4.8 (37-52)	-	-
Gubernaculum length	19	17 ± 2.8 (12-19)	20 ± 1.8 (16-22)	-	-

distinguished from the following species by a hermaphroditic vs. gonochoristic mode of reproduction: the morphologically and molecularly circumscribed species *P. aerivorus*, *P. elegans*, *P. lheritieri*, and *P. uniformis*; the molecularly and biologically circumscribed species *P. americanus*, *P. marianneae*, *P. pauli*, and *P. pseudaerivorus*; the morphologically, molecularly, and biologically circumscribed species *P. arcanus*, *P. exspectatus*, and *P. japonicus*.

Type host (carrier) and locality: The culture from which the type specimens were obtained was originally isolated by M. Herrmann from an adult *Cyclocephala amazonica* (Coleoptera: Scarabaeidae) collected 4 km south of Buena Vista, Bolivia (17°29.074' S, 63°38.775' W) in November 2006.

Distribution: Besides its collection from the type locality and type host, the species was isolated as strain RS5518 from an unidentified scarab beetle in Colombia.

Type material, type strain, and nomenclatural registration: Holotype eurystomatous male, two paratype stenostomatous males, one paratype eurystomatous hermaphrodite, and three paratype stenostomatous hermaphrodites deposited in the University of California Riverside Nematode Collection (UCRNC), CA. Four paratype stenostomatous hermaphrodites (SMNH Type-8421) deposited in the Swedish Natural History Museum, Stockholm, Sweden. Four paratype stenostomatous hermaphrodites deposited in the Natural History Museum Karlsruhe, Germany. The type strain is available in living culture and as frozen stocks under culture code RS5262 in the Department of Evolutionary Biology, Max Planck Institute (MPI) for Developmental Biology, Tübingen, Germany, and can be provided to other researchers upon request. The new species binomial has been registered in the ZooBank database (zoobank.org) under the identifier [94C3F8D7-AF07-4BB7-B377-881E112A6F04].

Pristionchus mayeri n. sp.[*]

= *Pristionchus* sp. 25 *apud* Herrmann et al. (2010)

(Figs. 7-9)

Measurements: See Table 4.

Description of species-specific characters:

Adults: Species androdioecious, consisting of males and self-fertile hermaphrodites.

Stenostomatous form: Stegostom bearing: a large, conspicuous, flint-shaped (or inverted "V"-shaped) dorsal tooth; in the right subventral sector, a crescent-shaped or half-circular ridge with a small, short, and pointed subventral denticle; in the left subventral sector, a crescent-shaped ridge with two small peaks, often with apparent cleavage between two main peaks. Dorsal tooth sclerotized at surface.

Eurystomatous form: Stegostom bearing: a large claw-like dorsal tooth; a large claw-like right subventral tooth; in the left subventral sector, a row of left subventral denticles of varying numbers and size, i.e., six to eight medium-sized and small cusps, sometimes with irregular shape, all projecting from a common cuticular plate that appears split midway along its length. Dorsal and right subventral teeth movable. Left subventral denticles immovable.

Male: Spontaneous males rare (< 1%, strain RS5460) to relatively common (up to 5%, RSA035) in culture. Spermatogonia arranged in four to 10 rows in reflexed part, then well-developed spermatocytes arranged as three to eight rows in anterior two-thirds of main branch, then mature amoeboid spermatids arranged in multiple rows in remaining, proximal part of gonad. Spicules smoothly curved in ventral view, adjacent to each other for distal third of their length, each smoothly tapering to pointed distal end. Spicule in lateral view smoothly ventrally arcuate, giving spicule about 100° curvature, with wide, rounded manubrium present at anterior end; lamina-calomus complex expanded just posterior to manubrium, then smoothly tapering to pointed distal end. Gubernaculum conspicuous, about one-third of spicule in length, slightly broader anteriorly such that dorsal and ventral walls separate at a 30° angle at posterior end. In lateral view, anterior part of gubernaculum with two serial curves separated by a ventrolaterally directed cusp and with deep, convex, terminal curvature two-fifths to half of gubernaculum length; posterior part forming a tube, about half of gubernaculum length, enveloping spicules. With usually nine pairs of genital papillae and a pair of phasmids present and arranged as <v1, (C, v2, v3d), v4, ad, Ph, (v5, v6, v7, pd)> (= <P1, (C, P2, P3d), P4, P5d, Ph, (P6, P7, P8, P9d)> in nomenclature of Kanzaki et al., 2012a, 2012b). Some individuals with extra papilla or pair of papillae ("v0") about two cloacal body widths anterior of v1. Single or pair of v1 sometimes missing. Positions of v1 papillae asymmetrical and located about one cloacal body width posterior to cloacal slit, v2 twice as far from v1 than from v4, v3d slightly or conspicuously anterior to v2, C and v3 close to (within one-half cloacal body width) of v4, ad located middle of v4 and v6, Ph around middle between ad and v5 or close to ad, v5–v7 linearly arranged, and pd variable, from same level as v7 to slightly anterior of v5.

Diagnosis and relationships: Besides its generic characters, *P. mayeri* n. sp. is diagnosed by male genital papillae arranged as <v1, (C, v2, v3d), v4, ad, Ph, (v5, v6, v7, pd)>, whereby v3 is within one-half cloacal body width of v4 and pd is at same level as or anterior to v7, and by the presence in some individuals of an additional, anterior "v0" papilla, either single or as a pair. *Pristionchus mayeri* n. sp. is distinguished from the closest known hermaphroditic species, *P. mayeri* n. sp., by a rounded (up to twice as long as wide) vs. slender (up to three times longer than wide) manubrium, although character states overlap in these two species; the posterior tube of gubernaculum being long (one-half gubernaculum length) vs. short (one-third length), and with the anterior opening of the tube being narrow, i.e., ventral and dorsal walls separating at 30° angle vs. open, i.e., walls separating at 45°; lamina-calomus complex distinctly vs. not ventrally expanded; v7 papilla in line with vs. consistently lateral to v5/v6; its unique SSU rRNA sequence, which differs from that of *P. boliviae* n. sp. in five to six nucleotide positions in a diagnostic 472-bp fragment of the gene. It is further distinguished from *P. boliviae* n. sp. by prezygotic reproductive isolation, namely the inability to form F1 hybrids. The species is distinguished from the following species by a hermaphroditic vs. gonochoristic mode of reproduction: the morphologically and molecularly circumscribed species *P. aerivorus*, *P. elegans*, *P. lheritieri*, and *P. uniformis*; the molecularly and biologically

[*] This species is named in honor of our colleague Dr. Werner E. Mayer (deceased), whose work in the molecular systematics of Diplogastridae provided the necessary framework for comparative studies in *Pristionchus*.

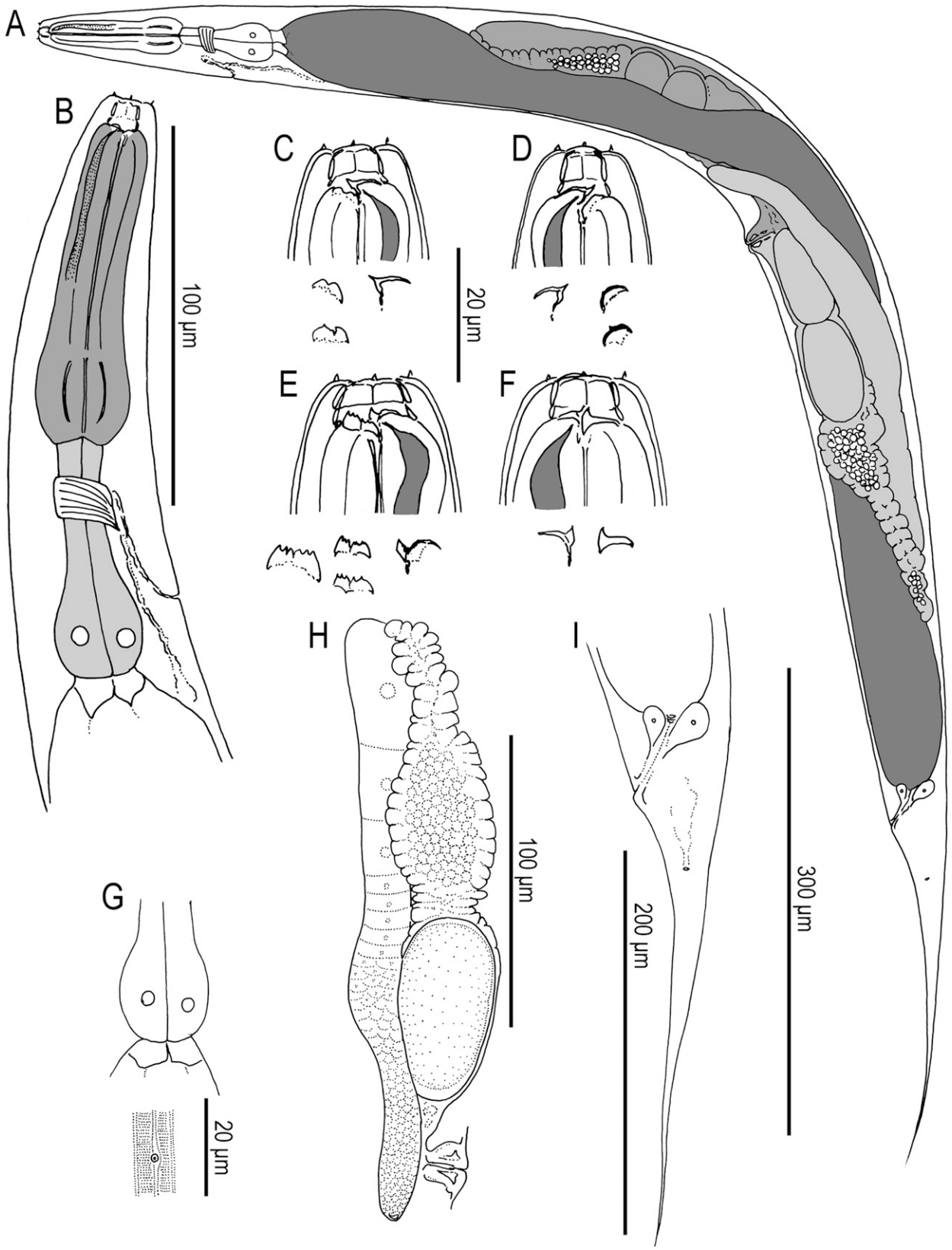

Fig. 7. Adult hermaphrodite of *Pristionchus mayeri* n. sp.: A. Whole body of stenostomatous individual in left lateral view. B. Neck region of stenostomatous individual in right lateral view. C. Stenostomatous form in left lateral view, showing two variants of left subventral ridge (below, left) and dorsal tooth (below, right). D. Stenostomatous form in right lateral view, showing dorsal tooth and two variants of left subventral ridge. E. Eurystomatous form in left lateral view, showing three variants of left subventral ridge (below, left) and dorsal tooth (below, right). F. Eurystomatous form in right lateral view, showing dorsal tooth (below, left) and right subventral tooth (below, right). G. Deirid. H. Anterior gonadal branch in right lateral view. I. Tail in left lateral view.

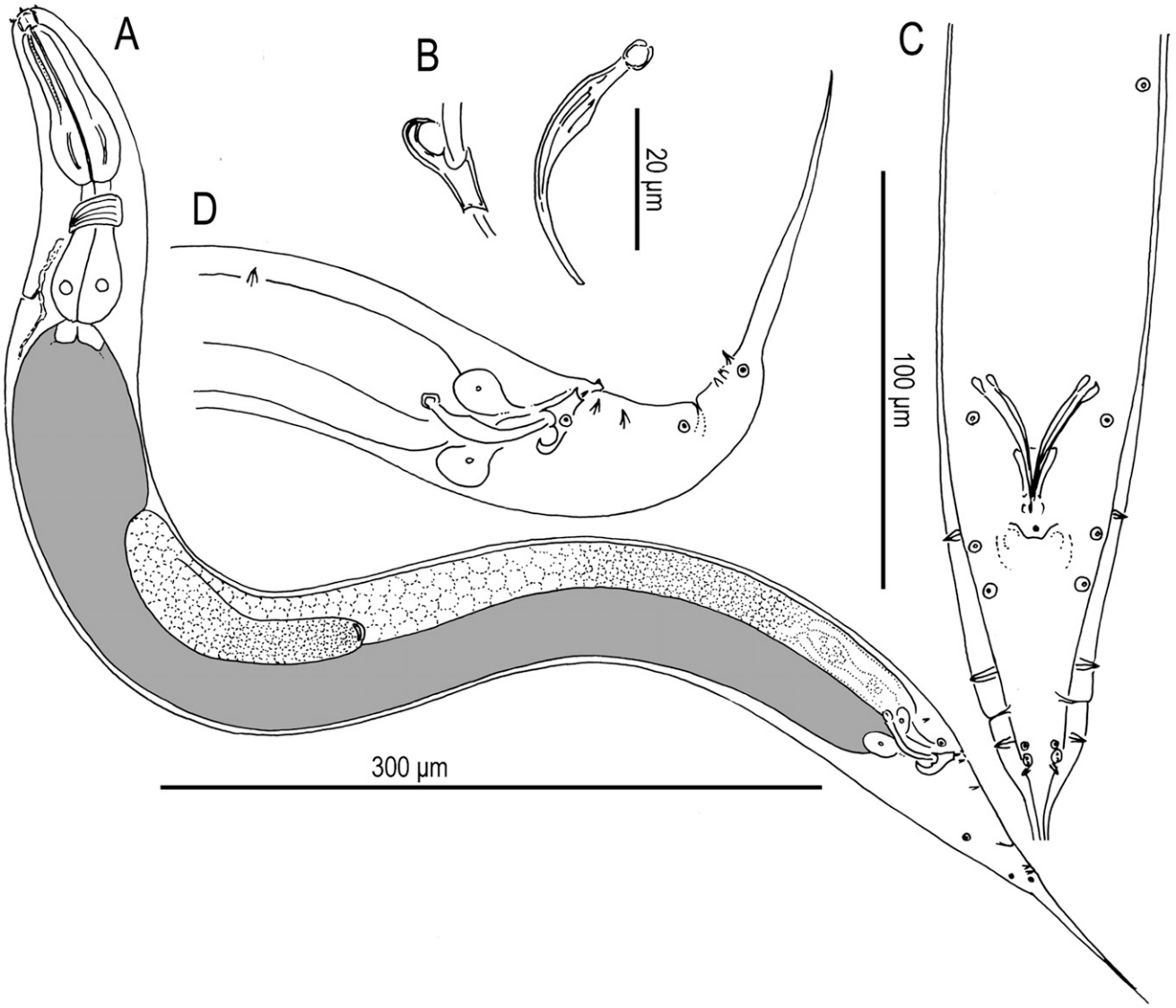

Fig. 8. Adult male of *Pristionchus mayeri* n. sp.: A. Whole body of stenostomatous individual in right lateral view. B. Gubernaculum and spicule in right lateral view. C. Tail in ventral view. D. Tail in right lateral view.

circumscribed species *P. americanus*, *P. marianneae*, *P. pauli*, and *P. pseudaerivorus*; the morphologically, molecularly, and biologically circumscribed species *P. arcanus*, *P. exspectatus*, and *P. japonicus*.

Type host (carrier) and locality: The culture from which the type specimens were obtained was originally isolated from an adult *Hoplochelus marginalis* (Coleoptera: Scarabaeidae) collected by M. Herrmann from Trois Bassins on La Réunion Island in January 2009 (Herrmann et al., 2010).

Distribution: Besides its collection from the type locality and type host, it was isolated from *Adoretus* sp. (Coleoptera: Scarabaeidae) at Grand Étang and Colorado during subsequent trips to La Réunion. The species was also isolated from soil in Madagascar and from *Adoretus* sp., *Heteronychus licas*, *Hyposerica tibialis*, *Hy. vinsoni*, and *Phyllophaga smithi* (Coleoptera: Scarabaeidae) in Lakaz Chamarel and Black River Gorges National Park in Mauritius.

Type material, type strain, and nomenclatural registration: Holotype stenostomatous hermaphrodite, three paratype stenostomatous hermaphrodites, one paratype eurystomatous hermaphrodite, and two paratype stenostomatous males deposited in the UCRNC, CA. Four paratype stenostomatous hermaphrodites (SMNH Type-8422) deposited in the Swedish Natural History Museum, Stockholm, Sweden. Four paratype stenostomatous hermaphrodites deposited in the Natural History Museum Karlsruhe, Germany. The type strain is available in living culture and as frozen stocks under culture code RS5460 in the Department of Evolutionary Biology, MPI for Developmental Biology, Tübingen, Germany, and can be provided to other researchers upon request. The new species binomial has been registered in the ZooBank

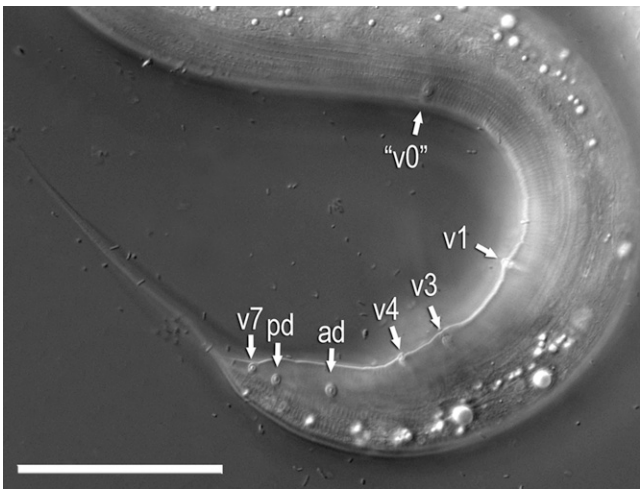

FIG. 9. Male genital papillae of *Pristionchus mayeri* n. sp.: View is left lateral. Scale bar is 20 μm. Characteristic of this species is closeness (less than one-half cloacal body width) of papilla v3 to v4 and a position of pd overlapping or anterior to v5–v7. Papilla arrangement is unusually variable in this species, as sometimes shown by the presence of an extra anterior papilla "v0."

database (zoobank.org) under the identifier [B15074FC-0903-4E7E-81A8-EC2040F229D2].

Pristionchus atlanticus n. sp.[*]
= *Pristionchus* sp. 3 *apud* Mayer et al. (2007, 2009)
(Figs. 10-11)

Measurements: See Table 5.

Description of species-specific characters:

Adults: Species gonochoristic (i.e., dioecious), with males and females.

Stenostomatous form: Stegostom bearing: a large, conspicuous, flint-shaped (or inverted "V"-shaped) dorsal tooth; a crescent-shaped right subventral ridge with minute denticle on medial (inner) side; two bump-like (blunt) left subventral denticles projecting from a common cuticular plate, often with apparent cleavage between two main peaks. Dorsal tooth sclerotized at surface.

Eurystomatous form: In type strain, typically smaller than stenostomatous form, possibly as a result of starvation. Stegostom bearing: a large claw-like dorsal tooth; a large claw-like right subventral tooth; in the left subventral sector, a row of usually four medium-sized to large pointed subventral cusps projecting from a common cuticular plate that appears split midway along its length. Dorsal and right subventral teeth movable. Left subventral denticles immovable.

Male: Spicules smoothly curved in ventral view, adjacent to each other for distal third of their length, each smoothly tapering to pointed distal end. Spicule in lateral view smoothly ventrally arcuate, giving spicule about 100° curvature, oval manubrium present at anterior end; lamina-calomus complex expanded just posterior to manubrium, then smoothly tapering to pointed distal end. Gubernaculum conspicuous, about one-third of spicule in length, relatively narrow anteriorly such that dorsal and ventral walls separate at a 15° angle at posterior end. In lateral view, anterior part of gubernaculum with two serial curves separated by anteriorly and ventrally directed process with shallow but distinctly concave terminal curvature; posterior part forming a tube enveloping spicules. Nine pairs of genital papillae and a pair of phasmids present and arranged as <v1, v3d, (C, v2), v4, ad, Ph, (v5, v6, v7), pd> (= <P1, P2d, (C, P3), P4, P5d, Ph, (P6, P7, P8), P9d> in nomenclature of Kanzaki et al., 2012a, 2012b). Positions of v1 papillae about one cloacal body width posterior to cloacal slit, C/v3 and v4 very close to each other (clustered within less than one-quarter cloacal body width), ad twice as far from v4 than from v5, Ph midway between ad and v5, v5 located less than ½ cloacal body width posterior to ad, v5–v7 linearly arranged. Tail spike about two cloacal body widths long.

Diagnosis and relationships: Besides its generic characters, *P. atlanticus* n. sp. is diagnosed by male genital papillae arranged as <v1, v3d, (C, v2), v4, ad, Ph, (v5, v6, v7), pd>, whereby v2d and v4 are very close to each other (within one-quarter cloacal body width) and also far from both v1 and ad, and whereby pd is clearly posterior to v7. *Pristionchus atlanticus* is separated from all other gonochoristic species in the *maupasi* group by reproductive isolation (Herrmann et al., 2006). The species is distinguished from the closest known gonochoristic species, *P. pauli*, by v3 and v4 being separated by less than one-quarter vs. about one-half cloacal body width. It is further distinguished from all other gonochoristic species by its unique SSU rRNA sequence, and it differs from *P. pauli* in at least two nucleotide positions in a diagnostic 472-bp fragment of the gene (Herrmann et al., 2006).

Type host (carrier) and locality: The culture from which the type specimens were obtained was originally isolated by Andrew Chisholm and Marie-Anne Félix from soil in a flowerbed at Cold Spring Harbor Laboratory, NY.

Type material, type strain, and nomenclatural registration: Holotype stenostomatous male, four paratype stenostomatous females, and three paratype eurystomatous females deposited in the UCRNC, CA. Two paratype stenostomatous males, two paratype stenostomatous females, and one paratype eurystomatous hermaphrodite (SMNH Type-8418–SMNH Type-8420) deposited in the Swedish Natural History Museum, Stockholm, Sweden. Three paratype stenostomatous males, two paratype stenostomatous females, and one paratype eurystomatous female deposited in the Natural History Museum Karlsruhe, Germany. The type strain is available in living culture and as frozen stocks under culture code CZ3975 in the Department of Evolutionary Biology, MPI for Developmental Biology, Tübingen, Germany and can be provided to other researchers upon request. The new

[*] The species epithet is a Latin adjective referring to the species' North American type locality near the Atlantic Ocean.

TABLE 4. Morphometrics of stenostomatous hermaphrodite holotype (in glycerin) and hermaphrodite and male specimens of *Pristionchus mayeri* n. sp. (temporary water mounts). All measurements made in μm and given in the form: mean ± sd (range).

Character	Stenostomatous hermaphrodite		Eurystomatous hermaphrodite	Stenostomatous male
	Holotype	Temporary water mounts	Temporary water mounts	Temporary water mounts
n	-	10	10	10
L	1194	1041 ± 48 (962-1115)	847 ± 81 (703-956)	921 ± 53 (830-995)
L′	1004	839 ± 53 (764-915)	698 ± 72 (551-768)	797 ± 54 (699-880)
a	16	15 ± 0.7 (14-16)	14 ± 1.4 (12-16)	12 ± 0.8 (10-13)
b	8.3	6.3 ± 0.2 (5.8-6.6)	5.6 ± 0.3 (5.1-6.1)	6.3 ± 0.3 (5.8-6.6)
c	6.3	5.2 ± 0.5 (4.3-5.8)	5.8 ± 0.8 (4.5-7.2)	7.5 ± 0.8 (6.4-8.7)
c′	5.1	6.6 ± 0.4 (5.9-7.3)	5.8 ± 0.8 (4.6-7.0)	3.1 ± 0.4 (2.5-3.9)
T or V	49	47 ± 2.5 (42-50)	46 ± 3.7 (38-50)	62 ± 3.1 (57-69)
Maximum body diam.	76	71 ± 3.6 (65-77)	60 ± 2.9 (56-64)	80 ± 2.6 (76-85)
Stoma width	5.7	6.6 ± 0.6 (5.4-7.2)	10.1 ± 0.6 (9.0-11.2)	6.0 ± 0.5 (5.4-6.8)
Stoma height (cheilo- + gymnostom)	6.2	7.9 ± 0.9 (6.7-9.4)	6.2 ± 0.5 (5.4-7.4)	6.3 ± 0.4 (5.6-6.7)
Stoma height (to base of stegostom)	9.8	10.4 ± 0.7 (9.0-11.4)	8.8 ± 0.8 (7.6-10.1)	8.9 ± 0.5 (8.3-9.8)
Neck length (head to base of pharynx)	144	166 ± 8.8 (154-182)	151 ± 7.7 (134-157)	147 ± 4.3 (141-152)
Anterior pharynx (pro- + metacorpus)	75	94 ± 5.2 (86-100)	85 ± 3.2 (79-90)	81 ± 2.3 (78-85)
Posterior pharynx (isthmus + basal bulb)	63	65 ± 6.4 (53-75)	60 ± 4.9 (49-64)	60 ± 2.3 (57-63)
Post./ant. pharynx ratio	84	69 ± 7.0 (58-79)	71 ± 4.1 (62-76)	74 ± 2.4 (71-80)
Excretory pore from ant. end	137	135 ± 11 (117-149)	116 ± 8.6 (104-131)	116 ± 3.8 (112-123)
Testis length	-	-	-	571 ± 51 (509-671)
Ant. female gonad	268	229 ± 11 (216-252)	184 ± 25 (133-221)	-
Post. female gonad	241	199 ± 27 (159-224)	169 ± 24 (130-223)	-
Vulva to anus distance	425	353 ± 17 (319-372)	286 ± 40 (212-356)	-
Cloacal or anal body diam.	37	31 ± 2.0 (27-34)	25 ± 1.8 (23-29)	40 ± 2.7 (36-43)
Tail length	190	202 ± 14 (186-230)	148 ± 23 (119-187)	124 ± 12 (111-143)
Spicule length (curve)	-	-	-	47 ± 2.1 (44-50)
Spicule length (chord)	-	-	-	39 ± 1.9 (37-42)
Gubernaculum length	-	-	-	16 ± 1.6 (14-19)

species binomial has been registered in the ZooBank database (zoobank.org) under the identifier [8F62BBFE-35DC-45E2-BAB4-E5F3307E8A12].

Informative male-specific characters in the maupasi *group:* To further diagnose *P. boliviae* n. sp., *P. mayeri* n. sp., and *P. atlanticus* n. sp. with respect to other species in the *maupasi* group, we examined previously unreported characters of the male tail in *P. americanus*, *P. marianneae*, *P. pauli*, and *P. pseudaerivorus*, and provide new, comparable character information for *P. aerivorus* and *P. maupasi* (Fig. 12A). Species in the *maupasi* group were previously circumscribed based on reproductive isolation and molecular sequence divergence (Herrmann et al., 2006). Male papilla characters clearly separating these species by morphology include: positions of v2d and v3 relative to C; position of v4 relative to v3 and v2d; position of pd relative to v5–v7. Character states for the arrangement of papillae v1–v3 in

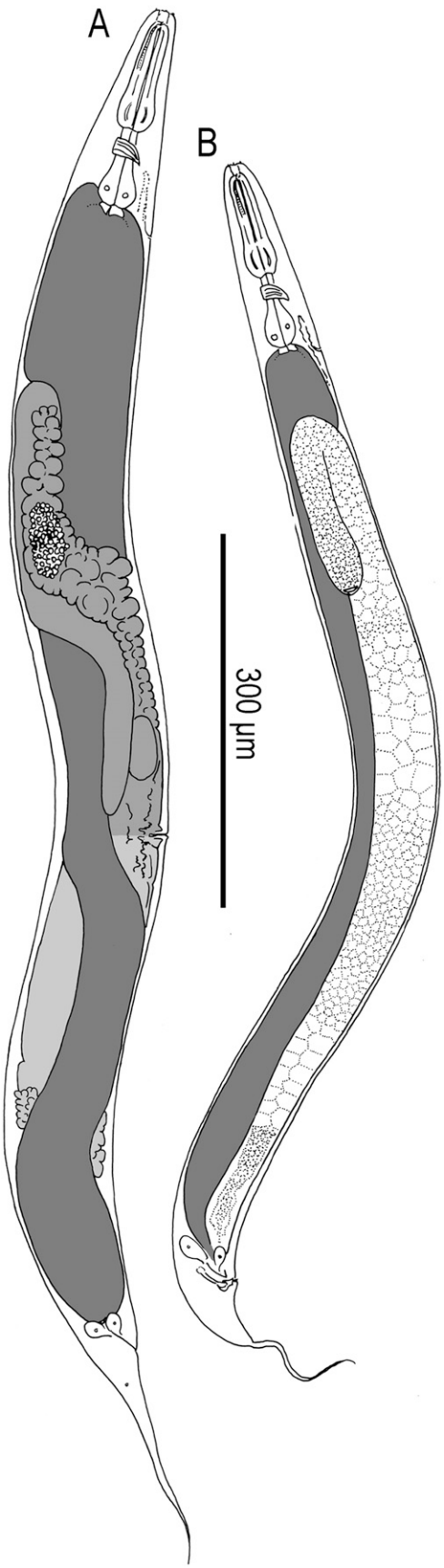

FIG. 10. Adults of *Pristionchus atlanticus* n. sp.: View is right lateral. A. Whole body of adult stenostomatous female. B. Whole body of adult stenostomatous male.

gonochoristic taxa and *P. maupasi* are informative of the phylogenetic structure within the *maupasi* group (Fig. 12B). Specifically, the position of the second ventral papilla relative to the first dorsal papilla is posterior in the basal species of the group, *P. pauli*, *P. marianneae*, and *P. americanus*, whereas it is anterior in *P. aerivorus*, *P. pseudaerivorus*, and *P. maupasi*. In both *P. boliviae* n. sp. and *P. mayeri* n. sp., the most posterior dorsal papilla (pd) overlaps or is anterior to the three posterior ventral papillae (v5–v7). The papilla patterns in *P. boliviae* n. sp. and *P. mayeri* n. sp. are variable within the species, including inconsistent position and presence of v1, the inconsistent presence of an extra anterior papilla "v0," the precise position of pd relative to v5–v7, and the absolute (but not relative) positions of v1–v4 in *P. boliviae* n. sp.

Of other valid *Pristionchus* species that have not been placed in a molecular phylogenetic context, *P. vidalae* (Stock, 1993) Sudhaus and Fürst von Lieven, 2003 has papillae arranged in an order similar to others in the *maupasi* group. This species, isolated from *Diabrotica speciosa* (Coleoptera: Chrysomelidae) in Argentina, shows a pattern of <v1, v2d, v3, C, v4, ad, [Ph], (v5, v6, v7), pd> (presumed phasmids were described as an extra pair of papillae), whereby v2d is far anterior to v3 and almost equidistant from v3 and v1, v4 is far anterior to ad and close to C, and ad is close to Ph. The arrangement in *P. vidalae* is thus closest to that of *P. atlanticus* n. sp. and *P. americanus*, and it is clearly distinguished from both species by the anterior positions of vd and presumed Ph. However, other morphological characters available for this species are presently insufficient to confidently place it in the *maupasi* group.

DISCUSSION

Description of androdioecious species in a model system introduces a resource for comparative studies on the evolution of reproductive mode. Characterizing the new *Pristionchus* species by morphological and molecular phylogenetic evidence, including 27 gene loci in the present study, lays the necessary foundation for future work on these species as potential models. Increasing outgroup representation by description of the gonochoristic species *P. atlanticus* n. sp. gives greater resolution to tracking evolutionary events leading to androdioecy. Between the two closest species described herein, *P. boliviae* n. sp. and *P. mayeri* n. sp., molecular phylogenetic divergence was greater than that separating several other *Pristionchus* species pairs (Herrmann et al., 2006; Kanzaki et al., 2012a). Their identities as unique biological species were confirmed by their reproductive isolation in hybrid mating tests. Morphological characters further distinguish all three species.

Characters diagnostic of Pristionchus *species:* Most morphological characters traditionally scored in Diplogastridae are invariant or vary to similar degrees within and across species of *Pristionchus* (Kanzaki et al., 2012a,

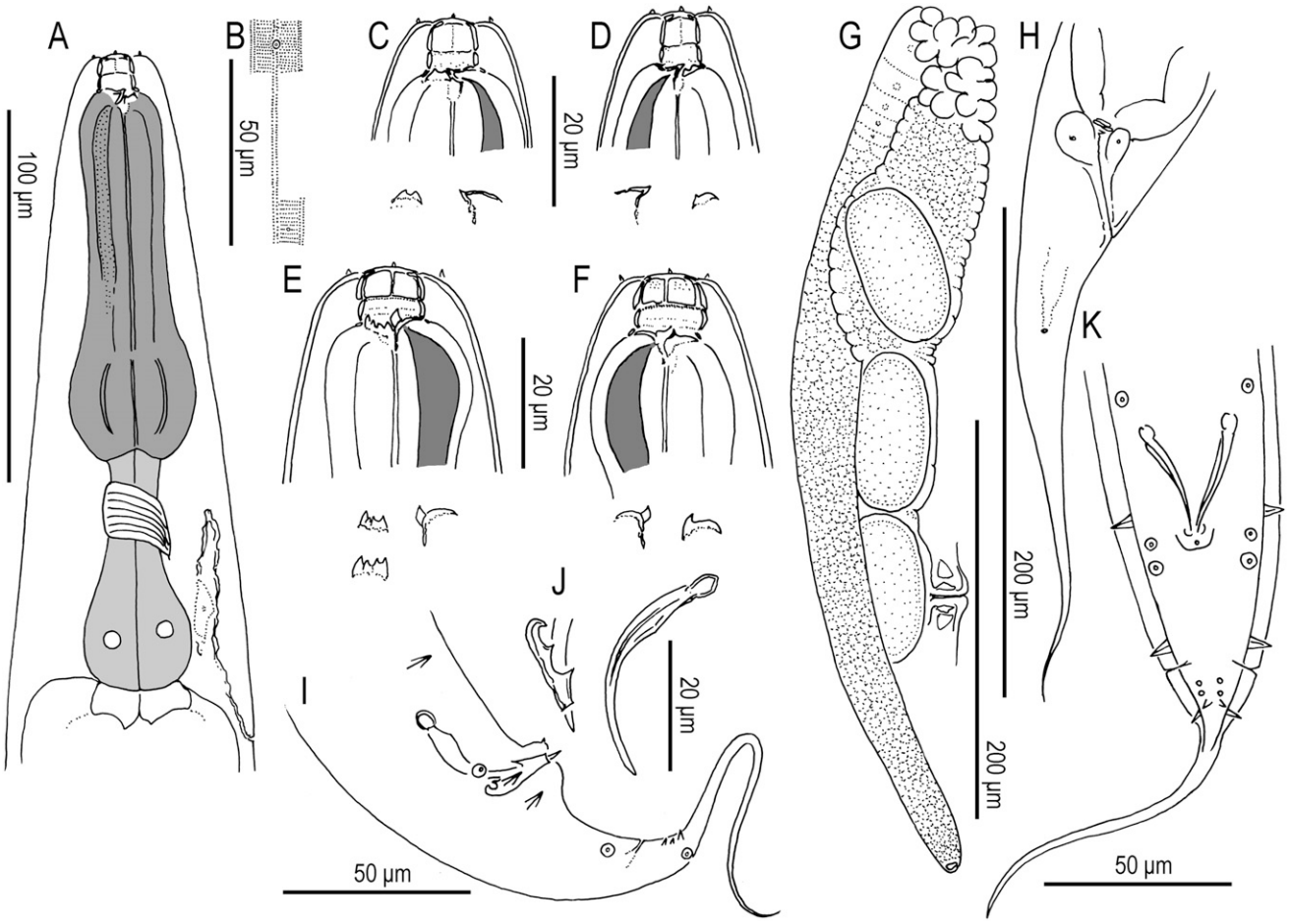

FIG. 11. *Pristionchus atlanticus* n. sp.: A–H. Adult female. I–K. Adult male. A. Neck region of stenostomatous individual in right lateral view. B. Deirid (above) and "postdeirid" (below). C. Stenostomatous form in left lateral view, showing left subventral ridge (below, left) and dorsal tooth (below, right). D. Stenostomatous form in right lateral view, showing dorsal tooth (below, left) and right subventral ridge (below, right). E. Eurystomatous form in left lateral view, showing two variants of the left subventral ridge, which is host to four pointed cusps (below, left), and dorsal tooth (below, right). F. Eurystomatous form in right lateral view, showing dorsal tooth (below, left) and right subventral tooth (below, right). G. Anterior gonadal branch in right lateral view. H. Tail in right lateral view. I. Tail in right lateral view. J. Gubernaculum and spicule in right lateral view. K. Tail in ventral view.

2012b; Fürst von Lieven and Sudhaus, 2000). In contrast, the morphology of the stoma, especially in the teeth and denticles, are often informative in characterizing *Pristionchus* species (Kanzaki et al., 2012a, 2012b), as they show topography complex enough to track minor differences by light microscopy. Within the *maupasi* group of species, however, much of this variability was also present within species, and so any particular denticle in the more complex arrangements cannot be reliably assigned a homologous state. Any variability of stomatal structures in *Pristionchus* species is therefore most useful for diagnosis in conjunction with other characters, especially those of the male sexual structures. A trait common to all three species and including other species in the *maupasi* group is the size of mouthparts, particularly the dorsal tooth, in the stenostomatous form (Ragsdale, unpubl. data). This tooth is typically large and often similar in size to the dorsal tooth of the eurystomatous form of the same species, although it is always flint-shaped and only sclerotized at the surface, as typical for the genus. Male genitalia, especially in the shape of the gubernaculum, were clearly distinct in all three new species. Arguably the most informative characters were in the arrangement of male genital papilla (Fig. 12). This interspecific variability, shown previously also for the *pacificus* group (Kanzaki et al., 2012a) and in more basal *Pristionchus* species (Kanzaki et al., 2012b), attests to the usefulness of these characters for diagnoses in the genus.

Divergence of male sexual structures in androdioecious species: In contrast to gonochoristic species, the two new androdioecious species showed substantial variation in male sexual characters. In particular, the presence of an additional single lateral papilla or pair of papillae ("v0") in *P. boliviae* n. sp. and *P. mayeri* n. sp. is unusual given the generally consistent number of nine papillae across the family (Sudhaus and Fürst von Lieven, 2003). The occasional appearance of an extra papilla was also observed in *P. maupasi* by Potts (1910), who noted increased variability in that androdioecious species compared with gonochorists. Furthermore, the position of

TABLE 5. Morphometrics of stenomatous male holotype (in glycerin) and male and female specimens of *Pristionchus atlanticus* n. sp. (temporary water mounts). All measurements made in μm and given in the form: mean ± sd (range).

Character	Stenostomatous male		Eurystomatous male	Stenostomatous female	Eurystomatous female
	Holotype	Temporary water mounts	Temporary water mounts	Temporary water mounts	Temporary water mounts
n	-	10	10	10	10
L	652	896 ± 191 (578-1084)	584 ± 24 (547-619)	1173 ± 276 (803-1530)	672 ± 65 (551-757)
L′	630	957 ± 181 (483-957)	479 ± 22 (448-505)	982 ± 253 (651-1304)	506 ± 64 (391-590)
a	15	17 ± 1.6 (14-19)	17 ± 1.1 (16-19)	14 ± 0.8 (13-15)	15 ± 2.1 (12-20)
b	5.8	6.6 ± 0.9 (4.9-7.6)	4.9 ± 0.2 (4.6-5.2)	7.8 ± 1.2 (6.0-9.1)	5.1 ± 0.5 (4.3-5.8)
c	6.0	7.4 ± 1.2 (7.1-10.1)	5.6 ± 0.3 (5.2-6.0)	6.1 ± 0.8 (4.7-7.3)	4.1 ± 0.5 (3.1-4.5)
c′	4.9	3.7 ± 0.5 (3.1-4.5)	4.2 ± 0.3 (3.8-4.8)	5.9 ± 0.5 (4.8-6.8)	7.3 ± 0.4 (7.0-8.1)
T or V	62	60 ± 8.6 (43-67)	46 ± 3.9 (40-54)	49 ± 1.6 (45-51)	49 ± 6.0 (44-64)
Maximum body diam.	44	55 ± 16 (32-72)	34 ± 2.3 (31-38)	86 ± 23 (59-121)	45 ± 4.3 (38-51)
Stoma width	4.3	4.8 ± 0.9 (3.7-6.5)	6.3 ± 0.3 (5.9-6.9)	5.4 ± 0.8 (4.0-6.7)	8.9 ± 0.9 (7.6-10.3)
Stoma height (cheilo- + gymnostom)	6.3	6.9 ± 1.0 (5.3-8.7)	6.0 ± 1.0 (4.8-7.7)	9.0 ± 0.9 (7.4-10.0)	7.0 ± 0.7 (5.5-7.8)
Stoma height (to base of stegostom)	10.2	10.4 ± 0.9 (8.4-11.7)	10.0 ± 0.9 (8.7-11.4)	12.7 ± 0.8 (11.6-14.2)	11.9 ± 0.9 (10.5-12.9)
Neck length (head to base of pharynx)	112	136 ± 15 (117-162)	119 ± 6.0 (107-126)	149 ± 15 (128-168)	132 ± 8.6 (115-148)
Anterior pharynx (pro- + metacorpus)	64	75 ± 7.5 (67-89)	65 ± 2.7 (60-69)	83 ± 7.1 (73-93)	73 ± 4.5 (66-81)
Posterior pharynx (isthmus + basal bulb)	42	53 ± 6.7 (44-64)	48 ± 3.0 (42-51)	57 ± 7.9 (44-67)	53 ± 4.6 (42-59)
Post./ant. pharynx ratio	66	71 ± 4.2 (66-78)	74 ± 3.5 (70-80)	68 ± 5.1 (59-74)	72 ± 4.3 (64-79)
Excretory pore from ant. end	116	140 ± 19 (108-173)	111 ± 8.0 (100-122)	160 ± 25 (115-192)	120 ± 6.8 (110-134)
Testis length	401	550 ± 173 (249-728)	269 ± 26 (227-319)	-	-
Ant. female gonad	-	-	-	286 ± 88 (154-390)	123 ± 20 (82-144)
Post. female gonad	-	-	-	250 ± 84 (122-352)	103 ± 12 (82-119)
Vulva to anus distace	-	-	-	403 ± 110 (252-535)	209 ± 21 (170-233)
Cloacal or anal body diam.	22	33 ± 5.2 (25-39)	25 ± 0.7 (24-26)	33 ± 6.5 (25-45)	23 ± 1.6 (20-26)
Tail length	108	121 ± 14 (95-137)	104 ± 5.7 (96-114)	191 ± 25 (151-226)	167 ± 17 (151-210)
Spicule length (curve)	45	45 ± 4.9 (36-51)	37 ± 3.1 (36-44)	-	-
Spicule length (chord)	38	38 ± 3.9 (31-44)	31 ± 2.4 (26-34)	-	-
Gubernaculum length	17	16 ± 1.9 (13-19)	14 ± 1.1 (12-15)	-	-

pd in *P. boliviae* n. sp. and *P. mayeri* n. sp. varied with respect to the ventral v5–v7, sometimes assuming in both species a unique, anterior position (Figs. 5,8,9). Variability in papilla position was especially pronounced in *P. boliviae* n. sp., in which the absolute positions of v1–v4 were variable, with bilateral asymmetry common for v1, and in which a single ad papilla was even duplicated in one specimen. The inconsistency of male sexual characters in *P. boliviae* n. sp., *P. mayeri* n. sp., and apparently also *P. maupasi* (Potts, 1910), is in line with predictions of "selfing syndrome," whereby mating-related traits become degenerate in males due to the reduced sexual selection pressure in a mostly self-fertilizing population (Thomas et al., 2012). In particular, the poor ability of males of *P. boliviae* n. sp. and *P. mayeri* n. sp. to cross in comparison with other *Pristionchus* species under similar experimental conditions (Herrmann et al., 2006) is consistent with the degeneracy of male

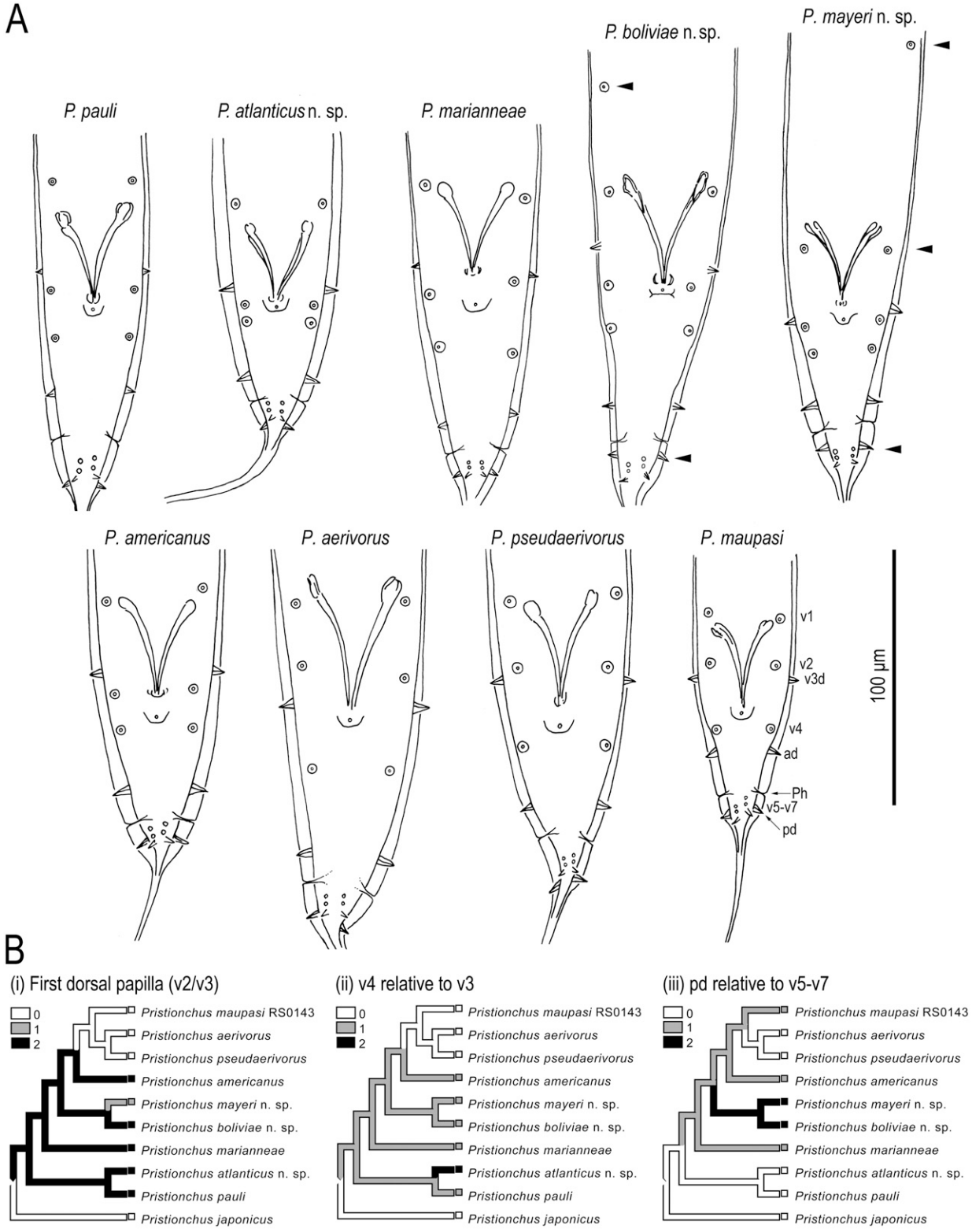

Fig. 12. Diagnostic and phylogenetically informative male tail characters of the male tail of *Pristionchus*: A. Line drawings of genital papilla arrangement, shown in ventral view, in *Pristionchus* species of the *maupasi* group. Diagnostic characters include: opportunistic presence of "v0"; distance of v1 form v2/v3; relative positions of v2 and v3; positions of v2 and v3 relative to (C); position of pd relative to v5–v7; position of pd as variable. B. Ancestral state reconstruction of three male papilla characters in the *maupasi* group by simple parsimony, as implemented in Mesquite v.2.5 (Maddison and Maddison, 2011). Tree is from maximum likelihood analysis (Fig. 2). Characters and states are as follows: (i) identity of first dorsal papilla is v3 (0), v2/v3 (papillae are at same level) (1), or v2 (2); (ii) position of v4 relative to v3 is two-thirds to more than one cloacal body width or "far" (0), about one-half cloacal body width or "close" (1), or less than one-third cloacal body width or "very close" (2); (iii) most anterior position of pd relative to v5–v7 is posterior (0), overlapping (1), or anterior (2). Character states for outgroup, *P. japonicus*, are from Kanzaki et al. (2012a).

sexual morphology in the former species. An extra, anterior male papilla has also been observed in the gonochoristic species *Micoletzkya masseyi* (Susoy et al., 2013) and *Koerneria* sp. (Kanzaki, unpubl. data), suggesting a latent propensity for this developmental aberration. The variable presence of "v0" and v1, as well as the intermediately located papillae in *P. boliviae* n. sp., raises the possibility that variability in v0 and v1 is linked to inappropriate cell division or apoptosis in the cell lineage of v1, the presumptive homolog of Rn.1 descendants in rhabditid nematodes (Fitch and Emmons, 1995).

Implications for the evolution of reproductive mode in Pristionchus*:* The existence of two closely related androdioecious species raises the question of how common speciation and thus diversification is in taxa with a self-fertilizing reproductive mode. In *Caenorhabditis* nematodes, transitions to androdioecy have been recent events (Kiontke et al., 2004; Cutter et al., 2008). Because the accumulation of deleterious mutations is predicted to cause rapid extinction in purely asexual lineages (Muller, 1964), occasional outcrossing may have contributed to the persistence of androdioecious *Pristionchus* species as it has in *Caenorhabditis* (Loewe and Cutter, 2008). Is the sister relationship of the species *P. boliviae* n. sp. and *P. mayeri* n. sp. evidence that androdioecious species are not only evolutionarily stable, but capable of divergence? Based on taxon representation thus far, this is the most parsimonious scenario. Although uncommon, cladogenesis of androdioecious species is possible, as inferred for the rhabditid genus *Oscheius* (Felix et al., 2001; Kiontke and Fitch, 2005) and *Eulimnadia* clam shrimps (Weeks et al., 2006, 2009). Conversely, is sampling incomplete in this clade of *Pristionchus*, in which case the evolution of hermaphroditism would have arisen twice in closely related taxa? This prediction would be consistent with the observation that hermaphroditic species often exist in pairs with morphologically close gonochoristic species (i.e., "complemental species pairs" sensu Potts, 1908), presumably sharing recent common ancestry and possibly having speciated in sympatry (Osche, 1954). Ongoing efforts for denser taxon sampling will hopefully test whether closer gonochoristic sister species exist for *P. boliviae* n. sp. or *P. mayeri* n. sp. The empirically poor outcrossing ability of both of these species hints at the presence of incipient reproductive barriers within them, which if present in nature would facilitate speciation in these lineages. The capacity of some strains of *P. boliviae* n. sp. (strain RS5262) and *P. mayeri* n. sp. (RSA035) to produce high numbers of spontaneous males, for example, in comparison with *P. pacificus* (Click et al., 2009), may also have an impact on the population structure of these species.

In an alternative to androdioecy, many strains of *P. entomophagus* lack males altogether (Steiner, 1929) and cannot be made to induce them (D'Anna and Sommer, unpubl. data), including by incubation conditions that increase their incidence in androdioecious *Caenorhabditis* species (Hodgkin, 1999). The elimination of males from self-fertilizing strains would be consistent with the theoretical difficulties of maintaining androdioecy (Charlesworth, 1984; Pannell, 2002). However, the selection of androdioecy against males would also select for those that are successful outcrossers, which would explain why they are not completely lost in androdioecious nematode species (Chasnov, 2010). Therefore, the buildup of deleterious mutations or the inability to respond through recombination to strong selection pressure in obligate self-fertilizers of *P. entomophagus* would be predicted and thus suggests the recent evolution of hermaphroditism in this species. Achieving more thorough taxon representation in the *entomophagus* group will be a valuable step in testing this hypothesis.

Literature Cited

Charlesworth, D. 1984. Androdioecy and the evolution of dioecy. Biological Journal of the Linnean Society 23:333–348.

Chasnov, J. R. 2010. The evolution from females to hermaphrodites results in a sexual conflict over mating in androdioecious nematode worms and clam shrimp. Journal of Evolutionary Biology 23:539–556.

Chitwood, B. G. 1937. Cephalic structure and stoma. P. 53 *in* B. G. Chitwood and M. B. Chitwood, eds. Introduction to nematology. Baltimore: Monumental.

Click, A., Savaliya, C. H., Kienle, S., Herrmann, M., and Pires-daSilva, A. 2009. Natural variation of outcrossing in the hermaphroditic nematode *Pristionchus pacificus*. BMC Evolutionary Biology. 9:75.

Cutter, A. D., Wasmuth, J. D., and Washington, N. L. 2008. Patterns of molecular evolution in Caenorhabditis preclude ancient origins of selfing. Genetics 178:2093–2104.

Darwin, C. 1877. The different forms of flowers on plants of the same species. New York: Appelton.

Denver, D. R., Clark, K. A., and Raboin, M. J. 2011. Reproductive mode evolution in nematodes: insights from molecular phylogenies and recently discovered species. Molecular Phylogenetics and Evolution 61:584–592.

Edgar, R. C. 2004. MUSCLE: Multiple sequence alignment with high accuracy and high throughput. Nucleic Acids Research 32:1792–1797.

Fedorko, A., and Stanuszek, S. 1971. *Pristionchus uniformis* sp. n. (Nematoda, Rhabditida, Diplogasteridae), a facultative parasite of *Leptinotarsa decemlineata* Say and *Melolontha melolontha* L. in Poland. Morphology and biology. Acta Parastiologica 19:95–112.

Félix, M. A., Vierstraete, A., and Vanfleteren, J. 2001. Three biological species closely related to *Rhabditis (Oscheius) pseudodolichura* Körner in Osche, 1952. Journal of Nematology 33:104–109.

Fitch, D. H. A., and Emmons, S. W. 1995. Variable cell positions and cell contacts underlie morphological evolution of the rays in the male tails of nematodes related to *Caenorhabditis elegans*. Developmental Biology 170:564–582.

Floyd, R., Abebe, E., Papert, A., and Blaxter, M. 2002. Molecular barcodes for soil nematode identification. Molecular Ecology 11:839–850.

Fürst von Lieven, A. 2008. *Koerneria sudhausi* n. sp. (Nematoda: Diplogastridae); a hermaphroditic diplogastrid with an egg shell formed by zygote and uterine components. Nematology 10:27–45.

Fürst von Lieven, A., and Sudhaus, W. 2000. Comparative and functional morphology of the buccal cavity of Diplogastrina (Nematoda) and a first outline of the phylogeny of this taxon. Journal of Zoological Systematics and Evolutionary Research 38: 37–63.

Haag, E. S. 2009. Convergent evolution: Regulatory lightning strikes twice. Current Biology R977–R979.

Herrmann, M., Kienle, S., Rochat, J., Mayer, W. E., and Sommer, R. J. 2010. Haplotype diversity of the nematode *Pristionchus pacificus* on Réunion in the Indian Ocean suggests multiple independent invasions. Biological Journal of the Linnean Society 100:170–179.

Herrmann, M., Mayer, W. E., and Sommer, R. J. 2006. Sex, bugs and Haldane's rule: The nematode genus *Pristionchus* in the United States. Frontiers in Zoology 3:14.

Hodgkin, J. 1999. Conventional genetics. Pp. 245-270 *in* I. A. Hope, ed. *C. elegans*: A practical approach. Oxford, UK: Oxford University Press.

Hooper, D. J. 1986. Handling, fixing, staining and mounting nematodes. Pp. 59–80 *in* J. F. Southey, ed. Methods for work with plant and soil nematodes. London: Her Majesty's Stationary Office.

Kanzaki, N., Ragsdale, E. J., Herrmann, M., Mayer, W. E., and Sommer, R. J. 2012a. Description of three *Pristionchus* species (Nematoda: Diplogastridae) from Japan that form a cryptic species complex with the model organism *P. pacificus*. Zoological Science 29:403–417.

Kanzaki, N., Ragsdale, E. J., Herrmann, M., and Sommer, R. J. 2012b. Two new species of *Pristionchus* (Rhabditida: Diplogastridae): *P. fissidentatus* n. sp. from Nepal and La Réunion Island and *P. elegans* n. sp. from Japan. Journal of Nematology 44:80–91.

Kiontke, K., and Fitch, D. H. A. 2005. The phylogenetic relationships of *Caenorhabditis* and other rhabditids. (August 11, 2005). The *C. elegans* Research Community, ed. WormBook. doi/10.1895/wormbook.1.11.1.

Kiontke, K., Gavin, N. P., Raynes, Y., Roehrig, C., Piano, F., and Fitch, D. H. A. 2004. *Caenorhabditis* phylogeny predicts convergence of hermaphroditism and extensive intron loss. Proceedings of the National Academy of Sciences of the United States of America 101:9003–9008.

Kiontke, K., Manegold, A., and Sudhaus, W. 2001. Redescription of *Diplogasteroides nasuensis* Takaki, 1941 and *D. magnus* Völk, 1950 (Nematoda: Diplogastrina) associated with Scarabaeidae (Coleoptera). Nematology 3:817–832.

Kreis, H. A. 1932. Beiträge zur Kenntnis pflanzenparasitischer Nematoden. Zeitschrift für Parasitenkunde 5:184–194.

Lewis, S. C., Dyal, L. A., Hilburn, C. F., Weitz, S., Liau, W. S., LaMunyon, C. W., and Denver, D. R. 2009. Molecular evolution in *Panagrolaimus* nematodes: Origins of parthenogenesis, hermaphroditism and the Antarctic species *P. davidi*. BMC Evolutionary Biology 9:15.

Loewe, L., and Cutter, A. D. 2008. On the potential for extinction by Muller's Ratchet in *Caenorhabditis elegans*. BMC Evolutionary Biology 8:125.

Maddison, W. P., and Maddison, D. R. 2011. Mesquite: A modular system for evolutionary analysis. Version 2.75. URL: http://mesquiteproject.org.

Maupas, E. 1919. Essais d'hybridation chez les nématodes. Bulletin Biologique de la France et de la Belgique 52:466–498.

Mayer, W. E., Herrmann, M., and Sommer, R. J. 2007. Phylogeny of the nematode genus *Pristionchus* and implications for biodiversity, biogeography and the evolution of hermaphroditism. BMC Evolutionary Biology 7:104.

Mayer, W. E., Herrmann, M., and Sommer, R. J. 2009. Molecular phylogeny of beetle associated diplogastrid nematodes suggests host switching rather than nematode-beetle coevolution. BMC Evolutionary Biology 9:212.

Merrill, J. H., and Ford, A. L. 1916. Life history and habits of two new nematodes parasitic in insects. Journal of Agricultural Research 6:115–127.

Micoletzky, H. 1922. Die freilebenden Erd-Nematoden. Archiv für Naturgeschichte. Abteiliung A 87:1–650.

Muller, H. J. 1964. The relation of recombination to mutational advance. Mutation Research 1:2–9.

Osche, G. 1954. Über die gegenwärtig ablaufende Entstehung von Zwillings- und Komplementärarten bei Rhabditiden (Nematodes). Zoologische Jahrbücher. Abteilung für Systematik 82:618–654.

Pannell, J. R. 2002. The evolution and maintenance of androdioecy. Annual Review of Ecology and Systematics 33:397–425.

Paramonov, A. A. 1952. Opyt ekologicheskoi klassifikatsii fitonematod. Trudy Gelmintologicheskii Laboratorii. Akademia Nauk SSSR (Moskva) 6:338–369.

Pires-da Silva, A., and Sommer, R. J. 2004. Conservation of the global sex determination gene *tra-1* in distantly related nematodes. Genes & Development 18:1198–1208.

Potts, F. A. 1908. Sexual phenomena in the free-living nematodes. Proceedings of the Cambridge Philosophical Society 14:373–375.

Potts, F. A. 1910. Notes on the free-living nematodes. Quarterly Journal of Microscopical Science 55:433–484.

Ronquist, F., Teslenko, M., van der Mark, P., Ayres, D. L., Darling, A., Höhna, S., Larget, B., Liu, L., Suchard, M. A., and Huelsenbeck, J. P. 2012. MrBayes 3.2: Efficient Bayesian phylogenetic inference and model choice across a large model space. Systematic Biology 61: 539–542.

Sommer, R. J. 2009. The future of evo-devo: Model systems and evolutionary theory. Nature Reviews Genetics 10:416–422.

Sommer, R. J., Carta, L. K., Kim, S. Y., and Sternberg, P. W. 1996. Morphological, genetic and molecular description of *Pristionchus pacificus* n. sp. (Nematoda: Neodiplogastridae). Fundamental and Applied Nematology 19:511–521.

Stamatakis, A. 2006. RAxML-VI-HPC: Maximum likelihood-based analyses with thousands of taxa and mixed models. Bioinformatics 22:2688–2690.

Steiner, G. 1929. *Diplogaster entomophaga* n. sp., a new *Diplogaster* (Diplogasteridae, Nematodes) found on a *Pamphilius stellatus* (Christ) (Tenthredinidae, Hymenoptera). Zoologischer Anzeiger 80:143–145.

Stock, S. P. 1993. *Micoletzkya vidalae* n. sp. (Nematoda: Diplogasteridae), a facultative parasite of *Diabrotica speciosa* (Coleoptera: Chrysomelidae) from Argentina. Research and Reviews in Parasitology 53: 109–112.

Sudhaus, W., and Fürst von Lieven, A. 2003. A phylogenetic classification and catalogue of the Diplogastridae (Secernentea, Nematoda). Journal of Nematode Morphology and Systematics 6:43–90.

Susoy, V., Kanzaki, N., and Herrmann, M. 2013. Description of the bark beetle associated nematodes *Micoletzkya masseyi* n. sp. and *M. japonica* n. sp. (Nematoda: Diplogastridae). Nematology 15:213–231.

Tamura, K., Peterson, D., Peterson, N., Stecher, G., Nei, M., and Kumar, S. 2011. MEGA5: Molecular evolutionary genetics analysis using maximum likelihood, evolutionary distance, and maximum parsimony methods. Molecular Biology and Evolution 28:2731–2739.

Thomas, C. G., Woodruff, G. C., and Haag, E. S. 2012. Causes and consequences of the evolution of reproductive mode in *Caenorhabditis* nematodes. Trends in Genetics 28:213–220.

Völk, J. 1950. Die Nematoden der Regenwürmer und aasbesuchenden Käfer. Zoologische Jahrbücher. Abteilung für Systematik 79:1–70.

Weeks, S. C. 2012. The role of androdioecy and gynodioecy in mediating evolutionary transitions between dioecy and hermaphroditism in the Animalia. Evolution 66:3670–3686.

Weeks, S. C., Chapman, E. G., Rogers, D. C., Senyo, D. M., and Hoeh, W. R. 2009. Evolutionary transitions among dioecy, androdioecy and hermaphroditism in limnadiid clam shrimp (Branchiopoda: Spinacaudata). Journal of Evolutionary Biology 22:1781–1799.

Weeks, S. C., Sanderson, T. F., Reed, S. K., Zofkova, M., Knott, B., Balaraman, U., Pereira, G., Senyo, D. M., and Hoeh, W. R. 2006. Ancient androdioecy in the freshwater crustacean *Eulimnadia*. Proceedings of the Royal Society of London B 273:725–734.

Weingärtner, I. 1955. Versuch einer Neuordnung der Gattung *Diplogaster* Schulze 1857 (Nematoda). Zoologische Jahrbücher. Abteilung für Systematik 83:248–317.